Mechanisms of Inflammation-induced Hepatocarcinogenesis and Prion Transmission via the Aerial Route

Dissertation

zur

Erlangung der naturwissenschaftlichen Doktorwürde

(Dr. sc. nat.)

vorgelegt der

Mathematisch-naturwissenschaftlichen Fakultät

der

Universität Zürich

von

Johannes Stephan Haybäck

aus Österreich

Promotionskomitee

Prof. Dr. Adriano Aguzzi (Vorsitz und Leitung)

Prof. Dr. Manfred Kopf

Prof. Dr. Burkhard Becher

Betreut durch Dr. Mathias Heikenwälder

Zürich 2009

Die vorliegende Arbeit wurde von der mathematisch-naturwissenschaftlichen Fakultät der Universität Zürich auf Antrag von Professor Dr. Adriano Aguzzi als Dissertation angenommen.

Meiner Frau Cornelia

To my wife Cornelia

Summary: Mechanisms of Inflammation-induced Hepatocarcinogenesis

The link between inflammation and carcinogenesis in general and more specifically in liver has been acknowledged for a long time. Hepatocellular carcinoma (HCC) is the most common primary liver cancer. It is associated with chronic liver damage as seen in Hepatitis B and Hepatitis C virus infection, chronic drug and alcohol abuse as well as autoimmune diseases which are typically accompanied by chronic hepatitis.

Interestingly, only 30-40% of all patients with chronic hepatitis develop HCC. The molecular, genetic and cellular events that drive chronic hepatitis induced liver carcinogenesis remain largely elusive.

Due to the lack of appropriate animal models with chronic hepatitis induced HCC research has focused either on (a) animal studies using carcinogenic substances to induce liver cancer or (b) on patient samples.

(a) In the past, scientists have used for example carcinogenic substances such as diethylnitrosamine (DEN) to induce liver cancer in mice. The pathogenesis of HCC in these mouse models differs from that in humans and thus may not be directly comparable to chronic hepatitis induced human HCC. However, DEN-induced HCC might have a genetic signature similar to that of human HCC with poor prognosis. Ablation of the multi-drug resistance gene 2 (*mdr2*) induces cholestatic hepatitis and liver cancer. Liver specific expression of the hepatitis B surface antigen (HBsAg) in mice demonstrates that chronic immune-mediated liver cell injury is critical for HCC formation.

(b) Alternatively, research in humans has centreed on patient liver samples, with sometimes limited ability to dissect cellular and molecular events of chronic hepatitis induced HCC. Recent work with liver samples from patients with chronic hepatitis associated HCC has demonstrated that pro-inflammatory cytokines, Lymphotoxin (LT) α and β, are specifically upregulated on hepatocytes and oval cells. In addition, a recent study has provided evidence that LTβ receptor (LTβR) and LTβ are actively involved in hepatitis C virus replication. In order to establish a mouse model for chronic hepatitis induced HCC LTα and LTβ were ectopically expressed in hepatocytes (AlbLTαβ mice, high expressing line 1223 and therefore named *tg*1223 throughout the following thesis). I can show that these mice develop laboratory evidence and histological signs of insidiously developing chronic hepatitis at 6 to 9 months of age persisting through life time. Indeed, at 12 months of age, about 20% (6/34) of *tg*1223 mice developed macroscopically visible nodules that were classified histologically as HCC. Tumor frequency increased with age reaching ~35% (18/51) by 18 months, whereas C57BL/6 mice did not develop HCC (0/35; $P<0.0001$).

Hepatitis B and C viruses (HBV, HCV) cause chronic hepatitis and HCC by poorly understood mechanisms. This work shows upregulation of the cytokines lymphotoxin (LT) α, β and their receptor (LTβR) in HBV- or HCV-induced hepatitis and HCC. Liver-specific LTαβ expression in mice induces liver inflammation and HCC causally linking hepatic LT overexpression to hepatitis and HCC. Development of HCC, composed in part of $A6^+$ oval cells, depends on lymphocytes and IKappa B kinase β expressed by hepatocytes but is independent of TNFR1. *In vivo* LTβR stimulation implicates hepatocytes as the major LT-responsive liver cells and LTβR inhibition in LTαβ-transgenic mice with hepatitis suppresses HCC formation. Thus, sustained LT signaling represents a hitherto unknown pathway involved in hepatitis-induced HCC.

Summary

Pharmacological inhibition of LTβR signaling reduces pathogen- and concavalin A (ConA)-induced liver injury while LTβR signaling on hepatocytes appears beneficial during liver regeneration. This work demonstrates that sustained hepatic LT expression in mice can be injurious causing chronic hepatitis and HCC. Enhanced hepatic LTβR signaling might be of potential clinical relevance since LTβR and its ligands are drastically increased in human HBV- and HCV-induced hepatitis and HCC when compared to normal livers or non-viral, benign liver diseases. Thus, hepatic LT signaling might be advantageous if transiently active during liver regeneration, but detrimental if chronically triggered. I propose that suppression of hepatic LTβR signaling might be beneficial in liver diseases with chronic LTα, LTβ or LIGHT overexpression.

Zusammenfassung: Mechanismen Entzündungs-induzierter Leberkarzinogenese

Die Assoziation von Entzündung und Karzinogenese wurde bereits vor langer Zeit, insbesondere auch für die Leber, beschrieben. Das hepatozelluläre Karzinom (HCC) ist der häufigste Primärtumor der Leber. Es ist assoziiert mit chronischer Leberschädigung, wie sie im Rahmen von Hepatitis B/C Virus-Infektionen, chronischer Medikamenteneinnahme und Alkoholabusus, ebenso wie auch bei Autoimmunerkrankungen auftritt. Diese Veränderungen sind typischerweise mit einer chronischen Hepatitis vergesellschaftet. Interessanterweise entwickeln lediglich 30-40% aller Patienten mit chronischer Hepatitis ein HCC, und die molekularen, genetischen und zellulären Ereignisse, welche ursächlich für durch chronische Hepatitis induzierte Leberkarzinomentstehung sind, sind bisher noch weitgehend unbekannt. Aufgrund des Fehlens von Mausmodellen für die durch chronische Hepatitis induzierten HCC hat sich die Forschung bisher in zweierlei Weise orientiert. Zum einen (a) wurden Tierstudien unter Verwendung von karzinogenen Substanzen zur HCC-Induktion, zum anderen (b) wurden Studien an Patientengewebe durchgeführt.

(a) In der Vergangenheit haben Forscher beispielsweise chemische Karzinogene wie Diethylnitrosamin (DEN) oder Mitogene wie z.B. Concavalin A (Con A) verwendet, um bei Mäusen Leberkrebs zu induzieren. Die Pathogenese von HCC unterscheidet sich in diesen Modellen deutlich von der humanen Situation und ist daher nicht direkt vergleichbar zum durch chronische Hepatitis induzierten humanen HCC. Allerdings hat das DEN-induzierte HCC möglicherweise eine genetische Signatur, welche ähnlich humanen HCC mit schlechter Prognose ist. Die Entfernung des multi-drug resistance-Gens 2 (*mdr2*) induziert eine cholestatische Hepatitis und Leberkrebs. Leber-spezifische Expression des Hepatitis B-Oberflächenantigens (HBsAg) bei Mäusen zeigte, dass ein chronischer Immun-vermittelter Leberzellschaden entscheidend für die HCC-Entstehung ist.

(b) Alternativ hat sich die Forschung auf Lebergewebe von Patienten gestützt, wobei die Möglichkeit zur genauen Auftrennung der zellulären und molekularen Ereignisse bei durch chronische Hepatitis bedingter Leber-Karzinogenese nur eingeschränkt bestand. Eine erst kürzlich erschienene Arbeit zu Lebergeweben von Patienten mit durch chronische Hepatitis induziertem HCC zeigte, dass die proinflammatorischen Cytokine, Lymphotoxin (LT) α und β spezifisch auf Hepatozyten und den sogenannten "Ovalzellen" hochreguliert sind. Zusätzlich zeigte eine aktuelle Studie, dass der LTβ-Rezeptor und LTβ aktiv in der Replikation des Hepatitis C-Virus involviert sind.

Um ein Mausmodell für ein durch chronische Hepatitis induziertes HCC zu etablieren, wurde LTα und LTβ ektop spezifisch in Hepatozyten (*tg*1223 Mäuse) exprimiert. Ich kann zeigen, dass diese Mäuse laborchemische und histologische Zeichen einer chronischen Hepatitis im Alter von 6 bis 9 Monaten entwickeln. Dieser Entzündungsstatus persistiert über die gesamte Lebensspanne der Tiere. Tatsächlich entwickelten etwa 20% (6/34) der *tg*1223 Mäuse im Alter von 12 Monaten makroskopisch erkennbare Knoten, die histologisch als HCC zu klassifizieren sind. Die Tumorhäufigkeit stieg mit dem Alter an um etwa ~35% (18/51) im Alter von 18 Monaten zu erreichen, wohingegen C57BL/6 Mäuse keine HCC

entwickelten (0/35; $P<0.0001$). Hepatitis B- und C-Viren (HBV, HCV) verursachen chronische Leberentzündung und HCC über bislang schlecht verstandene Mechanismen. Diese Arbeit zeigt eine Hochregulation des Cytokins Lymphotoxin (LT) α, β und seines Rezeptors (LTβR) in HBV- oder HCV-bedingter Leberentzündung und in HCC. Mittels Leber-spezifischer LTαβ-Expression in Mäusen, welche Hepatitis und HCC entwickeln, kann ein kausaler Zusammenhang zwischen Leber-spezifischer LTαβ-Überexpression, Hepatits und HCC hergestellt werden. Die Entwicklung von HCC, die in einem Teil aus $A6^+$ Oval-Zellen bestehen, hängt von Lymphozyten und der IKappa B Kinase β, welche von Hepatozyten exprimiert wird, ab. Sie ist aber unabhängig von TNFR1. *In vivo* LTβR-Stimulierung aktiviert Hepatozyten, welche sensitiv für LT sind. Eine Blockade des LTβR bei LTαβ-transgenen Mäusen mit Leberentzündung unterdrückt die HCC-Bildung. Somit stellt der LT-abhängige Signaltransduktionsweg einen bisher unbekannten, wesentlichen Pfad bei durch Hepatitis induzierter Leberkrebsentstehung dar. Die pharmakologische Hemmung der LTβR-Signaltransduktion reduziert Pathogen- und ConcavalinA-induzierten Leber-Schaden, während die Stimulierung des LTβR, der auf Hepatozyten signalisiert, vorteilhaft während der Leber-Regeneration zu sein scheint. Diese Arbeit zeigt, dass die verstärkte hepatische LT-Expression in Mäusen schädlich ist, indem sie chronische Hepatitis und HCC verursachen kann. Verstärkte hepatische LTβR-Signaltransduktion könnte potenziell von klinischer Relevanz sein, da LTβR und dessen Liganden bei HBV- und HCV-bedingter Leberentzündung und HCC beim Menschen im Vergleich zu normalen Lebern oder nichtviral induzierten Leber-Krankheiten drastisch erhöht sind. So könnte hepatisches LT, wenn es limitiert aktiv während der Leber-Regeneration sezerniert wird, vorteilhaft sein. Es kann aber schädlich sein wenn es dauerhaft getriggert wird. Ich schlage vor, dass die Unterdrückung des hepatischen LTβR Signaltransduktionsweges bei Leber-Krankheiten mit einer chronischen LTα-, LTβ-Überexpression vorteilhaft sein könnte.

A Lymphotoxin-Driven Pathway to Hepatocellular Carcinoma

Johannes Haybaeck,[1,15] Nicolas Zeller,[1,15,16] Monika Julia Wolf,[1] Achim Weber,[2] Ulrich Wagner,[3] Michael Odo Kurrer,[4] Juliane Bremer,[1] Giandomenica Iezzi,[5] Rolf Graf,[6] Pierre-Alain Clavien,[6] Robert Thimme,[7] Hubert Blum,[7] Sergei A. Nedospasov,[8,9] Kurt Zatloukal,[10] Muhammad Ramzan,[11] Sandra Ciesek,[12] Thomas Pietschmann,[12] Patrice N. Marche,[11] Michael Karin,[13] Manfred Kopf,[5] Jeffrey L. Browning,[14] Adriano Aguzzi,[1] and Mathias Heikenwalder[1,*]

1Department of Pathology
2Institutes of Neuropathology and Clinical Pathology
University Hospital Zurich, CH 8091 Zurich, Switzerland
3Functional Genomics Centre Zurich, University Zurich, CH 8057 Zurich, Switzerland
4Department of Pathology, Cantonal Hospital Aarau, CH 5001 Aarau, Switzerland
5Institute of Integrative Biology, Molecular Biomedicine, Swiss Federal Institute of Technology (ETH), Zurich, Schlieren,
CH 8952 Schlieren, Switzerland
6Swiss HPB (Hepato-Pancreatico-Biliary) Centre, Department of Surgery, University Hospital Zurich, CH 8091 Zurich, Switzerland
7Department of Internal Medicine, University of Freiburg, D-79095 Freiburg, Germany
8Engelhardt Institute of Molecular Biology, Moscow, 119991, Russia
9German Rheumatism Research Centre, Berlin, 10117, Germany
10Institute of Pathology, Medical University of Graz, A 8036 Graz, Austria
11INSERM and Universite´ Joseph Fourier-Grenoble, Unite´ 823, Institut Albert Bonniot UJF Site Sante´ BP 170 La Tronche,
F 38042 Grenoble, France
12Division of Experimental Virology, TWINCORE, Centre for Experimental and Clinical Infection Research, Medical School Hannover (MHH) and the Helmholtz Centre for Infection Research (HZI), D-30625 Hannover, Germany
13University of California, San Diego and University of California, Los Angeles, CA 92093-0723, USA
14Department of Immunobiology, Biogen Idec, Cambridge, MA 02142, USA
15Present address: Department of Neuropathology, University of Freiburg, D-79106 Freiburg, Germany
16These authors contributed equally to this work

*Correspondence: mathias.heikenwaelder@usz.ch

Published in **Cancer CELL**, 2009, Oct 6; 16(4):295-308

Selected Definitions

Cytokines: Cytokines are signaling proteins, which either exist in a soluble or membrane bound form and that regulate immune mediated signalings through interactions with specific receptors. The action of cytokines may be autocrine or paracrine.

Chemokines: Cytokines that recruit inflammatory cells to the site of inflammation by a process called chemoattraction. Therefore they are chemotactic cytokines. Some are considered pro-inflammatory and can be induced during immune responses in order to promote cells of the immune system to a site of infection, while others are considered homeostatic and are involved in controlling the migration of cells during normal tissue maintenance or development.

Germinal centre: A structure found in the follicles of secondary lymphoid tissues composed of specialized B-lymphocytes.

Follicular dendritic cells (FDCs): Mesenchymal, radio-resistant cells that reside within white pulp follicles of germinal centres of lymphoid tissue. These cells possess long dendrites and carry intact antigens in immune complexes on their surfaces. These cells differ from dendritic cells as the latter are of hematopoietic origin.

Inflammation: A complex response of the immune system to harmful stimuli like pathogens, cell death or other irritants, such as physical or chemical stimuli. Inflammation is an organism or organ specific strategy to remove damaging agents or stimuli in order to guarantee tissue remodeling and maintenance of organ integrity. The basic symptoms of inflammation are redness (*rubor*), swelling (*tumor*), heat (*calor*), pain (*dolor*) and deranged function (*functio laesa*). The first four have been known since ancient times. Loss of function was added to the definition of inflammation by Rudolf Virchow. Inflammation can be classified as either acute or chronic.

Acute inflammation is an early innate immune response that is generally short and self-limiting. Characteristically neutrophils and macrophages, under specific circumstances, also eosinophils are the main hallmark cells present at a cellular level in acute inflammation. Under certain conditions acute inflammation can develop into a chronic inflammatory state that lasts longer and which may be prolonged in a way that the inflammatory immune response can even lead to considerable tissue destruction and loss of proper functionality. The cellular components being characteristic for chronic inflammation are predominantly lymphocytes and plasma cells. It is well established that these cells often organize themselves in secondary lymphoid organs. Inflammation of the liver is termed hepatitis.

Lymphoreticular system (LRS): The lymphoreticular system is divided into primary and secondary lymphoid tissues. Primary lymphoid organs are anatomical sites where the cells of the LRS are generated, including bone marrow and thymus. Secondary lymphoid organs are specialized tissues to trap antigens, to allow the initiation of adaptive immune responses providing signals that sustain recirculating lymphocytes. Secondary lymphoid organs include the spleen, the lymph nodes, the appendix and the mucosa associated lymphoid tissues. Tertiary lymphoid tissues ectopically arise at sites of chronic inflammation.

Lymphotoxin (LT): LTα and LTβ are proinflammatory cytokines that are part of the tumor necrosis factor (TNF) superfamily. They are mainly expressed by B- and T- lymphocytes and natural killer (NK) cells. LTs exist as membrane bound heterotrimers ($LT\alpha_1\beta_2$ or $LT\alpha_2\beta_1$) or as secreted homotrimer ($LT\alpha_3$). LTs bind to TNFR1, TNFR2 or LTβR triggering a signaling pathway which is essential for the maturation and maintenance of secondary lymphoid organs and of follicular dendritic cells (FDCs).

1. Introduction

1.1 The most important signaling pathways in liver diseases

1.1.1 Overview about various signal transduction pathways

Liver homeostasis and appropriate liver cell function is ensured by the action of various well established signaling pathways. These include the function of the vascular endothelial growth factor, IL-6/gpl30/STAT3, insulin dependent pathways, the hepatic tumor necrosis factor signaling, the Fas/FasL signaling pathway, the TGF-β and the Smad pathway in hepatic fibrogenesis, interferon signaling, the interaction of CD14 and Toll-like receptors, the Wnt/β-Catenin pathway, the Notch signaling, calcium signaling, MAP kinase pathways, PI3K, PTEN, Akt, TOR-signaling and the NF-κB-signaling pathways.

The liver has an important role as the major detoxifying organ of the body and as the first line of defense against ingested toxins and infectious agents. Consequently, the liver has conserved various adaptive responses including the ability to regenerate and protect itself against tissue damage (Fausto, 1999, 2000; Michalopoulos and DeFrances, 1997). Interleukin-6 (IL-6) has been demonstrated as critical during the acute response phase, proliferation and protection against injury in hepatic regenerative processes. While STAT3 appears to be the dominant signal in the IL-6/glycoprotein 130 (gp130)-mediated acute phase response and provides a basis for many of the hepatoprotective properties of IL-6/gp 130 signaling (Taub, 2003), STAT3 does not account for the full proliferative effect of IL-6/gp 130, and it appears that the mitogen-activated protein kinase (MAPK) signaling downstream of IL-6/gp 130 also contributes to the proliferative effects. IL-6 binds to its receptor, IL-6R, that binds to the gp 130 receptor, activating a janus kinase (JAK), which is an intracellular tyrosine kinase (Heinrich et al., 2003).

Stimulation of JAK results in tyrosine phosphorylation of gp130 at several sites and its autophosphorylation. Then tyrosine phosphorylation of gp130-associated STAT3 and SHP2 (SH2 domain containing tyrosine phosphatase) follows. This leads to signal transduction via the STAT3 and MAPK signal transduction pathways. This again results in the activation of the MAPK pathway and activation of STAT3 by tyrosine phosphorylation. Dimerized STAT3 is able to translocate into the nucleus and to activate gene transcription. The described process has been reported to promote liver regeneration and hepatoprotection against Fas and toxic damage. STAT3 is activated by tyrosine phosphorylation at a single site (Y705) and by serine phosphorylation at a MAPK consensus site within its transactivation domain. Tyrosine phosphorylation mediated by JAK is required for STAT3 dimerization, nuclear translocation, and DNA binding.

Triggering gp130 leads not exclusively to STAT signaling but also to activation of the MAPK cascade. MAPK signaling is important for proliferation (Talarmin et al., 1999). IL-6 signaling might also directly activate PI3 kinase, protein kinase B and AKT which are other kinases that impact on cell survival (Heinrich et al., 2003). Efficient inhibitors of STATs include PIAS (protein inhibitor of activated STATs) and SOCS (suppressors of cytokine signaling) (Campbell et al., 2001; Chung et al., 1997). Knockout mice

for IL-6, gp130, STAT3 could demonstrate the importance of these molecules (Alonzi et al., 2001; Fattori et al., 1994; Kopf et al., 1994) in pathological liver states.

1.1.2 The VEGF (Vascular Endothelial Growth Factor) signaling pathway

Vascular endothelial growth factor (VEGF) has been reported to be the main inducer of angiogenesis. VEGF, targeting vascular endothelial cells, is known to play an important role in liver regeneration, hepatic fibrogenesis, portal hypertension and hepatocarcinogenesis (Benjamin et al., 1999; Ferrara and Davis-Smyth, 1997). In chronic hepatitis C, an increase in hepatic VEGF expression and angiogenesis in portal tracts has been reported by one group (Medina et al., 2003) while another group did not find any differences in *VEGF* mRNA expression ratios among steatohepatitis, chronic hepatitis C and HCC (Shimoda et al., 1999). Besides hypoxia, mutations in tumor suppressor genes, oncogenes and viral proteins also lead to the upregulation of VEGF during hepatocarcinogenesis. HCC is a strongly vascularized tumor and therefore depends on VEGF (Yamaguchi et al., 1998). During the process of hepatocarcinogenesis, expression of VEGF increases gradually from low-grade dysplastic nodules to high-grade dysplastic nodules and to early HCC (Park et al., 2000). The degree of VEGF expression during HCC development correlates with the vessel density (Park et al., 2000). High serum levels of VEGF significantly correlated with the presence of intrahepatic metastasis, presence of microscopic venous invasion, advanced stage and postoperative recurrence. Moreover, levels of biologically active VEGF in patients with malignant ascites are higher in comparison to patients with ascites due to non-malignant or cirrhotic causes (Zebrowski et al., 1999).

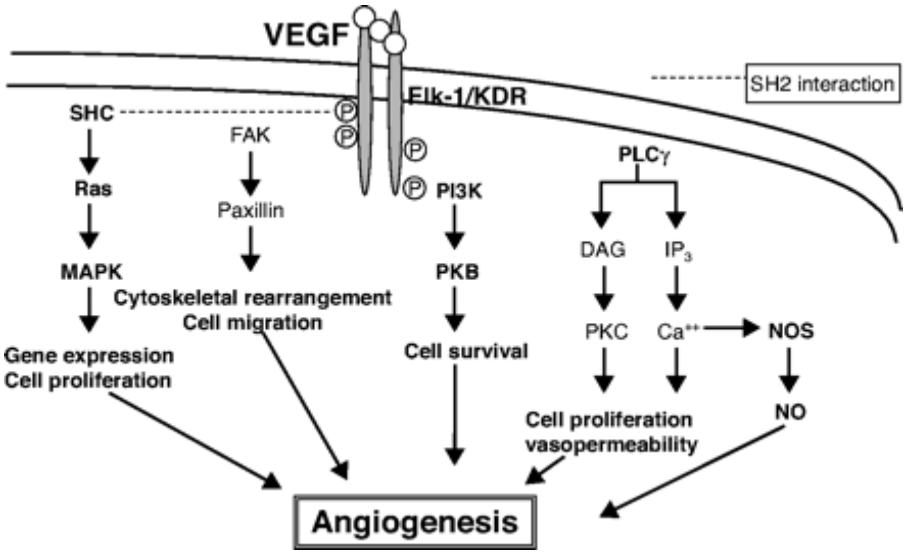

Figure 1. Signaling pathways triggered by VEGF. The activity of VEGF is mediated through three receptor tyrosine kinases: VEGFR-1 (Flt-1), VEGFR-2 (KDR/Flk-1), and VEGFR-3. VEGFR-1 is expressed on endothelial cells and monocytes mediating cell motility. The proliferative and mitogenic activities of VEGF, as well as vascular permeability, are mediated primarily through VEGFR-2. VEGFR-3, also known as Flt-4, being homologous with the neurophilin-1 receptor, is thought to mediate lymphoangiogenesis; adapted from (Giles, 2001).

1.1.3 The Tumor Necrosis Factor signaling pathway

Tumor necrosis factor-α (TNF) is a proinflammatory cytokine involved in liver regeneration, injury and inflammation. It is produced primarily by activated macrophages, but can also be produced by epithelial cells, adipocytes and endothelial cells (Kern et al., 2001; Loffreda et al., 1997). TNF is produced as a 26-kDa type II transmembrane protein with an extracellular C-terminal domain for receptor interaction, a single transmembrane domain, and an intracellular N-terminal domain essential for cell signaling. The membrane form of TNF is a homotrimer (Banner et al., 1993). A soluble form (sTNF) is generated through proteolytic cleavage of the transmembrane form by the metalloprotease TNFα converting enzyme (TACE), being a member of the mammalian adamalysin (ADAM) family (Black et al., 1997). The bioactivity of membrane-bound TNF is higher than that of sTNF.

TNF exerts its biological effects by binding to the TNF receptor type 1 (TNF-R1) or TNF receptor type 2 (TNF-R2). These receptors belong to the TNF receptor superfamily. Whereas the membranous and soluble forms of TNF induce equivalent activation of TNF-R1, full activation of TNF-R2 needs membrane-bound TNF (Grell et al., 1999). Recent studies have demonstrated that rather than receptor trimerization occurring after ligand binding, the TNF-R exists as a preformed multimer to which the ligand binds in its homotrimeric form (Aggarwal, 2003). Both receptor types are expressed in the liver, but it is unclear whether type II receptors are expressed only on non parenchymal cells (NPC) such as Kupffer cells, or on hepatocytes. TNF-R1 is generally required for the induction of apoptosis, while the role of TNF-R2 seems to be less well defined. TNF-R2 possesses a lower binding affinity and higher dissociation rate for TNF than TNF-R1. This suggests that TNF-R2 may transiently bind and then release TNF, in order to increase local concentrations of TNF that acts on TNF-R1 (Grell et al., 1998a; Grell et al., 1998b). This phenomenon is known as ligandpassing and may allow TNF-R1 activation at much lower TNF concentrations (Barbara et al., 1994). Alternatively, overexpression of TNF-R2 can also inhibit TNF signaling by competing with TNF-R1 for the ligand. This is why the overall biological effect of TNF might depend, at least partially, on the relative ratio of the two receptors (Fotin-Mleczek et al., 2002). Initially, the adaptor molecule TRADD binds to the TNF-R1. The survival pathway is activated following recruitment of TRAF-2 and RIP to TRADD. This complex triggers IKK, which phosphorylates IKB. Phosphorylated IKB undergoes proteasomal degradation, releasing NF-κB heterodimers which translocate to the nucleus and activate genes necessary for TNF-induced hepatocyte proliferation. In parallel, NF-κB-regulated gene products block the TNF driven apoptotic death pathway. Signaling through TRAF-2 leads to activation of the JNK/cJun/AP-1 pathway. AP-1-dependent gene expression promotes hepatocyte proliferation, but sustained AP-1 activation can also induce the apoptotic death pathway.

In the death pathway, the TRADD-TRAF-2-RIP complex dissociates from the TNF-R1 and recruits FADD and procaspase-8. Caspase-8 is released after its autolytic activation. Caspase-8 cleaves Bid, resulting in a truncated and active Bid which activates the pro-apoptotic Bcl-2 family members Bax and Bak. Their oligomerization and integration into the mitochondrial membrane leads to cytochrome c release. The complex of cytochrome c and APAF-1 recruits procaspase-3 resulting in apoptosis. Caspase-8 activation

also causes release of the lysosomal enzyme cathepsin B, which induces the mitochondrial death pathway. Binding between TNF and TNF-R occurs at the plasma membrane through interactions between the receptor and the trimeric ligand. This results in a conformational change in the receptor and translocation of the receptor-ligand complex to lipid-enriched membrane microdomains, known as lipid rafts. There is evidence that the sources of TNF production after partial hepatectomy are biliary and endothelial cells (Loffreda et al., 1997). Of note, neutralizing anti-TNF antibodies inhibit hepatocyte proliferation following partial hepatectomy, clearly implicating TNF as a hepatocyte mitogen in this model (Akerman et al., 1992). Studies of partial hepatectomy in *tnfr1*$^{-/-}$ mice have basically confirmed these data. Inhibition of the biological activities of TNF leads to reduced activation of the downstream transcriptional regulators NF-κB, STAT3 and AP-1 (Yamada et al., 1997). On the other hand, posthepatectomy liver regeneration was normal in *tnfr2*$^{-/-}$ mice. Absence of the type 2 receptor had essentially no effect on NF-κB and STAT3 binding or IL-6 production. However, it caused a delay in AP-1 binding. Therefore it is believed that TNF-induced proliferation occurs exclusively through TNFR1 mediated signaling. Infiltrating cytotoxic T-lymphocytes decrease HBV gene expression and replication in the liver of HBV transgenic mice through the secretion of TNF as well as IFβ and IFγ (McClary et al., 2000). In summary, TNF has been proposed to be important in human liver diseases (Khoruts et al., 1991; Streetz et al., 2000).

1.1.4 The NF-κB signaling pathway

Nuclear factor (NF)-κB was first described in 1986 as a nuclear factor necessary for immunoglobulin K light chain transcription (Sen and Baltimore, 1986a, b). It exists in virtually all known cell types, and regulates the transcription of many genes including those involved in immune and inflammatory response, cell death and proliferation (Karin and Lin, 2002). The mammalian the NF-κB family includes five cellular DNA-binding subunit proteins: p50 (NF-κB 1), p52 (NF-κB 2), c-Rel (Rel), p65 (Re1A) and RelB. The NF-κB DNA-binding subunits share an N-terminal Rel homology domain (RHD). It forms a unique butterfly-shaped structure composed of 13 strands arranged in a pattern similar to immunoglobulin domains. This region is responsible for DNA binding, dimerization, nuclear translocation and interaction with the inhibitory IKB proteins. RelA (p65), RelB and c-Rel contain C-terminal transactivation domains that trigger target gene transcription. Of these proteins, p65, which contains two potent transactivation domains (TADs) within its C-terminus, mediates the strongest gene activation (Schmitz and Baeuerle, 1991). The other two members, p52 and p50 become active by either constitutive (p105) or regulated (p100) processing steps (Amir et al., 2004). They are generally not activators of transcription, unless they form heterodimers with p65, RelB or c-Rel. NF-κB commonly refers to a p50/p65 heterodimer. The activity of NF-κB is controlled by IκBs, a family of cytoplasmic inhibitory proteins that share a number of protein/protein interaction domains called ankyrin repeats. The precursors p105 and p100 are also included in this family, since they contain IKB-like repeats and therefore inhibit NF-κB activation (Baeuerle and Baltimore, 1996). NF-κB is effectively sequestered in the cytoplasm by IκB in an inactive state via complex formation and the ability of

IKB to mask the nuclear localization site (NLS) of NF-κB. As IκBα is an NF-κB-target gene, it also terminates NF-κB activation at transcriptional level: increased synthesis of IKBα shuts down NF-κB-induced gene expression by IκBα-mediated nuclear export of the DNA-binding subunits, thereby acting in a negative feedback loop (Arenzana-Seisdedos et al., 1997). To date, the so-called canonical and non-canonical pathways and the DNA damage-induced NF-κB pathway are established. Moreover, further mechanisms such as p65 posttranslational modifications regulate the activity of this transcription factor. The canonical pathway is probably the most important mediator of NF-κB activation in response to cytokines. An essential step during this pathway is the disruption of cytoplasmic NF-κB. After phosphorylation, polyubiquitination of IκB-α by a specific, constitutively active ubiquitin ligase takes place (Karin, 1999). The ubiquitin-marked IκB proteins are quickly degraded by the 26S proteasome, resulting in unmasking of the nuclear localization site (NLS) of NF-κB. This allows nuclear entry, DNA binding and transcriptional activity of NF-κB. The activation of this IKB-independent pathway involves the IKK subunit IKKα and results in the release of p52/RelB and p50/RelB dimers (Senftleben et al., 2001; Xiao et al., 2001). It is induced for example by LTβ and leads to NIK- and IKKα-dependent processing of the p100 precursor protein, which results in the release of p52 (Pomerantz and Baltimore, 2002). LTβ employs canonical and non-canonical pathways. While in the canonical pathways, signaling is abrogated quickly by induction of IκBα, the non-canonical pathway comprises slower p100 processing, thus inducing a delayed NF-κB activation (Coope et al., 2002; Dejardin et al., 2002). DNA-damage-induced NF-κB activation, in contrast to the previously described pathways, occurs in an IKK-independent manner. It has been observed after doxorubicin stimulation or UV radiation and involves mitogen-activated protein kinase (MAPK)-dependent alternative IKBα phosphorylation (Kato et al., 2003). Post-translational modifications of NF-κB subunits may also influence NF-κB activation. In particular, the phosphorylation of p65 and also its acetylation appear to modify its transcriptional activity significantly. *In vitro*, IKKα and IKKβ can form homo- and heterodimers (Zandi et al., 1998).

Besides its anti-apoptotic function in TNF-mediated liver apoptosis, NF-κB might also play a role in other apoptotic pathways. ConA stimulation in mice leads to activation of NF-κB, and this pathway is blocked by anti-TNF treatment (Trautwein et al., 1998). HBV is the leading cause of hepatic failure worldwide, followed by HCV infection. Both HBV and HCV modulate the NF-κB pathway (Tai et al., 2000). Numerous chemical compounds and viral vectors that inhibit NF-κB have been developed or are under development (Karin et al., 2002). The ubiquitous presence of NF-κB in virtually all cells and its involvement in different cellular pathways makes administration of drugs which inhibit NF-κB non-specifically possibly dangerous. Especially, the subunits of the IKK complex are widely discussed as therapeutic targets for development of anti-inflammatory and anticancerous agents (Kato et al., 2003).

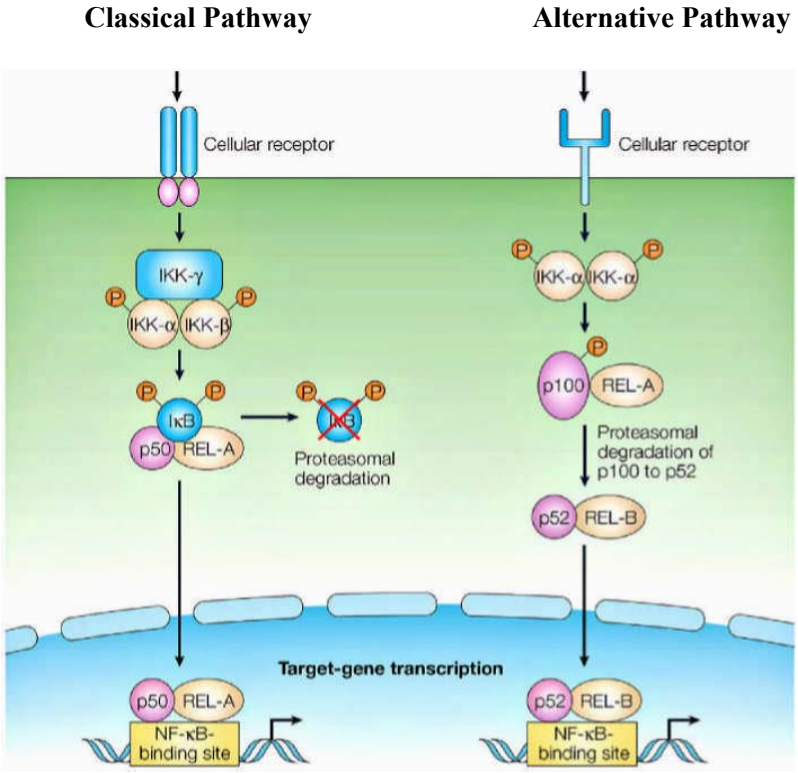

Figure 3. Signaling pathways leading to the activation of different nuclear factor κB transcription factors. The classical pathway is induced by pro-inflammatory triggers such as TNF, LPS and DNA-damaging agents. This leads to an IKKβ and IKKγ dependent phosphorylation of IKBs, resulting in their proteasomal degradation, and the subsequent liberation of NF-κB dimers. These subsequently translocate into the cell nucleus. The alternative NF-κB pathway is activated by certain TNF family members and leads, independent of IKKβ and IKKγ to the phosphorylation of P100 by IKKα and the degradation of its carboxy-terminal part by the action of the proteasome. Finally, p52-Rel-B dimers translocate to the nucleus; from (Karin and Greten, 2005).

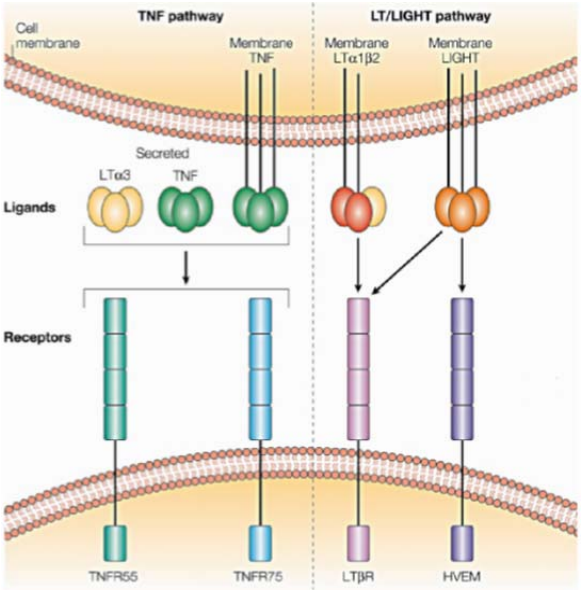

Figure 4. Selected ligands and receptors of the TNF / lymphotoxin family. The TNF signaling pathway is activated by TNF or $LT\alpha_3$-induced signaling through both TNF receptors, TNFR1 (p55) and TNFR2 (p75). Regarding the LT/LIGHT-dependent pathway signal transduction is mediated by the LTβ receptor (LTβR) that binds two

ligands, the $LT\alpha_1\beta_2$ heterotrimer or homotrimeric LIGHT. LIGHT might also signal via the HVEM; modified from (Gommerman and Browning, 2003).

1.1.5 The Interferon signaling pathway / JAK-STAT signaling pathway

The interferons (IFNs) are cytokines produced by many cell types responding to viral infections and other triggers. Two types of IFNs exist. Type I IFNs are secreted in response to viral infections by various cell types. Type II IFN, also known as IFNγ, is produced by activated T-cells and macrophages upon mitogenic or antigenic stimulation of the immune defense machinery. It is involved in antigen-specific immune responses. Upon recognizing viral antigens, the cell activates different signaling cascades in order to produce cytokines that both inhibit pathogen replication and stimulate immune responses (Akira et al., 2001; Huang et al., 2001). After specific phosphorylations, interferon regulatory factor 3 (IRF3) dimers migrate into the nucleus to stimulate the expression of certain IFNs during the very early phase of the cellular response to infections, whereas IRF7 is recruited later for amplifying the interferon response. Binding of endogenous secreted interferons, or of exogenous interferon in treated patients, to their cell surface receptors activates a tyrosine kinase signaling cascade which leads to the activation of latent cytoplasmic STATs. Current therapy of chronic hepatitis C virus (HCV) infection is based on type I interferon (IFN). Despite the introduction of new potent antiviral drugs able to inhibit hepatitis B virus (HBV) replication, type I IFNs are still commonly used in the treatment of HBV-infected patients and represent the only treatment that can efficiently achieve a permanent suppression of HBV replication and HBsAg loss. Both transformed and virally infected cells have evolved mechanisms to resist the biological activities of IFNs. Interferon-stimulated genes encode for proteins displaying strong antiviral, antiproliferative and anti-tumoral activity. IFNα/β also regulates antiviral immune responses involving dendritic and natural killer cells (Biron, 2001). However, the efficacy of IFN treatment in human tumors is hampered by rapid development of resistance. Viruses have developed different strategies to intercept IFN signaling, in order to inhibit IFN-induced antiviral responses (Katze et al., 2002). Many viruses perturb signaling components of the JAK-STAT pathway, thus preventing the proper cellular response to IFN. Among the viral factors, infection with HCV types 1 and 4, high viral load, long-lasting HCV infection, higher levels of HCV, NS5A variability within and outside the so-called interferon sensitivity determinant region (ISDR) are believed to be the best predictive factors of poor response to IFN. Decreased levels of IFNα receptor expression are found in HCV patients and IFN receptor mRNA levels are higher in the responders than in non-responders suffering from chronic active hepatitis irrespective of HCV genotypes (Fujiwara et al., 2004). While HCV products inhibit IFN signaling and IFN-induced antiviral activity, IFN itself inhibits HCV "replicon amplification" (Chung et al., 2001).

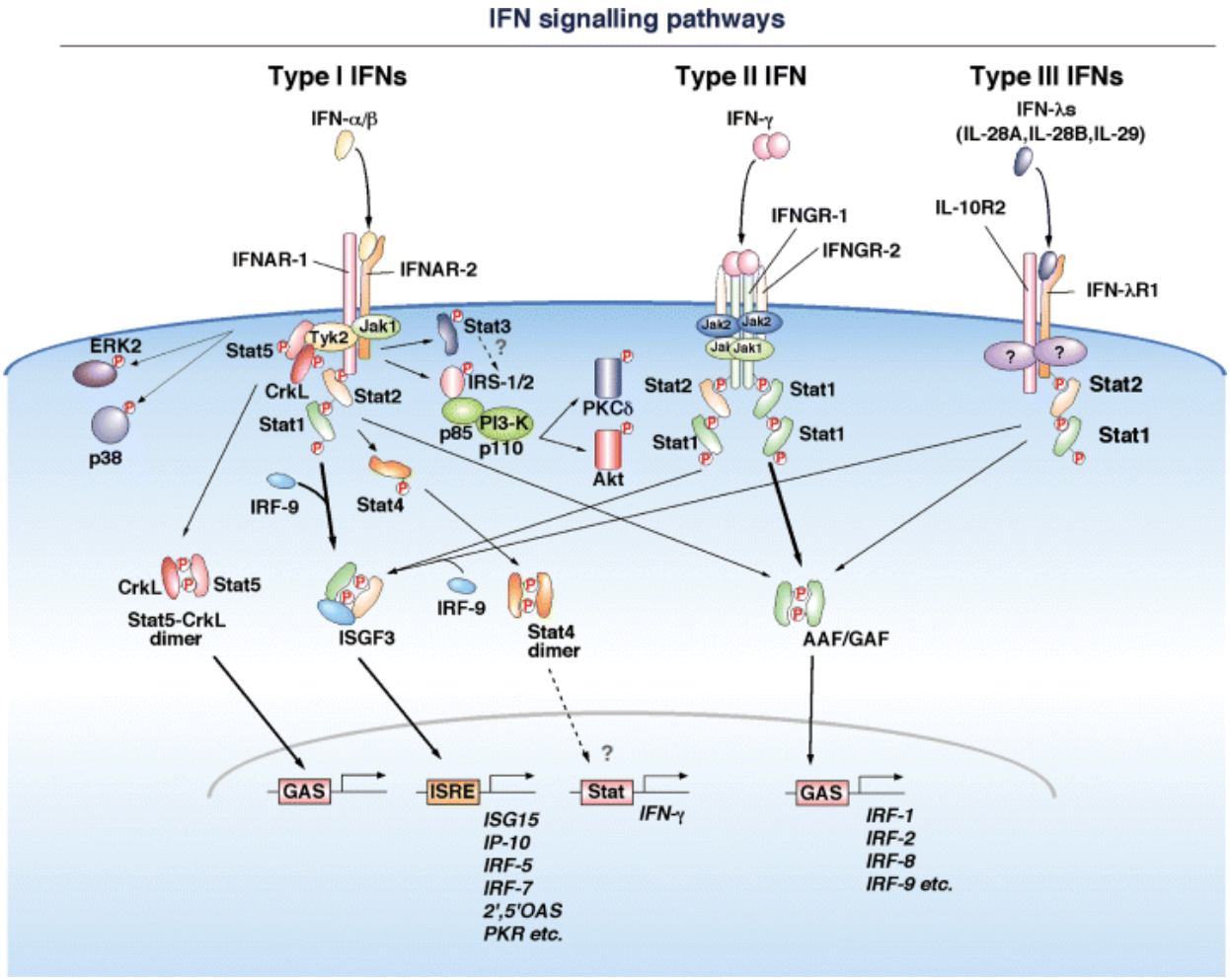

Figure 5. Activation of the JAK-STAT pathway and additional signaling pathways by three types of IFNs. Type I IFNs (only IFN-α and IFN-β are shown for simplicity), type II IFN (IFN-γ) and type III IFNs (IFN-λ1/ IL-29, IFN-λ2/IL-28A and IFN-λ3/IL-28B) bind to their receptor complex as shown. All of them activate the canonical JAK-STAT pathway. Type III IFNs were reported to activate STAT1 and STAT2 through the activation of JAK kinases, leading to downstream gene induction in an ISGF3- or GAF/AAF-dependent manner. It is not yet clear which JAKs are associated with the type III receptor subunit (IFN-λR1). STAT5 is associated with Tyk2, while v-*crk* sarcoma virus CT10 oncogene homologue (avian)-like (CrkL) constitutively associates with the guanine-nucleotide-exchange factor (GEF) C3G. Following type I IFN stimulation, CrkL is recruited to Tyk2, which phosphorylates both STAT5 and CrkL, resulting in heterodimer formation. This dimer translocates into the nucleus to activate GAS-mediated gene induction. Type I IFNs also activate the PI3-kinase-mediated signaling pathway downstream of JAK1 and Tyk2, through the phosphorylation of insulin receptor substrate (IRS)-1 and IRS-2, most probably independently of STATs. The activated PI3-kinase consequently increases the activities of v-*akt* murine thymoma viral oncogene homologue 3 (Akt) and protein kinase Cδ (PKCδ). Moreover, type I IFNs can activate MAP kinases, the so called extracellular-signal-regulated kinase 2 (ERK2) and p38, both of which are capable of phosphorylating Ser 727 of STAT1 *in vitro;* from (Takaoka and Yanai, 2006).

1.1.6 The Wnt/β-catenin signaling pathway

The role of the Wnt/β-catenin pathway is well established in vertebrates in embryogenesis and

carcinogenesis (Pennisi, 1998). The importance of the Wnt/β-catenin pathway in liver development and hepatocellular carcinogenesis has been discussed. The Wnt/β-catenin pathway appears to be critical for biliary epithelial cell growth (Sekhon et al., 2004). A significant increase in the total β-catenin protein within the first few minutes after hepatectomy was observed. This was mediated by an epigenetic or post-translational mechanism and it occurred independently of transcriptional modifications (Monga et al., 2001). Nuclear and cytoplasmic localization of β-catenin have been shown in 90 - 100% of hepatoblastomas (Jeng et al., 2000). In addition, abnormal cytoplasmic and/or nuclear localization of β-catenin was observed in 30 - 46% of hepatic adenomas (Chen et al., 2002). In contrast, no significant changes in the pathway were observed in FNH. Altered Wnt/β-catenin activation has been demonstrated in many cancers and it is one of the important aberrant pathways in HCC in man and animals (Laurent-Puig et al., 2001; Polakis, 2000). Moreover, more than 40% of HCV-associated HCC have been reported to display mutations in the β-catenin gene and nuclear accumulation of the respective protein (Huang et al., 1999) while HBV-related HCC display an overall lower frequency of β-catenin mutations (Boutros et al., 1998). Although mutations in its gene were infrequent, aflatoxin-driven HCC have been described to frequently accumulate β-catenin in around 45% of cases (Devereux et al., 2001).

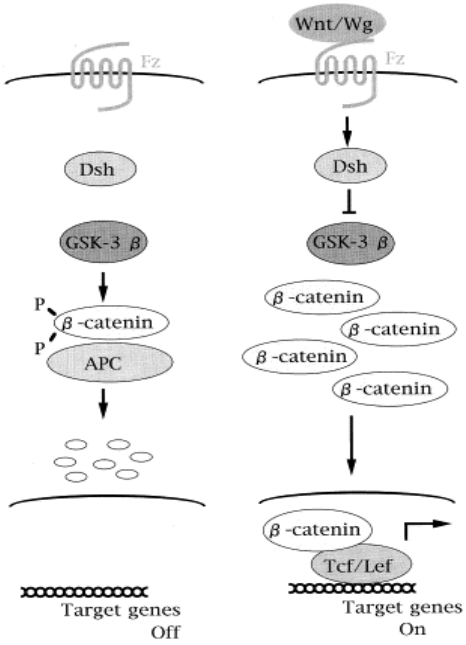

Figure 6. The Wnt signaling pathway. The Wnt family consists of more than 15 closely related secreted glycoproteins. Receptors for the Wnt proteins are members of the *frizzled* family of transmembrane proteins, and the Wnt signal is transduced to a cytoplasmic protein, Dishevelled (Dvl). Upon activation by the Wnt signal, Dvl inhibits the activity of glycogen synthase kinase-3β (GSK-3β). In the absence of the Wnt signal, GSK-3β phosphorylates β-catenin and induces the degradation of β-catenin. Thereby, the Wnt signal induces the accumulation of β-catenin, which in turn associates with TCF/LEF family transcription factors, altering the expression of Wnt signaling target genes; from (Akiyama, 2000).

1.2 The TNF superfamily with focus on Lymphotoxin

1.2.1 The TNF superfamily

Up to date, more than 40 members of the TNF superfamily are known (Aggarwal, 2003). Cytokines of this family can occur as secreted or membrane-bound proteins. They are critically involved in the regulation of cell growth, differentiation, and activation of immune cells by mediating signals to effector immune cells. LTs have been identified as one of the most important factors in lymphoid organogenesis, organization and maintenance of specified lymphoid tissue (Futterer et al., 1998; Mebius et al., 1997; Yoshida et al., 1999). LT is indispensable for maintenance of secondary lymphoid organ architecture (Fu et al., 1998b; Rennert et al., 1996; Tumanov et al., 2003; Wang et al., 2001). LT and TNF were first identified in 1975 and their respective cDNAs were then cloned (Locksley et al., 2001). LT and many ligands such as TNF, CD40L, LIGHT, FasL, BAFF, and their corresponding receptors belong to the TNF receptor superfamily (Aggarwal, 2003; Fu et al., 1998b; Locksley et al., 2001). LTα and LTβ which are proinflammatory cytokines are cytotoxic to normal and transformed cells *in vitro* (Ruddle and Waksman, 1967). LTα, LTβ and TNF are structurally similar, including their assembly into functionally active homotrimers and / or heterotrimers. Remarkably, the genes encoding for LTα, LTβ, and TNF are also in close proximity to each other, within the major histocompatibility locus (Muller et al., 1987). Most TNF superfamily members are expressed by immune cells. LTs are mainly expressed by natural-killer cells (NK-cells), by lymphoid tissue inducer cells (LTIs), on the surface of B-lymphocytes and by activated T-lymphocytes. The TNF superfamily ligands are type II transmembrane proteins (intracellular N-terminus) that are biologically active as self assembling, non-covalent bound trimers. The LTβ subunit in the heterotrimeric complex modifies the receptor binding specificity to engage with high affinity the LTβ receptor. This is expressed by stromal cells (Browning et al., 1993; Cupedo et al., 2004). LTα mRNA expression is inducible in B-cells, while LTβ mRNA is constitutively produced. The generation of surface LTβ depends on the formation of complexes with LTα (Worm and Geha, 1994). Surface LT expression enhances production and secretion of homeostatic chemokines by stromal cells within the spleen and other secondary lymphoid organs (Ngo et al., 1999; Shakhov et al., 2000). Homeostatic chemokines, which are expressed by LT-responsive cells like for example FDCs, upregulate surface expression of the LT complex on B-lymphocytes (Ansel et al., 2000), and signal as a positive feedback loop which is required for the organization of lymphoid follicles and for the formation of tertiary lymphoid follicles in non-lymphoid organs. It therefore becomes increasingly apparent that LT-signaling controls secondary lymphoid organogenesis (Browning et al., 1993; Drayton et al., 2003). Ectopic expression of LTα in the kidney or pancreas leads to the generation of lymphoid aggregates, resembling tertiary folliclels (Kratz et al., 1996; Picarella et al., 1992). These are quite similar to activated lymphoid follicles found in spleen or in lymph nodes.

1.2.2 The TNF superfamily members

The pro-inflammatory and homeostatic cytokines LTα and LTβ are members of the TNF superfamily. Under physiological conditions LTs are expressed by activated T-, B-, NK- and lymphoid tissue inducer cells (Fu et al., 1998b; Ware, 2005) and are crucial for organogenesis and maintenance of lymphoid tissues (Tumanov et al., 2003). Whereas LTβ contains a transmembrane domain, LTα is soluble. Consequently, LT can exist as membrane bound heterotrimers ($LT\alpha_1\beta_2$ or $LT\alpha_2\beta_1$) interacting with LTβR or as soluble secreted homotrimers ($LT\alpha_3$) triggering TNF receptor 1, 2 (TNFR1, TNFR2) and the herpes virus entry mediator receptor (HVEM) (Browning et al., 1997; Ware, 2005). LTβR and TNFR1 signaling can be activated by the HCV-core protein (Chen et al., 1997; Zhu et al., 1998) involving the canonical or non-canonical NF-κB signaling pathways (Ware, 2005; You et al., 1999). Furthermore, HBV- or HCV-infections lead to increased hepatic LT expression *in vivo* and *in vitro* (Lee et al., 2005; Lowes et al., 2003) and HCV replication has been demonstrated to depend on components of the LTβ signaling pathway *in vitro* (Ng et al., 2007).

LTs can directly act on hepatocytes which physiologically express high levels of LTβR but little LT (Browning and French, 2002). T-cell-derived LT and LIGHT (LT-like, exhibits inducible expression, competes with HSV glycoprotein D for HVEM, expressed by T-lymphocytes) signaling to hepatocytes controls lipoprotein homeostasis (Lo et al., 2007). In addition, LT signaling is important for liver regeneration through T-cell-derived LT expression (Tumanov et al., 2008) and regulates HSC function and wound healing (Ruddell et al., 2009). Thus, hepatic LTβR signaling controls liver homeostasis in both health and disease.

1.2.3 NF-κB and tumor development

Triggering TNFR1 or LTβR induces the classical and alternative NF-κB signaling pathways, which are linked to inflammation-induced carcinogenesis (Greten and Karin, 2004). However, the precise role of these pathways in HCC pathogenesis is controversial (Vainer et al., 2008). Mice lacking IKappa B kinase β (IKKβ specifically in hepatocytes ($IKK\beta^{\Delta hep}$) exhibit a marked increase in DEN-induced HCC formation suggesting a protective function of IKKβ in HCC development (Maeda et al., 2005). In contrast, NF-κB signaling promotes HCC development in $mdr2^{-/-}$ mice and anti-TNFα treatment is protective (Pikarsky et al., 2004). Interestingly, mice with a hepatocyte-specific deletion of IKKγ develop steatohepatitis and HCC (Luedde et al., 2007). Consequently, the role of NF-κB signaling in hepatocarcinogenesis might depend on the mouse model and the type or degree of liver inflammation and injury (Vainer et al., 2008). During my thesis, I investigated a possible causal relationship between sustained hepatic LTβR-signaling, chronic hepatitis and HCC development.

1.3 Overview on liver diseases

1.3.1 Liver anatomy and physiological function

The liver is divided by the ligamentum falciforme and the ligamentum teres hepatis in the bigger right lobe and the smaller left lobe. From the liver gate arches the quadrate lobe to the front, at the back the dorsal caudate lobe. The organ contains a crude capsule which is transected by sensitive nerves that are responsible for pain when stretching the liver capsule due to liver enlargement. The internal anatomical structure is given by the branching of the liver vessels defining liver segments. These allow segmental surgical resections. The morphological subunits, the liver lobes, are consisting of liver cell plates and intervening sinusoids. These sinusoids converge to the central vein. The main entrance fields lie between the liver cell plates and contain vessels, nerves and bile ducts. They are surrounded by liver cells of the parenchymal border plate. The sinusoids are lined by Kupffer cells and endothelial cells. The incoming blood is provided by the branches of the portal vein and the hepatic artery which lie in the main entrance field. The blood flows through the sinusoids into the central vein in the centre of the liver lobes. The central veins merge to sublobular veins and to the hepatic veins by which the blood from the liver runs off. The bile flows in the opposite direction. Bile is secreted into bile canaliculi which have a wall formed by the canalicular liver cell membranes. The other drain of the bile occurs via the canals of Herring (cholangioles), the ductuli and the interlobular cystic ducts in the main entrance fields, and about the right and left hepatic duct in the ductus choledochus. However, Rappaport description based on the functional circumstances does better justice to the acinar structure of the liver. The centre of the acinus gets blood from parts of the main entrance field and the smallest branches of the portal artery and the hepatic artery. The central veins lie within the acinar periphery. The Rappaport zone 1 lies around the main entrance field of the liver parenchyma for receiving oxygen and blood richer in nutrient and richer in hormone than the Rappaport zone 3 lying around the central vein. The intervening Rappaport zone 2 takes an interposition. The liver cells form approximately 80% of the hepatic cell population. They own functionally different membranes (sinusoidal, lateral, canalicular). The canalicular membranes form the bile canaliculi carrying numerous microvilli. Between the liver cell plates and the endothelial cells lies the space of Disse. The sinusoids lined by endothelial cells are fenestrated. As a continuous basal membrane is absent, a communication is possible between sinusoid and the space of Disse. The Kupffer cells represent the monocyte-macrophage system within the liver and play an important role in defense processes. In the space of Disse specified cells, the lipid and vitamin A containing, so called Ito- or stellate cells lie. The liver fulfils metabolic (glucose metabolism, fat metabolism), synthetic (serum proteins, coagulation factors), catabolic and biotransformatory duties (dismantling of serum proteins, hormones, transformation of foreign matters) as well as storage (glykogen, triglyceride, metals, vitamins) and removal functions (biliary components). Hence, a disturbance of the liver function is connected with a distinctive clinical symptomatology.

1.3.1.1 Liver cell types

1.3.1.1.1 Hepatocytes

Hepatocytes are the main cellular components of the liver. They display an eosinophilic cytoplasm, reflecting numerous mitochondria, and basophilic stippling due to large amounts of rough endoplasmic reticulum and free ribosomes. Brown lipofuscin granules are also detectable together with irregular unstained areas of cytoplasm corresponding to cytoplasmic glycogen and lipid stores which are removed during routine histological preparation. The average life span of a human hepatocyte is about 5 months. Hepatocytes display a high regenerative capacity. Their nuclei are round with dispersed chromatin and prominent nucleoli. Anisokaryosis is common and reflects tetraploidy and polyploidy, a normal feature of over 50% of hepatocytes. Binucleated cells are quite common. Hepatocytes are organised into plates separated by vascular channels (sinusoids), an arrangement supported by a reticulin (collagen type III) network. The hepatocyte cords are one cell thick in humans as well as in mice. Sinusoids display a discontinuous, fenestrated endothelial cell lining. The endothelial cells have no basement membrane and are separated from the hepatocytes by the space of Disse which drains lymph into the portal tract lymphatics. The hepatocyte manufactures serum albumin, fibrinogen, and the prothrombin group of clotting factors. It is the main site for the synthesis of lipoproteins, ceruloplasmin, transferrin, complement and glycoproteins. Hepatocytes manufacture their own structural proteins and intracellular enzymes as well. Synthesis of proteins is undertaken by the rough endoplasmic reticulum (RER), and both the rough and the smooth endoplasmic reticulum (SER) are involved in secretion of the proteins formed. The endoplasmic reticulum (ER) is involved in conjugation of proteins to lipid and carbohydrate moieties synthesized by, or modified within, the hepatocytes. The liver produces fatty acids from carbohydrates and synthesizes triglycerides from fatty acids and glycerol. Hepatocytes also synthesize apoproteins with which lipoproteins (VLDL, HDL) are exported. Hepatocytes are able to metabolize, detoxify, and inactivate exogenous compounds such as drugs, and endogenous compounds such as steroids. In addition, it should be mentioned that hepatocytes are polar, meaning that they contain two membrane domains. One is the apical membrane domain. This is formed by a small bile duct (canaliculus bilifer) and its neighbouring cell. This membrane carries numerous microvilli and secretes bile. The small bile ducts are sealed by a zonula occludens, zonula adhaerens and macula adhaerens. The other domain is the so called basolateral membrane. The wide basolateral membrane domain borders on the space of Disse or on the sinusoids being responsible for the material exchange with the blood.

1.3.1.1.2 Biliary epithelial cells

Beside from hepatocytes also from other cell types in the liver tumors can arise. These cell types are the so called cholangiocytes. These cells are the origin of cholangiocellular carcinomas (CCC). Cholangiocytes are polarized cells constituting about 5 % of the whole liver mass. These cells are critical for bile production as bile has to be modified several times until it reaches the duodenum. In man some primary biliary diseases

are well known, such as PBC, PSC, biliary atresia or cystic fibrosis. It has become clear that for the regulation of ductular bile secretion and bile duct proliferation cholangiocytes depend on second messengers like cAMP, calcium and kinases such as PKC, MAPK and PI3-K. As cholestasis is one of the major manifestation types of liver diseases it appears to be important to understand what the pathophysiological prerequisites for cholangiocellular dysfunction are as these lead to secretion impairment (Roberts et al., 1997). Various models of ductular cholestasis using for example bile duct ligation could show that expression of the secretin receptor and cAMP producrtion are still preserved. In contrast, these functions are even enhanced (Alpini et al., 1994). On the other hand, calcium signaling pathways are severely impaired in various cholestatic models and diseases (Alvaro et al., 1997). As I am mainly interested in inflammation driven carcinogenesis it is of high interest that a major predisposing factor for the development of CCC is an inflammatory state within the bile ducts. Here inflammation induces a p38 MAPK stress signaling cascade. Thereby cholangiocellular proliferation might be facilitated by translational regulation of protein synthesis. Therefore, gene silencing of eIF-4E (eukaryotic translation initation factor 4E), has been suggested as a possible therapeutic strategy (Yamagiwa et al., 2003). Since cholangiocytes are accessible by percutaneous or endoscopic interventions, and as at least in animal models introducing genes into cholangiocytes via retrograde biliary infusions has been demonstrated, gene therapies might become an attractive therapeutic strategy for treating CCC (Hommel et al., 2003).

1.3.1.1.3 Kupffer cells

These liver resident macrophages are named after the pathologist C. von Kupffer, who first recognized this non-parenchymal cell (NPC). Kupffer cells (KC) represent about 35% of the hepatic NPC in normal adult mice. These cells reside within the lumen of the liver sinusoids, adherent to the endothelial cells which form the blood vessel walls. KC, found in highest number in the periportal area, constitute the first macrophage line of the body to come in contact with bacteria, bacterial endotoxins, and microbial debris derived from the gastrointestinal tract, being transported to the liver via the portal vein (Fox et al., 1987). Thereby, KC are constantly exposed to factors which act as macrophage activators. Upon activation, KC themselves, release various products, including cytokines, prostanoids, nitric oxide, and reactive oxygen species (Decker, 1990). In other words, KC are intimately involved in the liver's response to infection, toxins, ischemia, resection and various other stresses. The most important activators of KC are the complement factors C3a and C5a (Schieferdecker et al., 2001; Su, 2002). LPS activates KC directly via TLR signaling (Su, 2002). In addition, high LPS concentrations can stimulate KC indirectly via complement activation in either the portal or the systemic circulation (Jaeschke et al., 1994). After complement activation, cleavage of C3 and C5 leads to the generation of the potent anaphylatoxins C3a and C5a followed by the activation of their receptors C3aR and C5aR (Ember and Hugli, 1997). Moreover, hepatic CD14 expression is increased in various liver diseases (Su, 2002). Signaling through TLR4 requires MD-2, a secreted protein closely linked to the extracellular domain of TLR4. Downstream of TLR4, signaling occurs via MyD88, which associates with the interleukin1 receptor-associated kinase (IRAK) and TNF-activated factor 6

(TRAF-6). TRAF-6 mediated signaling pathways activate NF-κB, which results in the production of proinflammatory cytokines (Akira et al., 2001). As KC eliminate activated neutrophils they suppress their production of toxic metabolic compounds and degradative enzymes. Thus, activation of KC is necessary for the optimal regenerative ability of the liver. Hepatocyte proliferation *in vivo*, at least in part, occurs through NF-κB and STAT3. The respective events have been shown to be triggered by leukocyte-KC interaction under the mediation of the intracellular adhesion molecule ICAM-1 (Selzner et al., 2003) as livers from ICAM-1-deficient mice exhibited impaired regenerative capacitiy after 70% hepatectomy, which was paralleled by a dramatic decrease in leukocyte recruitment and tissue TNF and IL levels. Taken together, KC are intimately involved in the hepatic response to various damaging insults.

1.3.1.1.4 Hepatic stellate cells

Hepatic stellate cells (HSC) are located along the sinusoids and they form the space of Disse as they are lying in close proximity to the hepatocytes as well as to the sinusoidal endothelium. The whole microcirculatory network is covered by the HSC although they just constitute about 5 - 8 % of the entire liver cell number. This cell type is important as it is potentially involved in the fibrogenic transformation of liver tissue following chronic injury. Because of their anatomical location, ultrastructural features, and similarities with pericytes regulating blood flow in other organs, HSC have been functionally described as liver-specific pericytes. The most evident ultrastructural feature of HSC in normal adult liver is the presence of cytoplasmic lipid droplets ranging in diameter from 1 to 2 μm. These lipid droplets are involved in the hepatic storage of retinyl esters, indicating the storage of retinoids by HSC (Blomhoff and Wake, 1991). Interestingly, after prolonged culture on plastic, HSC undergo activation from a quiescent "storing" phenotype to a highly proliferative "myofibroblast-like" phenotype. The activated phenotype is characterized by a dramatically increased synthesis of collagen types I and III, which appears predominant over the synthesis of collagen type IV and other ECM components. Various soluble factors, including growth factors, cytokines, chemokines and oxidative stress products, have been reported to influence the activation of HSC. After activation of stallate cells into myofibroblasts due to tissue injury, they start to proliferate and contribute to scarring, fibrosis or cirrhosis.

1.3.1.1.5 Hepatic sinusoidal endothelial cells

Hepatic sinusoidal endothelial cells (HSEC) are a morphologically distinct cell population that lines the liver sinusoids. Features that distinguish HSEC from endothelial cells in other organs and in larger hepatic vessels are the presence of multiple fenestrae throughout the cells and the lack of an underlying basement membrane. The sinusoids are located between hepatocyte plates and they start at the portal tract and terminate at the central vein. The sinusoids are separated from the adjacent hepatocytes by the perisinusoidal space, termed the space of Disse. HSEC are the first cells in contact with blood flow into the sinusoids and serve to compartmentalize the vascular sinusoidal channels from the hepatic parenchyma. As

they are smaller than red and white blood cells, there is distortion of both cell types and the sinusoids during passage of blood cells (Fraser et al., 1995). This process has been referred to as "endothelial massage", which allows efficient exchange of compounds from the blood through sinusoidal fenestrae into the space of Disse.

1.3.2 Liver cell injury

Obligate primary liver toxins usually induce liver cell necrosis at the periphery of the liver lobes (Rappaport zone 1), while secondary liver toxins cause areas of necrosis mainly in the centre of the liver lobes (Rappaport zone 3). This is due to higher transformation activity of liver cells in the centre of the liver lobe where more toxic products originate from. Examples of primary liver toxins are the yellow phosphorus, the secondary liver toxin carbon tetrachloride or amanita poisons. The toxins cause coagulation necrosis. No or mild inflammation is present. Fulminant hepatitis courses are found with 0.1-1% of the HBV infections. They frequently occur with concurrent HDV infection (2 - 20%). With HCV infections fulminant hepatitis is very rare.

1.3.2.1 Cholestasis

The term cholestasis can be defined in different ways. In general, it describes the disturbance of the bile outflow. The causes can lie within the liver cells themselves, therefore termed intrahepatic non-mechanical cholestasis or an impediment of the bile flow can be due to alterations in the intrahepatic bile ducts, named intrahepatic mechanical cholestasis. Alternatively, the cause for cholaestasis can also lie outside the liver, this is the so called extrahepatic cholestasis. From a morphological point of view cholestasis means the retention of bilious pigment in the liver cells (intracytoplasmic bilious pigment) and in the bile ducts as bile thrombi. Also, the simple stagnation of the bile flow can be called cholestasis. Clinically, the retention of substances ordinarily eliminated via the bile in blood and tissues are also called cholestasis. Several molecular defects of bile secretion cause cholestasis. Mutations of certain transport systems can lead to innate, autosomal recessive inherited syndromes of cholestasis like progressive informal intrahepatic cholestasis (PFIC). It is worth mentioning that the different PFIC-subtypes are assigned to different transport defects. Mutations of the bilirubin-export pump (multidrug resistance-related protein, MRP2) are responsible for the Dubin Johnson syndrome which is marked by a disturbed secretion of conjugated bilirubin and an unusually high concentration of other organic conjugates. Although up to now still no mutations of the drug-export pump (multidrug resistance protein 1, MDR1) have been described, these could be responsible for drug induced types of cholestasis, particularly as a disturbed elimination of drugs could lead to the intracellular accumulation in hepatocytes and secondary inhibition of other canalicular transport systems. The latter proteins are particularly of interest as *mdr2*$^{-/-}$ mice display a phenotype characterized by cholestatic hepatitis (Pikarsky et al., 2004). Extrahepatic cholestasis occurs as a result of a mechanical bilious drain obstacle beyond the liver (gallstones, tumors of the cystic duct, the papilla Vateri,

the pancreas, enlarged lymph nodes in the liver gate, inflammatory swelling of the head of the pancreas, bile duct stricture with scars and extrahepatic bile duct atresia). Above the obstruction the cystic ducts are extended. Bacterial infections are favored by the biliary holdup with development of a cholangitis. The morphology is similar in intra- and extrahepatic cholestasis, irrespective of the cause. The morphologically detectable effects of cholestasis arise from the retention of toxic bilious components, in particular from bilirubin and bile acids. Deposits of bilirubin can be detected in hepatocytes and KC as well as bile thrombi in bile canaliculi. These changes predominate in the early phases of the cholestasis in the central segment of the liver acini (Rappaport zone 3) and extend then towards the periphery (Rappaport zone 1). With more distinctive liver cell damage a net-like change of the cytoplasm in the firm of a so called net degeneration or fedory degeneration develops with time. Vaster necroses are termed bilious infarcts. Consequently, at the periphery of the liver lobes bile ductuli can start to proliferate. Periductal fibrotic changes, lengthening and serpentiform alterations of bile ducts, the so called cystic duct proliferation as well as the development of fibrous septae are often the result of a secondary inflammation. The secondary biliary cirrhosis is also a typical complication of the bile duct atresia. Clinically, hyperbilirubinemia often manifests as ikterus (jaundice). A rise of the bilirubin concentration in the blood at more than 1 mg/dl is called subikterus, more than 2 mg/dl as an ikterus. An ikterus appears clinically in a yellow color of the sklerae first, then of the skin, the body liquids as well as the inner organs. With respect to the pathogenesis different types of ikterus can be distinguished including the prehepatic, intrahepatic and posthepatic causes of hyperbilirubinemia.

1.3.3 General mechanisms of hepatitis

Inflammatory liver disorders can affect the liver parenchyma as hepatitis, the intrahepatic bile duct system as cholangitis or vessels. In addition to toxic agents, metabolic disturbances and immunological reactions, various possible causes (viruses, bacteria, mushrooms, parasites) are known to account for these disorders. The acute viral hepatitis is of high social importance as the number of new infections is very high (Wasley et al., 2007). The lethality of the acute illness is low. The acute viral hepatitis is marked by liver cell degeneration, liver cell necrosis, Kupffer cell proliferation, inflammatory infiltrates and does not continue longer than 6 months. Beside the classical hepatitis viruses (hepatotropic viruses), namely hepatitis A virus (HAV), hepatitis B virus (HBV), hepatitis C virus (HCV), hepatitis D virus (HDV) and hepatitis E virus (HEV), a list of other causes (e.g., Epstein Barr virus, yellow fever virus, Cytomegaly virus) is able to cause hepatits. Surprisingly, the different hepatitis viruses cause a similar clinical and morphological picture, although they belong to different virus families. Whether the hepatitis G virus (HGV) also concerns a hepatotropic virus with primary replication in the liver is still under debate.

1.3.4 Virus induced hepatitis

Viruses can cause either acute or chronic hepatitis. A chronic viral hepatitis lasts longer than 6 months and shows more or less distinctive clinical symptoms. As the most frequent causes, the hepatitis virus B, which

frequently occurs in combination with hepatitis D, and C can be named. Approximately 5-10% of the patients with acute hepatitis B develop a chronic HBV infection. Risk groups for chronic HBV infection are people with immune defects (e.g. dialysis patients, newborns, immunocompromised patients after transplantation), homosexuals, drug dependent and cognitively disabled persons (e.g. Down's syndrome). The HDV infection is bound to a concurrent HBV infection and HBV acts as "an assistant virus". The HCV infection leads in approximately 80% of the cases to chronic hepatitis. Positive virus carrier status is observed in about 1-2% of clinically healthy individuals in the population. The course of the chronic hepatitis C is usually made worse by alcoholism. With HBV-induced chronic hepatitis the liver cell damage decreases predominantly due to the effect of cytotoxic $CD8^+$ T-lymphocytes which are directed against cell membrane associated viral antigens (in association with HLA-class-I-molecules). A chronic infection results from an insufficiency of the immunological elimination mechanisms. Morphologically, in the light form of chronic hepatitis, lymphocytic infiltrates are limited to the main entrance field. The parenchymal border plate remains intact. Liver cell necroses and inflammatory infiltrates in the liver lobes are discrete. In HBV associated cases hepatocytes with milk-glassy homogenised cytoplasm ("milk glass cells") can be seen. These cytoplasmic changes correspond to increased SER. In these cells, the presence of HBsAg and often also HBcAg can be shown by immunhistochemistry. A reliable distinction between B and C hepatitis based on the light-microscopic picture is not possible while specific features are suggestive of the underlying cause. However, milk glass cells are absent in hepatitis C, while steatosis, cystic duct changes with irregular, several cell layers thick epithelium and lymphatic follicles are frequently found in the main entrance fields. In the severe form of chronic hepatitis lymphohistiocytic inflammation is seen in addition to the main entrance field inflammation in which also more or less plasma cells are detected in the liver lobes. Thereby the so called border zone hepatitis or interface hepatitis which esentially represents apoptosis of the liver cells at the parenchymal border plate is generated. Single cell degeneration with apoptosis, hepatocyte ballooning and lytic necrosis is found in irregular distribution, accompanied by activated KC, in form of so called KC nodule and lymphocytic infiltrates. In clinically severe courses, also confluent and bridge-forming necrosis can be seen. In addition, often fibrosis with formation of liver septae and, finally, in approximately 20-50% destruction of liver lobes occurs. This manifests as liver cirrhosis. Clinicopathological correlations with clinically asymptomatic HBV bearers found a regular liver architecture in 75% of the patients without inflammatory changes. The rest regularly shows minimum hepatitis or a chronic hepatitis with different activity stages. Most patients with chronic hepatitis B are free of pain. Laboratory-diagnostics of blood from most patients display a mild elevation of aminotransferase levels. A part of the cases heals; a low percentage can pass into a severe chronic hepatitis. Patients suffering from a highly active chronic hepatitis B mention variable complains picture with decreased power, loss of appetite, steady elevation of aminotransferase levels and occasional ikterus (Mellen et al., 2009). Liver biopsies, as they were used in the presented work, are required for defining the entity one is dealing with, to control the illness course and the therapy efficiency. About 20-50% of all chronically infected patients develop liver cirrhosis within 5-10 years. Only in few patients the HBV is eliminated in the course of time. Chronic hepatitis D resembles chronic hepatitis B, however, shows often a heavier course. Chronic hepatitis

C is a progressive liver illness and, however, a statement about the course of the illness is difficult in many cases. After many years' course liver cirrhosis often develops. There is a correlation between progression and the degree of histologically provable inflammation and fibrosis in the liver. Stop of alcohol consumption is extremely important as alcohol accelerates the cirrhotic process. The autoimmune hepatitis is often accompanied by a distinctive clinical symptomatology with tiredness, feeling of sickness, appetite loss, fever, joint pains, and the illness often starts with an acute hepatitis. Primarily women (about 80%) are affected before the 30th year or in the menopause. The illness is often accompamied by endocrinological disturbances and extrahepatic autoimmune phenomena like thyreoiditis, vasculitis, colitis, anaemia or urtikaria. The aminotransferase levels are steady, while the inflammatory boosts raises. The appearance of antinuclear antibodies (ANA), antibodies against smooth muscle actin and of antibodies against mikrosomal antigens and against cytosolic proteins is regularly observed. The illness has untreated a bad prognosis. Hence, untimely diagnosis and immunsuppressive treatment are of great importance (Fernandez Rodriguez and Alonso Lopez, 2009).

1.3.4.1 Hepatitis B Virus

The main cause of HCC worldwide is HBV. HBV is an enveloped hepatotropic DNA virus causing several liver diseases such as acute to chronic hepatitis, cirrhosis and HCC. During prolonged infection, viral DNA sequences integrate into the host genome, causing mutations, chromosomal instability and general genomic rearrangements. The genome of HBV is a circular, partially double-stranded DNA molecule and it is characterized by its four overlapping open reading frames (ORF) that encode for surface (S), core (C), polymerase (P) and X proteins (HBx). The expression of viral genes, in particular genes encoding for HBx, may deregulate the control of cellular growth and viability and sensitize hepatocytes to exogenous and endogenous carcinogens (Wu et al., 2001). The oncogenic capacity of HBx is a result of the fact that some of the genes activated by HBx, such as ICAM-1 (Hu et al., 1992), c-myc (Terradillos et al., 1997) and c-fos (Avantaggiati et al., 1993), are important for cell adhesion and proliferation.

The frequency of virus carriers is especially high in South-East Asia and Africa while in Central Europe and Northern Europe only approximately 0,1-0,5%, in Africa and Asia up to 15% of the population are infected with HBV. The transfer of the virus occurs through blood and blood products as well as through saliva, seminal liquid, vaginal secretion, mother's milk and other body liquids. The "vertical" transfer from the mother to the child, usually during birth, also plays an important role. The transfer by blood and blood products during transfusions today has drastically decreased due to the regular testing for HBsAg of donated blood products.

HBV is not or only mildly cytopathic. However, the destruction of virus-infected liver cells seems to occur about a cellular immunological reaction against cell surface antigens dependent on the virus. After infection with HBV in 20-30% of the cases an acute and in approximately 60% a subclinical course is observed. In most cases spontaneous healing occurs. Through cell destruction acute hepatitis leads to virus elimination,

and is therefore selflimiting.

1.3.4.2 Hepatitis C Virus

The HCV is a linear single-phase RNA virus. It counts to the family of the Flaviviridae. HCV is transferred by blood and blood products and is responsible for approximately 80% of the earlier so called Non-A-Non-B-hepatitis forms. Antibodies against HCV appear in blood circulation 1-3 months after onset of the acute illness. The virus is found in a low concentration in blood and can be diagnosed by means of PCR. The RNA genome encodes three structural proteins like core and cover proteins and four enzymes which are necessary for the virus replication. The virus shows a distinctive genetic instability with a high mutation rate. Currently it is calculated that in the USA alone, nearly 4 million HCV infected individuals, many of which appear to be clinically healthy virus carriers. This represents a major health issue as infection maybe spread by intravenous drug abuse and dialysis treatment.

After an incubation time of approximately two months only to 15-20% of the cases develop an acute ikteric illness which is similar to hepatitis B. However, the spontaneous healing is very limited, with only about 15-20% of the infected population. The majority will develop a chronic course and a chronic virus carrier's status. The trend towards development of a chronic course after acute hepatitis is high and remains at approximately 80%. Of this approximately 20% spontaneously develop liver cirrhosis. At a later stage HCC can develop in the cirrhotic liver. Currently, the therapy of choice is interferon α for both, acute as well as chronic hepatitis C.

1.3.5 Non virus induced hepatitis

Non-virus related liver diseases with hepatitis include alcoholic steatohepatitis (ASH), cholestasis (CH), which is also frequently associated with inflammation, primary biliary cirrhosis/autoimmune cholangitis (PBC), end stage liver cirrhosis due to alcoholic liver disease (CIR), α1-antitrypsin deficiency (α1-AT) and focal liver fibrosis (FLF).

1.3.5.1 Primary biliary cirrhosis / Autoimmune hepatitis

Autoimmune hepatitis accounts for 5-20% of all chronic hepatitis cases. It appears preferentially in women at a younger age and after menopause (women: men = 8: 1). It is associated with hypergammaglobulinemia, HLA-B8- and -DR3-status and circulating autoantibodies (anti-actin antibody, antinuclear and other antibodies). In PBC a T-cell attack against hepatocellular membrane antigens is the underlying pathomechanism. Besides, a suppressor-T-cell-defect also seems to play a role. Also a cellular cytotoxicity dependent on antibodies is involved and the autoimmune attack could be initiated by viral infection. In drug induced chronic hepatitis immune phenomena could also be involved. HCC often complicates PBC, in

which copper accumulates in the liver (Melia et al., 1984; Nakanuma et al., 1990).

1.3.5.2 Alcoholic hepatitis

Mallory bodies, intracytoplasmic irregular inclusions, occur in HCC cells of alcoholic and non-alcoholic patients alike (Nakanuma and Ohta, 1985, 1986) as they do also in liver-cell adenomas (Malatjalian and Graham, 1982). This observation suggests a link in the pathogenesis of alcoholic liver disease and of liver cancer. Alcoholic hepatitis or nutritional and toxically induced steatohepatitis is histologically characterized predominantly by necrosis in the centre of the liver lobes. It is accompanied by neutrophilic infiltrates and the appearance of Mallory-Denk bodies or alcoholic hyalin and enlarged, balloned hepatocytes. The Mallory bodies show a filamentous ultrastructure and contain unusual keratin, but also non-keratin derived components like Ubiquitin. In a rather high percentage of patients distinctive signs of cholestasis are also found. The often co-existing fatty liver does not correlate with the severity of the alcoholic hepatitis. Fibrotic changes also occur frequently. However, the morphological changes are not specific for alcohol and can occur in the setting of morbid obesity, type-II-diabetes-mellitus, Wilson`s disease, various metabolic illnesses or induced by drugs that lead to liver damage.

The prognosis of alcoholic hepatitis depends on the gravity of liver cell damage. The lethality rate reaches 30%. With abstinence from alcohol consumption alcoholic hepatitis is reversible. However, often residual damaged foci remain. With continuous alcohol abuse a rather high percentage of approximately 30% of the patients with alcoholic hepatitis develop liver cirrhosis in a relatively short time, mostly within 1-2 years

1.3.5.3 Non alcoholic steatohepatitis

Non-alcoholic steatohepatitis (NASH) has gained increasing interest as it is the most severe form of non-alcoholic fatty liver disease (NAFLD), characterized by the presence of macrovesicular steatosis along with inflammatory activity, and sometimes associated with fibrosis. The molecular mechanisms involved in tissue damage during NASH are poorly understood. However, it has recently been demonstrated that Fas expression, activation of caspase-3 and -7 and hepatocyte apoptosis are enhanced in the liver of NASH patients, and positively correlated with the biochemical and histopathologic markers of liver injury (Feldstein et al., 2003a; Feldstein et al., 2003b). Mitochondrial function is often impaired in the liver of subjects with NASH (Perez-Carreras et al., 2003). Activation of Fas results in mitochondrial dysfunction which is associated with generation of reactive oxygen species, which are able to induce apoptosis, further exacerbating tissue injury and inflammation. Thus, Fas inhibition may be an effective therapy to reduce liver damage and prevent development of cirrhosis in NASH.

1.3.6 Other non virus related liver disorders

Non-virus related liver diseases without hepatitis include steatosis (ST), hemochromatosis / siderosis (HE/SID), and Wilson's disease (WD) while it has to be mentioned that in all of these diseases inflammation, to various degree, may also occur. Especially iron and copper storage is often paralleled by drastic inflammation. Focal nodular hyperplasia (FNH) represents a benign primary liver tumor. Diseases such as α1AT (●), FLF (▲), HE/SID (•), and WD (Δ) are listed under "other liver diseases" (OLD) in the experimental chapter.

1.3.6.1 Steatosis hepatis

The content of lipids in the normal liver amounts to approximately 5% of the liver weight. In fatty liver disease a prevailing accumulation of triglycerides can be observed. The lipid content increases to 40-50% of the liver weight under these conditions. The fatty liver is a frequent finding in liver biopsies. The underlying disturbance of the fat metabolism determines the clinical picture. The morphology proves the definitive diagnosis. The fatty liver is reversible with discontinuation of the causing agent. However, this can be the starting point for a progressive liver disorder e.g. alcoholic hepatitis or NASH. Fatty acids are taken up by the hepatocyte from blood and are converted partly again into triglycerides, are used partly for the synthesis of cholesterol and phospholipids. They are also oxidized in part. Besides, fatty acids can also originate in the liver. The triglyceride synthesis of free fatty acids can be supported by the gylcolysis and the formation of gylcerine. The fatty liver is based on a disturbance of the fatty acid and triglyceride metabolism. Fat storage "per se" does not lead to liver cirrhosis.

1.3.6.2 Hemochromatosis / Liver siderosis

Hereditary hemochromatosis is an autosomal recessive disorder. The responsible HFE-gene has been located on the short arm of chromosome 6. A single G to A mutation, resulting in a cysteine to tyrosine substitution (C282Y) is the cause for most cases. The genetic defect leads to iron accumulation in the liver, resulting in a progression to liver cirrhosis. Males are predominantly affected (Crawford et al., 1998; Niederau et al., 1999). The risk to develop HCC on the basis of hemochromatosis is high. An association with additional risk factors such as alcohol consumption and chronic infection with HBV and HCV has been reported (Fargion et al., 1994). Of note, proliferative, frequently dysplastic iron-free areas of liver cells are present in most cases before HCC develop (Deugnier et al., 1993). The treatment of hemochromatosis remains symptomatic with phlebotomy as an effective therapy.

1.3.6.3 Wilson`s disease

Large amounts of copper accumulate in Wilson's disease, which is an autosomal recessively inherited

disease that tends to affect males and frequently results in liver cirrhosis (Cheng et al., 1992).

1.3.6.4 α1-Antitrypsin deficiency

α1AT is an inhibitor of serine proteinases. It is synthesized in hepatocytes and secreted into the blood stream. The pattern of inheritance of α1-Antitrypsin (α1AT) deficiency is complex and is under the control of Pi (protease inhibitor) genes. α1AT deficiency leads to the accumulation of PAS-positive, diastase-resistant globules that consist of α1AT. The disease is associated with neonatal jaundice and cirrhosis in early childhood, with pulmonary emphysema and liver cirrhosis in adult life (Rubel et al., 1982).

1.3.6.5 Liver fibrosis and cirrhosis

Liver fibrosis means connective tissue increase in liver which can be proven in an objective manner by chemical regulation of the whole collagen content. The normal lobular liver architecture is still, at least partially, protected. During fibrogenesis collagen type I is increasingly deposited by activated stellate cells. Morphologically one can divide liver fibrosis into portal fibrosis, perisinusoidal fibrosis, central pericellular or perivenular fibrosis or in fibrosis affecting the periphery of the liver lobes (periportal fibrosis). Many chronic liver disorders lead to liver fibrosis as the primary disorders are accompanied by inflammation. Certain substances (e.g., alcohol, acetic aldehyde, iron) can directly stimulate the collagen synthesis. The responsible mechanisms seem to be quite complicated. Various cytokines (TNF-α, TGF-β) are involved as stimuli of the collagen synthesis. The development of the fibrosis stands in relationship with duration and gravity degree of the damage. The duration of the development of liver fibrosis is variable. Liver cirrhosis, also termed liver fibrosis stage IV, is a final stage of various severe inflammatory and necrotizing liver damages with soft tisssue production. Thereby the normal liver architecture is lost. Most HCC arise in cirrhotic livers though the proportion varies. The pattern of cirrhosis tends to be macronodular and inactive in chronic alcoholic patients and in HBV infected patients whereas it is frequently micronodular and active in HCV-related cases (Takenaka et al., 1995).

1.3.7 Human liver tumors

In clinical practice, a wide variety of benign and malignant lesions present as hepatic masses and are subjected to needle biopsy. For practical purposes, these lesions can be broadly classified into: (1) clearly hepatocytic and malignant; (2) clearly hepatocytic and of uncertain clinical nature and malignant potential; (3) clearly malignant and of uncertain lineage; and (4) neither clearly hepatocellular nor malignant. The diagnostic approach to each of these requires integration of clinical, laboratory and imaging data. Work-up usually requires histochemical and immunohistochemical stains. Liver biopsies are generated by percutaneous, transjugular, laparoscopic or open surgical routes, with or without imaging guidance. Recent

advances in imaging techniques allow better distinction among these lesions. However, diagnostic challenges are often encountered in clinical practice. In general, liver biopsies are assigned to one of three categories, based on the clinical indication: (1) medical disorders, (2) tumor evaluation, and (3) post-transplant biopsy. In many laboratories routinely, nine initial sections from the paraffin block are obtained, and levels 1, 3 and 7 are stained with H&E. Sections from biopsies for evaluation of medical disorders are stained with trichrome, reticulin, Berlin blue and diastase with periodic acid-Schiff reaction (DPAS) stains. For other categories, the unstained sections are held for stains that are determined after evaluating the HE-stained sections.

Mass lesions found in liver biobsies (Table 1) can be classified into four categories. The first category consists of lesions that are clearly hepatocytic in nature and appear malignant. This is represented largely by well to moderately differentiated HCC. The second category includes lesions that are well differentiated and clearly hepatocytic in nature, and the diagnostic issue is the clinical nature and potential malignant behavior. This category includes regenerative nodules, dysplastic nodules (DN), FNH, hepatic adenoma (HA) and well differentiated HCC. The third category includes lesions that clearly appear malignant, and the diagnostic issue is the lineage of the neoplasm, e.g. HCC versus non-hepatocytic tumor, such as CCC, other primary liver tumors and metastases. The last category is composed of a very small number of cases that do not belong to any of these well-defined categories, and appear neither clearly hepatocellular nor clearly malignant.

The number of people affected by liver masses in Africa and South-East Asia is large, over one million per year. Numerous studies indicate that the marked geographical variability in incidence is due to just one tumor type, namely HCC, which predominates in tropical Africa and South-East Asia but also in other regions of the world. Intrahepatic duct carcinoma is the next commonest. It occurs with approximately the same frequency everywhere, except in South East Asia where its high incidence is clearly associated with liver fluke infestation.

All other liver tumor types are rare. Overall, liver cancer ranks eighth in frequency in the world (sixth among men and eleventh among women). In general, the outlook for malignant hepatobiliary tumors is extremely poor. Epidemiological and etiologic aspects of liver tumors have been largely reported (Bosch et al., 1999; Okuda, 1997).

Table 1: The following tumor entities in liver are known:

Benign epithelial tumors	Malignant epithelial tumors	Benign non-epithelial tumors	Malignant non-epithelial tumors	Tumor-like lesions
Hepatocellular adenoma	Hepatocellular carcinoma	Hemangioma	Rare primary tumors	Various reactive conditions
Bile-duct adenoma	Hepatoblastoma	Angiomyolipoma	Metastatic tumors	
Bile-duct cystadenoma	Bile-duct carcinoma (cholangiocellular carcinoma)	Other benign tumors	Hemangiosarcoma	
Biliary papillomatosis	Bile-duct cystadenocarcinoma		Epithelioid hemangioendothelioma	
	Mixed liver-cell and bile-duct carcinoma		Embryonal sarcoma	
	Sarcomatoid, hepatoid and other malignant epithelial tumors		Rhabdomyosarcoma	
	Combined and mixed carcinomas		Other sarcomas, lyrnphomas or germ-cell tumors	

1.3.7.1 Focal nodular hyperplasia

This lesion occurs in both sexes and at all ages but most commonly in young adult women. Most of them are discovered incidentally and only about 15% cause symptoms, usually recognized as a mass or upper abdominal pain. Rupture and hemoperitoneum are rare. Focal nodular hyperplasia (FNH) is usually solitary, around 5 cm in size and typically forms a well-circumscribed fibrous globular mass. It tends to bulge on its cut surface and displays multiple yellow-brown nodules of liver parenchyma separated by fibrous septs. Histologically, it resembles cirrhosis except that the lesion occurs focally and the rest of the liver is normal. A central stellate scar is often seen and may contain thick-walled vessels. A mild to moderate lymphocytic infiltrate is present in the septs. Whether or not this condition is related to oral contraceptive use and pregnancy has been debated for years but the evidence speaks against it. Gonadal steroids and pregnancy may, however, increase the vascularity of the lesion and predispose it to rupture. It has been suggested that FNH is essentially a vascular malformation with arteriovenous anastomoses and localized overgrowth of all liver constituents. Its polyclonal nature has been confirmed by chromosome studies. Most patients are treated conservatively and surgery is only necessary for those with symptoms.

1.3.7.2 Hepatocellular carcinoma

HCC represents the most frequent, aggressive hepatocyte driven tumor with poor prognosis. Its occurrence is known to be related to chronic hepatitis B and C virus infections and exposure to aflatoxin. Genetic factors have been shown not to be of significant importance.

The macroscopic and microscopic appearances of HCC have been described in detail over the years and criteria for diagnosis and nomenclature have been defined many times (Okuda, 1997). Classifications (Yuki et al., 1990) have divided liver-cell carcinomas into infiltrative or expansive, single or multinodular, and mixed types with observations on encapsulation, intrahepatic venous spread and special subtypes. HCC form soft, haemorrhagic, occasionally bile-stained nodules and masses with a tendency to necrosis. As HCC have an arterial blood supply but both the hepatic and portal veins proliferate alongside and cavernous structures develop in collaterals (Terada et al., 1989) intra- and extrahepatic spread can take place to all parts of the liver (Toyosaka et al., 1996), hepatic veins, inferior vena cava, right atrium (Kojiro et al., 1984) and the portal system. The likelihood of HCC for local intravascular spread has been noted for many years but distant metastases may not occur until quite late.

HCC microscopically show broadening of liver cell cords, loss of reticulin fiber networks and increased proliferation rates of hepatocytes. HCC are characterized by cellular pleomorphism with often huge and multiple bizarre hepatocyte nuclei. These are seldom numerous but at times occupy large areas and form solid masses; in some instances. Then the trabecular or plate-like growth pattern is almost or completely lost. Clear cells can predominate but are usually still arranged in cords separated by sinusoids. The clarity of the cytoplasm is most often due to massive glycogen storage. Sometimes it can be also due to water or fat. An oncocytic appearance is characteristic for the fibrolamellar variant of liver-cell carcinoma. Such cells, containing numerous mitochondria can also be seen in small numbers in otherwise ordinary HCC.

Pedunculated liver-cell carcinoma

The pedunculated liver-cell carcinoma does not greatly differ from an ordinary HCC with regard to age and sex distribution, association with cirrhosis and chronic HBV infection, production of AFP and microscopic appearances. The main characteristics are a small size, ranging from 2 to 3 cm, slow growth, fibrous encapsulation, an almost invariable association with cirrhosis, low prevalence of HBV infection and serum levels of AFP usually below the level of 500ng/ml. The histological features do not differ from those of 'ordinary' HCC except for the fact that these tumors usually appear well differentiated.

Fibrolammelar liver-cell carcinoma

The fibrolamellar carcinoma differs in most aspects from common HCC yet it is of liver-cell origin and malignant. Fibrolamellar carcinomas often occur under 35 years of age and less than 5% over the age of 50. Very rarely, cases have been described in patients aged 70 - 85 years (Hodgson, 1987). There is no gender

disparity or association with cirrhosis. Patients present with abdominal pain, malaise and weight loss. Serum AFP is seldom raised and less than 10% of patients show evidence of HBV or HCV infection. Jaudice does not occur in most cases. In rare cases, an elevated level of CEA has been reported.

Fibrolamellar carcinomas are usually solitary and often large, 5-25 cm in size and can weigh up to 1000g. The surgical resectability rate is high. Multiple tumors may still be cured by hepatectomy and transplantation (Pinna et al., 1997; Ringe et al., 1992; Schlitt et al., 1999). The 5-year survival rate recorded in large series has been around 50% and progress is slow even when the tumor has not been completely eradicated. Tumor cells are large, eosinophilic and polygonal, with vesicular nuclei and prominent, usually single, nucleoli.

1.3.8 Epidemiology on human hepatitis and hepatocellular tumorigenesis

The highest rates of all HCC cases are seen in South-East Asia and tropical Africa where frequencies have been estimated to be up to 150/100.000/year. In these areas, the tumor is the commonest or next commonest in the list of all cancers. The lowest rates are found in Western countries, South America and Australia. Intermediate rates prevail in Japan, the Middle East and the Mediterranean countries (Simonetti et al., 1991). The possible role of racial and genetic factors has been extensively studied but discounted in favor of environmental agents.

Variation in incidence might be explained by differences in alcohol consumption and smoking. In the latter, it may be related to variable levels of exposure to aflatoxins (Omata, 1987). The relationships between HCC and viral infections, chemical substances, hormones, alcoholism, nutrition and presence or absence of cirrhosis were investigated in detail (Kaldor and Bosch, 1990; Okuda, 1992). The incidence of HCC increases with age in all populations but there is a tendency for it to fall off in the elderly. Overall, the age peak is inversely related to the frequency of the tumor, patients being the youngest in high and the oldest in low incidence areas. A male to female predominance is observed everywhere and ranges from 4:1 in low to 8:1 in high incidence areas. Malnutrition is common in most areas with a high HCC incidence but so are hepatitis B and C virus infections and exposure to hepatotoxic agents. Existing knowledge on diet and cancer indicates that it is over-nourishment, rather than lack of calories or deficiency of protein, that promotes tumor development (Willett and MacMahon, 1984). Epidemiological reports indicate a relationship between high dietary fat, cholesterol, obesity and carcinomas of the breast and endometrium in women, carcinoma of the prostate in men, and carcinomas of the colon and pancreas in both sexes. In one study from Japan, inadequate and unbalanced nutritional intake were more common in patients with cirrhosis and HCC than in the general population but it was unclear whether this was based on a causal relationship. HCC incidence was also correlated to various substances that have been found in drinking water, foodstuffs and native remedies (Willett and MacMahon, 1984). Most of them are simply suspected to carry carcinogenic potential. Aflatoxins induce acute liver necrosis, dysplasia and HCC in man and animals (Ross et al., 1992). Other mycotoxins are less efficient inducers of HCC. Chronic alcohol abuse frequently

leads to cirrhosis and HCC, particularly in low incidence areas where hepatitis B and C virus infections are uncommon (MacSween, 1982; MacSween and Anthony, 1982). Alcohol might act as a co-carcinogen with hepatitis B and C virus infections, aflatoxins and smoking, in addition to its general role as a cirrhosis-inducing agent.

It is certain that continued alcohol consumption is not necessary for the development of HCC once cirrhosis is established and the risk actually increases with time after cessation of drinking (Lee, 1966). Currently, the incidence of HCC is rising in Western countries and in Japan (Akriviadis et al., 1998; Omata, 1987; Simonetti et al., 1991). The reasons are not entirely clear but the spread of chronic hepatitis C infection is most probably the cause. To sum it up, risk factors in all parts of the world are male sex, age and cirrhosis (Simonetti et al., 1991).

1.3.9 Murine HCC models

Chemically induced HCC mice models mimic the injury-fibrosis-malignancy cycle by administration of a genotoxic compound alone or, if necessary, followed by a promoting agent. In xenograft models, the tumor nodules are generated by injecting human cancer cells from a lab culture into immune deficient mice (Heindryckx et al., 2009). Alternatively, transgenic mice can be used as model system. Promotion of HCC formation by chronic inflammatory stimuli has been recapitulated in various models. Ablation of the multi-drug resistance gene 2 (*mdr2*) induces cholestatic hepatitis and liver cancer (Pikarsky et al., 2004) and administration of the chemical carcinogen diethylnitrosamine (DEN) causes acute liver injury and HCC (Maeda et al., 2005). Liver specific expression of the hepatitis B surface antigen (HBsAg) in transgenic mice demonstrates that chronic immune-mediated liver cell injury is critical for HCC formation (Nakamoto et al., 1998). In various animal models a gender disparity has been observed as apparently experimental liver tumors are more easily induced in males than in females. Moreover, orchiectomy reduces the carcinogenic effect of chemicals in male rodents to the level found in females. It is very unlikely that sex steroids are carcinogenic by themselves but they might possibly promote tumor growth (Carr and Van Thiel, 1990; Eagon et al., 1985; Ohnishi et al., 1986; Porter et al., 1987). Chemically induced models include several compounds that induce tumor formation when administered in sufficiently high doses. DEN is often used as a carcinogenic substance as it can alkylate DNA and thereby induces hepatocarcinogenesis. Reactive oxygen species (ROS) generated by the P450-dependent enzymatic system might induce oxidative stress by the formation of hydrogen peroxide and superoxide anions. Production of ROS is known to cause DNA, protein and lipid damage. Therefore, oxidative stress most probably plays an important role in liver carcinogenesis (Heindryckx et al., 2009). Tumors in mice that have been induced by DEN harbor activating mutations in the H-ras proto-oncogene. These are rarely seen in humans and they correlate with metastasis and poor prognosis. After a long-term repetitive administration of DEN, 100% of male mice and 30% of female mice develop HCC. DEN can be used as an initiator and phenobarbital (PB) as a promoting agent. PB can increase the expression of cytochrome P450 a 100-fold, supporting an enhanced effect of DEN

(Waxman and Azaroff, 1992). Promotion with PB leads to tumors that exhibit mutations in the β-catenin proto-oncogene (Loeppen et al., 2002). β-catenin mutations are associated with non-invasive tumors and a significantly higher 5-year survival rate in humans. Aflatoxin B1 (AFB) is also used as inducer of HCC in mice (Ghebranious and Sell, 1998; Heindryckx et al., 2009). Carbon tetrachloride (CCl4) is a very potent hepatotoxin. Mice subjected to a long-term choline deficient ethionine supplemented (CDE) diet develop HCC at the age of 50–52 weeks (Knight et al., 2000). The proposed mechanism of carcinogenicity by CDE diet is through the formation of oval cells, which are believed to represent the precursors of hepatocytes. Thioacetamide (TAA) is an additional hepatotoxin. Its repeated administration over a period of 10–15 weeks results in liver fibrosis in mice (Heindryckx et al., 2009).

Different aspects of HBV-induced hepatocarcinogenesis have been investigated by generating transgenic mice expressing complete fragments of the HBV genome, under control of either the HBV promoter, or constitutive (mouse albumin) or inducible (mouse metallothionein) liver-specific promoters. The first HBV-related transgenic mouse model were generated in 1985 (Chisari et al., 1985). Others followed (Koo et al., 2005). Transgenic lineages with lower HBx copy number showed lower tumor incidence comparable with that of wild-type mice (Koike et al., 1994), while other experiments did not encounter any tumors in HBx transgenic mice (Lee et al., 1990). HBx transgenic mice have been reported to be more sensitive for HCC development after a single DEN-injection when compared with their non-transgenic counterparts (Sell et al., 1991).

A number of HCV proteins, such as core, NS3 and NS5A (Heindryckx et al., 2009) play an important role in hepatocarcinogenesis. When the complete viral protein is expressed, steatosis and HCC occur in 15% of the mice after approximately 90–100 weeks (Heindryckx et al., 2009). The expression of HCV core leads to progressive hepatic steatosis in several lines of constitutive transgenic mice, followed by HCC after 80–105 weeks in 32% of the male mice (Heindryckx et al., 2009). Inducible expression of core protein by tetracycline and Dox administration leads to a peak in steatosis after 2 months but no HCC occurs (Chang et al., 2008). Transgenic mice expressing core, E1 and E2 structural proteins developed HCC after 60 weeks in 23% of the male mice (Naas et al., 2005). The Myc protein is a transcription factor that activates the expression of several genes through binding on consensus sequences and recruitment of histone acetyltransferases (Nilsson and Cleveland, 2003). Transgenic mice over-expressing c-myc develop liver tumors after a long period of latency (35–90 weeks) (Thorgeirsson and Santoni-Rugiu, 1996). Interestingly, *Myc* transgenic mice are genetically close to human HCC that have a good prognosis. β-catenin mutations are considered to be an early event in hepatocarcinogenesis (Laurent-Puig and Zucman-Rossi, 2006). When mutations in both the β-catenin and H-ras genes are introduced by adenovirus-mediated Cre expression, early HCC are found in mice already 8 weeks after induction. High grade HCC could be established after approximately 26 weeks. Transgenic mice over-expressing human TGF-α under the inducible metallothionein 1 promoter get tumors in their livers. These lesions are genetically similar to human HCC associated with poor prognoses. Double transgenic mice carrying both c-myc (albumin promoter) and TGF-α (metallothionein promoter) display a massive acceleration of HCC development compared to the single

transgenic mice overexpressing either c-myc or TGF-α (Thorgeirsson and Santoni-Rugiu, 1996). Moreover, over-expression of the secreted form of the epidermal growth factor (EGF) results in multiple highly malignant hepatic tumors after 24–36 weeks (Tonjes et al., 1995). In double transgenic mice expressing EGF and myc, HCC development has been reported as accelerated (Tonjes et al., 1995). One model that does not require liver- specific expression for the onset of HCC is a transgenic mouse model over-expressing fibroblast growth factor 19 (FGF19) in skeletal muscle which leads to the occurrence of HCC in 50% of the mice after approximately 52 weeks (Nicholes et al., 2002). The Simian vacuolating virus 40 (SV40) is a DNA-virus that can cause tumor formation. When the SV40 T-antigen is expressed under a promoter like albumin, α1 antitrypsin, serum amyloid P component or antithrombin III, liver tumors can arise after a short period of latency (4–12 weeks). Metastasis to the lungs may occur in these models (Heindryckx et al., 2009). Alpha-1 antitrypsin (AAT) -deficient mice develop HCC after 52–90 weeks (Geller et al., 1994). Phosphatase and tensine homolog (PTEN) is a tumor suppressor gene. Liver-specific PTEN-deficient mice develop hepatic steatosis, inflammation, fibrosis and tumors, alterations resembling the ones seen in human livers affected by non-alcoholic steatohepatitis (NASH) (Watanabe et al., 2007). Members of the platelet-derived growth factor (PDGF) family are important for tumorigenesis. In addition, they have been associated with several diseases, including hepatic fibrosis. Liver cirrhosis induced by over-expression of PDGF-A, PDGF-B, PDGF-C or PDGF-D is associated with hepatic stellate cell activation possibly as a result of the induction of profibrotic genes such as TGF-β1 (Campbell et al., 2005; Thieringer et al., 2008). Long-term over-expression of the PDGF genes induces HCC after approximately 52 weeks (Campbell et al., 2005) TGF-β1 is known to be an important player in the pathogenesis of liver fibrosis (Williams and Knapton, 1996). Transgenic mice over-expressing TGF-β1 present the most extensive liver fibrosis after approximately 10 weeks. In addition, tumor formation has also been described in this model as well (Schnur et al., 2004).

1.4 Inflammation and cancer

1.4.1 Chronic inflammation and carcinogenesis

The link between inflammation and cancer has been acknowledged for a long time (Lu et al., 2006). Interestingly, chronic inflammatory diseases may be associated with increased cancer risk, mostly in an organ specific manner, while in other areas of the body chronic inflammatory states rather lead to degenerative disorders, as observed in articular joints. The association between the immune system and cancer has been known for a long time. Already Rudolf Virchow speculated ~150 years ago about inflammatory origins of cancer. Moreover, epidemiological data clearly demonstrate that susceptibility to cancer increases when tissues are chronically inflamed.

Chronic inflammation of the liver, as seen in chronic viral hepatitis, is associated with HCC. Chronic gastritis, as seen in *helicobacter* infection, is associated with stomach cancer (Oh et al., 2005). Chronic esophagitis, as seen in chronic gastroesophageal reflux disease, can lead to Barrett's esophagus and

esophageal carcinoma (Gomes et al., 2005). Finally chronic ulcerative colitis is tightly linked to the development of colorectal carcinomas (Itzkowitz and Yio, 2004). Some of these associations have been investigated and are currently being confirmed and studied in mouse models of chronic inflammation. Bacterial infections can result in chronic colitis associated colorectal cancer in immune compromised mice (Erdman et al., 2003; Greten et al., 2004). Helicobacter felis infection results, also in mice, in chronic gastritis and eventually gastric cancer (Goldenring and Nomura, 2006). Different patterns of gastritis, associated with different helicobacter genotypes and host factors, have been linked to distinctly increased or reduced (Meireles et al., 2004; Wen et al., 2004) risks of cancer. While antral gastritis is associated with duodenal ulceration, multifocal or diffuse gastritis that is associated with atrophy shows a strong association with gastric cancer. Similarly, chronic colitis in diverticular disease is not associated with an increased cancer risk while chronic ulcerative colitis is. In line, it has been shown that long-term use of non-steroidal anti-inflammatory drugs (NSAIDs) is capable of reducing the risk of several cancer types (Gupta and Dubois, 2001). In general, it is suggested that a single mutagenic event does not result in formation of a malignant tumor. Additional genetic and epigenetic events are necessary for the progression to a tumor state. The essential requirements being characteristic of a tumor cell are self-sufficiency in growth signals, insensitivity to growth-inhibitory signals, evasion of programmed cell death (apoptosis), limitless replicative potential, sustained angiogenesis, and tissue invasion and metastasis (Hanahan and Weinberg, 2000). Carcinogenesis is commonly regarded as a three step process. These phases are the initiation phase with first genomic alterations. During the promotion phase proliferation of genetically altered cells is ongoing and finally, during the progression phase the tumors increase in size. In summary, the formation of malignant tumors is the result of uncontrolled growth of a given cell type which then gains the ability to invade the surrounding tissue and then malignant cells spread theoretically at least, throughout the whole body. Functionally, various factors, either directly or indirectly, suffice to induce cell proliferation, recruitment of inflammatory cells and to trigger production of reactive oxygen species leading to oxidative DNA damage. In parallel reduced DNA repair leads to a lack of protection against pro-tumorigenic events.

On the effector level different mechanisms have been proposed, including HIF-1α, COX-2, iNOS and peroxynitriles, NF-κB signalling, and numerous cytokines (Lu et al., 2006). Most research efforts have addressed the sequence of events associated with the progression of chronic inflammation to overt carcinoma. While these studies have brought insight into the genetic alterations that accumulate within target cells during their progression from normal tissue to cancer, they have brought little knowledge on the characteristics of the inflammation itself that drives the critical events during tumorigenesis. Little is known on the characteristics of the inflammations that are associated with cancer and many open questions remain to be answered.

1.4.2 Chronic inflammation and hepatocellular carcinoma

While in most cases, inflammatory responses of the immune system are beneficial as a defense mechanism

against pathogenic agents, when tissue homeostasis is constantly disturbed by inflammation, this can lead to dramatically increased cell death, excessive tissue remodeling with compensatory proliferation and oxidative stress-related protein and DNA alterations. In addition, in the past, research efforts were directed to understand the sequence of tumorigenic processes by treating animals with chemical carcinogens like DEN which most probably does not reflect virus triggered hepatic carcinogenesis. A causal relationship between chronic hepatitis, hepatocellular damage and regeneration with fibrosis and carcinogenesis is well established from epidemiological studies (Berasain et al., 2009; El-Serag, 2002; El-Serag et al., 2007). Various etiologies, including chronic alcohol consumption, drug abuse, autoimmune disorders, exposure to toxins (e.g. aflatoxin B) or infections with hepatotropic viruses (e.g. HBV, HCV) can lead to chronic hepatitis, liver fibrosis and finally cirrhosis. HBV- and HCV-infections are by far the most common cause of chronic hepatitis in humans (Malhi et al., 2006). Chronic HBV- and HCV-infections are frequently associated with HCC, the most prevalent primary human liver cancer (El-Serag and Rudolph, 2007), and except for HBV-infections, liver cirrhosis precedes HCC in most cases. The exact mechanisms driving chronic hepatitis-induced liver cancer remain elusive. Among others, aberrant expression of cytotoxic cytokines is thought to be critically involved (Greten and Karin, 2004; Karin, 2006; Lee et al., 2005; Lowes et al., 2003; Maeda and Omata, 2008; Vainer et al., 2008).

Many cell types that are susceptible to the actions of cytokines are residing in the liver. Hepatocytes express a variety of cytokine receptors such as for IL-1, TNF-α, LTα, LTβ and IL-6. NPC, such as the resident liver macrophages (KC) not only synthesize various cytokines, but the actions of these cells is also affected by cytokines.

1.5 The role of NF-κB in liver pathology

1.5.1 Impact of NF-κB on hepatitis and chronic hepatitis induced liver carcinogenesis

The pro-inflammatory and homeostatic cytokines LTα and LTβ are members of the TNF superfamily. Under physiological conditions LTs are expressed by activated T-, B-, NK- and lymphoid tissue inducer cells (Fu et al., 1998a; Ware, 2005) and are crucial for organogenesis and maintenance of lymphoid tissues (Rennert et al., 1996; Tumanov et al., 2003). Whereas LTβ contains a transmembrane domain, LTα is soluble. Consequently, LT can exist as membrane bound heterotrimers ($LT\alpha_1\beta_2$ or $LT\alpha_2\beta_1$) interacting with LTβR or as soluble secreted homotrimers ($LT\alpha_3$) triggering TNF receptor 1, 2 (TNFR1, TNFR2) and the herpes virus entry mediator receptor (HVEM) (Browning et al., 1995; Ware, 2005). LTβR and TNFR1 signaling can be activated by the HCV-core protein (Chen et al., 1997; Zhu et al., 1998) involving the canonical or non-canonical NF-κB signaling pathways (Ware, 2005; You et al., 1999). Furthermore, HBV- or HCV-infections lead to increased hepatic LT expression *in vivo* and *in vitro* (Lee et al., 2005; Lowes et al., 2003) and HCV replication has been demonstrated to depend on components of the LTβR signaling pathway *in vitro* (Ng et al., 2007).

LTs can directly act on hepatocytes which physiologically express high levels of LTβR but little LT (Browning and French, 2002). T-cell-derived LT and LIGHT (LT-like, exhibits inducible expression, competes with HSV glycoprotein D for HVEM, expressed by T- lymphocytes) signaling to hepatocytes controls lipoprotein homeostasis (Lo et al., 2007). In addition, LT signaling is important for liver regeneration through T-cell-derived LT expression (Tumanov et al., 2008) and regulates hepatic stellate cell function and wound healing (Ruddell et al., 2009). Thus, hepatic LTβR signaling controls liver homeostasis in both health and disease. Promotion of HCC formation by chronic inflammatory stimuli has been recapitulated in various models. Ablation of the multi-drug resistance gene 2 (*mdr2*) induces cholestatic hepatitis and liver cancer (Pikarsky et al., 2004) and administration of the chemical carcinogen diethylnitrosamine (DEN) causes acute liver injury and HCC (Maeda et al., 2005). Liver specific expression of the hepatitis B surface antigen (HBsAg) in transgenic mice demonstrates that chronic immune-mediated liver cell injury is critical for HCC formation (Nakamoto et al., 1998).

Triggering TNFR1 or LTβR induces the classical and alternative NF-κB signaling pathways, which are linked to inflammation-induced carcinogenesis (Greten and Karin, 2004). However, the precise role of these pathways in HCC pathogenesis is controversial (Vainer et al., 2008). Mice lacking IKappa B kinase β (IKKβ specifically in hepatocytes ($Ikk\beta^{\Delta hep}$) exhibit a marked increase in DEN-induced HCC formation suggesting a protective function of IKKβ in HCC development (Maeda et al., 2005). In contrast, NF-κB signaling promotes HCC development in $mdr2^{-/-}$ mice and anti-TNFα treatment is protective (Pikarsky et al., 2004). Interestingly, mice with a hepatocyte-specific deletion of IKKγ (also called NEMO) develop steatohepatitis and HCC (Luedde et al., 2007). Consequently, the role of NF-κB signaling in hepatocarcinogenesis might depend on the mouse model and the type or degree of liver inflammation and injury (Vainer et al., 2008). Here, I investigated a possible causal relationship between sustained hepatic LTβR-signaling, chronic hepatitis and HCC development.

In my thesis I describe a new mouse model for HCC development. I also aimed at elucidating the impact of NF-κB and of inflammatory cells for HCC formation. Moreover, I was interested in TNFR1 and I wanted to find out which parallels do exist between the presented murine model and human liver data. I hypothesized that liver disorders with inflammation would significantly differ from diseases without inflammation, irrespectively of a viral background. I thought that most probably liver tumors would not differ regarding their origin. I also did not expect to be able to prove metastasis in the presented mouse model based on preliminary data where I had not found any lung metastases. In order to disprove all these hypotheses and to address the questions I have performed various experiments with the following experimental outcome.

1. Results Mechanisms of Inflammation-induced Hepatocarcinogenesis

1.6 LT-driven mechanisms inducing chronic hepatitis and HCC

1.6.1 Upregulation of LTα, LTβ and LTβR in HBV or HCV infected human livers

The specific role of LT signaling in the pathogenesis of virus-induced hepatitis and HCC formation is not completely defined. I analyzed transcriptional levels of *LTα*, *LTβ*, *LIGHT*, *TNFα*, *LTβR* and *TNFR1* in human HBV- or HCV-induced chronic hepatitis and HCC or in non-viral HCC compared to healthy liver specimens (Figs. 7 and 8).

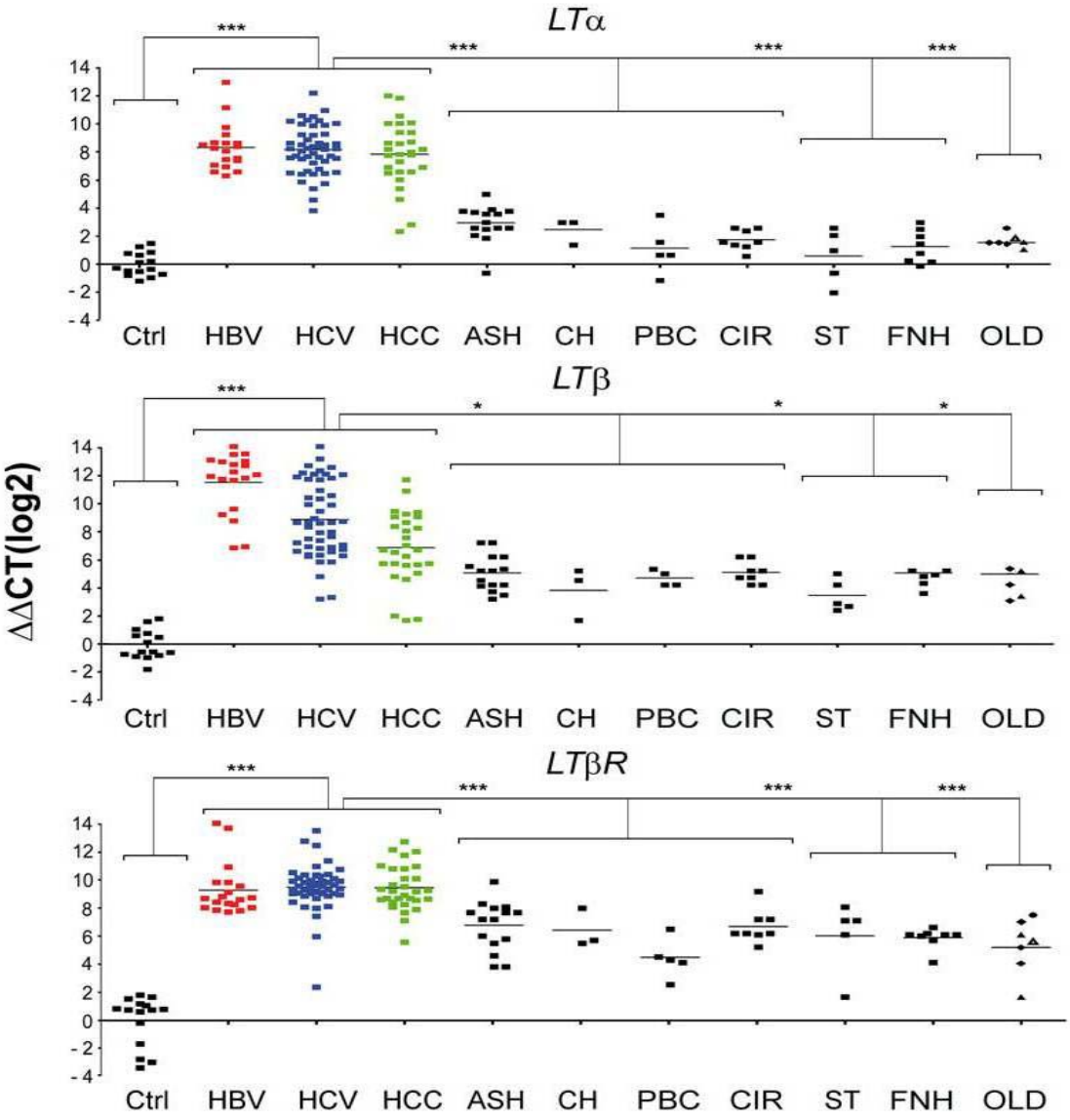

Figure 7: mRNA expression of TNF-superfamily members in viral (HBV, HCV induced) and non-viral liver diseases. Analysis of hepatic *LTα*, *LTβ* and *LTβR* transcription by real-time PCR. Healthy individuals (Ctrl; n=1 5), patients chronically infected with HBV (n=19), HCV (n=49), affected by HCC (n=30) or suffering from various non-virus related liver disorders were investigated. Non-virus related liver diseases with hepatitis include alcoholic

steatohepatitis (ASH; n=13), cholestasis (CH; n=3), primary biliary cirrhosis/ autoimmune cholangitis (PBC; n=5), end stage liver cirrhosis due to alcoholic liver disease (CIR; n=8), α1-antitrypsin deficiency (α1AT; n=1) and focal liver fibrosis (FLF; n=2). Non-virus related liver diseases without hepatitis include steatosis (ST; n=5), hemochromatosis/siderosis (HE; n=3), and Wilson's disease (WD; n=1). Focal nodular hyperplasia (FNH; n=8) was investigated as a benign primary liver tumor. Diseases such as α1AT (●), FLF (▲), HE/SID (•'), and WD (Δ) are listed under "other liver diseases" (OLD). Horizontal bars represent the average mRNA expression level. The y-axis describes the ΔΔCT values on a log2 scale. *, **, *** indicate statistical significance: * = p≤0.05; ** = p<0.001; *** = p<0.0001.

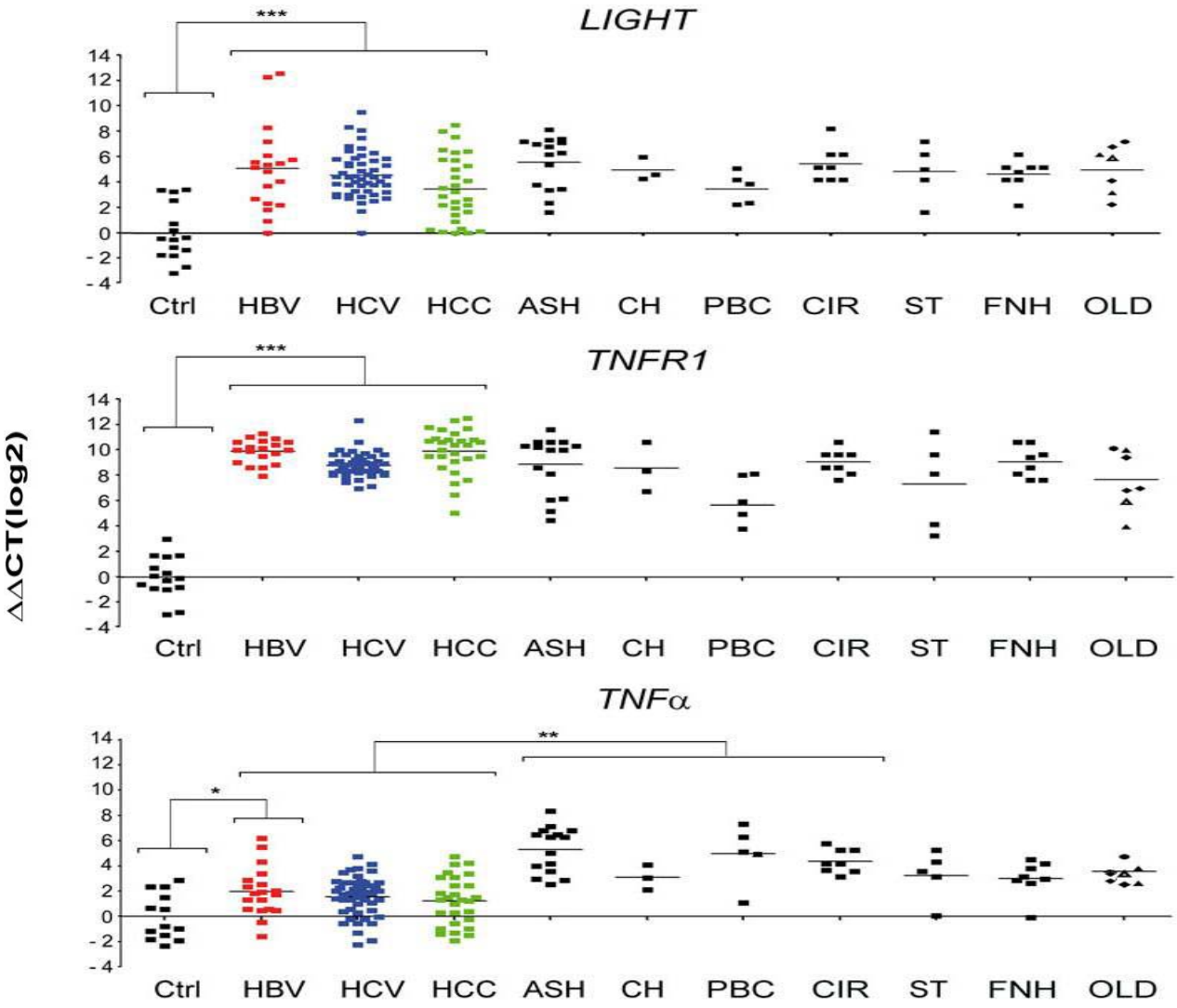

Figure 8: mRNA expression of TNF-superfamily members in viral (HBV, HCV induced) and non-viral liver diseases. Analysis of hepatic *LIGHT, TNFR1, and TNFα* transcription by real-time PCR. Healthy individuals (Ctrl; n=1 5), patients chronically infected with HBV (n=19), HCV (n=49), affected by HCC (n=30) or suffering from various non-virus related liver disorders were investigated. Non-virus related liver diseases with hepatitis include alcoholic steatohepatitis (ASH; n=13), cholestasis (CH; n=3), primary biliary cirrhosis/ autoimmune cholangitis (PBC; n=5), end stage liver cirrhosis due to alcoholic liver disease (CIR; n=8), α1-antitrypsin deficiency (α1AT; n=1) and focal liver fibrosis (FLF; n=2). Non-virus related liver diseases without hepatitis include steatosis (ST; n=5), hemochromatosis/siderosis (HE; n=3), and Wilson's disease (WD; n=1). Focal nodular hyperplasia (FNH; n=8) was

investigated as a benign primary liver tumor. Diseases such as α1AT (●), FLF (▲), HE/SID (•'), and WD (Δ) are listed under "other liver diseases" (OLD). Horizontal bars represent the average mRNA expression level. The y-axis describes the ΔΔCT values on a log2 scale. *, **, *** indicate statistical significance: * = p≤0.05; ** = p<0.001; *** = p<0.0001.

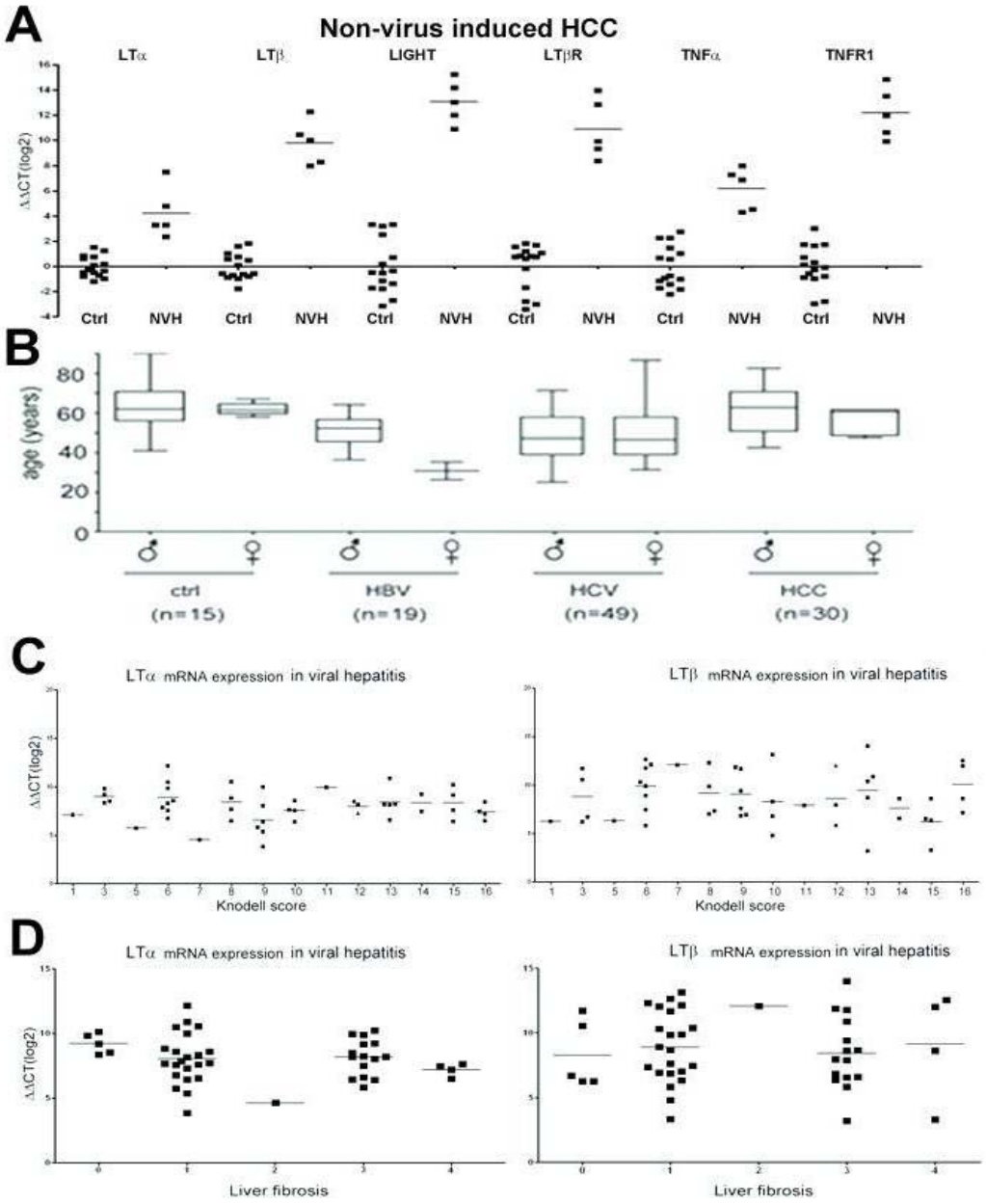

Figure 9: mRNA expression in non-virus related HCC; gender distribution, correlation analysis of *LTα* and *LTβ* mRNA expression with Knodell score, fibrosis, as well as mRNA expression analysis of chemokines in non virus related HCC. (A) Real-time PCR analysis for *LTα, LTβ*, *LIGHT*, *LTβR*, *TNFα* and *TNFR1* transcripts in non-virus related HCC (NVH). Each symbol represents one individual patient. Horizontal bars represent the average *LTα* and *LTβ* mRNA expression level. The y-axis describes the ΔΔCT values on a log2 scale. Ctrl left and NVH right. **(B)** Box plot analysis depicts age and gender distribution of respective patients. Ctrl: healthy control patients. HBV: Hepatitis B virus. HCV: Hepatitis C virus. HCC: Hepatocellular carcinoma. Each symbol represents one individual patient. Horizontal bars represent the average *LTα* or *LTβ* mRNA expression level. The y-axis describes the ΔΔCT

values on a log2 scale. **(C)** Correlation analysis of *LTα* and *LTβ* mRNA expression with Knodell score (ranging from 0-16) in HCV-infected livers. **(D)** Correlation analysis of *LTα* and *LTβ* mRNA expression with fibrosis score (ranging from 0-4) in HCV-infected liversHorizontal bars represent the average mRNA expression level. The y-axis describes the ΔΔCT values on a log2 scale. Standard deviation (+/- SD) is indicated by error bars.

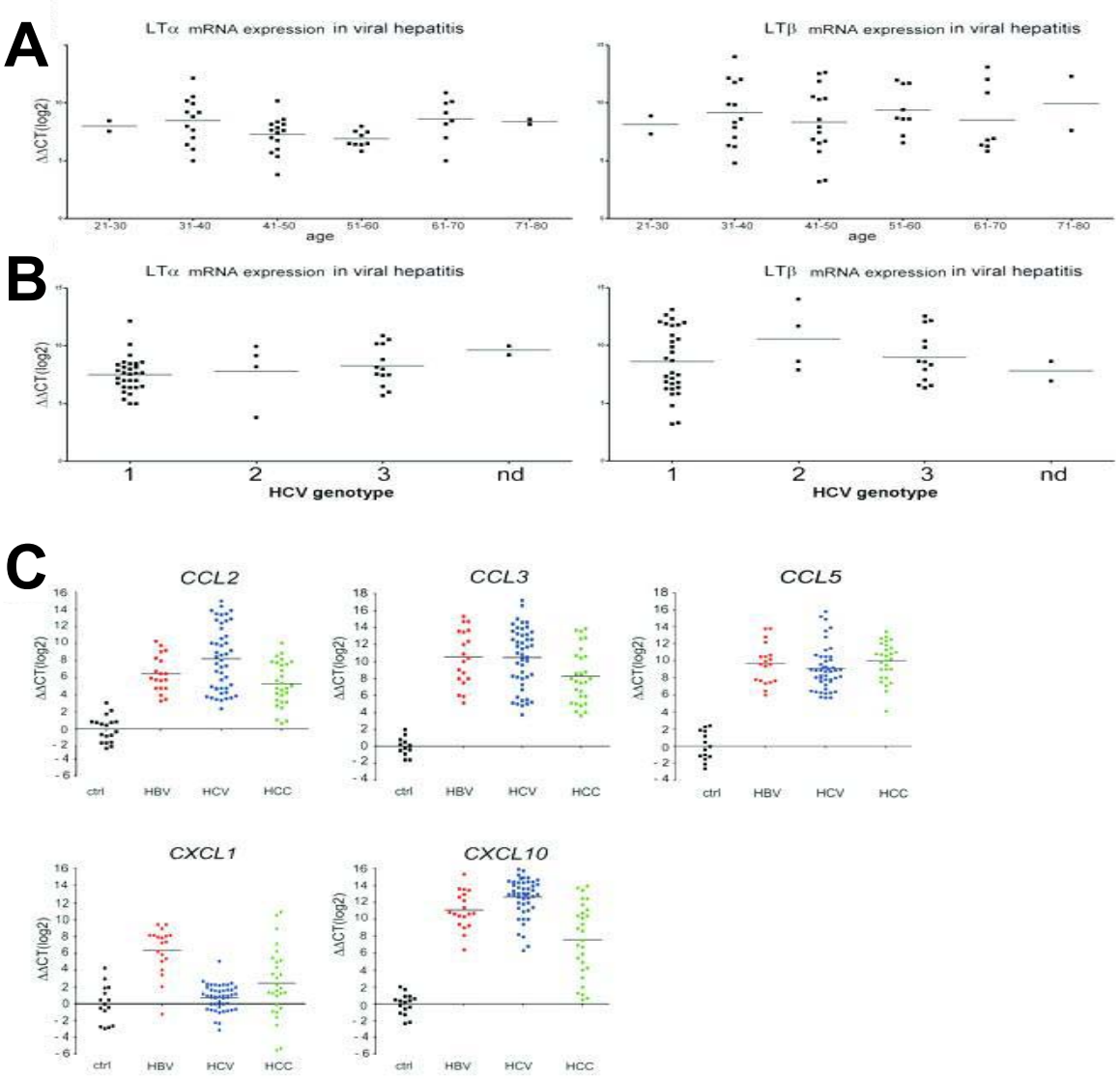

Figure 10: mRNA expression in non-virus related HCC; age and gender distribution, correlation analysis of *LTα* and *LTβ* mRNA expression with Knodell score, fibrosis, age, and HCV genotype, as well as mRNA expression analysis of chemokines in HBV- or HCV-infected livers and HCC. (A) Correlation analysis of *LTα* and *LTβ* mRNA expression with age (ranging from the 3rd to the 8th decade) in HCV-infected livers. **(B)** Correlation analysis of *LTα* and *LTβ* mRNA expression with HCV genotypes. **(C)** Analysis of *CCL2, CCL3, CCL5, CXCL1*, and *CXCL10* mRNA expression by real-time PCR in human livers of healthy controls (n=15), patients chronically infected with HBV (n=19) or HCV (n=49) and patients suffering from HCC (n=30). Horizontal bars represent the average mRNA expression level. The y-axis describes the ΔΔCT values on a log2 scale. Standard deviation (+/- SD) is indicated by error bars.

LTα, *LTβ* and *LTβR* mRNA expression was increased on average ~2^7 to 2^{10} fold in HBV- or HCV-induced

hepatitis and HCC (P<0.001), whereas *LIGHT* transcripts were less elevated (on average ~2^3 to 2^5 fold; P<0.001). Likewise, *TNFR1* mRNA expression was significantly increased in HBV- or HCV-induced hepatitis and HCC (on average ~2^7 to 2^9 fold; P<0.0001).In contrast, *TNFα* was only slightly upregulated in HBV-induced hepatitis (P=0.04), while no significant increase was observed in HCV-induced hepatitis (P=0.3) and HCC (P=0.4). In most cases, HCV genotype, degree of inflammation (Knodell score), fibrosis (Metavir score) and liver enzyme levels (ALT; AST) were assessed (Tables 2-5).

Levels of *LTα*, *LTβ* and *LTβR* mRNA expression did not correlate with the degree of liver inflammation (P=0.5), fibrosis (P=0.5), patient age (P=0.5), gender (P=0.5), HCV genotype or type of virus infection (HBV; HCV; HBV/HCV co-infection in the case of some HCC; P=0.5) (Figures 9 and 10; data not shown).

To determine whether upregulation of LT ligands and receptors was specific for HBV- or HCV-induced liver diseases, I examined transcript levels in non-viral liver diseases. These included liver disorders with hepatitis [alcoholic steatohepatitis (ASH); cholestasis (CH); primary biliary cirrhosis/autoimmune cholangitis (PBC); end-stage liver cirrhosis due to alcoholic liver disease (CIR)] and liver diseases without inflammation [steatosis (ST), focal nodular hyperplasia (FNH)]. Additionally, other liver diseases (OLD) such as hemochromatosis/siderosis, Wilson's disease, focal liver fibrosis, α1-antitrypsin deficiency and non-viral HCC (NVH) were investigated.

Levels of *LTα, LTβ* and *LTβR* mRNA were significantly lower in all non-viral liver diseases analyzed except NVH when compared to virus-induced chronic hepatitis and HCC (*LTα: P*<0.0001; *LTβ: P*=0.05; *LTβR: P*<0.0001; Figs. 7 - 101). This was irrespective of whether non-viral liver diseases were associated with inflammation or not. *LIGHT* and *TNFR1* mRNA expression in non-viral liver diseases including NVH was similar to HBV- or HCV-induced chronic hepatitis and HCC. In contrast, *TNFα* mRNA expression was significantly higher in non-viral liver diseases with inflammation and NVH compared to healthy livers (P<0.0001), HBV- or HCV-induced hepatitis and HCC (P<0.0001).

Levels of *LTα*, *LTβ* and *LTβR* mRNA expression did not correlate with the degree of liver inflammation (P=0.5), fibrosis (P=0.5), patient age (P=0.5), gender (P=0.5), HCV genotype or type of virus infection (HBV; HCV; HBV/HCV co-infection in the case of some HCC; P=0.5) (Figures 9 and 10; data not shown).

Table 2: Overview of HCV infected chronically inflamed human livers that were incorporated in the analysis. Etiology, patient age, patient gender, degree of inflammation (0-2), deg ree of fibrosis (0-4), transaminase levels [Aspartat-Aminotransferase (AST), Alanin-Aminotransferase (ALT)], and HCV subtype are indicated. Degree of inflammation and fibrosis was evaluated by using the Metavir Score; nd: not determined.

Etiology	Age (years)	Gender	AST (U/l)	ALT (U/l)	Inflammation	Fibrosis	HCV genotype
HCV	44	F	20	34	1	3	3
HCV	45	M	42	91	1	3	1
HCV	47	M	33	79	0	2	1
HCV	36	M	9	6	0	0	2
HCV	57	F	58	71	1	2	3
HCV	34	M	77	152	1	1	1
HCV	45	M	40	72	1	2	3
HCV	35	F	44	93	0	1	1
HCV	57	M	18	32	1	1	1
HCV	38	F	36	44	0	1	3
HCV	64	M	nd	nd	nd	nd	nd
HCV	47	M	13	6	2	3	1
HCV	52	M	53	43	nd	nd	3
HCV	66	M	16	33	2	3	1
HCV	37	M	20	45	1	1	1
HCV	45	M	59	55	1	2-3	1
HCV	25	M	54	147	2	2	1
HCV	69	F	36	71	1	2	1
HCV	37	M	28	32	1	2	3
HCV	45	F	113	182	2	3	3
HCV	39	F	36	34	1	2	3
HCV	55	M	43	50	1	2	1
HCV	47	M	56	38	1	0	1
HCV	45	F	20	26	1	2	1
HCV	75	F	83	91	2	3	1
HCV	54	M	24	26	1	2	2
HCV	66	M	16	33	2	3	1
HCV	58	F	131	59	2	4	1
HCV	25	M	60	144	1	1	1
HCV	66	F	71	89	2	3	1
HCV	49	M	30	38	1	1	3
HCV	39	M	46	39	1	1	nd
HCV	38	M	86	177	2	3	3
HCV	31	F	32	51	1	2	1
HCV	45	F	30	32	0	1	3
HCV	42	F	13	26	0	0	1
HCV	64	M	52	52	2	2	1
HCV	71	M	51	106	1	1	1
HCV	54	F	28	24	1	1	2
HCV	54	F	28	24	1	1	2
HCV	42	M	27	44	2	3	1
HCV	69	F	86	144	1-2	2	1
HCV	46	M	72	109	1	1	1
HCV	58	M	29	36	1	3	1
HCV	40	F	25	22	0	0	3
HCV	57	F	35	57	1	2	1
HCV	40	M	36	103	1	2	3
HCV	38	M	64	129	1	2	1
HCV	64	M	67	91	1	3	1

Table 3: Overview of HCV and HBV infected chronically inflamed human livers that were incorporated in the analysis. Etiology, periportal inflammation (0-10), intralobular inflammation (0-4), portal inflammation (0-4), degree of fibrosis (0-4) and Knodell score (0-16) are indicated. Degree of hepatitis activity and fibrosis was evaluated by using the Knodell necroinflammatory score; nd: not determined.

Etiology	Periportal (0-10)	Intralobular (0-4)	Porta (0-4)	Score (sum)	K fibrosis score	Entire score
HCV	nd	nd	nd	nd	nd	nd
HCV	1	1	3	5	1	6
HCV	4	3	4	11	4	15
HCV	3	1	4	8	3	11
HCV	4	3	4	11	3	14
HCV	4	1	4	9	1	10
HCV	4	4	4	12	4	16
HCV	1	1	3	5	1	6
HCV	1	1	4	6	3	9
HCV	3	1	3	7	1	8
HCV	1	1	3	5	1	6
HCV	4	4	4	12	4	16
HCV	4	1	3	8	3	12
HCV	3	1	4	8	1	9
HCV	1	3	1	5	1	6
HCV	1	3	3	7	1	8
HCV	1	3	3	7	1	8
HCV	3	3	3	9	1	10
HCV	4	4	4	12	1	13
HCV	1	1	3	5	1	6
HCV	3	3	4	10	3	13
HCV	3	1	4	8	1	9
HCV	4	4	4	12	3	15
HCV	4	4	4	12	3	15
HCV	3	1	3	7	1	8
HCV	3	1	3	7	3	10
HCV	4	4	4	12	3	15
HCV	4	3	4	11	3	14
HCV	1	1	1	3	0	3
HCV	4	4	4	12	1	13
HCV	3	3	3	9	1	10
HCV	3	1	3	7	1	8
HCV	4	4	4	12	4	16
HCV	3	1	4	8	1	9

Etiology	Periportal (0-10)	Intralobular (0-4)	Porta (0-4)	Score (sum)	K fibrosis score	Entire score
HCV	3	3	4	10	3	13
HCV	1	1	3	5	2	7
HCV	1	1	4	6	3	9
HCV	1	1	1	3	0	3
HCV	4	3	4	11	1	12
HCV	3	1	1	5	1	6
HCV	1	1	3	5	1	6
HCV	1	1	1	3	3	6
HCV	3	3	4	10	3	13
HCV	3	1	3	7	0	7
HCV	3	3	4	10	4	14
HCV	1	1	1	3	0	3
HCV	4	4	4	12	3	15
HCV	4	4	4	12	3	15
HCV	1	1	3	5	1	6
HCV	3	1	3	7	1	8
HCV	4	3	4	11	3	14
HCV	4	3	4	11	1	12
HCV	3	1	3	7	1	8
HCV	4	3	4	11	4	15
HCV	3	4	3	10	1	11
HCV	3	1	3	7	1	8
HCV	3	1	3	7	1	8
HCV	1	1	3	5	1	6
HCV	3	0	3	6	1	7
HCV	4	1	4	9	3	12
HCV	1	1	3	5	0	5
HCV	3	1	3	7	3	10
HCV	0	0	3	3	0	3
HBV	1	1	3	3	0	3
HBV	4	1	9	9	3	12
HBV	1	2	4	4	1	5
HBV	1	1	3	3	0	3

Table 4A: Overview of HBV infected chronically inflamed human livers that were incorporated in the analysis. Etiology, patient age, patient gender, degree of inflammation (0-2), degree of fibrosis (0-4) and transaminase levels [Aspartat-Aminotransferase (AST), Alanin-Aminotransferase (ALT)] are indicated. Degree of inflammation and fibrosis was evaluated by using the Metavir Score; nd: not determined.

Etiology	Age (years)	Gender	AST (U/l)	ALT (U/l)	Inflammation	Fibrosis	HCV genotype
HBV/HCV	55	M	60	98	0	0	nd
HBV	34	M	34	79	1	0	nd
HBV	33	F	38	104	0	0	nd
HBV	44	M	56	95	2	3	nd
HBV	42	M	nd	nd	nd	nd	nd
HBV	51	M	nd	nd	nd	nd	nd
HBV	69	M	nd	nd	nd	nd	nd
HBV	23	F	nd	nd	nd	nd	nd
HBV	54	M	nd	nd	nd	nd	nd
HBV	61	M	nd	nd	nd	nd	nd
HBV	48	M	nd	nd	nd	nd	nd

Table 4B: Overview of HBV infected chronically inflamed human livers that were incorporated in the analysis. Diagnosis, HBsAg and HBcAg status, patient age and gender; nd: not determined. HBsAg: Hepatitis B virus surface antigen. HBcAg: Hepatitis B virus core protein antigen.

Diagnosis	HbsAg	HBcAg	Age	Gender
HBV	+++	-	nd	nd
HBV	+++	-	nd	nd
HBV	+++	+	nd	nd
HBV	+++	+	nd	nd
HBV	+++	-	nd	nd
HBV	+++	-	nd	nd
HBV	++	+	nd	nd
HBV	++	-	nd	nd

Table 5: Overview of human HCC that were incorporated in the analysis. Additional diagnosis, viral genotype, patient age and patient gender are indicated. HBsAg: Hepatitis B virus surface antigen. HBcAg: Hepatitis B virus core protein antigen.

Diagnosis	HbsAg	HBcAg	Age	Gender
HCC,HBV	+++	+++	51	M
HCC,HBV	+++	-	nd	nd
HCC,HBV	+++	++	32	M
HCC,HBV	++	-	50	M
HCC,HBV	+	-	45	M
HCC,HBV	+++	-	55	M
HCC,HBV			62	M
HCC,HBV			42	M
HCC,HBV,HCV			47	M
HCC,HBV			63	M
HCC,HBV			70	M
HCC,HBV			82	M
HCC,HBV			45	M
HCC,HBV			71	M
HCC,HBV			67	M
HCC,HBV,HCV			51	M
HCC,HBV			77	M
HCC,HBV			70	M
HCC,HBV			56	M
HCC,HBV			62	M
HCC,HBV			48	M
HCC,HBV			51	M
HCC,HBV			50	M
HCC,HBV			69	M
HCC,HBV,HCV			47	F
HCC,HBV,HCV			61	F
HCC,HBV			60	F
HCC,HBV			49	F
HCC,HBV			61	F
HCC,HBV			55	F

1.6.2 Increased chemokine expression in HBV- or HCV-induced hepatitis and HCC

To confirm that pro-inflammatory signaling cascades are activated during HBV- or HCVinduced hepatitis and HCC formation, chemokine mRNA expression levels were measured (Fig. 10). *CCL2, CCL3, CCL5* and *CXCL10* mRNA expression was significantly higher in human HBV- (P<0.0001) or HCV- (P<0.0001) induced hepatitis and HCC (P<0.0001) compared to healthy controls. *CXCL1* mRNA expression was significantly increased in HBV-induced hepatitis (P<0.0001) and HCC (P=0.02) but not in HCV-induced hepatitis (P=0.07).

1.6.3 Upregulation of LTα, LTβ, LIGHT upon HCV infection *in vitro*

I next investigated whether *LTα*, *LTβ*, *LIGHT and LTβ*R transcripts can be directly upregulated by hepatocytes as a consequence of viral infection. Thus, a human hepatocyte cell line (Huh-7.5; (Blight et al., 2002)) was challenged with infectious HCVcc (Pietschmann et al., 2006) and cytokine as well as chemokine expression was measured (Fig. 11A).

At 48 to 72 hrs post infection, *LTα* (P=0.05), *LTβ* (P=0.05), *LIGHT* (P=0.05), *LTβR* (P=0.05) and chemokine transcripts (*CCL2*, *CCL3*, *CXCL1* and *CXCL10*) were increased (2-32 fold) in HCVcc-infected compared to non-infected Huh-7.5 cells.

1.6.4 Identification of liver cells expressing LTβR and its ligands in HBV or HCV infections

To identify the cellular source of *LTα*, *LTβ*, *LTβR* and *LIGHT* expression in human HCV-infected livers, cells were collected from HCV-induced hepatitis and HCC (Figs. 11A and 12). Liver cells were sorted according to their CD45 surface expression, resulting in CD45-enriched (T-, B-cells; monocytes, macrophages/Kupffer cells; dendritic and NK-cells) or CD45-depleted fractions (hepatocytes, oval cells, bile duct epithelial and endothelial cells). Purity of CD45-enriched or -depleted fractions was assessed by real-time PCR for lymphocyte (CD3; CD20; CD45) or hepatocyte (cytokeratin 18) markers. CD45-depleted fractions displayed only a minor contamination with CD45 mRNA (~1-10%). Vice versa, CD45-enriched fractions showed only a minor amount of cytokeratin 18 mRNA transcripts (~2-20%; Fig. 11C; data not shown).

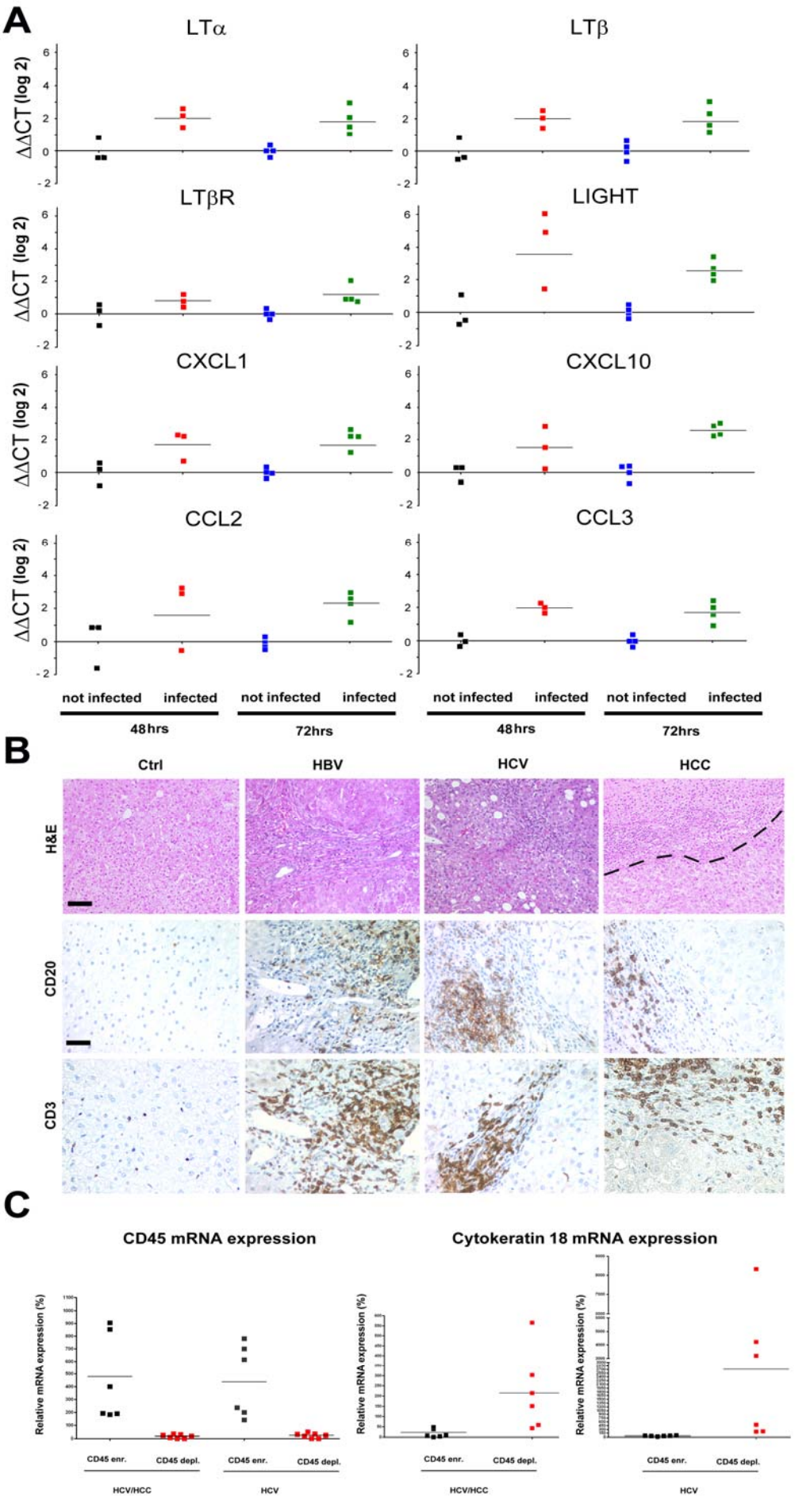
A
LTα
LTβ
LTβR
LIGHT
CXCL1
CXCL10
CCL2
CCL3
ΔΔCT (log 2)
not infected
infected
48hrs
72hrs
B
Ctrl
HBV
HCV
HCC
H&E
CD20
CD3
C
CD45 mRNA expression
Cytokeratin 18 mRNA expression
Relative mRNA expression (%)
CD45 enr.
CD45 depl.
HCV/HCC
HCV

Fig. 11: HCVcc infection of human hepatocytes *in vitro* and analysis of HCV-infected liver cells *in vivo*. (A) Real-time PCR analysis for the mRNA expression of *LTα*, *LTβ*, *LIGHT*, *LTβR*, *CXCL1*, *CXCL10*, *CCL2* and *CCL3* in a human hepatocyte cell line (Huh7.5) upon challenge with infectious HCVcc at 48 and 72 hrs post infection. Horizontal bars represent the average mRNA expression levels. The y-axis describes the ΔΔCT values on a log2 scale. For control, non-infected, time-matched control Huh7.5 cells were investigated. hrs: hours postinfection. Standard deviation (+/- SD) is indicated by error bars. **(B)** Immunohistological analysis of human healthy controls, HBV- and HCV-infected livers or HCC: H&E staining and staining for CD20 (B-cells) and CD3 (T-cells) was performed. H&E staining indicates morphological features of inflamed and fibrotic liver tissues (HBV- and HCV infected livers). HCC display transformed hepatocytes. The HCC border zone is indicated by a dashed line (upper row, right column). Inflammatory infiltrates were detected in HBV- or HCV-infected livers as well as at the border zones of HCC (scale bar: 100μm). **(C)** Real-time PCR analysis for *CD45* and *Cytokeratin 18* mRNA expression to quantify the purification efficiency of CD45-enrichment or CD45-depletion. Cells were prepared from HCV-infected, inflamed livers (HCV) or from HCC with HCV etiology (HCV/HCC). Horizontal bars represent the average mRNA expression level. The y-axis describes the ΔΔCT values on a log2 scale. Standard deviation (+/- SD) is indicated by error bars.

Within HCV-induced HCC, CD45-enriched and -depleted liver cells expressed similar *LTα* or *LTβ* mRNA levels (LTα: P=0.8; LTβ: P=0.1) that were significantly higher than in unsorted liver cells of healthy individuals (P<0.0001) (Fig. 11A).

1.6.5 Hepatocyte-specific LTα and β overexpression induces chronic progressive hepatitis

Whether sustained hepatic LTβR signaling is causally linked to chronic hepatitis and liver cancer was investigated in transgenic mice. Two independent lines expressing LTα and β under the control of the albumin enhancer/promoter embedded in a *Prnp* half genomic construct (phgPrP; Raeber et al., 1999) were generated by Mathias Heikenwälder and Nicolas Zeller and analyzed by the three of us. These two lines express LTα and β in a liver specific manner, either at low (i.e. *tg*1222) or at high level (i.e. *tg*1223; (Heikenwalder et al., 2005)). Although livers of *tg*1222 and *tg*1223 mice were histologically indistinguishable from those of negative littermates at three months of age (Fig. 13), the hepatic transcriptome was already considerably altered in *tg*1223 and to a lesser degree in *tg*1222 mice (Fig. 15; data not shown). Genes with the most dramatic expression changes were identified by DNA microarray analysis and confirmed by real-time PCR (Fig. 15).

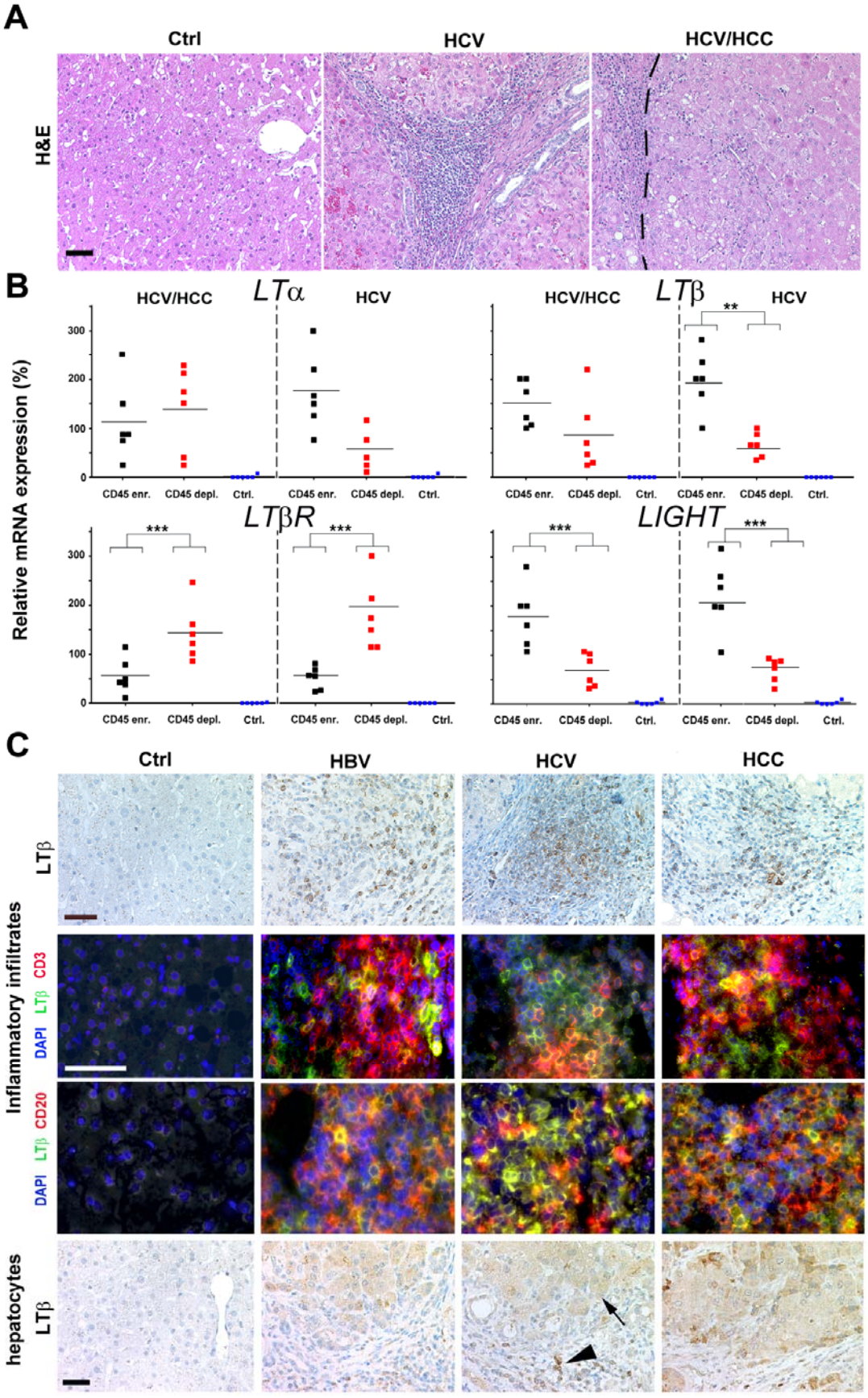

Figure 12: Identification of cell types expressing TNF-superfamily members in virus-infected or HCC-affected

livers. (A) Histology of representative paraffin sections of healthy controls, HCV-infected livers, and HCC with HCV etiology. HCV-infected livers (HCV) and tumors (HCV/HCC) display leukocytic infiltrates. H&E: Hematoxylin and eosin staining. The tumor border is indicated by a dashed line (scale bar: 100μm). **(B)** Real-time PCR analysis of sorted, CD45-enriched or CD45-depleted liver cells. For control, whole liver cell populations derived from healthy or diseased livers (HCV infected/HCC) were used. mRNA expression levels are normalized to unsorted, total cell populations of the respective liver disease and calculated as 100%. The average expression level is indicated as percentage of control (unsorted cells of the respective disease) and demarcated by horizontal bars. *, **, *** indicate statistical significance (Student's T-test): * = $p \leq 0.05$; ** = $p < 0.001$; *** = $p < 0.0001$. **(C)** Immunohistochemical (upper and lower panel) and immunofluorescence analysis for LTβ expression in healthy, HBV- or HCV-infected and HCC-affected livers (scale bar: 50μm). Arrowhead depicts $LT\beta^+$ leukocytes, arrow $LT\beta^+$ hepatocytes. *LTβR* mRNA transcript levels were significantly higher in CD45-depleted compared to CD45-enriched (P=0.006) or unsorted liver cells of healthy individuals (P<0.0001). In contrast, *LIGHT* mRNA expression was significantly increased in CD45-enriched when compared to CD45-depleted (P=0.008) or unsorted liver cells of healthy individuals (P=0.0007). Within HCV-induced hepatitis, CD45-enriched cells exhibited a trend towards increased *LTα* mRNA levels (P=0.089) and a significant rise in both *LTβ* and *LIGHT* transcripts compared to CD45-depleted or unsorted cells of healthy individuals (*LTβ*: P=0.006; *LIGHT*: P=0.01). Similar to HCV-induced HCC, *LTβR* mRNA expression was significantly higher in CD45- depleted compared to CD45-enriched (P=0.002) or unsorted control liver cells (P<0.0001). Thus, CD45-enriched liver cells but also CD45-depleted cell fractions express *LTα*, *LTβ* and *LIGHT* in HCV-induced hepatitis and HCC. Immunohistochemical analysis for LTβ protein expression corroborated these data: $CD3^+$, $CD20^+$ lymphocytes and hepatocytes express LTβ protein in HBV- or HCV-induced hepatitis and HCC, which was in contrast to healthy liver specimens (Fig. 12C).

As expected, *LTα* and *LTβ* transcripts were increased in *tg*1222 and *tg*1222 livers (Fig. 15A; data not shown). Additionally, mRNA expression of chemokines (*Ccl2*, *Ccl7, Cxcl1*, *Cxcl10*), genes involved in early growth response (e.g. *Egr1, Egr2*), cholesterol metabolism (e.g. *Ch25h*) and immediate early response (e.g. *c-Fos, Jun-b, Socs-3*) were significantly (P<0.0001) elevated. In contrast, genes involved in cell cycle control, histone modifications and cell metabolism were significantly downregulated (P<0.0001) (Fig. 15A; data not shown). *In situ* hybridization at 3 months of age revealed *LTα*, *LTβ*, *Cxcl10, Ccl2 and Egr1* mRNA transcripts in *tg*1223 hepatocytes (Fig. 14 and 15B). The latter experiment was mainly performed together with Juliane Bremer.

At the age of 4 months a slight increase in intrahepatic $CD11b^+$, $CD68^+$ and $MHCII^+$ cells was detected in *tg*1223 mice compared to age-matched *tg*1222 or C57BL/6 mice (Fig. 16; data not shown). At this time point, no significant increase in IL1β, IFNγ, IL6 and TNFα protein levels was found (data not shown). At 4-6 months transgenic livers started to develop strong portal and lobular (*tg*1223) or weak portal (*tg*1222) inflammation consisting of $CD4^+$, $CD8^+$ T-cells, B220+ B-cells and $CD11c^+$ dendritic cells (Fig. 16; (Heikenwalder et al., 2005)).

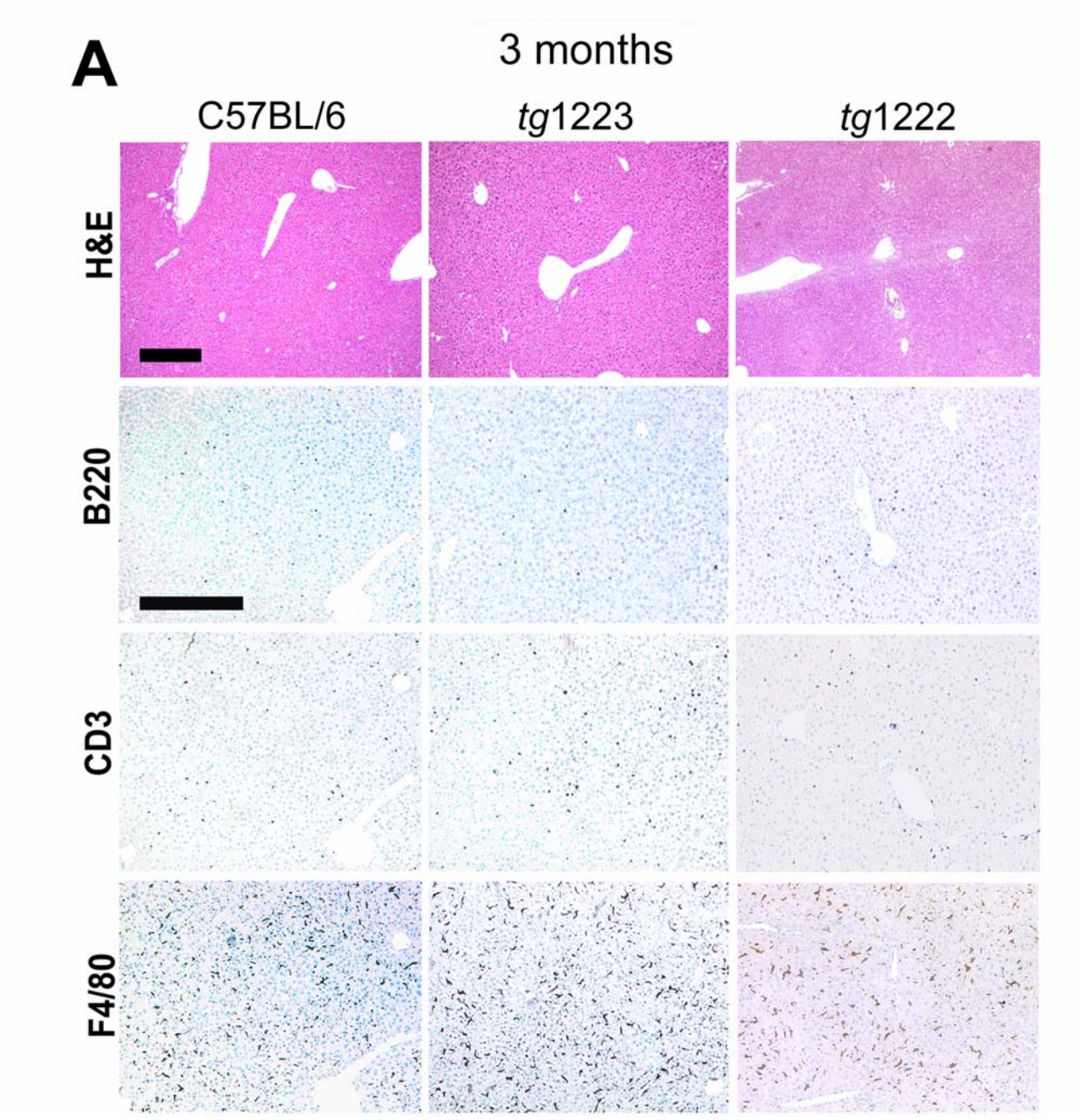

Figure 13: Immunohistological analysis of paraffin- or cryo-sections derived from 3 or 4-6 month-old C57BL/6 and transgenic livers. (A) C57BL/6, *tg*1222 and *tg*1223 livers lacked detectable inflammatory infiltrates as highlighted by H&E (scale bar: 200µm), by staining for B-cells (B220), T-cells (CD3), macrophages, Kupffer cells (F4/80) (scale bar: 100µm).

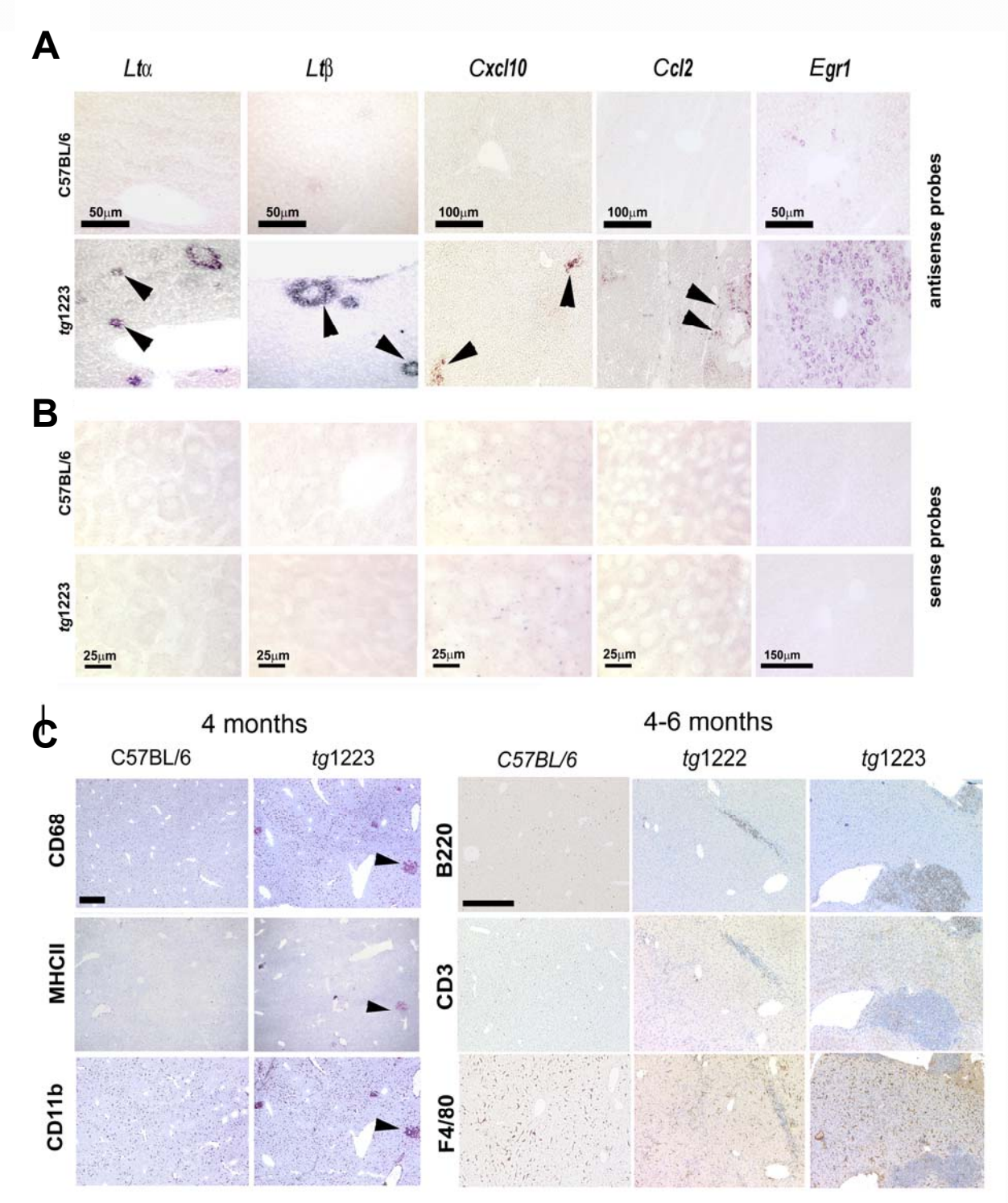

Figure 14: *In situ* hybridization of paraffin- or cryo-sections derived from 3 or 4-6 month-old C57BL/6 and transgenic livers. (A) *In situ* hybridization of liver cryo-sections from C57BL/6 and *tg*1223 mice with antisense probes for the indicated mRNAs. Arrowheads indicate focal hepatocyte-specific expression of *Ltα*, *Ltβ*, *Cxcl10, Ccl2* mRNA as well as broad *Egr1* mRNA expression. The size of scale bars is indicated. **(B)** Hybridization with sense probes served as negative control and did not lead to detectable signals for *Ltα*, *Ltβ, Cxcl10, Ccl2* and *Egr1* mRNA expression. The size of scale bars is indicated. **(C)** Immunohistochemical analysis for myeloid cells at the age of 4 months in *tg*1223 and C57BL/6 livers. A slight increase in the number of $CD11b^+$, $CD68^+$ and $MHCII^+$ cells was

detected in *tg*1223 livers at 4 months of age when compared to age matched *tg*1222 or C57BL/6 livers (left panel). I could already detect small aggregates at this particular time point, mainly consisting of myeloid cells (arrow heads). At the age of 4-6 months, $B220^{+}$, $CD3^{+}$ or $F480^{+}$ cells accumulated at portal sites of *tg*1223 livers (right panel). In *tg*1222 livers, only small portal inflammatory infiltrates could be observed at that time point (scale bar: 200µm).

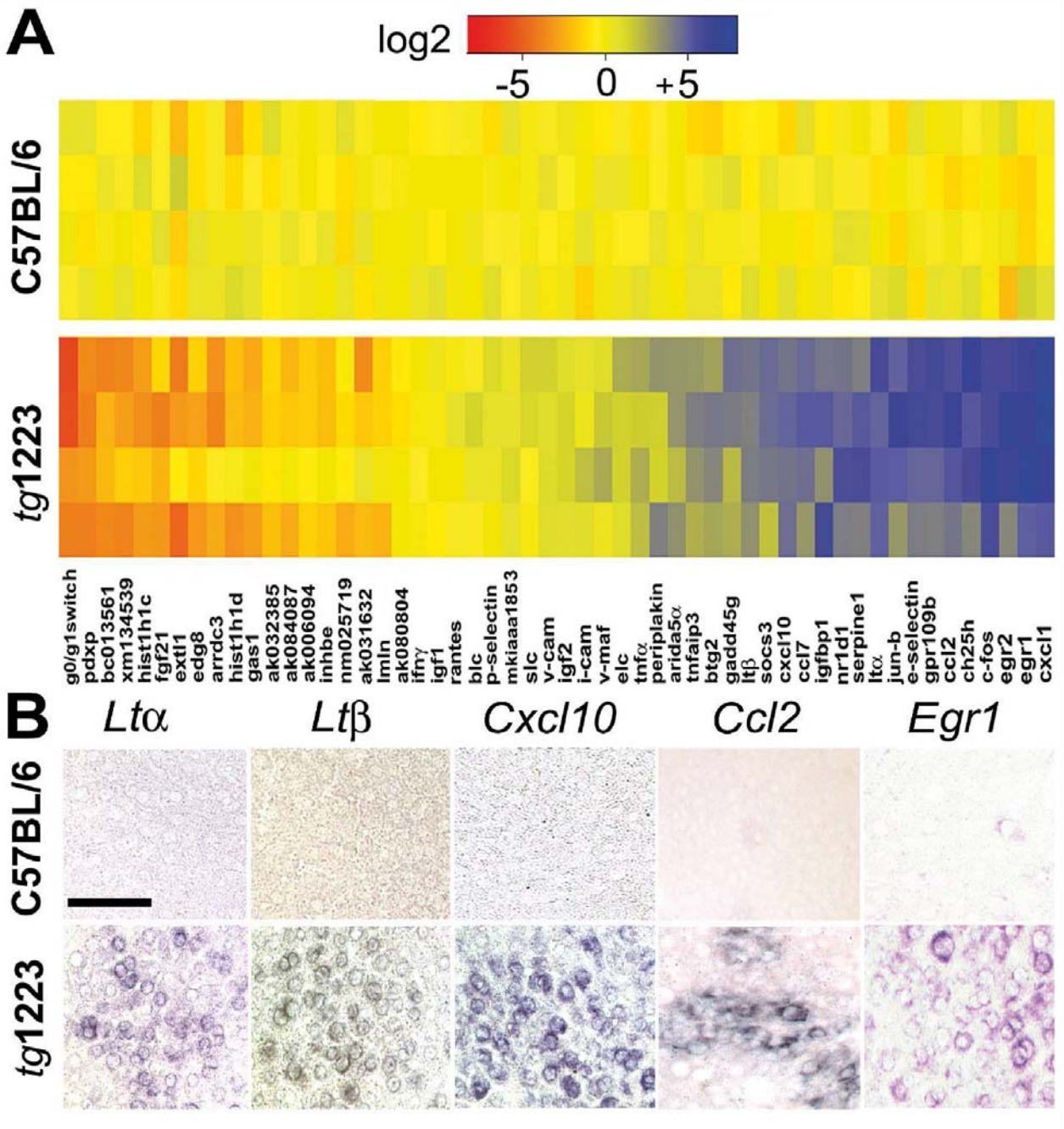

Figure 15: Characterization of *tg*1223 livers. (A) Real-time PCR analysis for mRNA expression in liver of candidate genes at the age of 3 months. Data are presented in a log2 scale (blue: upregulated; red: downregulated). Rows indicate individual mice; columns represent particular genes. Each data point reflects the median expression of a particular gene resulting from 3-4 technical replicates, normalized to the mean expression value of the respective gene in C57BL/6 livers. **(B)** *In situ* hybridization of C57BL/6: *Ccl2* and *Egr1* antisense probes (age of 3 months). Multiple

scattered foci of hepatocyte-specific *LTα, LTβ, Cxcl10*, *Ccl2* and *Egr1* mRNA were detected (scale bar: 50µm).

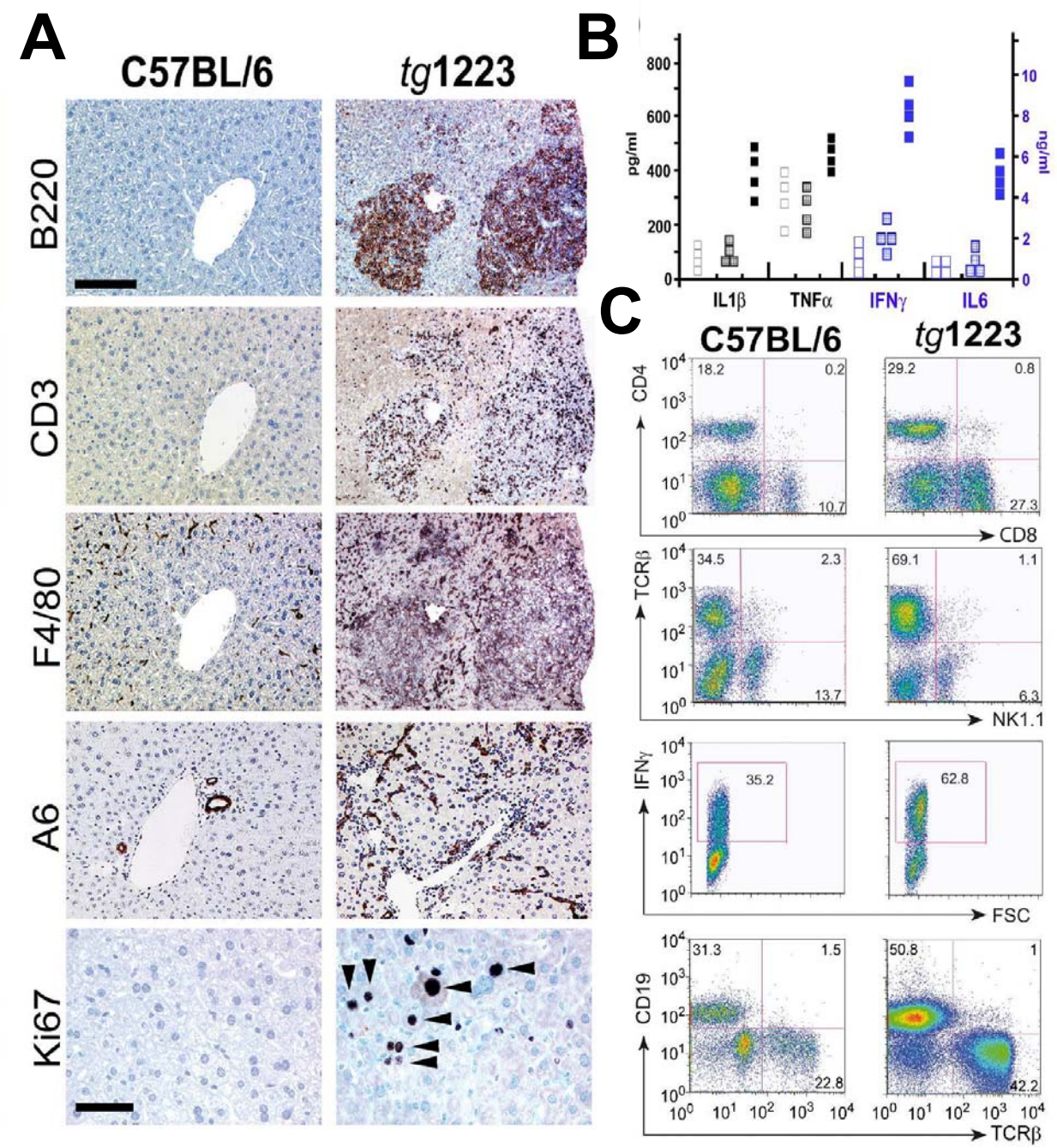

Figure 16: Characterization of *tg*1223 livers. (A) Immunohistochemical analysis of representative 9 month-old C57BL/6 and *tg*1223 livers. B220 stained B-cells, CD3 T-cells, F4/80 macrophages, Kupffer cells and A6 oval cells (scale bar: 150µm). Ki67^{+} proliferating hepatocytes (arrow heads) and inflammatory cells are indicated (scale bar: 50µm). **(B)** ELISA for IL1β, TNFα, IFNγ and IL6 in C57BL/6 (hollow symbols), *tg*1223 (filled symbols) or *tg*1222 (dotted symbols) liver homogenates (9 months). **(C)** Flow cytometry of intrahepatic lymphocytes at 9 months of age. CD4 (T-helper cells), CD8 (cytotoxic T-cells), TCRβ (T-cells), CD19 (B-cells), IFNγ (Interferon γ). IFNγ expression was monitored on CD4/CD8 gated T-cells. Representative flow cytometry analyses are shown. Numbers in each quadrant indicate the relative percentage of cells. Staining intensity is depicted on a log scale. FSC: Forward scatter.

At ≥9 months of age, *tg*1223 livers exhibited strong portal and lobular lymphocytic infiltrates (Fig. 16A). A pronounced influx of F4/80$^+$ macrophages and proliferation of A6$^+$ oval cells was observed. Chronic inflammation coincided with increased proliferating Ki67$^+$ hepatocytes (*tg*1223: 17±5 Ki67 cells/mm^2 liver section; C57BL/6: 0.5±0.3 Ki67$^+$ cells/mm^2 liver section; *P*=0.003), which was not significant in age-matched *tg*1222 livers (*P*=0.08; Fig. 16A; data not shown).

At this stage, hepatitis was accompanied by increased protein levels of IL1β (P=0.05), IFNγ (P=0.05) and IL6 (P=0.05) and, to a lesser degree, of TNFα in *tg*1223 livers. In tg1222 livers I observed only a slight elevation of these cytokines compared to C57BL/6 (Fig. 16B). Quantitative analysis of total intrahepatic lymphocytes revealed an increase in *tg*1223 livers (C57BL/6: 17-24x10^6 cells/liver; *tg*1223: 35-73x10^6 cells/liver P<0.05). Intrahepatic lymphocytes were further characterized by flow cytometry (Fig. 16C) in cooperation with Giandomenica Iezzi. Frequencies of CD8$^+$ (C57BL/6: 18±11%; *tg*1223: 38±10%), CD4$^+$ (C57BL/6: 16±3%; *tg*1223: 26±6%) and TCRβ$^+$ T-cells (C57BL/6: 33.5±9%; *tg*1223: 63.5±4%) were elevated (n=4), while NK1.1$^+$ cells (C57BL/6: 12±2%; tg1 223: 7±2%) were reduced in *tg*1223 livers. Furthermore, an increase in the frequency of CD19$^+$ B-cells was found in *tg*1223 livers (C57BL/6: 25±7%; *tg*1223: 52±4%). Elevated frequencies of IFNγ-producing CD4$^+$ and CD8$^+$ T-cells were found in *tg*1223 mice, while IL17-producing cells remained unchanged (Fig. 16C; data not shown).

1.6.6 LTα and LTβ overexpression induces hepatotoxicity

To determine whether chronic hepatitis leads to hepatocyte cell death in *tg*1222 or *tg*1223 mice, I analyzed serum transaminase levels (ALT and AST). From the age of 19 weeks on, serum ALT and AST levels were significantly elevated (*P*=0.05) in *tg*1223 but not in *tg*1222 mice (Fig. 17A).

In line, apoptotic hepatocytes were frequently detected in *tg*1223 mice (*tg*1223: 40.3±11.4 TUNEL$^+$ cells/mm^2 liver section; C57BL/6: 3.9±6.2 TUNEL$^+$ cells/mm^2 liver section; *P*=0.0005) but rarely in *tg*1222 and virtually absent in C57BL/6 mouse livers from the age of 6 months on (Fig. 17B and 19A, data not shown for *tg*1222 mice).

Hepatitis persisted in both transgenic lines for ≥18 months. Phenotypes were much milder in *tg*1222 mice, implying that the LT expression level determined the severity of inflammation and liver injury. Therefore, *tg*1223 mice were selected for additional experiments and further key results were obtained from this mouse line.

Nine month-old *tg*1223 and C57BL/6 livers were compared by DNA microarray and real-time PCR analysis. This revealed elevated mRNA expression of genes involved in embryogenesis (e.g. *Dmrta1*), liver inflammation (e.g. *Pbfe1*), carcinogenesis (e.g. *Phlda3, Thrsp*; (Kawase et al., 2009)), glucose homeostasis and insulin sensitivity (e.g. *Fgf21*), while mRNAs responsible for cell cycle control (*Gadd45g*) and protease inhibition (*SerpinA9*) were consistently downregulated (Fig. 19; data not shown). In contrast, genes found

to be strongly up- or downregulated at 3 months (Fig.15A) returned to normal levels in 9 month-old *tg*1223 livers, except *Lt*α and β mRNA, which remained at high levels. I found a significant upregulation of genes involved in cell division, liver inflammation, lipid metabolism, wound healing and tumorigenesis in 9 month-old compared to 3 month-old *tg*1223 livers (P<0.001). Genes involved in growth arrest and apoptosis were significantly downregulated (P<0.001) (Figs. 19 and 20; data not shown).

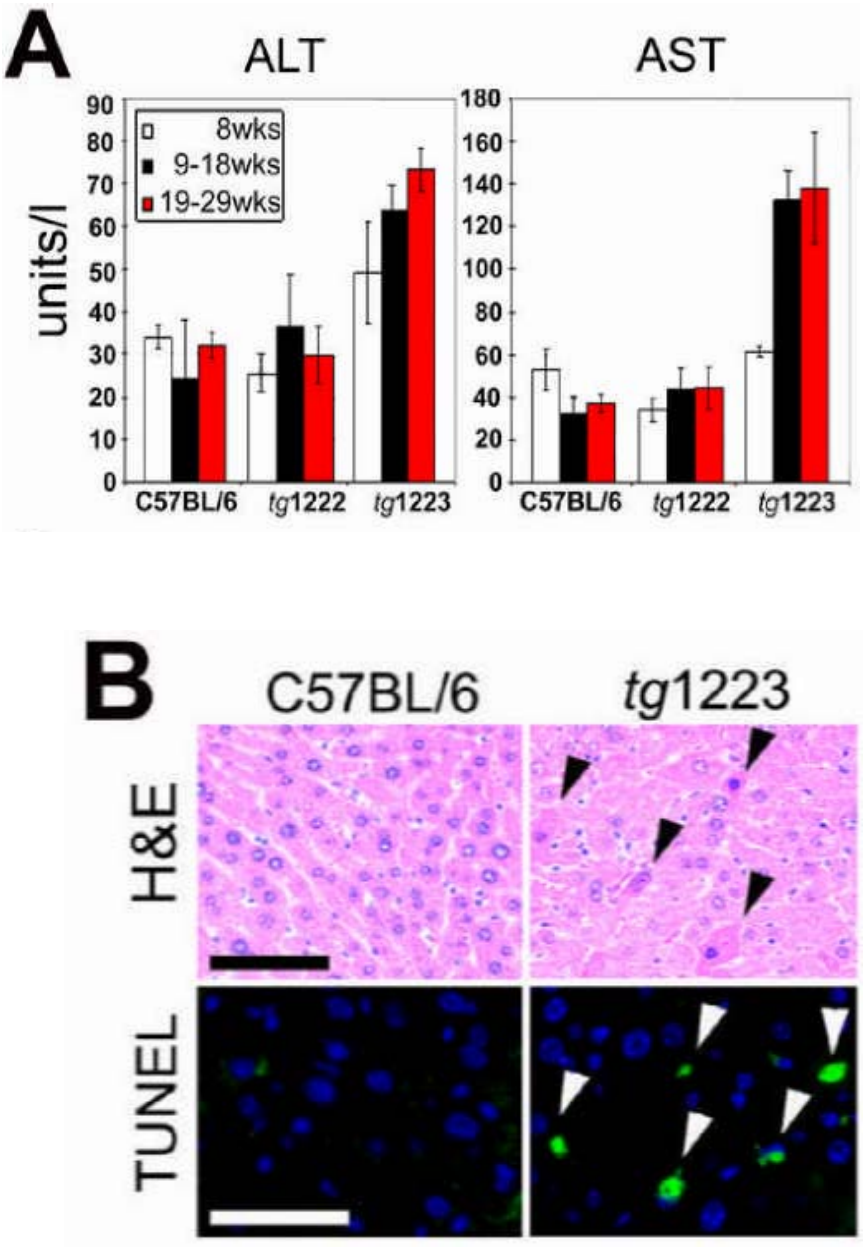

Figure 17: Chronic liver injury and HCC development in *tg*1223 mice. (A) Significant elevation of transaminases (ALT, AST) in sera of *tg*1223 mice from 19 weeks of age. Standard deviation (+/- SD) is indicated by error bars. **(B)** Increased hepatocyte cell death in *tg*1223 livers documented by H&E staining and TUNEL/DAPI assay. H&E: Hematoxylin & eosin: Black arrowheads indicate apoptotic hepatocytes. TUNEL: Green TUNEL$^+$ hepatocyte nuclei indicate apoptosis (white arrowheads; scale bars: 50μm).

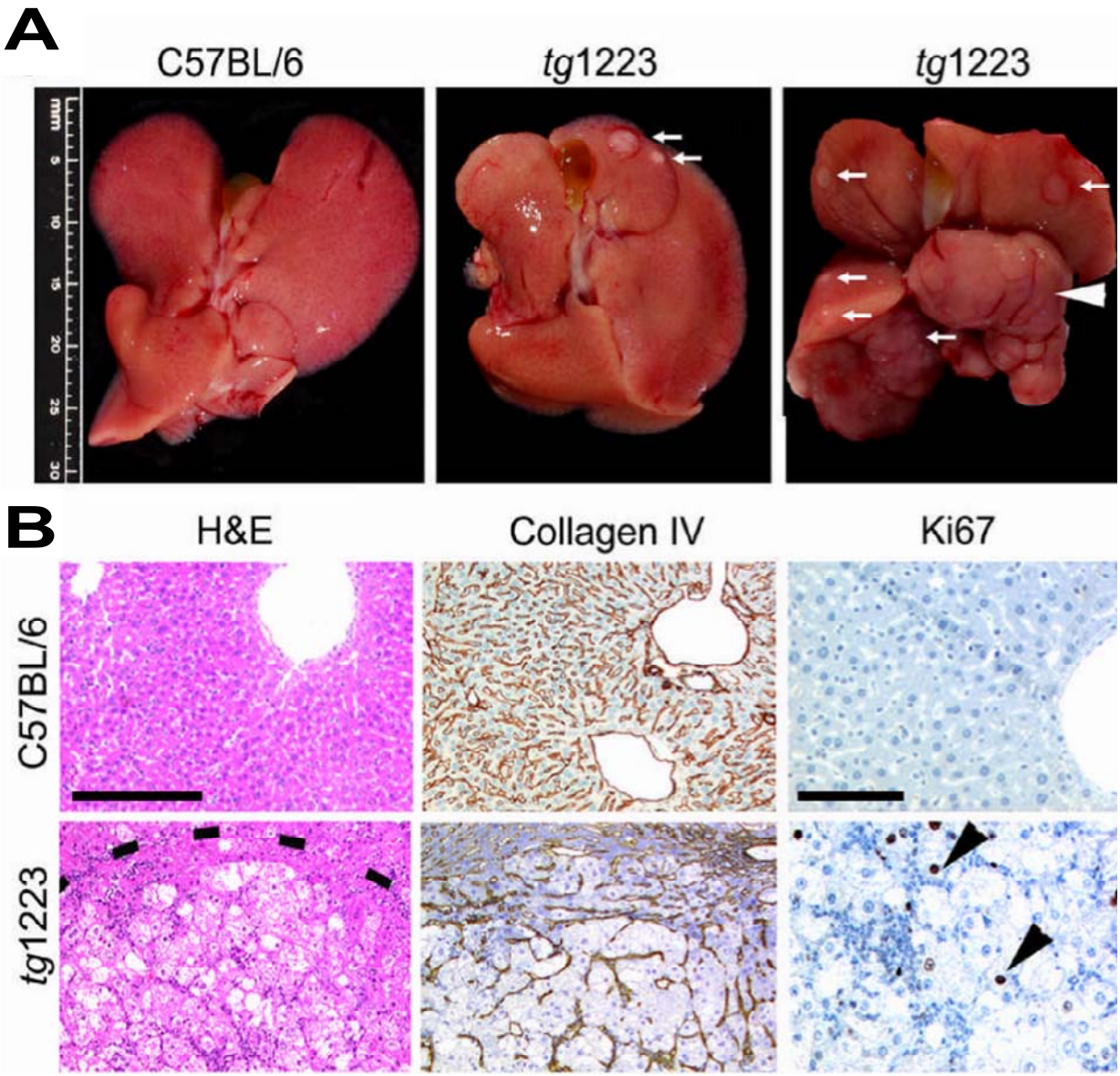

Figure 18: HCC development in *tg*1223 mice. (A) Macroscopy of C57BL/6 (left panel) and *tg*1223 livers at the age of 12 (middle panel) and 18 months (right panel). White arrows indicate tumor nodules. White arrowhead indicates a liver lobe completely affected by HCC. Scale bar size is indicated. **(B)** Histological analysis of livers derived from C57BL/6 and *tg*1223 mice. Dashed line depicts the HCC border. Collagen IV staining highlights the broadening of the liver cell cords and loss of collagen IV networks indicative of HCC in *tg*1223 mice (scale bar: 200µm). High numbers of $Ki67^+$ proliferating hepatocytes (arrowheads) are onlyfound in *tg*1223 HCC (rightcolumn; scale bar: 100µm).

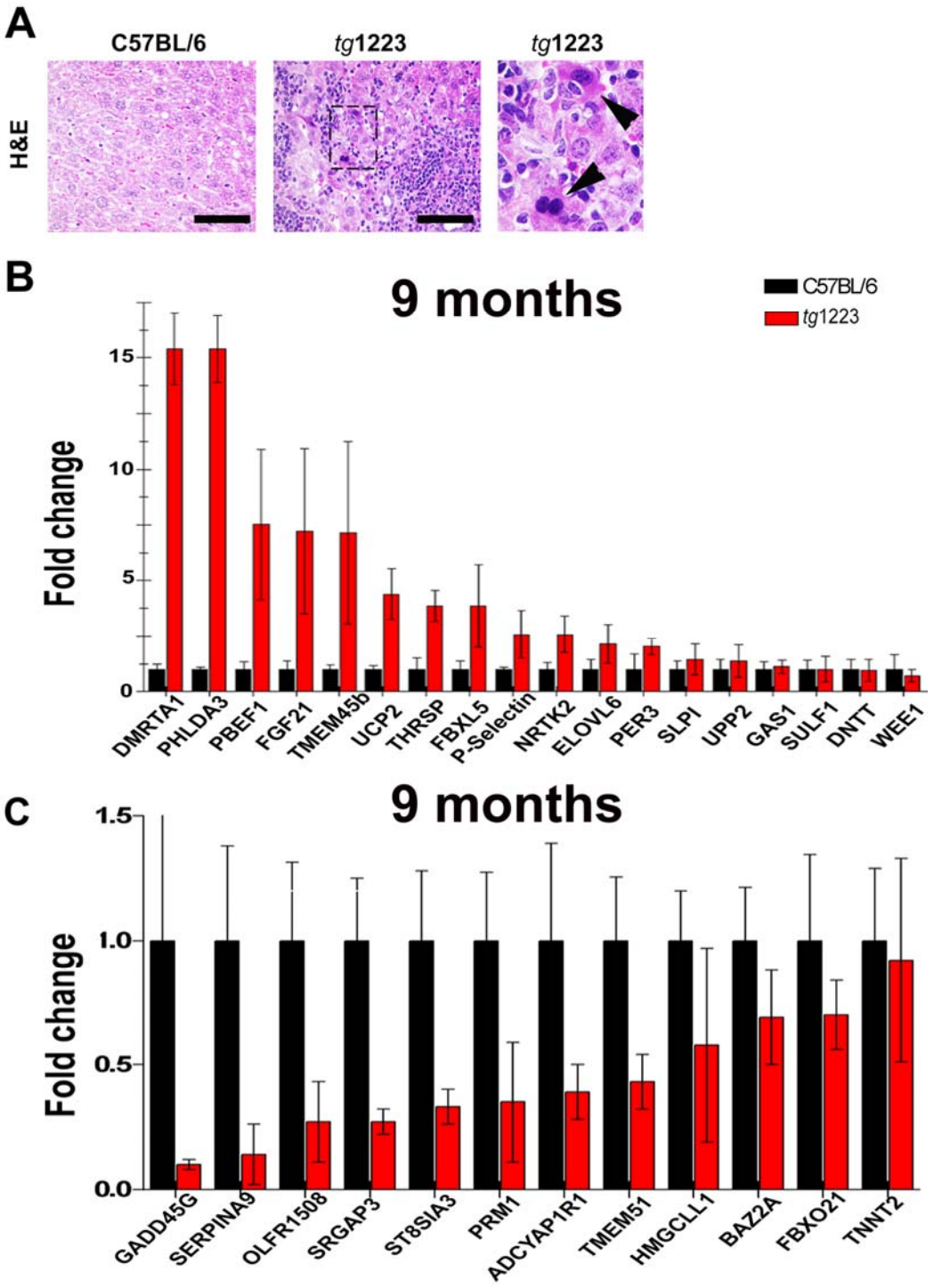

Figure 19: Hepatocyte apoptosis and analysis of mRNA expression in 9 month-old *tg*1223 compared to age-matched C57BL/6 livers. (A) Apoptotic hepatocytes were frequently observed in chronically inflamed *tg*1223 livers. Paraffin-sections of C57BL/6 and *tg*1223 livers were stained with H&E. Arrowheads indicate apoptotic hepatocytes with eosinophilic cytoplasms and shrunken nuclei surrounded by inflammatory cells in *tg*1223 but not in C57BL/6 livers at the age of 9 months. Right panel: insert with higher magnification. (scale bars: 100µm). **(B, C)** Based on a non-supervised DNA-microarray analysis, the expression of candidate genes was assessed by real-time PCR. Differences are reported as fold change. Standard deviation (+/- SD) is indicated by error bars. **(B)** At 9 months of age, strong upregulation of various genes involved in inflammatory processes and carcinogenesis (e.g. *Spl1, Dmrta1,*

Phlda3), cell adhesion and metastasis (e.g. *P-Selectin*), fibrogenesis (e.g. *Fgf21*), or carcinogenesis (*Nrtk2, Tmem45b*) were detected. **(C)** Genes responsible for cell cycle control (e.g. *Gadd45g*) were significantly downregulated in *tg*1223 livers compared to C57BL/6 livers at the same age.

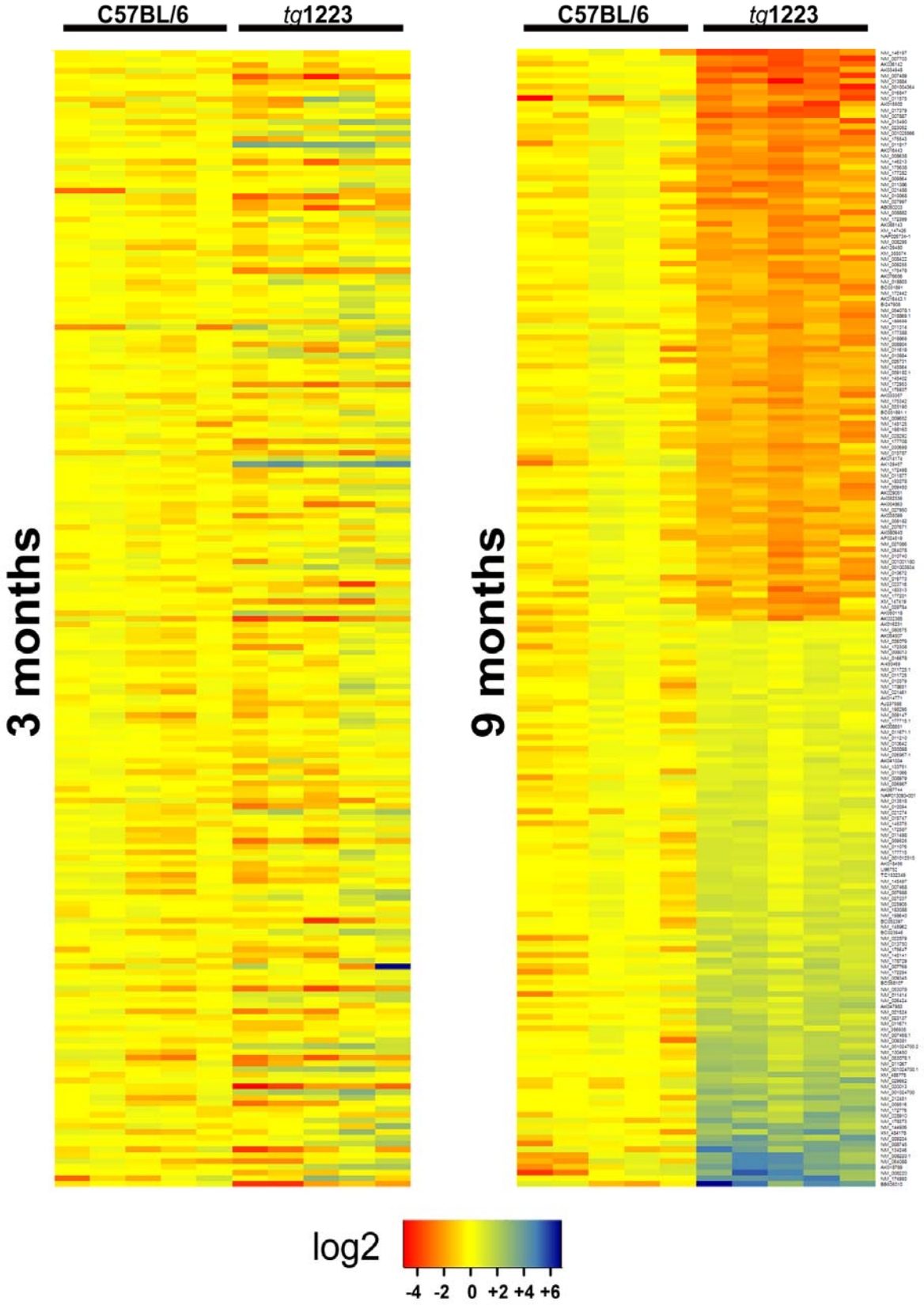

Figure 20: Analysis of mRNA expression in 9 month-old *tg*1223 compared to age-matched C57BL/6 livers. (A)

DNA-microarray analysis of C57BL/6 and *tg*1223 livers at 3 and 9 months of age. Indicated are the 100 highest up- and downregulated genes in 9 month-old *tg*1223 livers, when compared to 9 and 3 month-old C57BL/6 as well as 3 month-old *tg*1223 livers. Columns indicate individual mice; rows represent particular genes. Data are presented in a log2 scale (blue: upregulated; red: downregulated).

1.6.7 HCC development in *tg*1223 mice

At 12 months of age, about 20% (6/34) of *tg*1223 mice developed macroscopically visible nodules that classified histologically as HCC, including broadening of liver cell cords, loss of collagen IV networks and increased proliferative activity. In contrast, age-matched C57BL/6 livers lacked HCC (0/20; P=0.05) (Figs. 18A, B and Table 6 and 7). Tumor frequency increased with age reaching ~35% (18/51) by 18 months, whereas C57BL/6 mice did not develop HCC (0/35; P<0.0001) (Figs 19 - 21 and Table 6 and 7).

Table 6: Chronic hepatitis and HCC incidence in *tg*1223 mice, *tg*1223 mice intercrossed with various knockout mice. (A) Chronic hepatitis and HCC incidence in 12 month-old *tg*1223 and C57BL/6 mice. **(B)** Chronic hepatitis and HCC incidence in 18 month-old *tg*1223 and intercrossed *tg*1223 mice. Statistical evaluation: *, **, *** indicate the degree of statistical significance: * = p<0.05; ** = p<0.001; *** = p<0.0001.

A

12 months

C57BL/6		*tg*1223	
chronic hepatitis	HCC	chronic hepatitis	HCC
0/25	0/25	34/34	6/34

***

*

B

18 months

C57BL/6		*tg*1223		*tg*1223 x *Ikkβ*$^{\Delta hep}$		*tg*1223 x *Rag1*$^{-/-}$		*tg*1223 x *Tnfr1*$^{-/-}$	
chronic hepatitis	HCC	chronic hepatitis	HCC	chronic hepatitis	HCC	chronic hepatitis	HCC	chronic hepatitis	HCC
0/35	0/35	51/51	18/51	0/25	0/25	0/26	0/26	12/12	4/12

**

*** ***

***

Table 7: (A) *Tg*1223 and **(B)** *tg*1223/*tnfr1*$^{-/-}$ mouse identification number (mouse ID), mouse age and sex, numbers of HCC/entire liver and HCC characteristics (size, cytological features) are described. I have divided the cytological variants found in HCC based on the diameter of hepatocytes and the mitosis frequency detected. Small cell: hepatocytes with a diameter < 18 μm. Medium cell: hepatocytes with a diameter from 18 to < 21 μm. Large cell: hepatocytes with a diameter > 21 μm. Clear cell: Broad transparent cytoplasmic rim with strong increase of cytoplasm to nuclear ratio. All liver tumors were well differentiated HCC.

(A)

Mouse ID	Age (months)	Number of tumors	Largest tumor (mm)	Cytological variants	Sex (F/M)
1	12	4	2	Medium cell	F
2	12	2	5	Medium cell	M
3	12	3	4	Medium cell	F
4	12	2	12	Large cell	M
5	12	1	4	Medium cell	F
6	12	2	8	Large cell	M
7	18	7	9	Medium cell	M
8	18	10	11	Clear cell	M
9	18	2	25	Medium cell	M
10	18	1	4	Medium cell	F
11	18	3	12	Medium cell	F
12	18	1	16	Large cell	F
13	18	8	5	Clear cell	F
14	18	4	22	Medium cell	M
15	18	4	18	Small cell	M
16	18	5	9	Medium cell	M
17	18	10	4	Clear cell	F
18	18	2	17	Large cell	F
19	18	7	10	Medium cell	M
20	18	7	15	Clear cell	M
21	18	3	5	Small cell	M
22	18	5	7	Medium cell	M
23	18	2	6	Clear cell	F
24	18	2	3	Medium cell	F

(B)

Mouse ID	Age (months)	Number of tumors	Largest tumor (mm)	Tumor histology	Sex (F/M)
19	18	4	18	Medium cell	M
20	18	4	17	Medium cell	F
21	18	1	12	Clear cell	F
22	18	5	23	Medium cell	F

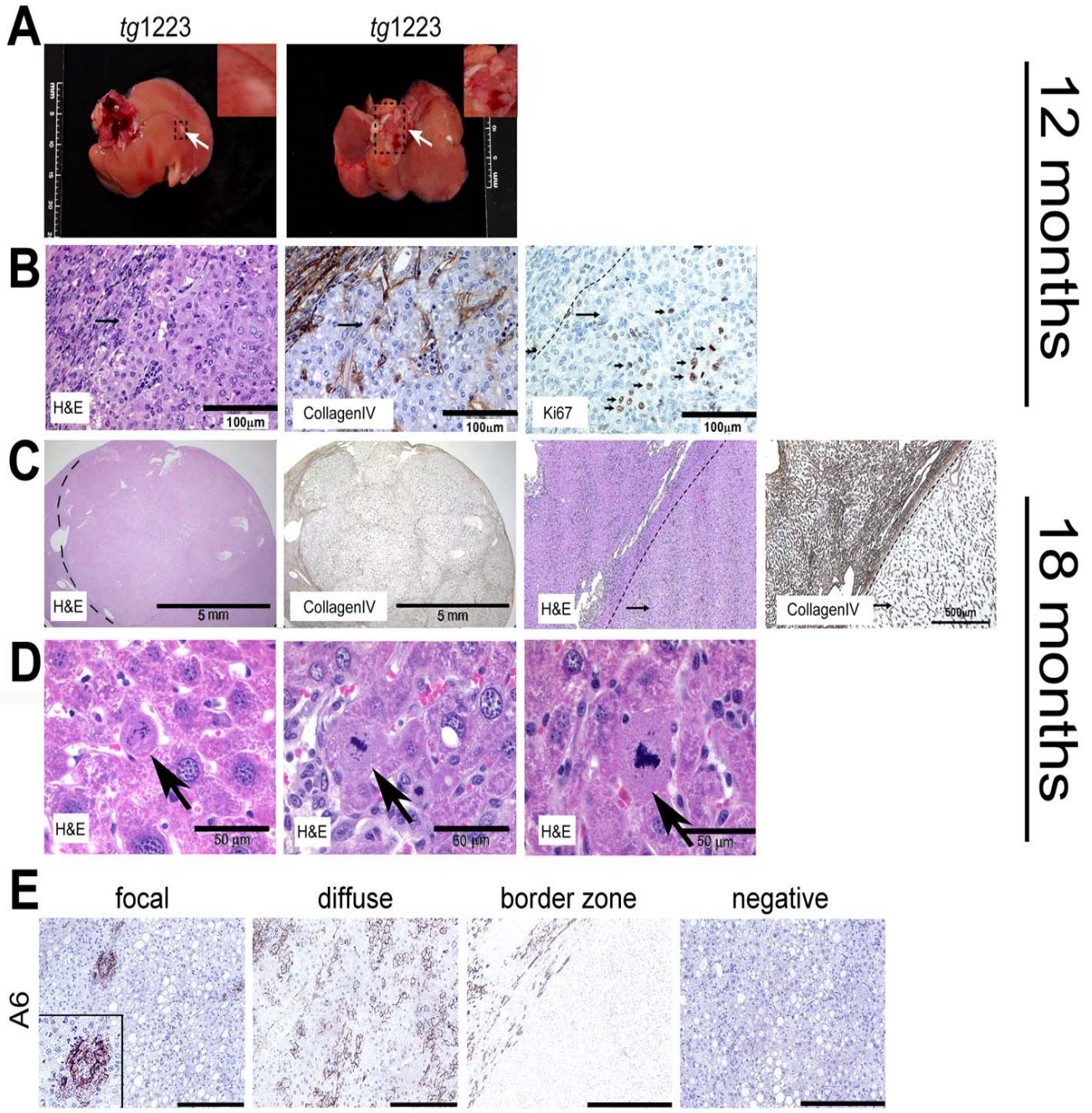

Figure 21: Macroscopic and histological analysis of HCC in 12 or 18 month-old *tg1223* livers. (A) Macroscopic analysis of *tg*1223 HCC from 12 month-old mice. White arrows indicate HCC nodules. (inserts with higher magnification). Size of scale bars is indicated. **(B)** Consecutive sections of a *tg*1223 HCC revealed broadening of liver cell cords, loss of collagen IV networks (H&E; Collagen IV; arrow), and increased proliferative activity of hepatocytes. Ki67 cells are indicated by short arrows (scale bar: 100μm). **(C)** Consecutive sections of a *tg*1223 HCC at the age of 18 months. The HCC compresses the adjacent hepatic parenchyma (scale bar: 5mm or 500μm, respectively). Broadening of liver cell cords and loss of collagen IV networks was detected (H&E; Collagen IV). **(D)** Higher magnification of H&E stained liver sections from 18 month-old *tg*1223 mice reveals cellular changes (arrows) including apoptosis (left panel) or frequently observed atypical mitoses (middle and right panel) in *tg*1223 hepatocytes. **(E)** Immunohistochemical analysis for $A6^+$ cells (presumably oval cells) in or around HCC. Approximately 45% of *tg*1223 HCC were composed of $A6^+$ cells, which were either focally or diffusely distributed. Other *tg*1223 HCC lacked $A6^+$ cells within the tumor (very right panel) but were surrounded by these cells at the border zone of the tumor (second right panel). Tumor border is marked by dashed line (scale bar: 200μm; insert: higher magnification). Tumors varied in size (1-25mm), histology and affected both genders with similar frequencies (males:females = 13:11; P=0 .3)(Fig. 18; Table 7).

1.6.8 Chromosomal aberrations and local spread of HCC in *tg*1223 mice

I further investigated micro-dissected *tg*1223 HCC (n=9) and age-matched C57BL/6 livers (n=5) for chromosomal aberrations. Array comparative genomic hybridization analysis (aCGH) revealed chromosomal aberrations in all *tg*1223 HCC (Fig. 22A and B; data not shown).

Amplifications and deletions of chromosomal regions ranged from ≤ 1 mega-base (MB) to 160 MB and were detected in most autosomes of all analyzed *tg*1223 HCC. Of note, the pattern of chromosomal aberrations varied in HCC from different individual *tg*1223 mice (P=0.34). For control, aCGH analysis of independent C57BL/6 liver DNA samples did not reveal significant chromosomal aberrations (data not shown).

I did not detect lung metastases but often saw multifocal intrahepatic disease in 18 month-old *tg*1223 mice. I therefore investigated whether multifocal *tg*1223 HCC represented intrahepatic spread of clonal tumors. Independent HCC (n=6) from different lobes of the same *tg*1223 liver were micro-dissected and subsequently analyzed by aCGH (Fig. 22B). All HCC taken from the same liver displayed significantly overlapping chromosomal aberrations throughout the entire genome (P<0.05), suggesting a clonal relationship of a tumor that has locally spread within the liver (Fig. 22B; data not shown).

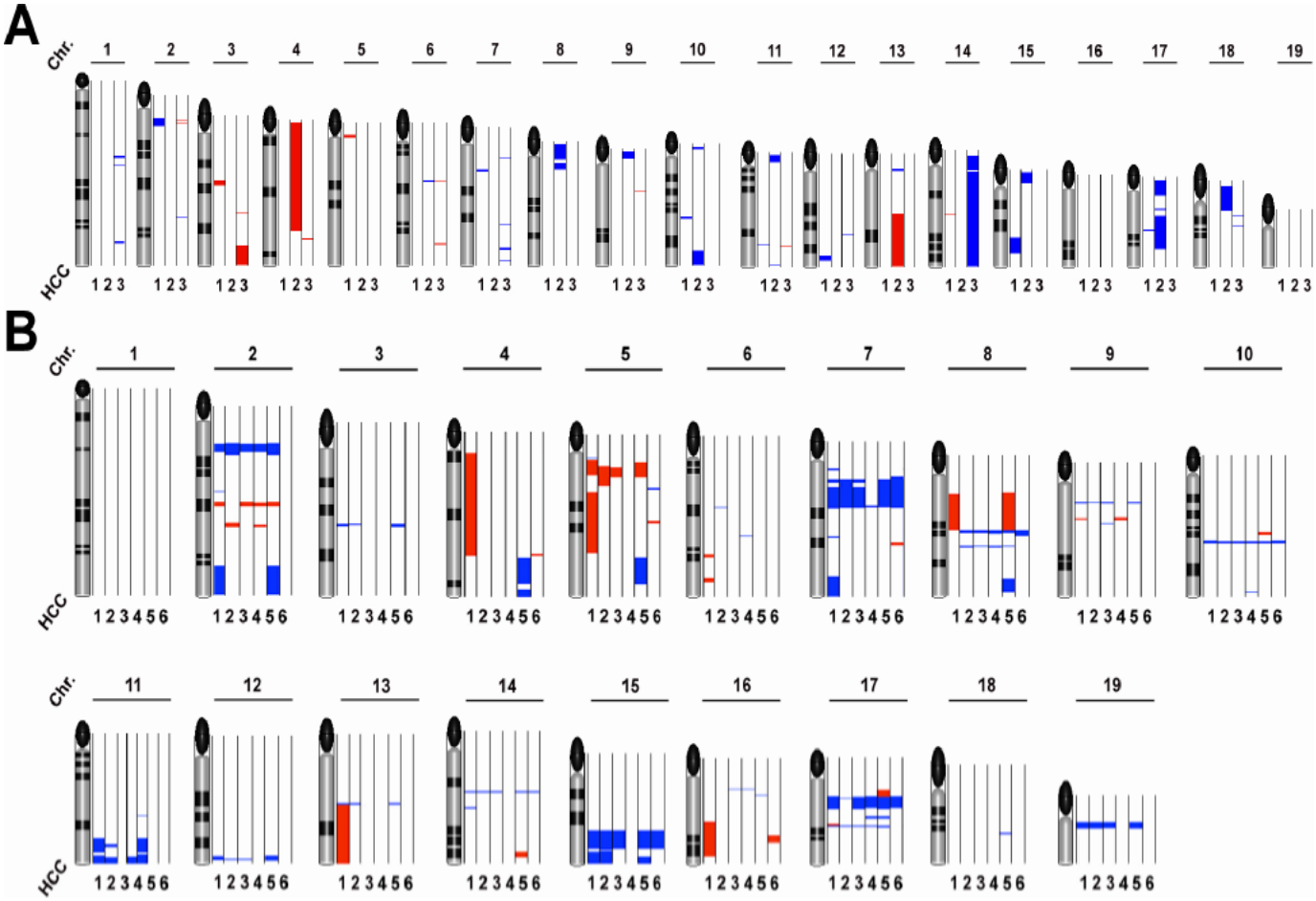

Figure 22: aCGH analysis of *tg*1223 HCC. The q-arm of each chromosome is shown and chromosome numbers are indicated. Black ellipses on the top of each q-arm represent the centromere. Dark horizontal bars within the symbolised chromosomes represent G bands. Chromosomal deletions are indicated in blue, amplifications in red (see methods for details). **(A)** HCC of individual *tg*1223 mice were hybridized against liver tissue of age matched C57BL/6 mice and analyzed by aCGH analysis. Columns next to each chromosome represent individual HCC (1; 2; 3) with numerous chromosomal aberrations on the q-arm of various autosomes. No common pattern of chromosomal aberrations could be detected. **(B)** aCGH analysis of six representative HCC (1, 2, 3, 4, 5 and 6) taken from different lobes of the same *tg*1223 liver.

1.6.9 Expression of tumor markers GP73, GS and AFP in *tg*1223 HCC

I then evaluated expression of human liver tumor markers golgi protein 73 (GP73), glutamine synthetase (GS) and α-fetoprotein (AFP) in *tg*1223 livers (Bachert et al., 2007; Marrero and Lok, 2004; Marrero et al., 2005; Sakamoto, 2009). GP73, GS and AFP protein expression was elevated in most *tg*1223 HCC as detected by immunohistochemistry and immunoblot analysis compared to C57BL/6 livers or unaffected liver regions adjacent to HCC (Fig. 23A-C; data not shown).

1.6.10 Mechanisms driving LTαβ-induced chronic hepatitis and liver cancer

To identify other receptors and molecular mediators potentially involved in LT-induced chronic hepatitis and HCC development, I intercrossed *tg*1223 with *Tnfr1*$^{-/-}$, *Tnfr2*$^{-/-}$ or *Ikkβ*$^{\Delta hep}$ mice. The requirement of lymphocytes in chronic hepatitis and HCC formation was investigated by intercrossing with *Rag1*$^{-/-}$ mice, which lack mature lymphocytes.

The absence of IKKβ, TNFR1 or lymphocytes per se did not appear to influence transgenic *LTα and LTβ* mRNA expression (Figs. 15A and 23D; data not shown). Initially, at three months of age, *tg*1223/*Ikkβ*$^{\Delta hep}$, *tg*1223/*Tnfr1*$^{-/-}$, *tg*1223/*Tnfr2*$^{-/-}$ and *tg*1223/*Rag1*$^{-/-}$ mice lacked histological evidence of hepatitis similar to *tg*1223 mice (data not shown). The aberrant hepatic gene expression pattern described for 3 month-old *tg*1223 mice developed only partially in *tg*1223/*Ikkβ*$^{\Delta hep}$ and *tg*1223/*Rag1*$^{-/-}$ mice, whereas *tg*1223/*Tnfr1*$^{-/-}$ livers displayed an expression profile rather similar to that of *tg*1223 mice (Figs. 21 and 23D).

At 9 months of age *tg*1223/*Rag1*$^{-/-}$ (n=26) and *tg*1223/*IKKβ*$^{\Delta hep}$ (n=18) livers lacked hepatitis, hepatocyte or oval-cell proliferation (Fig. 24), whereas *tg*1223/*Tnfr1*$^{-/-}$ (n=8) or *tg*1223/*Tnfr2*$^{-/-}$ (n=8) livers were indistinguishable from those of *tg*1223 mice (Figs. 21, 24A and B). At this age inflammatory foci were detectable in *tg*1223 and *tg*1223/*IKKβ*^{FF} livers. In contrast, no inflammation could be observed in livers of C57BL/6, *IKKβ*$^{\Delta hep}$ and *tg*1223/*IKKβ*$^{\Delta hep}$ mice. Further investigation of liver paraffin sections of 9 month-old *tg*1223/*Tnfr1*$^{-/-}$ and *tg*1223/*Tnfr2*$^{-/-}$ mice showed severe inflammation within the liver while age-matched *Tnfr1*$^{-/-}$ and *Tnfr2*$^{-/-}$ mice lacked signs of chronic hepatitis (Figs. 25 and 26).

At the age of 18 months, *tg*1223/*Rag1*$^{-/-}$ (n=26) and *tg*1223/*IKKβ*$^{\Delta hep}$ (n=25) mice were devoid of hepatitis and HCC (P<0.0001) (Fig. 24C; Table 6) suggesting that both lymphocytes and hepatocyte-specific IKKβ expression are required for LT-induced chronic hepatitis and HCC development. Notably, *tg*1223/*tnfr1*$^{-/-}$ mice displayed HCC (4/12) with an incidence similar to *tg*1223 mice (Figs. 24C; Table 6 and 7) indicating that TNFR1 signaling is not essential for LT-induced HCC formation in *tg*1223 mice.

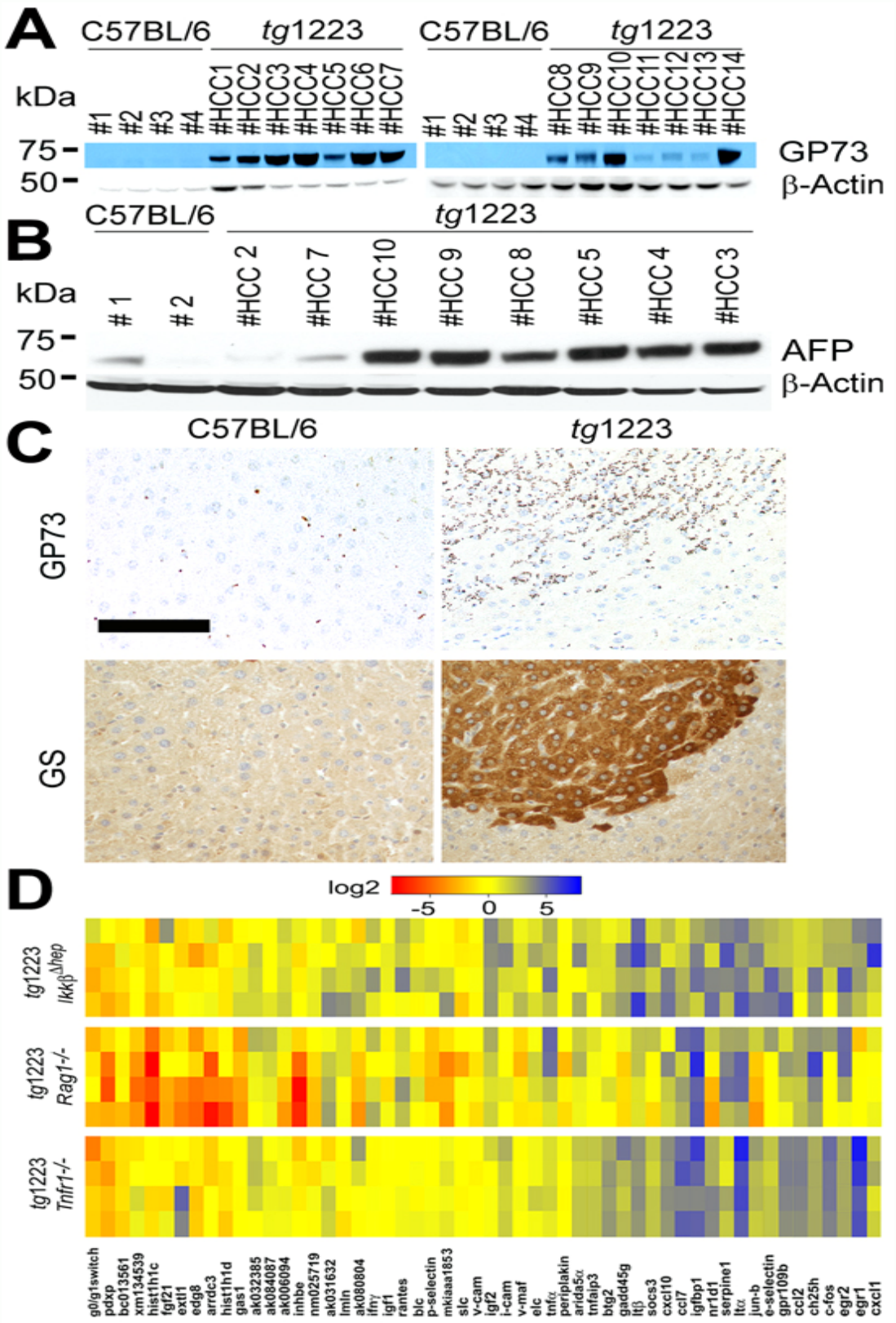

Figure 23: Expression of tumor markers in *tg*1223 HCC and mechanistic characterization of liver carcinogenesis in *tg*1223 mice. (A) Immunoblot analysis of C57BL/6 and *tg*1223 HCC homogenates for GP73. Strong to moderate signal intensities were detected in all *tg*1223 HCC, but not in C57BL/6 livers. **(B)** Immunoblot

analysis of C57BL/6 and *tg*1223 HCC homogenates for AFP. β-Actin served as a loading control (kDa: kilo Dalton). **(C)** Immunohistochemistry for GP73 and GS in a representative *tg*1223 HCC and age-matched C57BL/6 control (scale bar: 100tm). **(D)** mRNA expression of candidate genes in livers of 3 month-old *tg*1223/*Ikkβ*$^{\Delta hep}$, *tg*1223/*Rag1*$^{-/-}$ and *tg*1223/ *TNFR1*$^{-/-}$ mice. Data are presented in a log2 scale (blue: upregulated; red: downregulated). Rows indicate individual mice; columns represent particular genes. Each data point reflects the median expression of a particular gene resulting from 3-4 technical replicates, normalized to the mean expression value of the respective gene in C57BL/6 livers.

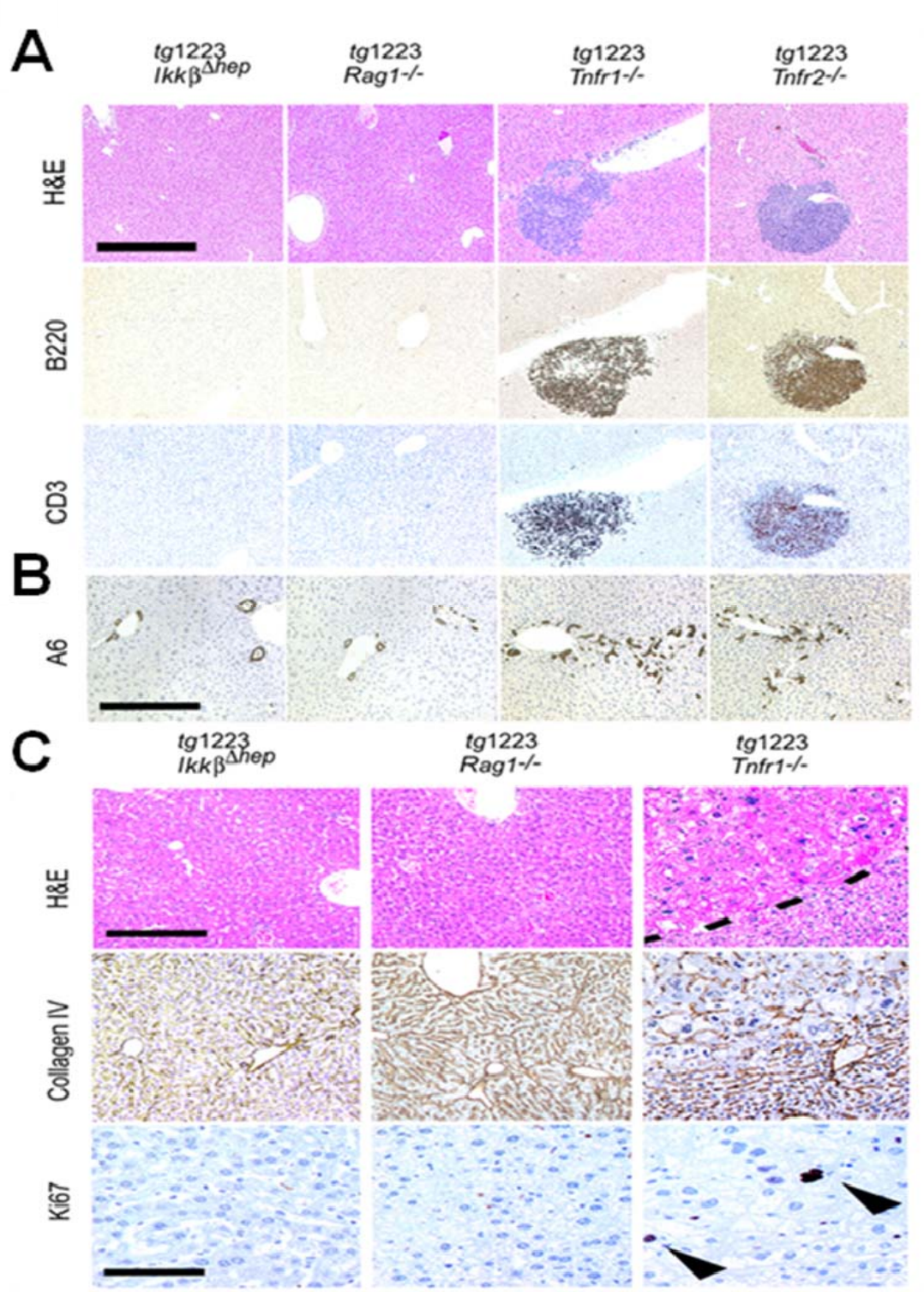

Figure 24: Expression of tumor markers in *tg*1223 HCC and mechanistic characterization of liver carcinogenesis in *tg*1223 mice. (A) Histological analysis of *tg*1223/*Ikkβ*$^{\Delta hep}$, *tg*1223/*Rag1*$^{-/-}$, *tg*1223/*TNFR1*$^{-/-}$ and *tg*1223/*TNFR2*$^{-/-}$ livers at 9 months of age. H&E, B220 for B-cells, CD3 for T-cells (scale bar: 500µm). **(B)** Immunohistochemical analysis of A6^{+} cells (oval cells) in livers of *tg*1223/*Ikkβ*$^{\Delta hep}$, *tg*1223/*Rag1*$^{-/-}$, *tg*1223/*Tnfr1*$^{-/-}$, and *tg*1223/*Tnfr2*$^{-/-}$ mice at 9 months of age (scale bar: 500µm). **(C)** Immunohistochemical analysis of *tg*1223/*Ikkβ*$^{\Delta hep}$, *tg*1223/*Rag1*$^{-/-}$, and *tg*1223/*Tnfr1*$^{-/-}$ livers (18 months of age). Dashed line depicts the HCC border (upper row; scale bar: 200µm). Collagen IV staining highlights the broadening of liver cell cords and loss of collagen IV networks in *tg*1223/*Tnfr1*$^{-/-}$ HCC. Ki67^{+}-proliferating hepatocytes are indicated by arrowheads (lower row; scale bar: 50µm).

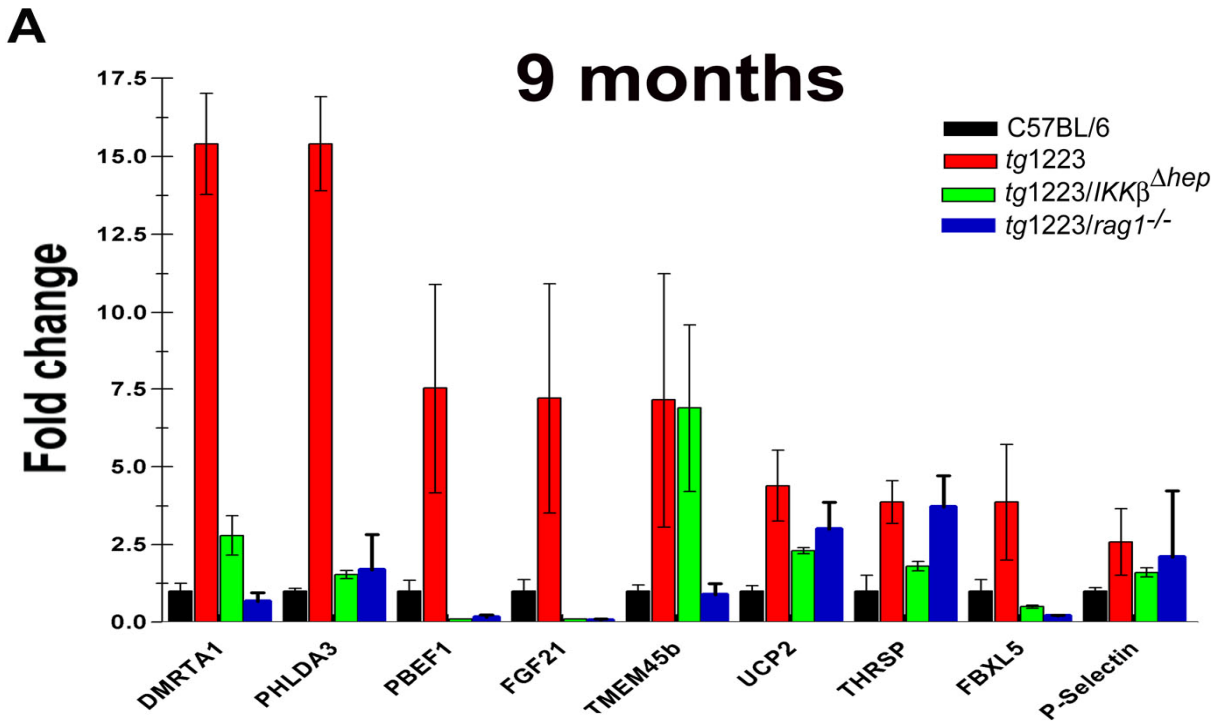

Figure 25: mRNA expression analysis of 9 month-old *tg1223*, *tg*1223/*IKKβ*$^{\Delta hep}$ and *tg*1223/*Rag1*$^{-/-}$ compared to age-matched C57BL/6 livers. Based on a non-supervised DNA-microarray analysis expression of candidate genes was assessed by real-time PCR. Differences are reported as fold change. Backcrossing of *tg*1223 mice to *IKKβ*$^{\Delta hep}$ or to *Rag1*$^{-/-}$ mice resulted in a significant downregulation of some genes that were highly upregulated in 9 month-old *tg*1223 livers (*Dmrta1, Phlda3, Pbef1, Fgf21; P*=0.05). Standard deviation (+/- SD) is indicated by error bars.

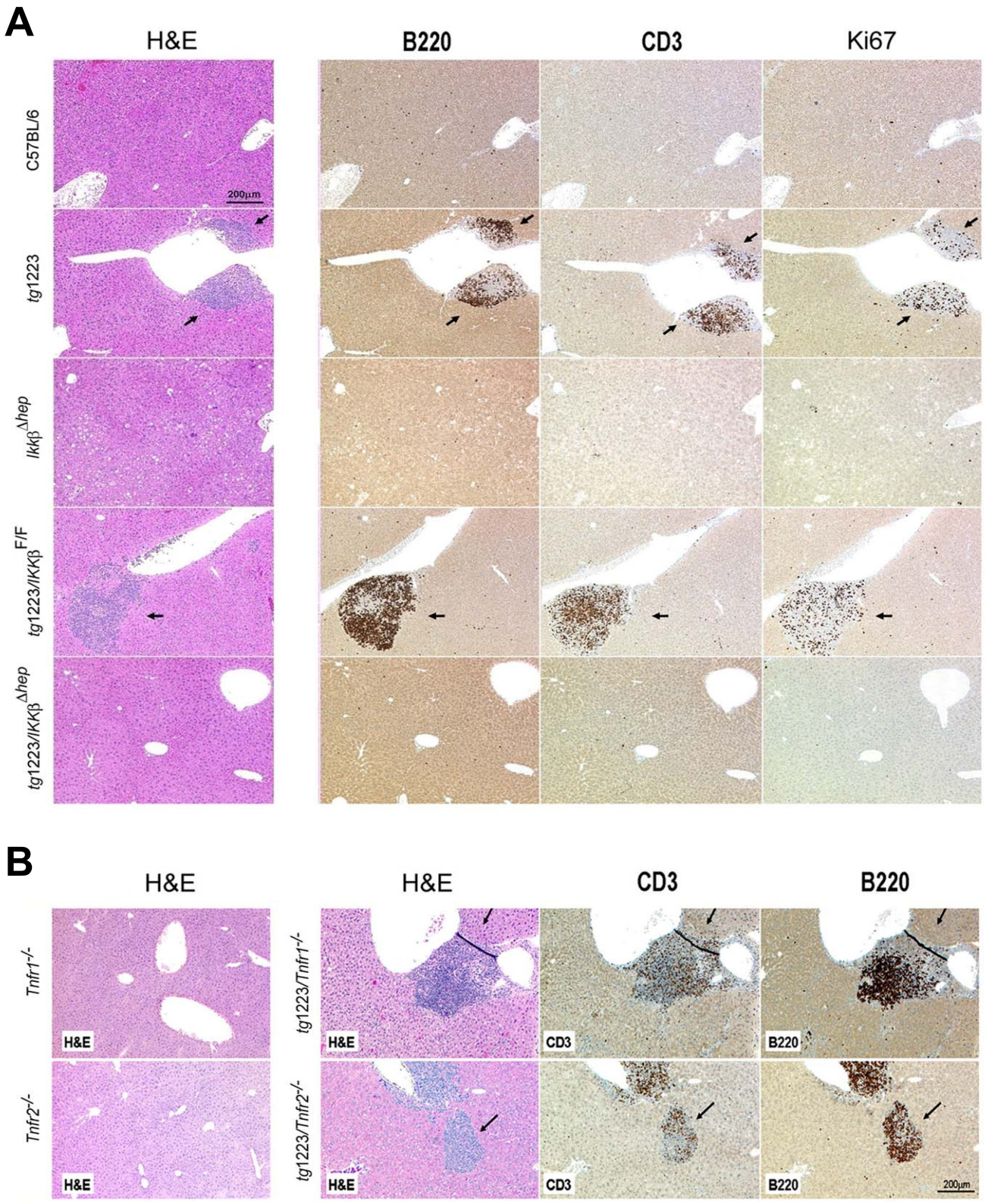

Figure 26: Histological analysis of 9 month-old *tg1223*, *tg*1223/*IKKβ*$^{\Delta hep}$ and *tg*1223/*Rag1*$^{-/-}$ compared to age-matched C57BL/6 livers. (A) Hepatocyte-specific deletion of *IKKβ*$^{\Delta hep}$ prevents LTαβ-induced inflammation in livers of *tg*1223 mice, whereas depletion of *TNFR1* or *TNFR2* does not affect chronic hepatitis development in *tg*1223 mice. Histological and immunohistological analysis of liver paraffin sections from 9 month-old C57BL/6, *tg*1223,

IKKβ$^{\Delta hep}$, *tg*1223/*IKKβ*^{FF}, and *Tg1223* /*IKKβ*$^{\Delta hep}$ mice. Sections were stained with H&E and antibodies detecting B- (B220), T- (CD3), and proliferating cells (Ki67). This revealed inflammatory foci in *tg*1223 and *tg*1223/*IKKβ*^{FF} livers. In contrast, no inflammation was observed in livers of C57BL/6, *IKKβ*$^{\Delta hep}$ and *tg*1223/*IKKβ*$^{\Delta hep}$ mice (scale bar:200 μm). **(B)** Immunohistological analysis of liver paraffin sections of 9 month-old *tg*1223/*Tnfr1*$^{-/-}$ and *tg*1223/*Tnfr2*$^{-/-}$ mice. Consecutive liver sections were stained with H&E and with antibodies detecting T- (CD3), and B-cells (B220). Age-matched *Tnfr1*$^{-/-}$ and *Tnfr2*$^{-/-}$ mice lacked signs of chronic hepatitis. Arrows denote foci of lymphocytic inflammation (scale bar: 200μm).

1.6.11 Hepatocytes are the major responsive liver cells to agonistic LTβR antibody treatment

To investigate whether hepatocytes represent the major LT-responsive liver cells and to investigate LTβR signaling in *Tnfr1*$^{-/-}$ and *Ikkβ*$^{\Delta hep}$ livers, TNFα (positive control), agonistic LTβR antibody (3C8) and appropriate negative controls (PBS; rat IgG) were administered intravenously (i.v.) to C57BL/6 and various knock-out mice (Figs. 27-30; Table 7). Administration of 3C8 induced nuclear p65 translocation primarily in hepatocytes and some NPC of C57BL/6 livers (Fig. 27A), as well as transcriptional changes and upregulation of selected chemokines reminiscent of those observed in 3 month-old *tg*1223 livers (Fig. 27A). Similar results were obtained after 3C8 treatment of *Tnfr1*$^{-/-}$ mice, in contrast to *IKKβ*$^{\beta hep}$ livers which were devoid of nuclear p65 translocation in hepatocytes and NPC (Fig. 27A).

As expected, TNFα but not PBS treatment induced nuclear p65 translocation in hepatocytes and NPC of C57BL/6 mice. Moreover, transcription of selected NF-κB target genes was elevated in these mice similar to livers from 3 month-old *tg*1223 mice. Livers of TNFα treated *Ikkβ*$^{\Delta hep}$ mice did not exhibit nuclear p65 translocation in hepatocytes but did in NPC. However, this sufficed to upregulate selected NF-κB target genes. Livers of TNFα treated *ltβR*$^{-/-}$ mice were indistinguishable from TNFα treated C57BL/6 livers.

Furthermore, upregulation of selected NF-κB target genes could not be detected. For control, *LtβR*$^{-/-}$ mice were treated with 3C8, lacking nuclear p65 translocation in hepatocytes or NPC as well as upregulation of selected NF-κB target genes.

To examine whether lack of functional IKKα on hepatocytes and NPC would suppress LTβR induced upregulation of selected NF-κB responsive genes, I investigated livers of mice expressing a non-phosphorylatable *Ikkα*$^{AA/AA}$ knock-in allele (*Ikkα*$^{AA/AA}$; (Cao et al., 2001). Upon 3C8 treatment *Ikkα*$^{AA/AA}$ mice upregulated selected NF-κB responsive genes (Fig. 29). The degree of mRNA upregulation in liver was similar to 3C8-treated C57BL/6 mice. In contrast, control treated (rat IgG) *Ikkα*$^{AA/AA}$ mice lacked upregulation of selected NF-κB responsive genes. This suggests that 3C8-mediated hepatic LTβR signaling is mainly integrated by hepatocytes involving canonical NF-κB pathway.

Moreover increased levels of chemokines were detectable in sera and liver homogenates of C57BL/6 mice

after 3C8 but not after rat IgG treatment (Figure 30):

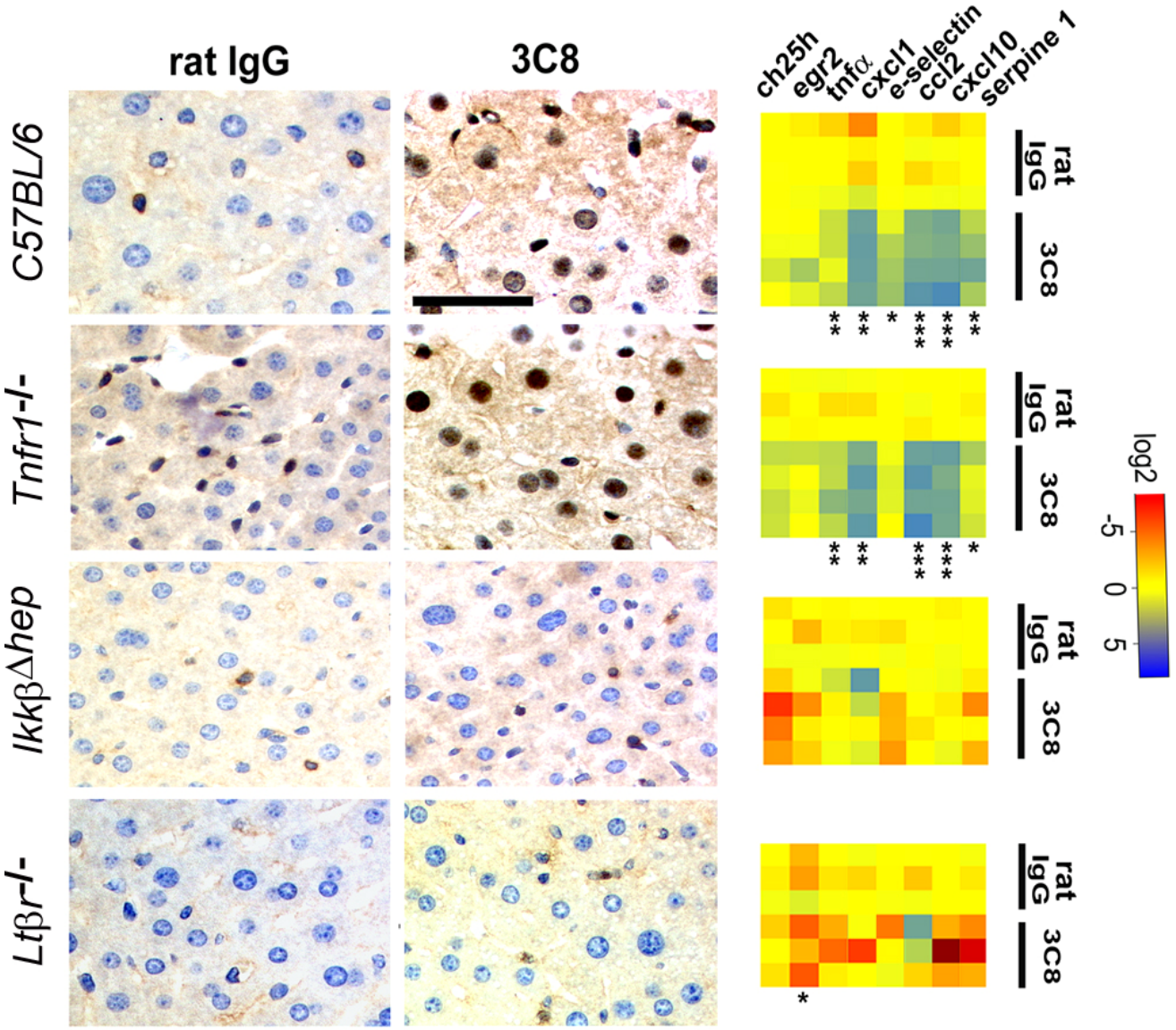

Figure 27: Effects of acute 3C8 treatment in mice. Immunohistochemical analysis of nuclear p65 translocation and real-time PCR for mRNA expression of selected NF-κB target genes in livers of C57BL/6 and various knock-out mice treated with 3C8. Data are presented on a log 2 scale (blue: upregulated; red: downregulated). Rows indicate individual mice; columns represent particular genes. Each data point reflects the median expression value of a particular gene resulting from 3-4 technical replicates, normalized to the mean expression value of the respective gene in C57BL/6 livers. (scale bar: 50tm). Expression data are depicted according to treatment group: rat IgG (control) or 3C8 (LTI 3R agonist). Statistical significance was evaluated by t-test: * = $p \leq 0.05$; ** = $p < 0.001$; *** = $p < 0.0001$.

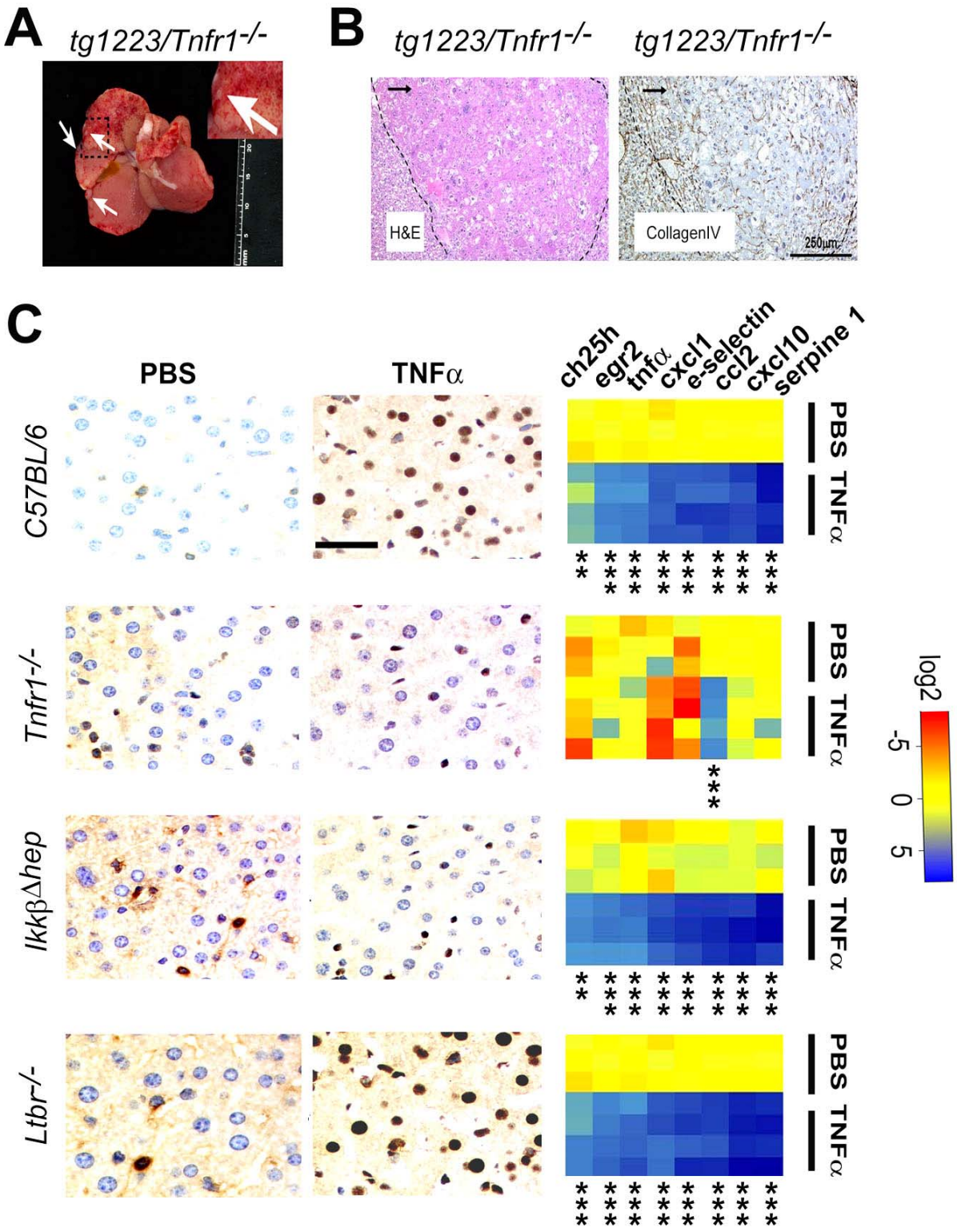

Figure 28: Macroscopy and histology of 18 month-old *tg*1223/*Tnfr1*$^{-/-}$ HCC, as well as molecular and histological characterization of hepatic signaling induced by acute TNFα treatment. (A) Macroscopic analysis of *tg*1223/*Tnfr1*$^{-/-}$ HCC (white arrows indicate liver tumors; insert, higher magnification). **(B)** Consecutive paraffin sections of a *tg*1223/*Tnfr1*$^{-/-}$ HCC compressing the adjacent hepatic parenchyma. Dashed lines indicate the border zone of the HCC. Arrow highlights the tumor nodule. Collagen IV stain reveals abnormally broad liver cell plates (scale bar: 250µm). **(C)** Immunohistochemical analysis of nuclear p65 translocation and real-time PCR for mRNA

expression of selected NF-κB target genes. Data are presented on a log2 scale (blue: upregulated; red: downregulated). Rows indicate individual mice; columns represent particular genes. Each data point reflects the median expression value of a particular gene resulting from 3-4 technical replicates 45 min after treatment. Data points were normalized to the mean expression value of the respective gene in C57BL/6 livers. Statistical significance was evaluated by t-test: * = p≤0.05; ** = p<0.001; *** = p<0.0001.

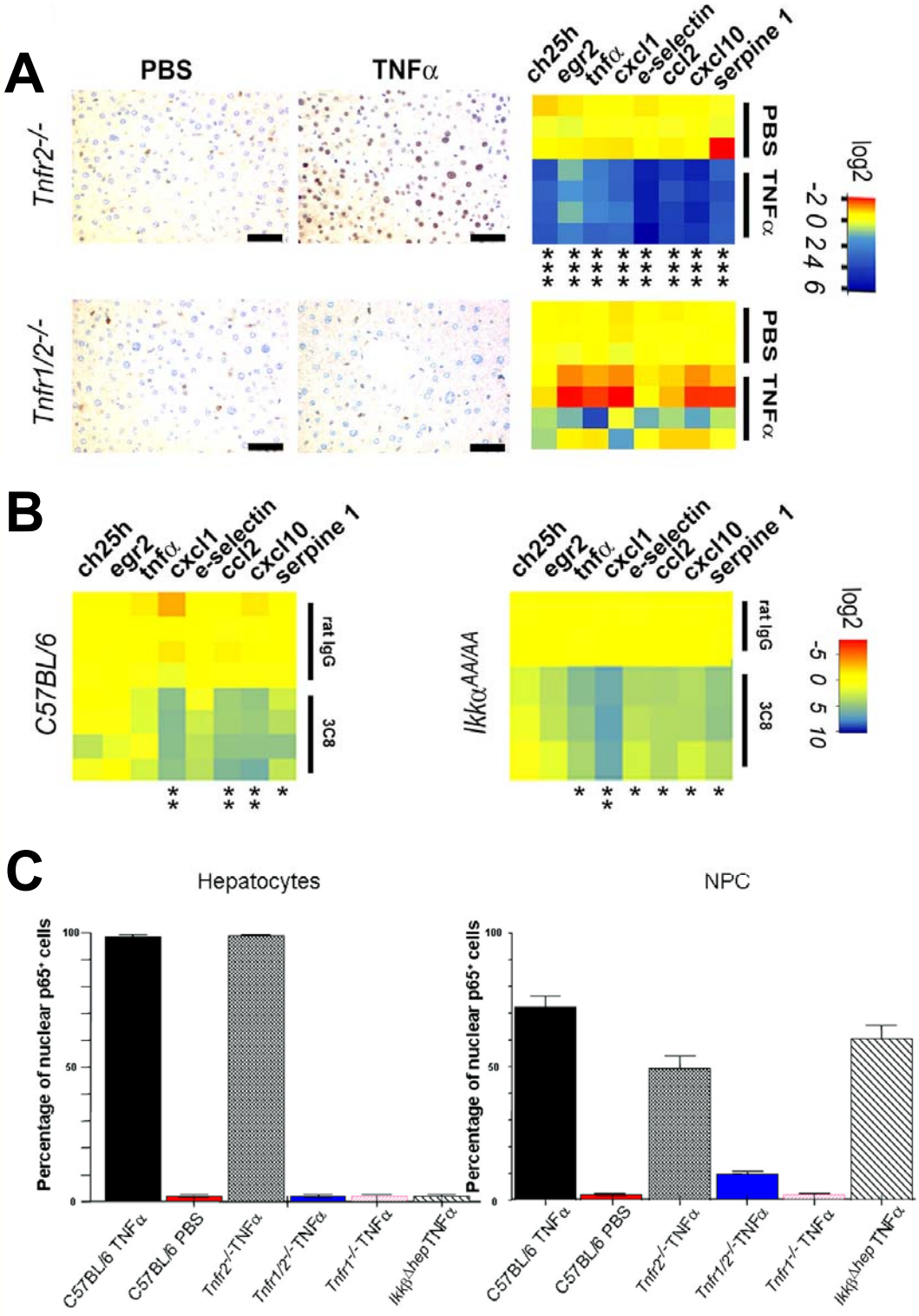

Figure 29: Molecular and histological characterization of hepatic signaling induced by acute TNFα treatment.

Results

(A) Immunohistochemical analysis of nuclear p65 translocation and **(A, B)** real-time PCR for mRNA expression of selected NF-κB target genes. Data are presented on a log2 scale (blue: upregulated; red: downregulated). Rows indicate individual mice; columns represent particular genes. Each data point reflects the median expression value of a particular gene resulting from 3-4 technical replicates 45 min after treatment. Data points were normalized to the mean expression value of the respective gene in C57BL/6 livers. Statistical significance was evaluated by t-test: * = $p \leq 0.05$; ** = $p < 0.001$; *** = $p < 0.0001$. **(A)** Acute i.v. administration of TNFα in *Tnfr2*$^{-/-}$ livers caused nuclear p65 translocation in hepatocytes and NPC, as well as elevated expression of selected NF-κB target genes (e.g. *Ch25h, Egr2, Cxcl1, Ccl2, Cxcl10*) (scale bar: 50µm). In contrast, acute i.v. administration of TNFα in *Tnfr1/2*$^{-/-}$ mice failed to induce nuclear p65 translocation in hepatocytes and NPC, as well as upregulation of selected NF-κB target genes (scale bar: 50µm). The described changes upon TNFα treatment were mainly TNFR1-mediated. *Tnfr1*$^{-/-}$ or *Tnfr1/2*$^{-/-}$ livers lacked nuclear p65 translocation in hepatocytes or NPC, as well as upregulation of all selected NF-κB target genes except *Ccl2*. **(B)** Selected NF-κB target genes were also investigated in livers of *Ikkα*$^{AA/AA}$ (right panel) and C57BL/6 (left panel) mice either treated with 3C8 or rat IgG. **(C)** Quantification of p65^{+}- hepatocytes and NPC after TNFα treatment in C57BL/6, *Tnfr1*$^{-/-}$, *Tnfr2*$^{-/-}$, *Tnfr1/2*$^{-/-}$ and *Ikkβ*$^{\Delta hep}$ livers. Percentages of nuclear p65^{+} hepatocytes or NPC/ mm^2 liver section are indicated. Acute i.v. administration of TNFα into *Tnfr1*$^{-/-}$, *Tnfr1/2*$^{-/-}$ and *Ikkβ*$^{\Delta hep}$ livers failed to induce nuclear p65 translocation in hepatocytes, whereas TNFα injection into C57BL/6 or *Tnfr2*$^{-/-}$ mice caused hepatic nuclear p65 translocation. The same results were found for NPC; apart from pronounced nuclear p65 translocation detected in TNFα-treated *Ikkβ*$^{\Delta hep}$ livers. Standard deviation (+/- SD) is indicated by error bars. Nuclear p65 (RelA) translocation in hepatocytes and non-parenchymal cells (NPC: e.g. Kupffer cells, lymphocytes), alterations in the hepatic transcriptome and protein expression of selected chemokines were examined.

Table 7: Hepatocytes are the major LT responsive liver cell type. Nuclear p65 translocation was analyzed in hepatocytes and NPC and mRNA expression of selected NF-κB target genes was quantified in C57BL/6 or knockout livers. (-) indicates that the number of cells with nuclear p65 translocation does not exceed the one of the background controls. (+) indicates that nuclear p65 translocation does exceed the background controls. (%) indicates the percentage of a particular cell type displaying nuclear p65 translocation.

Acute PBS or TNFα administration

Mouse genotype	Nuclear p65 translocation in hepatocytes	Nuclear p65 translocation in NPC	Upregulation of NF-κB target genes	Treatment
C57BL/6	-	-	-	PBS
	+ (95±3%)	+ (73±6%)	+	TNFα
tnfr1-/-	-	-	-	PBS
	-	-	- (*)	TNFα
Ikkβ$^{\Delta hep}$	-	-	-	PBS
	-	+ (62±7%)	+	TNFα
ltβr$^{-/-}$	-	-	-	PBS
	+	+	+	TNFα

(*) CCL2 was upregulated in all TNFα treated *tnfr1*$^{-/-}$ mice investigated. This upregulation was however abolished in *tnfr1/2*$^{-/-}$ mice.

Acute rat IgG or 3C8 administration

Mouse genotype	Nuclear p65 translocation in hepatocytes	Nuclear p65 translocation in NPC	Upregulation of NF-κB target genes	Treatment
C57BL/6	- + (90±3%)	- + (35±10%)	- +	Rat IgG 3C8
tnfr1-/-	- + (86±3%)	- + (38±9%)	- +	Rat IgG 3C8
$Ikk\beta^{\Delta hep}$	- -	- -	- -	Rat IgG 3C8
$lt\beta r^{-/-}$	- -	- -	- -	Rat IgG 3C8

1.6.12 Inhibition of LTβR signaling reduces chronic hepatitis and carcinogenesis

I further investigated the involvement of LTβR signaling in the transition of chronic hepatitis to HCC by long-term LTβR-Ig administration in *tg*1223 mice. Nine month-old *tg*1223 mice with chronic hepatitis (n=31) or age-matched C57BL/6 mice (n=23) were treated with LTβR-Ig for 2 months, remained untreated for another 4 weeks and were then sacrificed. LTβR-Ig treatment significantly reduced chronic hepatitis incidence in *tg*1223 mice compared to untreated *tg*1223 mice (*tg*1223 mice LTβR-Ig treated: 4/31; *tg*1223 mice untreated: 34/34; $P<0.0001$). Furthermore, LTβR-Ig treatment suppressed chronic hepatitis-driven HCC formation (*tg*1223 mice LTβR-Ig treated: 0/31; *tg*1223 mice untreated: 6/34; $P<0.05$) (Table 8; Figs. 31 and 32). LTβR-Ig treatment did not lead to overt histopathological alterations in C57BL/6 livers nor did I detect overt changes in lymphocyte (B-, T-cells) or macrophage populations within spleens of LTβR-Ig treated compared to untreated C57BL/6 or *tg*1223 mice (data not shown). Efficiency of LTβR-Ig treatment was ascertained by the loss of LTβR-dependent follicular dendritic cells (FDCs) within C57BL/6 and *tg*1223 spleens (Fig. 33).

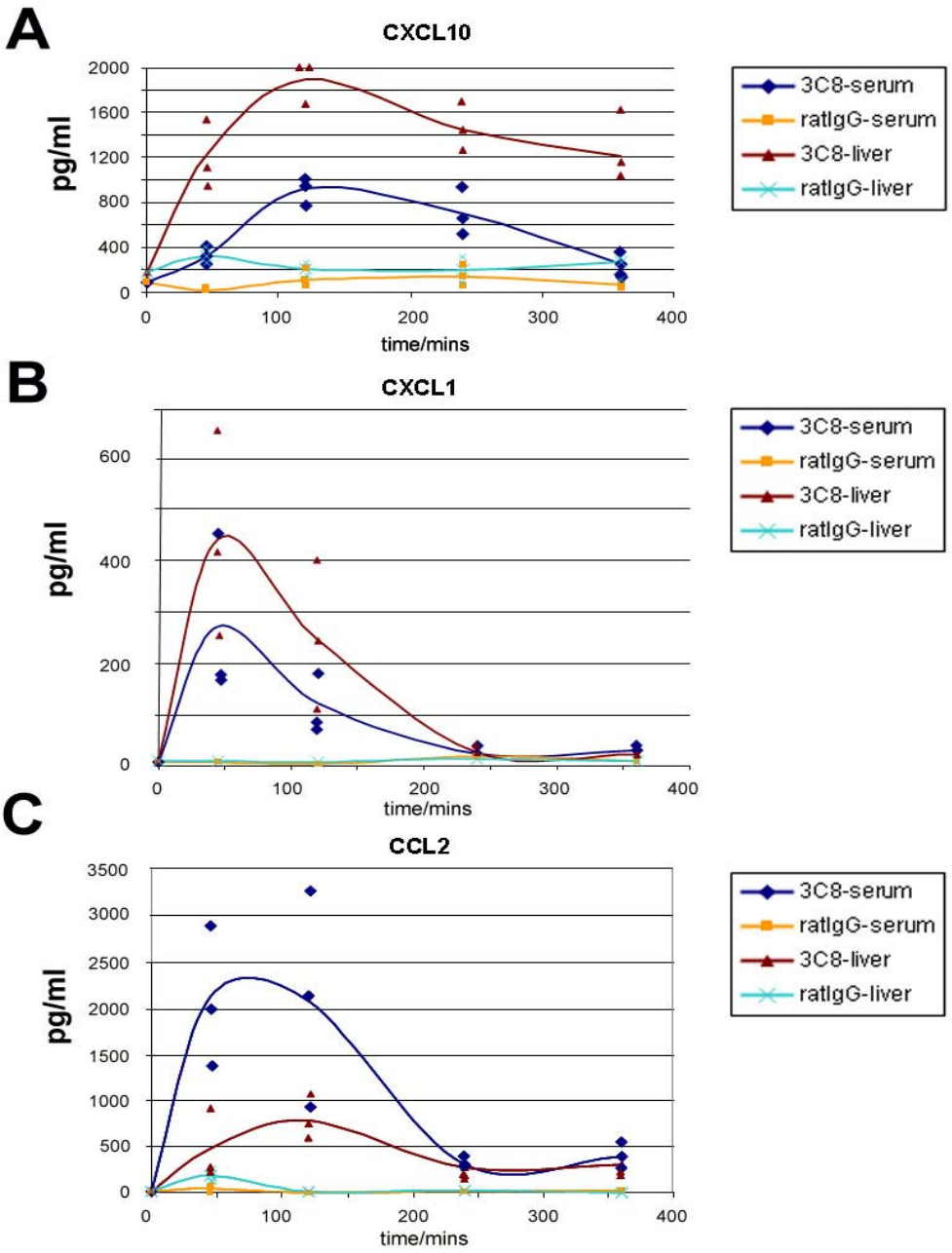

Figure 30: Increase of chemokines in sera and liver homogenates of C57BL/6 mice after 3C8 treatment. ELISA and multiplex-bead assay analysis of sera and liver tissue. I.v. injection of 3C8 into C57BL/6 mice led to a rapid upregulation of **(A)** CXCL10, **(B)** CXCL1 and **(C)** CCL2 in contrast to rat IgG. Hepatic upregulation of CXCL10 and CXCL1 occurred earlier and was stronger in C57BL/6 liver homogenates than in sera. Lines depict the average result (+/- SD) from three individual mice analyzed (symbols).

Table 8: Chronic hepatitis and HCC incidence in *tg*1223 mice and LTβR-Ig treated *tg*1223 mice. (A) Reduced chronic hepatitis and HCC incidence in 12 month-old *tg*1223 mice treated with LTβR-Ig. Statistical evaluation: *, **, *** indicate the degree of statistical significance: * = $p<0.05$; ** = $p<0.001$; *** = $p<0.0001$.

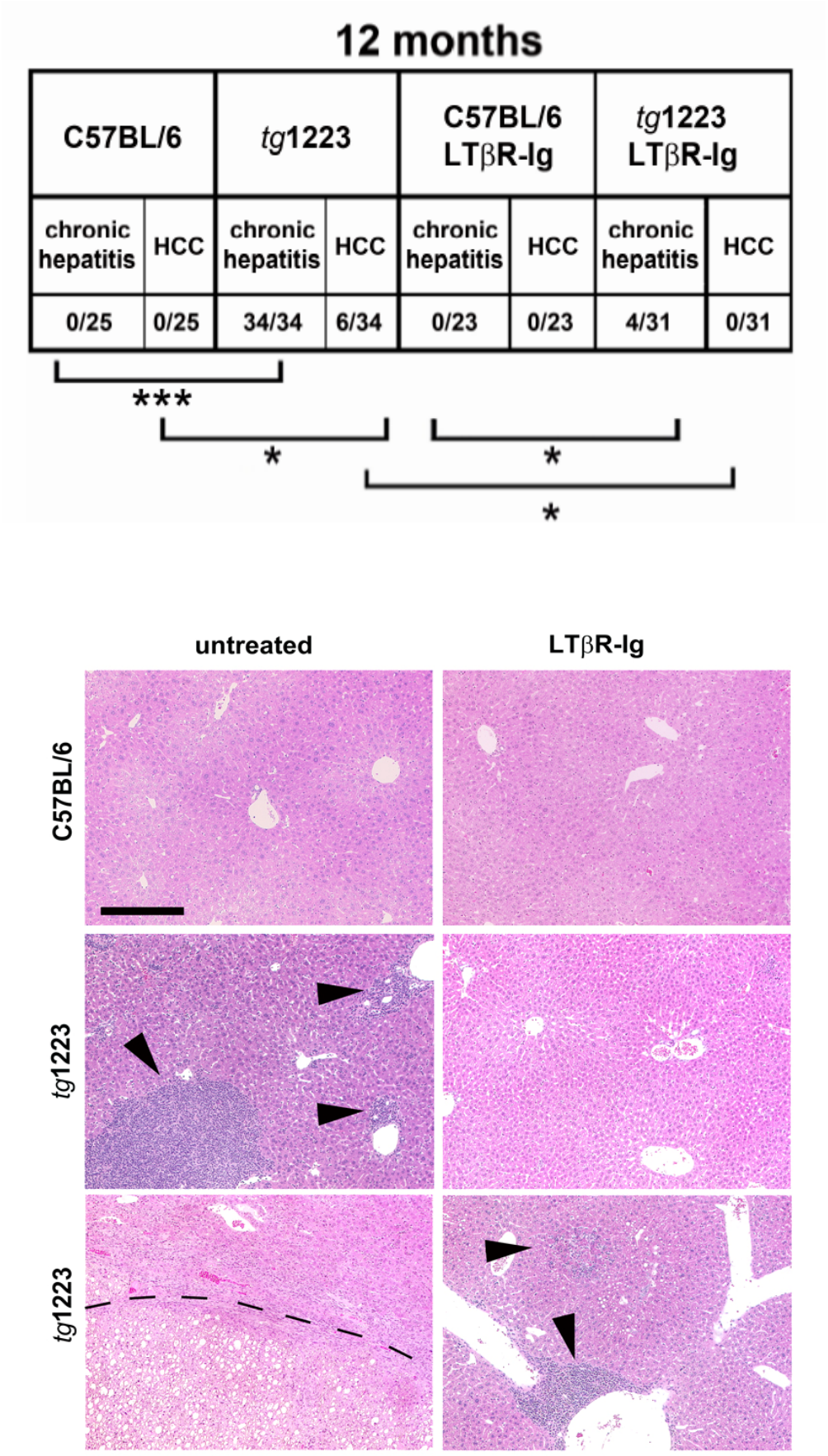

Figure 31: Effects of long-term LTβR-Ig treatment in *tg*1223 mice. Histological analysis (H&E) of livers from

untreated (left column) and LTβR-Ig treated (right column) C57BL/6 or *tg*1223 mice (12 months ofage). Representative sections show no hepatitis or HCC in untreated or LTβR-Ig-treated C57BL/6 livers (upper row). Untreated *tg*1223 livers display hepatitis in 34/34 (middle panel, left column) and HCC in 6/34 cases (lower panel, left column). LTβR-Ig treatment reduces the incidence of hepatitis (middle and lower panel, right column) and prevents HCC formation in LTβR-Ig treated *tg*1223 mice. Arrowheads indicate inflammatory foci. Tumor border is indicted by a dashed line (scale bar: 200 μm).

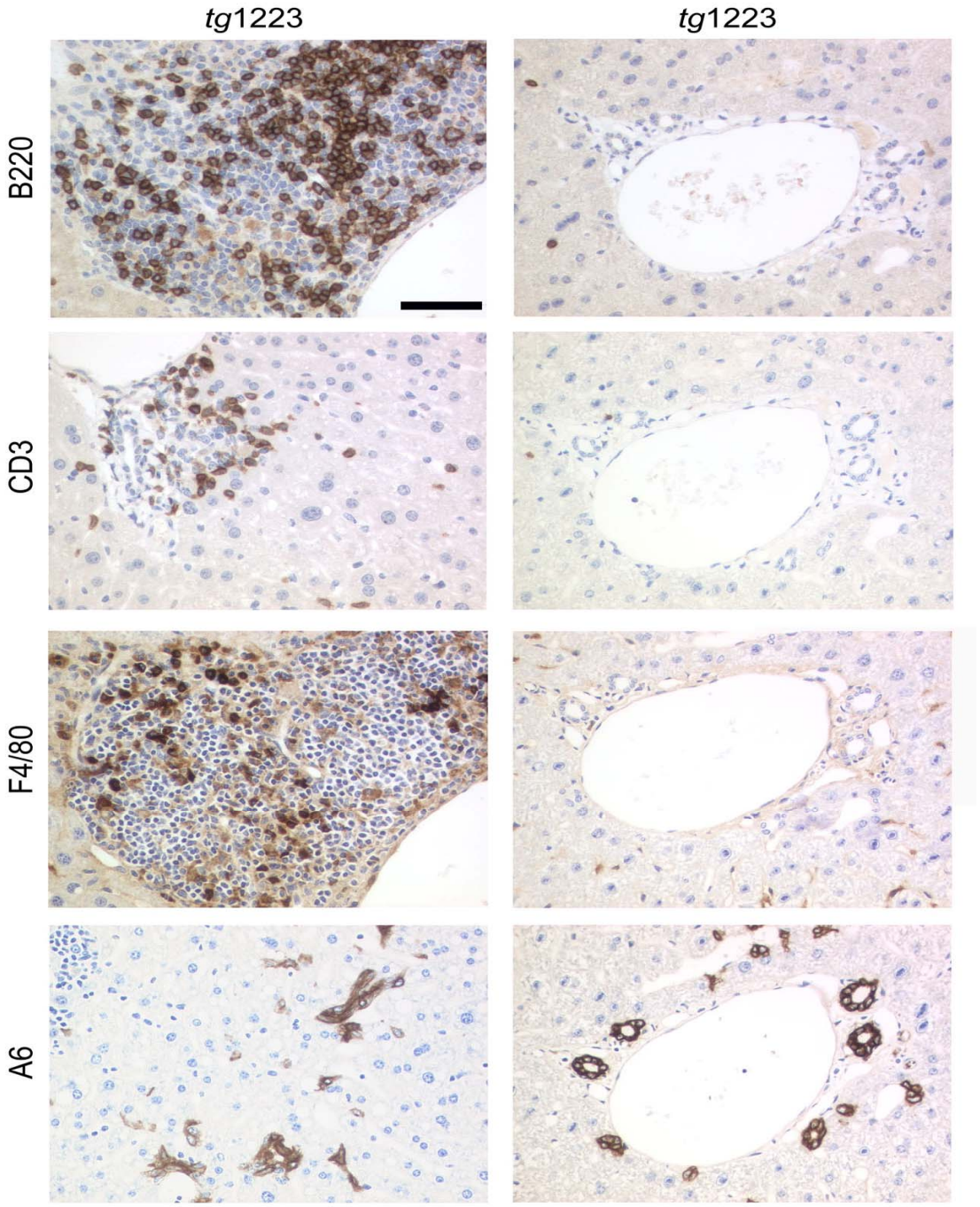

Figure 32: Immunohistological analysis of livers derived from LTβR-Ig-treated mice. Liver sections were stained

with antibodies detecting T- (CD3), and B-cells (B220), macrophages and Kupffer cells (F4/80) as well as $A6^+$ oval cells. LTβR-Ig treatment reduced the incidence of chronic hepatitis significantly (*tg*1223 untreated: 34/34 mice; *tg*1223 LTβR-Ig treated: 4/31). In the case of persistent inflammation in livers of LTβR-Ig-treated mice I found B- (B220), T-cell (CD3) infiltrates, macrophages and Kupffer cells (F4/80), as well as oval cell proliferation (representative case with hepatitis in left panel, without any significant inflammation in right panel) (scale bar: 50µm).

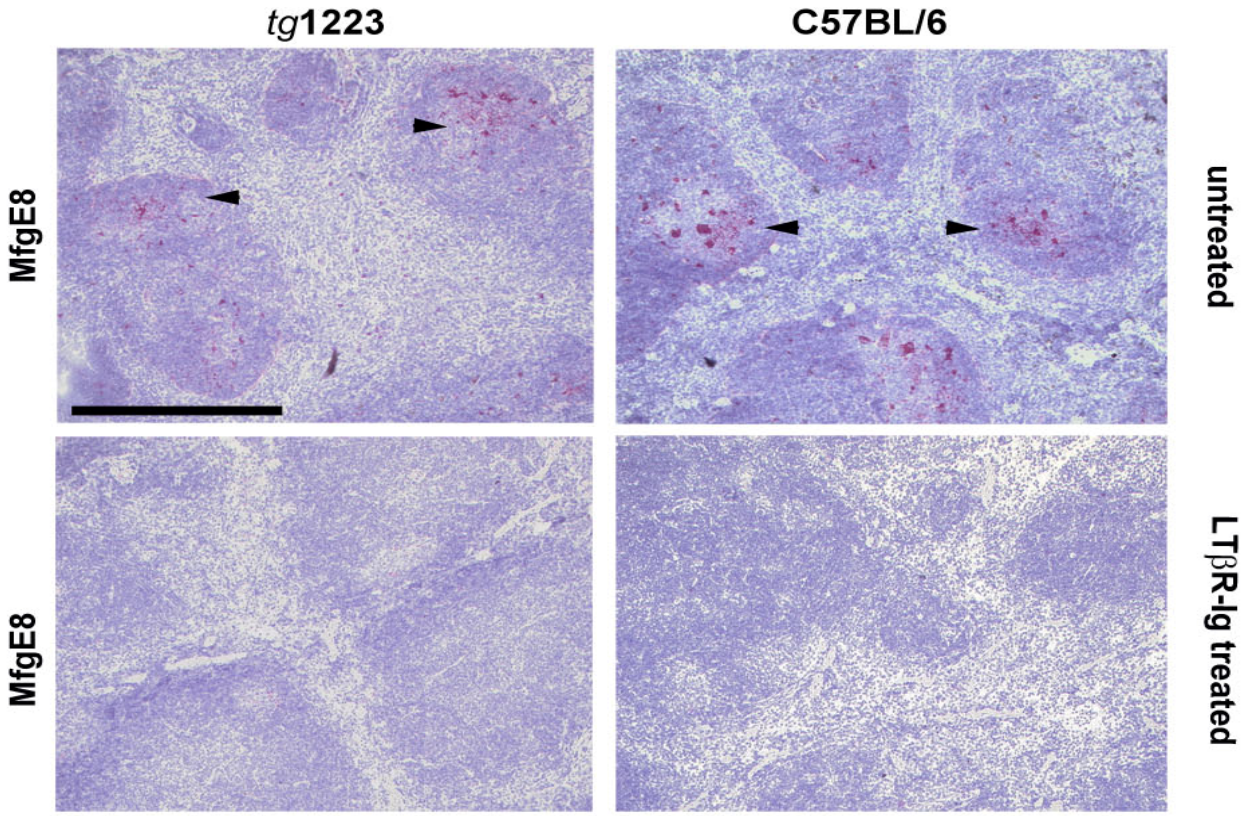

Figure 33: Loss of LTβR-dependent follicular dendritic cells (FDCs) within tg1223 and C57BL/6 mice upon LTβR-Ig treatment. Immunohistologcial analysis for the presence of FDC networks in spleens of LTβR-Ig-treated C57BL/6 or *tg*1223 mice. MFGE8 (FDC-M1) staining reveals a complete dedifferentiation of FDC networks in LTβR-Ig-treated C57BL/6 or *tg*1223 spleens. Arrowheads indicate FDC networks in spleens of untreated mice (scale bar: 200µm).

These results can be summarized in a murine (Fig. 34) and a human model (Fig. 35) without claiming that these models already completely explain all facettes of carcinogenesis in the liver.

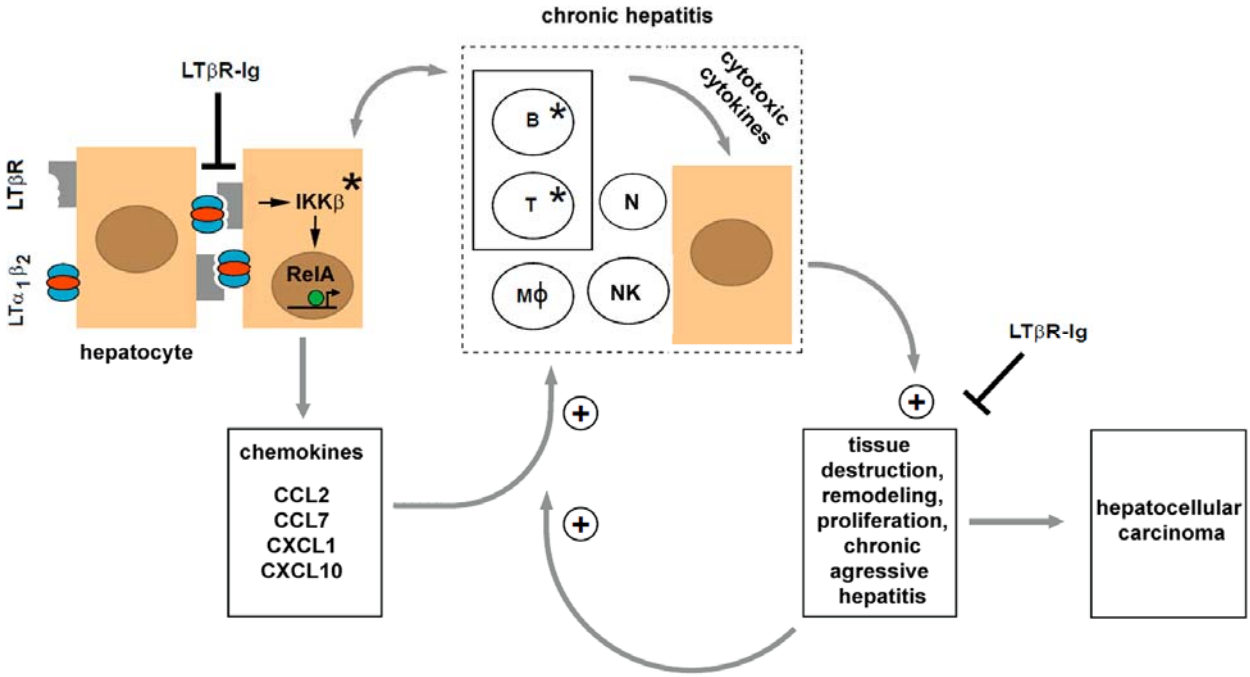

Figure 34: A model of chronic inflammation-induced hepatocarcinogenesis in *tg*1223 mice. Scheme of chronic inflammation-induced liver carcinogenesis in *tg*1223 mice: Transgenic hepatocytes (brown) express LTα, β and induce chemokine production (e.g. CCL2, CCL7, CXCL1, CXCL10) in the presence of IKKβ and intrahepatic lymphocytes. Chemoattraction and activation of myeloid cells and lymphocytes expressing particular chemokine receptors (e.g. CXCR3, CXCR2, CCR2, CCR1) cause hepatitis: CXCL10 attracts $CXCR3^+$ T- and NK-cells, CXCL1 $CXCR2^+$ T-, B-cells and neutrophils, CCL2 $CCR2^+$ macrophages and $CCL7^+$ attracts $CCR1^+$ monocytes. Activated, infiltrating immune cells secrete cytotoxic cytokines (e.g. IL6; IL1β, TNFα, IFNγ, LTαβ that cause tissue destruction, hepatocyte proliferation, cell death and tissue remodeling. In such an environment, hepatocytes are susceptible to chromosomal aberrations leading to HCC. Tissue destruction and remodeling supports the infiltration of activated inflammatory cells (e.g. myeloid cells) leading to a feed-forward loop towards chronic aggressive hepatitis. Asterisks indicate that genetic depletion ofthose components (IKKβ; T- and B-cells) blocks chronic hepatitis development and HCC. Blocking LTβR signaling with LTβR-Ig in 9 month-old *tg*1223 mice reduces chronic hepatitis incidence and prevents HCC. +: indicates the fortification of a described process. ⊣: indicates the suppression of a described process. The transcription factor RelA is schematically depicted as a green circle, inducing transcription of NF-κB target genes (e.g. chemokines) (arrow). B, T: B- and T-cells. Mø: macrophages. N: neutrophils. NK: NK-cells.

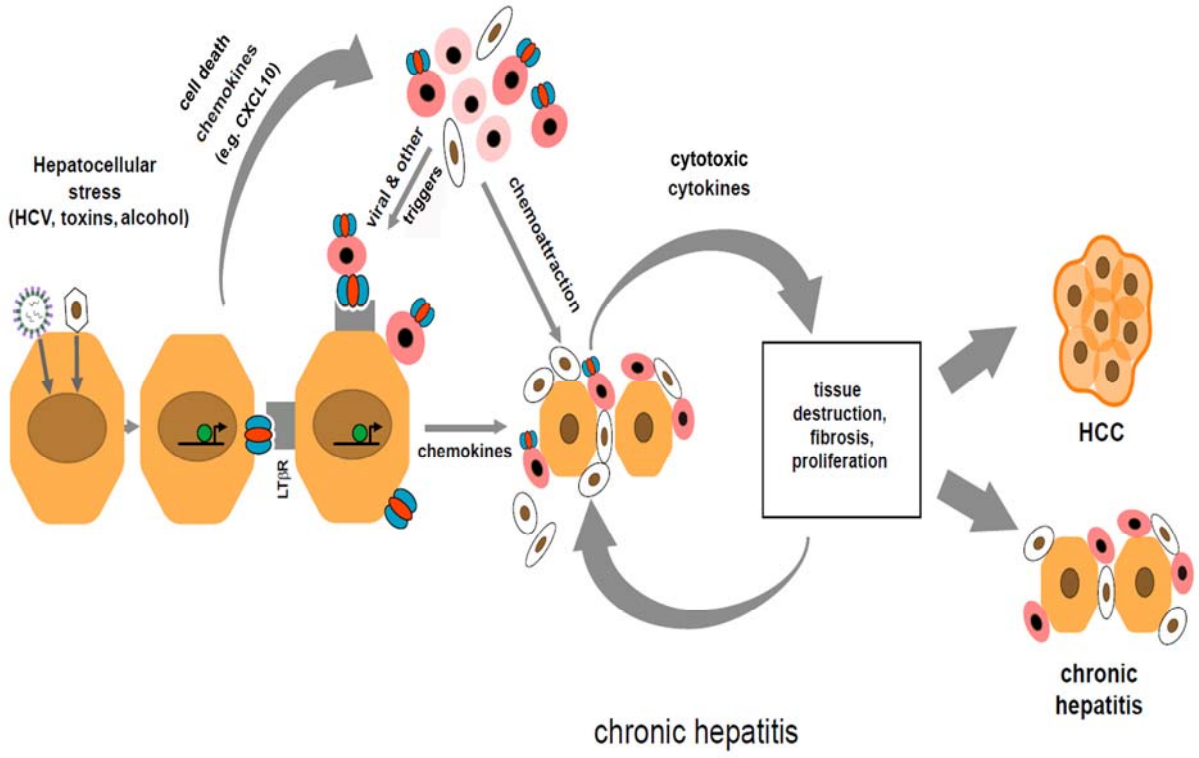

Figure 35: Model describing chronic inflammation-induced liver carcinogenesis in humans. Hepatocytes are schematically shown in brown. Various factors can lead to hepatocyte cell stress: These include toxins (aflatoxin-b), chronic alcohol uptake, drug abuse, and most frequently viral infections (e.g. HBV or HCV). These stress conditions induce cell death and may lead to transcription of chemokines (e.g. CXCL10 leading to the attraction of neutrophils and macrophages (pink circles and white ellipses) as well as lymphocytes (red circle). Infiltrating lymphocytes attracted by chemokines or viral particles presented on MHC molecules, might become activated and upregulate cytokines (e.g. TNFα, IL6, IFNγ, LT) and may induce LTβR signaling on hepatocytes. In the case of HBV- or HCV-infection, LT is also upregulated on hepatocytes further promoting hepatocyte-specific chemokine expression (e.g. *CXCL10* targeting $CXCR3^{+}$ T- and NK-cells) and attraction of inflammatory cells. Chronic hepatitis leads to the sustained expression of cytotoxic cytokines in liver, inducing cell death and compensatory proliferation of hepatocytes. This drives secretion of chemokines and cytokines by hepatocytes and activated Kupffer cells, promoting a positive feed-forward-loop. Ultimately, local ongoing tissue remodeling and hepatocyte proliferation stochastically induces chromosomal aberrations in hepatocytes leading to a clonal progression towards HCC. Alternatively, chronic hepatitis can persist without resulting in HCC formation. Thus, these results imply that long-term suppression of LTβR reduces chronic hepatitis incidence and can prevent the transition from chronic hepatitis to HCC in *tg*1223 mice.

1.7 DISCUSSION

This study uncovered drastic and robust mRNA upregulation of LTβR, LTα and LTβ in HBVor HCV-induced hepatitis and HCC. LT and LIGHT transcripts were mainly expressed by $CD3^+$ T- and CD20+ B-cells; a significant proportion of LTα and LTβ expression was also attributable to hepatocytes. Notably, upregulation of LTβR, LTα and LTβ transcripts was also detected in non-virus related HCC, which could stem from activated, tumor infiltrating lymphocytes and/or from neoplastic hepatocytes that have upregulated LT, possibly in response to IL6. It was demonstrated that HCC derived cell lines express IL6 (Baffet et al., 1991) and that LT levels are increased in response to IL6 in the latter (Subrata et al., 2005). Infection with HCVcc induced transcription of LTα, LTβ, LTβR, LIGHT and various chemokines in Huh-7.5 cells recapitulating in part HCV-driven LT and chemokine expression of HCV-infected livers *in vivo.*

LT signaling induces both, the canonical and the non-canonical NF-κB signaling pathways, whose role in controlling liver cancer formation remains controversial (Vainer et al., 2008). In a mouse model with acute DEN exposure, depletion of functional NF-κB signaling ($IKK\beta^{\Delta hep}$ mice) increased hepatocyte cell death, enhanced Kupffer-cell activation and elevated HCC incidence (Maeda et al., 2005). In contrast, NF-κB signaling promotes HCC development in $mdr2^{-/-}$ mice (Pikarsky et al., 2004) and hepatocyte-specific depletion of IKKβ prevents HCC formation in *tg*1223 mice.

How can this contradictory role of IKKβ signaling in HCC formation be reconciled? On the one hand IKKβ signaling might be required for hepatocytes to appropriately respond to and survive carcinogenic stimuli and acute liver injury (e.g. DEN exposure). On the other hand, IKKβ signaling might enable chemokine expression by hepatocytes leading to hepatitis and HCC. Consistent with this hypothesis, *tg*1223/$Rag1^{-/-}$ mice were devoid of chronic hepatitis, hepatocyte or oval-cell proliferation and failed to develop HCC.

Why could immune cells contribute to liver tumorigenesis? One explanation might be that $CD4^+$ or $CD8^+$ T-cells expressing inflammatory cytokines (e.g. IL1β, TNFα, IFNγ) as well as cytolytic proteins (e.g. Granzyme B) contribute to hepatocyte cell death, tissue remodeling and transformation, finally leading to HCC (Budhu and Wang, 2006; Nakamoto et al., 1998). Intrahepatic lymphocytes may also influence the production of inflammatory mediators, as 3 month-old *tg*1223/*Rag1-/-* livers displayed markedly reduced cytokine and chemokine levels. I propose that rather than directly acting as a cell-autonomous oncogene on hepatocytes or $A6^+$ oval cells, hepatic LTαβ expression induces local upregulation of chemokines (e.g. *Ccl2; Cxcl10, Cxcl1, Ccl7*) by hepatocytes. This leads to the attraction of circulating inflammatory cells and a hyperproliferative, hepatotoxic environment stochastically leading to HCC formation (Figs. 34 and 35). It is worth mentioning that some chemokines found in this study (e.g. CXCL10) have been reported to be mainly expressed by human hepatocytes in chronic hepatitis C (Zeremski et al., 2007).

Ablation of TNFR1 signaling did not prevent chronic hepatitis and HCC formation in *tg*1223 mice although anti-TNFα antibody treatment prevents HCC development in $mdr2^{-/-}$ mice (Pikarsky et al., 2004). I

investigated the mode of LT signaling in *Tnfr1*$^{-/-}$ livers upon 3C8 treatment. This induced analogous hepatic changes seen in *tg*1223 mice at 3 months of age. Similar to my results with *tg*1223/*Tnfr1*$^{-/-}$ mice, this suggests that heterotrimeric LT causes p65 translocation in hepatocytes and induces a TNFR1-independent signaling cascade via LTβR, presumably contributing to chronic hepatitis and HCC. Most probably, HCC formation in *mdr2*$^{-/-}$ mice depends on pathways involving TNFR1 distinct from the LTβR-dependent pathways described in my thesis.

I sought to indentify the major LT responsive liver cell-type by using *IKKβ*$^{\Delta hep}$ mice. I.v. administration of TNFα into *IKKβ*$^{\Delta hep}$ mice did not cause p65 translocation in hepatocytes but upregulated NF-κB target genes, presumably through TNFα-activated NPC. In contrast, 3C8 treatment in *IKKβ*$^{\Delta hep}$ mice neither induced nuclear p65 translocation in hepatocytes or NPC nor upregulation of selected NF-κB target genes. Therefore, hepatocytes but not NPC are likely to be the major liver cells integrating LT signaling. This explains why *tg*1223/*IKKβ*$^{\Delta hep}$ mice lack hepatitis and HCC although LTα and β were constitutively expressed by transgenic hepatocytes.

Upon 3C8 treatment, *IKKα*$^{AA/AA}$ livers upregulated selected NF-κB target genes similar to C57BL/6 mice (Fig. 29). Therefore, the absence of *IKKα* in both, hepatocytes and NPC, still allows NF-κB target gene expression upon 3C8 treatment, suggesting the involvement of the classical NF-κB pathway in LTβR-induced hepatic signaling.

LTβR signaling was reported to induce oval-cell proliferation (Akhurst et al., 2005), which is thought to contribute to the development of liver tumors (Lee et al., 2006). I observed proliferation of A6$^+$ oval cells in chronically inflamed *tg*1223 livers at the age of 9 months and found A6$^+$ cells within and at the border of *tg*1223 HCC. Whether those A6$^+$ cells represent transformed oval cells contributing to liver carcinogenesis or whether A6 is upregulated on aberrant hepatocytes within HCC remains elusive.

Lack of lymphocytes or chronic hepatitis prevented oval-cell proliferation, although LTα, β transgene expression was unaltered. Therefore, it is conceivable that activated, infiltrating lymphocytes or Kupffer cells may contribute to oval cell proliferation by providing further LT or other cytokines in *tg*1223 livers. Based on the presented data, a sequence of events leading to chronic hepatitis and HCC in *tg*1223 mice can be proposed (Figs. 34 and 35).

What are the possible clinical implications of my findings? Pharmacological inhibition of LTβR signaling reduces virus-, bacteria- and concavalin A-induced liver injury (An et al., 2006; Anand et al., 2006; Puglielli et al., 1999), while triggering LTβR signaling on hepatocytes appears beneficial during liver regeneration (Tumanov et al., 2008). Side-effects of pharmacologically inhibiting LTβR signaling include alterations in the microarchitecture of white pulp follicles and disappearance of FDCs in non-human primates (Gommerman et al., 2002). Despite the loss of FDCs and a reduced capacity to trap immune complexes the primary antibody response to keyhole limpet hemocyanin was not significantly altered

(Gommerman et al., 2002). In *tg*1223 mice, inhibition of LTβR signaling at the stage of chronic hepatitis partially reverted inflammation and prevented HCC formation, suggesting that LTβR-Ig treatment might be beneficial in liver pathologies with sustained *LTβR, LTα* and *LTβ* expression. siRNA knock- down of various components of the LTβR signaling pathway (e.g. LTβ; Rel A) interferes with HCV replication *in vitro* (Ng et al., 2007). Therefore, inhibition of LTβR signaling might also impede the efficiency of HCV replication.

Through this study I can report that LTβR and its ligands are drastically upregulated in chronic hepatitis B, C and in HCC. Immunohistochemistry and mRNA expression analysis revealed that LTs are expressed on both, lymphocytes and hepatocytes. Consistent with this result, challenge with infectious, cell culture derived HCV caused upregulation of LTα, LTβ, LIGHT, LTβR and various chemokines by a human hepatocyte cell-line *in vitro*.

Sustained hepatic LTα, β-expression caused chronic hepatitis and HCC formation in transgenic mice. Hepatitis and HCC development were prevented by the ablation of lymphocytes or hepatocyte-specific removal of IKKβ, yet HCC induction was TNFR1-independent. *In vivo* LTβR stimulation with an agonistic LTβR antibody identified hepatocytes as the major LT responsive liver cells and pharmacological in hibition of LTβR signaling in LTαβ-transgenic mice with hepatitis reduced liver inflammation and prevented HCC. These results demonstrate that sustained hepatic LT signaling is critically involved in hepatitis and HCC development.

The presented results show that LT signaling is critically involved in hepatitis and subsequent HCC development and imply that blocking LTβR signaling might become a beneficial therapeuticapproach in the context of HBV- or HCV-induced chronic hepatitis and other liver diseases displaying sustained hepatic LTβR signaling.

Additional tables with results that are not presented in this thesis and which are described as “data not shown” are found online under (Haybaeck et al., 2009) because these data sets are very large.

Summary: Prion transmission via the aerial route

Transmissible spongiform encephalopathies (TSEs) are fatal neurodegenerative diseases of humans and animals. The cellular prion protein (PrP^{C}) is absolutely required for disease development. In the central nervous system (CNS), prion infections cause spongiform vacuolation, neuronal loss and astrogliosis finally leading to the death of the infected individuals. In addition, the accumulation of misfolded, aggregated PrP (PrP^{Sc}) can be detected. The underlying infectious agent, the prion, was shown to accumulate not only in the CNS but also in secondary lymphoid organs of affected hosts. Only hosts with an intact immune system can be infected by a variety of extracerebral routes, including parenteral injection, transdermal administration after skin scarification, and oral administration. Up to date prions were not largely considered to be transmissible by aerial routes. Here I have investigated the transmissibility potential of prions administered by (1) aerosols in collaboration with Prof. Lothar Stitz's laboratory and (2) intranasally (i.n.) together with Dr. Claire Bridel. Various transgenic mouse models expressing the cellular prion protein (PrP^{C}) in specific compartments or cells (e.g. exclusively in the CNS) were investigated to identify the cellular and molecular mechanisms of prion infection via the (1) aerosolic and (2) intranasal route. Results of this study identify (1) inhaled prion aerosols and (2) prions administered i.n. as a startlingly efficacious pathway of prion transmission. Remarkably, in both paradigms prion transmission also occurred in the absence of B- and T-cells pointing towards a direct transmission route after exposure to prion aerosols or upon i.n. inoculation. The brains of all diseased or subclinical mice contained PrP^{Sc}. These results identify (1) inhalation and (2) contact mediated absorption as a surprisingly efficacious route of prion transmission, and call for appropriate revisions of the current prion-related biosafety guidelines as these data may have important clinical implications.

Zusammenfassung: Prionen-Übertragung über die Luftwege

Übertragbare spongiforme Encephalopathien (TSEs) sind tödliche neurodegenerative Krankheiten von Mensch und Tier. Das zelluläre Prion-Protein (PrP^{C}) ist für die Krankheitsentwicklung absolut erforderlich. Im Zentralnervensystem (ZNS), verursachen Infektionen durch Prionen eine spongiforme Vakuolisierung, einen neuronalen Zellverlust und eine Astrogliose, was mit dem Tod der infizierten Individuen endet. Außerdem kann, angehäuftes, falsch gefaltetes PrP (PrP^{Sc}) detektiert werden. Es konnte gezeigt werden, dass das zu Grunde liegende, ansteckende Agens, das Prion, nicht nur im ZNS, sondern auch in sekundär lymphatischen Organen von betroffenen Wirten akkumuliert. Nur Wirtsorganismen mit einem intakten Immunsystem können über eine Vielzahl von extrazerebralen Wegen, einschließlich der parenteralen Injektion, transdermal nach Hautabschürfung, und nach oraler Aufnahme angesteckt werden. Bisher wurden Prionen generell nicht als über die Luftwege übertragbar angesehen. Hier haben ich gemeinsam mit meinen Kooperationspartnern aus dem Labor von Prof. Lothar Stitz das Übertragbarkeitspotenzial von Prionen über (1) Aerosole und gemeinsam mit Frau Dr. Claire Bridel nach (2) intranasaler Inokulation untersucht. Verschiedene transgene Maus-Modelle, die das zelluläre Prion-Protein (PrP^{C}) an spezifischen Lokalisationen oder in speziellen Zellen (z.B. exklusiv im ZNS) exprimieren, wurden untersucht, um die zellulären und molekularen Mechanismen der Prionen-Übertragung durch (1) Aerosole und über den (2) intranasalen Weg herauszufinden. Die Ergebnisse dieser Studie identifizieren, dass Prionen in Form von (1) eingeatmeten Aerosolen und nach (2) intranasaler Applikation, erschreckend wirksam übertragbar sind. Bemerkenswerterweise konnten in beiden Experimenten Prionen auch in der Abwesenheit von B- und T-Zellen übertragen werden, was auf einen direkten Übertragungsweg nach Aerosolexposition oder nach intranasaler Inokulation von Prionen hindeutet. Die Gehirne aller erkrankten oder subklinischen Mäuse enthielten PrP^{Sc}. Diese Ergebnisse identifizieren das (1) Einatmen bzw. die (2) Kontakt-vermittelte Aufnahme von Prionen als einen überraschend wirksamen Weg der Prionen-Übertragung, und verlangen somit nach einer entsprechenden Revision der derzeit gültigen Prionen-bezogenen Biosicherheits-Richtlinien, da diese Daten von grosser klinischer Bedeutung sein könnten.

Selected Definitions

Amyloid: Fibrillary, mostly β-sheet-rich protein deposits. Amyloid is usually identified by apple-green birefringence when stained with congo red and analyzed under polarized light. PrP in amyloid form is found in some but not all forms of prion diseases in humans and animals.

Incubation time: Period of time between exposure to the infectious agent and the manifestation of clinical signs (in animals) or symptoms (in humans).

Prion: The term "prion" stands for protein-containing infectious agent causing TSEs, with unconventional biochemical properties, like resistance to agents known to inactivate nucleic acids, like proteinase K.

'Protein-only' hypothesis: This hypothesis, stated by Stanley Prusiner in 1982 suggests that prions harbour a protein, which is basically a glycoprotein, as the exclusive pathogenic component and not any nucleic acid. The essential genetic evidence indicates that the protein is an abnormally folded form of PrP, perhaps identical with PrP^{Sc}. However, the association with other non-informational molecules, such as lipids, glycans or nucleic acids, is not excluded.

PrP^{C}: The physiologically occurring form of PrP, or prion protein ('C' refers to 'cellular') which can be glycosylated on one or both of two asparagine residues with a variety of glycans. Its presence in a given cell type is necessary, but not sufficient, for replication of the prion.

PrP^{Sc}: An 'abnormally folded' form of the mature *Prnp* gene product that is almost invariably detectable in TSE-infected cells and tissues ('Sc' refers to 'scrapie', a prion disease occurring in sheep and mice). It is defined as being partly resistant to digestion by proteinase K under standardized conditions and is considered to be the major component of the transmissible agent.

***PRNP*:** The gene encoding the human prion protein.

***Prnp*:** The gene encoding PrP in animals.

Prion strains: Types of prions differing either in the clinical course of the respective disease, their

neuropathlogical presentation, their transmissibility and the physicochemical properties of the PrP isoforms that they are associated with.

Proteinase-K (PK): Proteinase-K is a proteolytic enzyme obtained from the fungus *Tritirachium album*, which is grown on keratins. Under specific, controlled digestion conditions it degrades PrP^{C} and removes approximately 90-100 amino acids from the N-terminus of PrP^{Sc}. A large protease resistant C-terminal fragment remains. PK digestion is generally used to differentiate PrP^{C} from its pathological misfolded isoform PrP^{Sc}.

Peripheral prion inoculation: This defines any administration route of prion agents other than into the CNS, including intraperitoneal (i.p.), intravenous (i.v.), intranasal (i.n.), aerosolic, transdermal and oral (po) administration.

TSE: Transmissible spongiform encephalopathies are fatal neurodegenerative diseases caused by prions. Not only the CNS but also extraneural tissues can contain prion infectivity.

2. INTRODUCTION: Prion transmission via the aerial route

2.1 Prion diseases/Transmissible spongiform encephalopathies (TSEs)

2.1.1 Prions affecting humans and animals

Transmissible spongiform encephalopathies (TSEs), known as prion disorders, are fatal neurodegenerative diseases that affect humans and a wide variety of animals. Prion diseases are a major challenge to biomedical research. To date, no therapy other than palliation is available. TSEs in humans include diseases, such as Creutzfeldt-Jakob disease (CJD), fatal familial insomnia (FFI), Gerstmann-Sträussler-Scheinker syndrome (GSS) and Kuru (Chesebro, 2003). In mammals, bovine spongiform encepaholopathy (BSE) is found in cattle, scrapie in sheep and goats, and chronic wasting disease (CWD) in elk and deer (Sigurdson and Miller, 2003). There are as well transmissible spongiform encephalopathies in cats and minks (Sigurdson and Miller, 2003).

The neuropathological alterations within the central nervous system (CNS) include spongiform vacuolation, drastic neuronal cell loss and astrogliosis (Aguzzi et al., 2007). The main hallmark of prion diseases is the accumulation of the misfolded form of the host-encoded celluar prion protein PrP^{C}, designated as PrP^{Sc}. "Sc" stands for scrapie, as an example of prion diseases in animals. The Prp^{Sc} deposits are detectable in the brain of affected individuals. An additional important of this disease entity is the extended incubation time between exposure to the infectious agent and manifestation of clinical symptoms. This time in humans can last from months to decades even (Collinge et al., 2006). Despite the fact that prion diseases show certain morphologic and pathophysiologic similarities to other progressive encephalopathies, such as Alzheimer's and Parkinson's disease (Aguzzi and Haass, 2003), TSEs are unique inthat they are transmitted through prion-contaminated material. This essential detail was identified more than half a century ago in the case of scrapie (Cuille and Chelle, 1939) and other TSEs.

2.1.2 *Prnp*, the gene encoding the cellular prion protein (PrP^{C})

The gene encoding the cellular isoform of the prion protein is located on chromosome 20 in humans and on chromosome 2 in mice (Basler et al., 1986).

The *Prnp* genes of mice, sheep and cattle contain three exons, while those of humans and hamsters span over two exons (Lee et al., 1998). *Prnp* mRNA is constitutively expressed in a wide range of tissues in the adult organisms of the various species. In the CNS for example, high PrP^{C} levels can be found in synaptic membranes of neurons, and in astrocytes. Apart from the CNS, *Prnp* is ubiquitously expressed (Doi et al., 1988). Interestingly, this also includes lymphocytes (Cashman et al., 1990) and stromal cells of lymphoid and non-lymphoid organs (Aguzzi and Polymenidou, 2004; Heikenwalder et al., 2008). During embryogenesis *Prnp* mRNA is found in the central and the peripheral nervous system and in specific non-neuronal populations (Miele et al., 2003). The mature form of murine PrP^{C} consists of 210 amino acids.

Posttranslational modifications include glycosylation at two sites (aa 181 and 197) and plasma-membrane attachment via a glycosyl-phosphatidyl-inositol (GPI)-anchor (Riek et al., 1996; Stahl et al., 1987). Like other GPI-anchored proteins, it is enriched in detergent-resistant membranes (Naslavsky et al., 1997; Vey et al., 1996). The structure of mature PrP^C from mice, humans, Syrian hamsters and cattle has some common features: a long, flexible amino-terminal tail (aa residues 23-128), three α-helices, and two anti-parallel β-sheets that flank the first α-helix (Riek et al., 1997). The second β-sheet and the third α-helix are connected by a large loop. The carboxyl terminus of PrP^C is stabilized by a disulfide bond that links helices two and three (Riek et al., 1996). Despite the fact that the N-terminal portion of the molecule is probably structurally less defined, it contains two conserved regions. One region consists of a segment of five repeats of an octameric amino-acid sequence (octarepeat region: OR). This region has been reported to be involved in copper binding (Brown et al., 1997). The other region (central domain CD), downstream relative to the first region, contains a very hydrophilic, positively charged amino acid cluster (CC formerly known as stop transfer effector domain STE) followed by a highly hydrophobic and conserved profile, which was originally termed transmembrane region 1 (hydrophobic core HC, Fig. 1). It still remains unclear whether this domain indeed functions as a transmembrane region under physiological conditions.

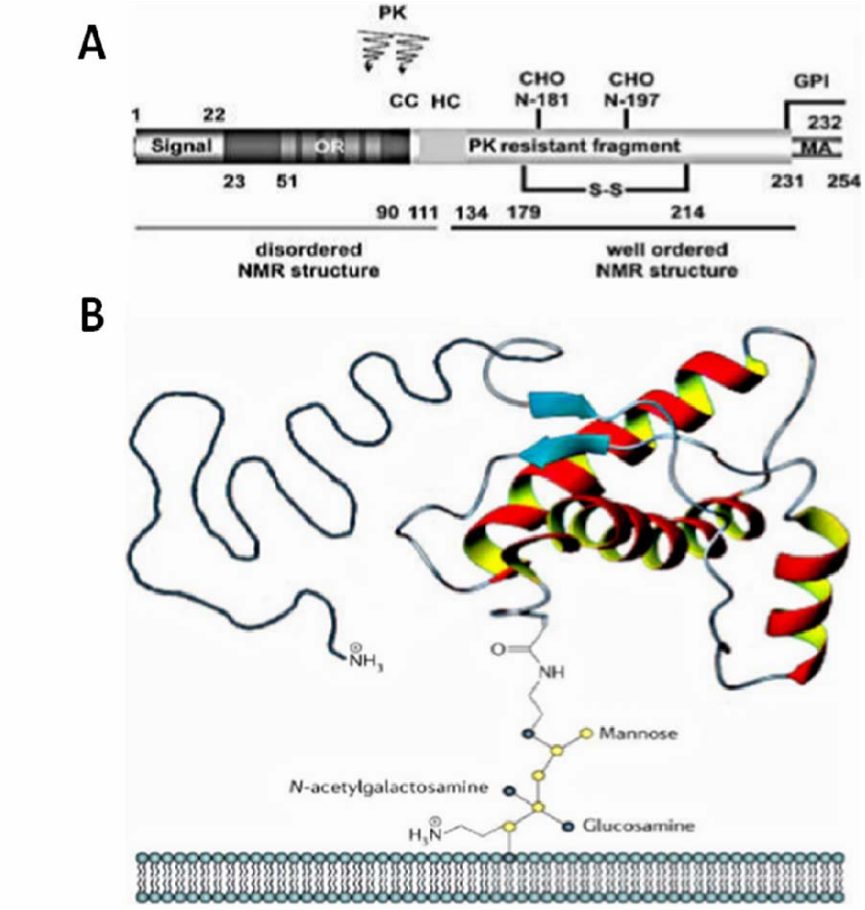

Figure 1. Structural features of the cellular prion protein. **(A)** Scheme of the primary structure of the prion protein and its posttranslational modifications. A secretory signal peptide resides at the extreme N-terminus. The numbers

describe the position of the respective amino acids. CC, charged cluster; HC, hydrophobic core; S-S, single disulfide bridge; MA, membrane anchor region; GPI, Glycosyl-phosphatidyl-inositol anchor: OR, octarepeat region; PK, proteinase K. The approximate cutting site of PK within PrP^{Sc} is indicated by the arrow. **(B)** Tertiary structure of the cellular prion protein inserted into a lipid bilayer, as deduced from NMR spectroscopy; modified from (Heikenwalder et al., 2007).

2.1.3 The physiological role of PrP^C

The *Prnp* gene was identified in 1986 (Basler et al., 1986) and *Prnp*$^{-/-}$ mice were first generated in 1992. PrP^C is a highly conserved protein in mammals. Up to date, clear knowledge about the physiological function of PrP^C is still lacking. Various functions have been attributed to PrP^C, including signal transduction (Mouillet-Richard et al., 2000), copper binding (Brown et al., 1997), synaptic transmission (Herms et al., 1999), induction of apoptosis (Paitel et al., 2003) and anti-apoptotic effects (Bounhar et al., 2001; Kuwahara et al., 1999) regulation of circadian rhythm (Tobler et al., 1997; Tobler et al., 1996) and others (Aguzzi and Polymenidou, 2004; Bounhar et al., 2001; Brown et al., 1997; Chiarini et al., 2002; Hutter et al., 2003; Kuwahara et al., 1999; Paitel et al., 2003; Zanata et al., 2002). PrP^C is also believed to be critical for axonal and dendritic outgrowth and synapse formation as well as their maintenance (Santuccione et al., 2005). The retrograde transport of PrP^C from the endoplasmic reticulum to the cytoplasm as a key neurotoxic mechanism has been extensively discussed (Kunz et al., 1999; Ma et al., 2002). It is also thought that PrP^C might act as a receptor for bacterial species like Brucella (Watarai et al., 2003). PrP^C seems to display similarities to membrane-anchored signal peptidases (Watarai et al., 2003). Paralogues are present in turtles (Simonic et al., 2000), amphibians (Strumbo et al., 2001) and fish (Rivera-Milla et al., 2003). Furthermore, *Prnp* null alleles have not been observed in any mammalian species (Mead et al., 2003b). The expression pattern of *Prnp* (Miele et al., 2003) in skeletal muscle, kidney, heart, secondary lymphoid organs and the CNS, highlights a conserved and widely distributed function of the protein (Bendheim et al., 1992; Ford et al., 2002a; Ford et al., 2002b), but *Prnp*$^{-/-}$ mice display a normal life expectancy (Büeler et al., 1992; Manson et al., 1994).

PrP has been reported to be expressed on long-term, re-populating hematopoietic stem cells being important for their self-renewal (Zhang et al., 2006) and the protein promotes neural precursor proliferation during developmental and adult mammalian neurogenesis (Steele et al., 2006). Surprisingly, postnatal depletion of PrP^C in neurons does not result in neurodegeneration (Mallucci et al., 2002). Neuronal cell death was shown in the hippocampus and cerebellum following intracranial application of crosslinking anti-PrP-antibodies (Solforosi et al., 2004). Transgenic expression of PrP variants carrying amino-proximal interstitial deletions causes ataxia, progressive cerebellar granule cell degeneration in *Prnp*$^{-/-}$ mice (Baumann et al., 2007; Radovanovic et al., 2005; Shmerling et al., 1998). Most phenotypic changes reported in *Prnp*$^{-/-}$ mice have been moderate. Possible PrP-interaction partners are currently investigated, besides the anti-apoptotic protein Bcl-2 (Kurschner et al., 1995), the laminin receptor precursor (Rieger et al., 1997) and N-CAM

(Schmitt-Ulms et al., 2001). The conversion of PrP^{C} to PrP^{Sc} results in neurodegeneration (Aguzzi et al., 2007). The only definite phenotype of *Prnp*$^{-/-}$ mice is their resistance to prion inoculation (Büeler et al., 1993).

2.1.4 The "Protein only hypothesis"

Transmission studies of TSEs showed not only the transmissibility of scrapie, Kuru and CJD to genetically appropriate recipients, they also revealed the existence of different prion strains. As indicated by incubation time, transmission of prions from one species to another is mostly less efficient than among individuals of the same species. This species barrier can, at least in some cases, be overcome, by introducing the *Prnp* gene of a donor into a recipient. Further transmission into individuals of the recipient species usually results in shortening of the incubation time. Therefore, prions can obviously adapt to different hosts (Perrier et al., 2002; Prusiner et al., 1990). Purification of the infectious agent from the brain of scrapie-infected rodents was undertaken by using an animal bioassay to track infectivity (Prusiner et al., 1984). This resulted in the isolation of highly infectious particles that contained a single type of protein molecule, named PrP^{Sc}. Careful characterization of the infectious particles resulted in the finding of exclusive biochemical properties like resistance to high temperatures, to formaldehyde treatment or to UV irradiation and, important from a diagnostic point of view, partially to proteinase K digestion (Griffith, 1967; Lehmann and Harris, 1996; Pattison, 1965; Prusiner, 1982). In contrast, PrP^{C} is a cell surface protein that is sensitive to proteases. PrP is encoded by an endogenous gene. It exists in two isoforms (Basler et al., 1986). In TSE infected cells, PrP^{Sc} is partly protease resistant and extremely stable (Lehmann and Harris, 1996; Nunziante et al., 2003). Due to its biochemical properties and the fact that it is the main component of purified infectious material (Aguzzi et al., 2007), this protein was itself proposed to be the infectious agent causing TSEs. The important observation that PrP^{C} and PrP^{Sc} are of the same amino-acid sequence, but differ significantly in their conformations, and the fact that the infectious agent lacks nucleic acids (DNA and RNA $\geq$ 50-60 nucleotides) (Riesner et al., 1993), resulted in the designation prion (for proteinaceous infectious particle) and a new hypothesis, the "protein only" hypothesis (Prusiner, 1982), which basically states that the causative agent is exclusively composed of a single kind of protein. Prion diseases are hypothesized to result from a conformational conversion of PrP^{C} into PrP^{Sc}. In contrast to PrP^{C}, PrP^{Sc} is enriched in β-sheet content and it is characterized by its poor solubility in non-denaturing detergents and its propensity for aggregation, and partial resistance to proteinase K (PK) digestion (McKinley et al., 1983). Digestion of PrP^{Sc} with PK (under certain conditions) results in an N-terminally truncated fragment. The causative agent of prion disorders is thereby clearly distinguishable from other pathogens such as bacteria or viruses (Prusiner, 1982). However, PrP^{Sc} is a surrogate marker for prion infectivity, which cannot be fully equated with prion infectivity (Aguzzi and Polymenidou, 2004). The process of conversion from PrP^{C} to PrP^{Sc} is believed to be induced by a physical interaction between host-encoded PrP^{C} as a substrate and exogenous PrP^{Sc} as a template, which results in the PrP^{Sc} conformation being imposed on PrP^{C}. It is well

established that PrP^{Sc} contains signicantly more β-sheet than PrP^{C} (Pan et al., 1993). For PrP^{C}, a three helix-structure has been determined by nuclear magnetic resonance (Donne et al., 1997; Riek et al., 1996; Riek et al., 1998) but it has not yet been possible to obtain a complete structure of PrP^{Sc}. Two models proposing a molecular mechanism of the conversion of PrP^{C} into PrP^{Sc} are discussed: the template assistance or "refolding" model, and the nucleation-polymerization or "seeding" model (Cohen et al., 1994; Gajdusek, 1988; Jarrett and Lansbury, 1993) (Fig. 2).

1) The refolding model suggests that the conformational change is kinetically controlled and that a high activation energy barrier prevents spontaneous conversion at detectable rates. The interaction with exogenously introduced PrP^{Sc} leads to an induced conformational change of PrP^{C}, resulting in the formation of PrP^{Sc}. This high energy barrier can be overcome by the catalytic action of PrP^{Sc}. It is believed that the process of unfolding and refolding is executed in conjunction with so far not determined enzymes and/or chaperones (Prusiner, 1991). This results in an exponential conversion cascade. In inherited prion disease, a rare pathogenic mutation is thought to favor spontaneous conversion of PrP^{C} into PrP^{Sc}, without the requirement of an exogenous infectious agent. This is the cause why inherited prion diseases can spontaneously arise, albeit late in life. Sporadic CJD may be due to an extremely rare event (occurring in about one in a million individuals per year) leading to a spontaneous conversion of PrP^{C} to PrP^{Sc} (Goldfarb et al., 1992).

2) The seeding model hypothesizes that the conformational change is in a thermodynamically controlled equilibrium strongly favoring PrP^{C} over PrP^{Sc}. PrP^{Sc} is only stabilized when it adds onto a crystal-like seed or aggregate of PrP^{Sc}. Seed formation most probably is a rare event. However, once a seed is formed, monomers are quickly added (Jarrett and Lansbury, 1993). The rate limiting step in this model is the formation of the seed. To explain exponential conversion rates, aggregates must be continuously fragmented, producing an increasing number of seeds and thereby new surfaces for accretion (Aguzzi and Sigurdson, 2004).

A Refolding model

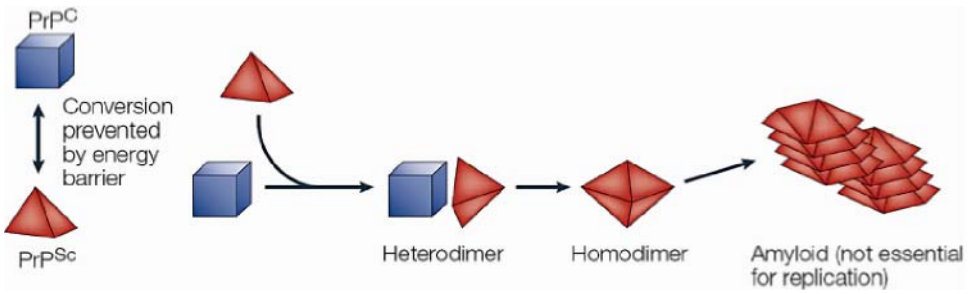

B Seeding model

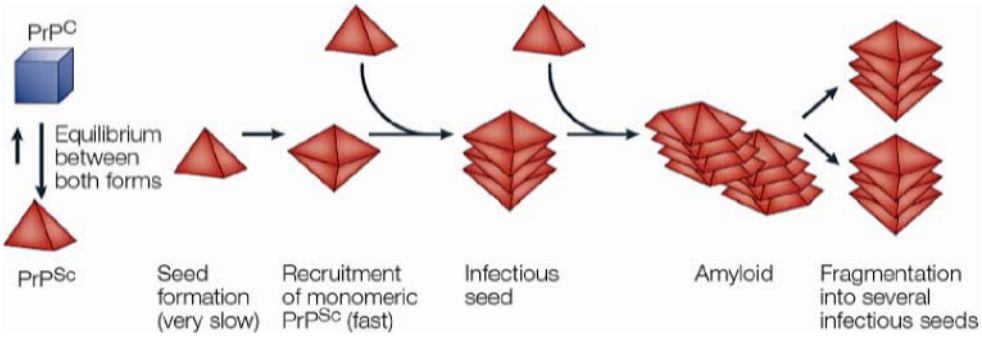

Figure 2. Models for the conformational conversion of PrP^{C} to PrP^{Sc}. (A) The refolding or template-directed assistance model and **(B)** the seeding or nucleation polymerization model; adapted from (Aguzzi and Sigurdson, 2004).

One of the most compelling lines of evidence supporting the protein only hypothesis derives from studies of PrP transgenic and knockout mice. In a particularly important experiment, it was demonstrated that *Prnp*$^{-/-}$ mice are resistant to prion infection (Büeler et al., 1993). This demonstrates conclusively that endogenous PrP^{C} substrate is essential for propagation of prion infectivity and disease development. It was also shown that the introduction of a hamster PrP transgene can abolish the species barrier that normally prevents infection of mice with hamster prions. Although a high degree of identity between the sequence of the incoming PrP^{Sc} and the resident PrP^{C} is often observed (Priola and Chesebro, 1995; Prusiner et al., 1990), it is not always essential for efficient prion replication. Even a single amino acid change in the PrP^{C} that is expressed by a susceptible host might confer protection against susceptibility to prion disease (Manson et al., 1999; Perrier et al., 2002). The data propose that prion propagation involves a species-specific physical interaction between exogenous PrP^{Sc} and host encoded PrP^{C}. Furthermore, grafting experiments revealed that the presence of PrP^{C} is required for neuronal damage in infected individuals (Brandner et al., 1996).

One, if not the final proof of the "protein only hypothesis" would be the reproducibility of the conversion process from non-infectious PrP^{C} to infectious material in a cell free environment. This strategy is based on the *in vitro* induction of full-length or truncated recombinant PrP protein misfolding, as well as on synthetic fragments of the polypeptide (Soto and Castilla, 2004). While various synthetic polypeptides were demonstrated to harbour PrP^{Sc}-like properties (for example formation of aggregates and enriched β-sheet structures) (Bocharova et al., 2005; Jackson et al., 1999; Zhang H, 1995), none of the constructs tested have been able to induce TSE like diseases in wild-type animals. Biochemical studies of cell-free conversion of PrP have shown that partially purified hamster PrP^{C} is not converted when mixed with purified PrP^{Sc}; on the other hand, conversion is restored when cell lysate is added to the sample (Deleault et al., 2005; Saborio et

al., 1999).

PrP^{Sc} can be generated *in vitro* by a method named PMCA (for protein misfolding cyclic amplification), which was shown to generate infectivity in wild-type Syrian hamsters (Castilla et al., 2005). However, this experiment still could not completely rule out the involvement of other components in the infectious units since PrP^{Sc} was formed in brain homogenates. Whereas the prion hypothesis is very likely to be true, other mechanisms have also been proposed, suggesting viruses, virinos and other infectious agents containing small RNAs as the infectious agents (Chesebro, 1998; Manuelidis et al., 1995). The putative participation of nucleic acids as part of the infectious particle still remains a matter of debate. Retroviral RNA for example has been shown to co-sediment with PrP^{Sc} (Akowitz et al., 1994; Murdoch et al., 1990) and short RNA fragments are released after nuclease digestion from purified infectious fractions (Akowitz et al., 1990) and several reports have demonstrated that PrP^{Sc} can interact with RNA with variable affinity (Weiss et al., 1997). However, the specificity of these interactions still remains to be determined (Safar et al., 2005).

Rarely, a particular protein in a yeast cell can flip into a different conformation, causing conversion of its counterparts to the same state and giving rise to functionally inactive aggregates. These changed conformations can be transmitted to daughter cells (Glover et al., 1997; King and Diaz-Avalos, 2004; Tanaka et al., 2004). Though yeast proteins, displaying the "prion phenomenon" are not homologous to vertebrate PrP^{C} at the amino acid sequence level, they share basic biochemical features like the formation of amyloid fibers and a highly specific species barrier. Therefore, the prion hypothesis appears not to be restricted to rare neurodegenerative disorders in mammals. Prion transmission represents a fascinating biological phenomenon.

2.1.5 Prion transmission routes

Studies of natural and experimental prion diseases have revealed various possible transmission routes. Oral, corneal, intraperitoneal (i.p.), intravenous (i.v.), intramuscular (i.m.), transdermal and intracerebral (i.c.) prion inoculation result in prion disease, where the intracerebral route has been shown to be the most efficient way of experimental prion transmission (Aguzzi, 2004 5849; Heppner et al., 2001; Herzog et al., 2004; Hill et al., 1997a; Maignien et al., 1999 681 9; Weissmann et al., 2002; Zhang et al., 2004). Horizontal transmission is believed to be critical for the natural spread of transmissible spongiform encephalopathies (TSEs) among animals (Biacabe et al., 2004 6832; Dickinson et al., 1974; Foster et al., 2006a; Foster et al., 2006b; Miller and Williams, 2003), although the pathway followed by the infectious agents from infected to healthy hosts is only partially understood. Different biological materials (e.g. saliva, milk, urine, blood, placenta) were reported to harbour significant levels of prion infectivity (Mathiason et al., 2006; Seeger et al., 2005; Vascellari et al., 2007), which may be the source for transmission of prion infectivity (Brown and Gajdusek, 1991; Georgsson et al., 2006; Johnson et al., 2006; Seidel et al., 2007). Infectivity dispersion in the environment may lead to disease transmission by feeding or drinking (Hadlow

et al., 1982; Miller et al., 2004). Superficial wounds of the tongue of animals have been suggested as possible source of prions (Bartz et al., 2003 1 877).

While the presence of PrP^{C} in many tissues has been well established during the past (Brown et al., 1990; Brown, 1990; DeArmond et al., 1987; Fournier et al., 1998) it has been clarified that PrP^{Sc} is not necessarily confined to central nervous and lymphoid tissues, but can also deposit in muscle (Glatzel et al., 2003), in inflamed organs (Heikenwalder et al., 2008; Heikenwalder et al., 2005; Ligios et al., 2005) and in the olfactory epithelium of the nasal cavity, even in the olfactory epithelium of sCJD patients (Tabaton et al., 2004; Zanusso et al., 2003 1821). So far, unidentified routes of infection, such as airborne transmission, may occur as some evidence has already been provided for the natural spread of TSEs (Corona et al., 2009; DeJoia et al., 2006; Diringer, 1995; Doty, 2008; Hamir et al., 2008; Kincaid and Bartz, 2007; Park et al., 2002; Sbriccoli et al., 2009) (Fig.3). In areas with high environmental contamination, infectivity adsorbed onto small soil particles may come in contact with the olfactory neuroepithelium and other nerve endings in the nasal mucosa. It has been proposed that inhaled dust particles from feed contaminated with the bovine spongiform encephalopathy (BSE) agent could lead to infection through the olfactory pathway (Shaw, 1995b). Significant PrP^{TSE} deposition and vacuolisation in the olfactory tract was reported in one patient suffering from variant CJD (vCJD) and presenting with loss of smell and taste as initial clinical symptoms (Reuber et al., 2001), and in genetic CJD cases associated with a novel 144-base pair insertion of the prion protein gene (Kovacs et al., 2007). Other studies showed that in deer with chronic wasting disease (Spraker et al., 2002b) and in BSE-affected cows (Vidal et al., 2005) the olfactory system is a permissive site for PrP^{TSE} accumulation. I.c. challenged animals displayed Prp^{Sc} in the olfactory bulb (OB), olfactory epithelium (OE), vomeronasal organ (VNO), and nasal-associated lymphoid tissue (NALT) of animals killed at the terminal disease stage, indicating that the infectious agent spreads from the CNS to the nasal mucosa (DeJoia et al., 2006). Investigating the HY-TME strain in hamsters, nasal administration was shown to be 10–100 times more efficient in transmitting prion disease than oral uptake (Kincaid and Bartz, 2007). In the same study, NALT was reported to be the earliest site of PrPTSE deposition, followed by the submandibular and cervical lymph nodes and, eventually, by mesenteric lymph nodes, Peyer's patches, and spleen. Therefore a primary involvement of the lymphoreticular system (LRS) in the spread of prion infectivity after i.n. administration has been proposed. The absence of PrP^{TSE} deposition in the OE throughout the experiment (Kincaid and Bartz, 2007) has been claimed to indicate that the olfactory nerves are not involved in the spread of prion infection. The authors interpreted the presence of PrP^{TSE} deposition in the dorsal motor nucleus of the vagus nerve (DMVN) and solitary tract nucleus (STN) during the pre-symptomatic stage of the infection as suggestive that the scrapie agent is taken up by extrinsic nerve fibres and terminals of the vagus nerve in the respiratory tract (Getchell and Getchell, 1992; Kulkarni et al., 1994) or in the gastrointestinal system, following partial leaking of the inoculum from the nasal cavity. Finally, the finding that immunostaining was confined to the trigeminal nuclei in some animals was thought to be indicative of an involvement of the trigeminal nerve as an additional way of entry to the brain after i.n. application (Fig. 3).

Horizontal prion transmission may play a critical role in the maintenance of prion infection, in particular of scrapie in sheep flocks or CWD in free ranging deer and elk (Mathiason et al., 2006). From a mechanistic point of view it is believed that after peripheral application the pathological prion protein replicates in the LRS before it starts to invade the CNS (Sbriccoli et al., 2009). It is thought that besides direct contact predominantly environmental contamination by infectious saliva (Mathiason et al., 2006; Shaw, 1995a) urine (Seeger et al., 2005), milk (Konold et al., 2008; Ligios et al., 2005), blood (Mathiason et al., 2006) or placental tissue can serve as a reservoir for prion infectivity (Salman, 2003). In hamsters neuroinvasion could be experimentally shown (Bartz et al., 2003). Experimental transmission of scrapie by nasal routes has been reported in 2 out of 3 genetically susceptible sheep (Hamir et al., 2008). The HY-TME agent did not enter the CNS via the olfactory nerves in hamsters. Instead, $PrP^{(Sc)}$ accumulated in elements of the cranial LRS prior to neuroinvasion (Kincaid and Bartz, 2007). In the nasal cavity, PrP^{Sc} accumulation was found in the olfactory and vomeronasal epithelium, where its location was consistent with a distribution in cell bodies and apical dendrites of the sensory neurons (DeJoia et al., 2006)These reports have inspired me to test the possibility of prion transmission by aerosols and i.n. application since no clear evidence and mechanistic explanation for the transmission of prions by aerosols has been reported yet (CDC/NIH Manual “Biosafety in Microbial and Biochemical Laboratories”, Section VII: Agents Summary Statements. Section VII-D: Prions. Office of Health and Safety (OHS)(1999).

Based on immunohistochemical data it has been postulated that neuroinvasion of the 263K pathways (Sbriccoli et al., 2009). In the mentioned study analysis at different time points revealed deposition of the pathological prion protein in NALT in the absence of brain involvement from 80 days post infection. Therefore, also the olfactory system is thought to be a feasible route by which inhaled prion containing dust particles of BSE contaminated feedstuffs is conveyled to the infection (Sawcer et al., 1993; Siso et al., 2006a; Siso et al., 2006b; Smith et al., 1995; Spraker et al., 2002a). Recently, Bessen et al. (Bessen et al., 2009) claimed that neuroinvasion from the tongue and nasal cavity can be independent of LRS infection. Their experimental outcome partially depended on the strain of the prion agent and/or the host species.

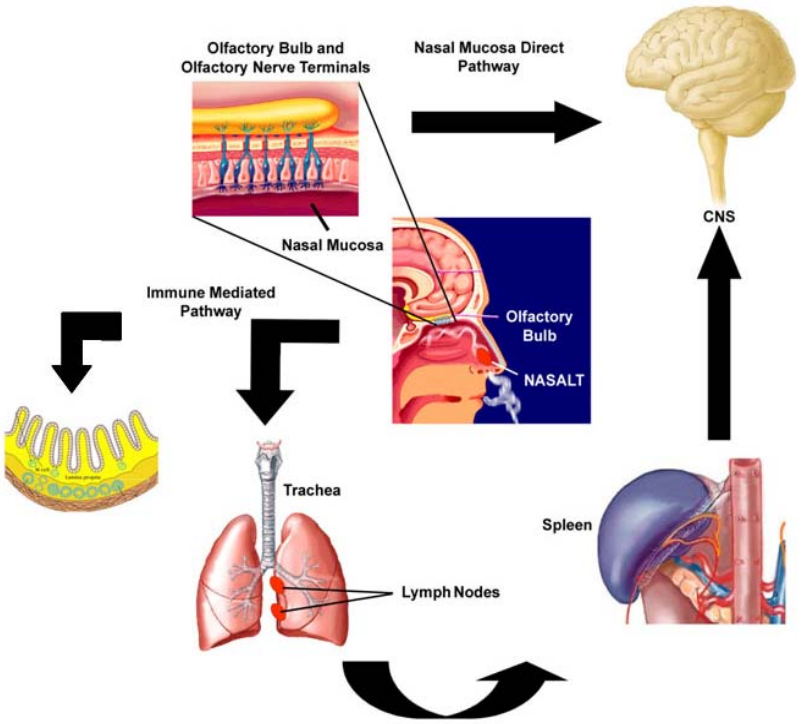

Figure 3. Possible prion transmission pathways to the CNS upon airway challenge. Prion transmission to the CNS may occur directly through the nasal mucosa via olfactory nerves (*direct pathway*) involving uptake of prions by the olfactory nerve terminals. Alternatively, uptake may require a lymphoid replication phase (*immune mediated pathway*): e.g. in the BLNs, the NALT or the spleen before entering the CNS.

2.2 Human prion diseases

In humans, prion diseases can be subdivided into three groups: infectious, sporadic and familial cases. All of them can be transmitted to non-human primates by ingestion or inoculation of brain tissue (Johnson and Gibbs, 1998), thus exemplifying one of the major hallmarks of TSEs. Creutzfeldt-Jakob disease (CJD) is the most common human TSE. The sporadic form accounts for about 85% of cases, about 10-15% of cases are familial, 1% of cases are iatrogenic. Variant CJD (vCJD) is largely limited to the UK and, to a much minor extent, other countries including France, Italy and Canada (Andrews et al., 2003).

2.2.1 Sporadic Creutzfeldt-Jakob-Disease (sCJD)

Sporadic Creutzfeldt-Jakob disease (sCJD) is rare and occurs throughout the world without overall geographic or seasonal clustering (Ladogana et al., 2005). Countries with surveillance programmes usually report a low yearly incidence (Baumann et al., 2007; Brandel et al., 2000), although higher incidences have also been reported (Glatzel et al., 2002). The first cases of sCJD were described more than 80 years ago (Creutzfeldt, 1920; Jakob, 1921); however, the etiology of sCJD is still unclear. The disorder appears to affect both men and women equally. The average age of onset is 60 years and is rare in people under the

age of 40. In contrast to other neurodegenerative diseases like Alzheimer‘s and Parkinson‘s disease, the incidence of sCJD declines after the age of 70 (Collins et al., 2004). Approximately one third of patients suffer from general symptoms such as fatigue, sleep disturbances and diminished appetite. Another third shows behavioral or cognitive alterations. The final third of patients display focal neurological symptoms such as visual loss, cerebellar ataxia, aphasia or motor deficits (Johnson, 2005). The disease progresses rapidly with prominent cognitive decline and the development of myoclonus. The median survival time from the onset of disease is five months and 90% of the patients suffering from sCJD die within one year (Johnson and Gibbs, 1998). The pathological changes in CJD are limited to the CNS and include neuronal cell loss and vacuolation within cell bodies and dendrites that give a spongiform appearance to the cortex and deep nuclei. The misfolded prion protein (PrP^{Sc}) can be detected by immunohistochemical staining and by Western blot analysis. It was originally thought that disease-associated PrP^{Sc} in sCJD patients was restricted to the nervous system; however, recent data indicate that it can also be detected in extraneural organs (Glatzel et al., 2003). sCJD can also be transmitted among humans through medical procedures (Brown et al., 1998; Matthews and Will, 1981). It is widely believed that spontaneous misfolding of the endogenous prion protein (PrP^{c}) into the pathogenic isoform, and/or somatic mutations in the gene encoding the prion protein might be the causal event in sCJD. However, if this were the case, one might expect a continuously increasing incidence with age, which is not supported by the observation that the age-specific onset curve of sCJD peaks in the 6^{th} decade of life.

2.2.2 Variant CJD (vCJD)

Variant CJD (vCJD) was first reported in 1996 in theUK (Will et al., 1996). The sudden onset of this disease in the United Kingdom (UK) and the young age of the affected individuals suggested a possible link to the BSE epidemic in cattle in the UK (Will et al., 1996). Subsequent biochemical analysis, neuropathological examination, and transmission studies have supported the idea that the disease might be zoonotically linked to BSE (Bruce et al., 1997; Hill et al., 1997a). Prions from patients with vCJD share some characteristics with those from cattle infected with BSE, indicating that they have a common source (Hill et al., 1997a). Furthermore, vCJD can be distinguished from sCJD based on several charcteristics. For example, patients suffering from vCJD display a disease course and pathology distinctive from that of sCJD, with younger age of onset, prominent psychiatric and sensory symptoms, and a longer disease course (Spencer et al., 2002). Neuropathological analysis reveals widespread vacuolation with multiple PrP^{Sc}-containing plaques. The vast majority of cases analyzed so far have been homozygous at codon 129 for methionine (Spencer et al., 2002). In contrast to sCJD in which PK-resistant PrP^{Sc} seems to be present in the skeletal muscles and spleens of some affected individuals (Glatzel et al., 2003), the variant form of CJD is characterized by high amounts of PrP^{Sc} in lymphoreticular tissues such as tonsils and spleen, and to a lesser degree, in lymph nodes (Hill et al., 1999); (Wadsworth, 2001). It is likely that sCJD spread might have occurred through consumption of BSE-contaminated meat products. Over the past several years, about 170

cases of a new variant of CJD in the UK have been reported (www.cjd.ed.ac.uk). Outside the UK, only very few cases have occurred (e.g. France, Italy and Canada). Since 2000 the numbers in the UK seem to have subsided (Andrews et al., 2003) (www.cjd.ed.ac.uk). As 15 years have passed since the peak of BSE incidence in the UK and corresponding peak has never been observed in the human population, it has been proposed that humans are either partially resistant to BSE-induced disease and/or that the dose of BSE infectivity to which the population has been exposed was quite low. However, there are still concerns that some individuals exposed to BSE might be asymptomatic carriers of the infection and that these individuals might pose a risk of further transmission to others (e.g. iatrogenically by surgical instruments or via blood transfusions) (Aguzzi and Glatzel, 2006; Brandel et al., 2000; Houston et al., 2000).

2.2.3 Kuru

Kuru was the first human spongiform encephalopathy to be experimentally transmitted to non-human primates(Gajdusek et al., 1966). This slowly progressing neurodegenerative disease was initially identified in the eastern highlands of Papua New Guinea in the mid 1950s (Gajdusek and Zigas, 1957; Poser, 2002). At the peak of the epidemic, an annual prevalence of up to 10% was observed in some Fore villages (Gajdusek and Zigas, 1957; Zigas and Gajdusek, 1957). Kuru in the Fore language means “to shiver” or “to tremble” which refers to the cerebellar ataxia that occurs in this disorder. Various data indicate that Kuru is transmitted via cannibalistic rituals as part of the mourning for deceased relatives (Gajdusek, 1977). Since cessation of cannibalism in the late 1950s, the prevalence of Kuru has steadily declined, but a few Kuru cases are still observed in the Fore Tribe, indicating that the incubation time of the infectious agent can be even higher than four decades (Mead et al., 2003a). Interestingly, the polymorphism at codon 129 of the *Prnp* gene is one important factor that appears to influence susceptibility to Kuru (Cervenakova et al., 1998; Lee et al., 2001).

2.2.4 Genetically determined human prion diseases

Familial TSEs are caused by mutations in the *PRNP* gene (Aguzzi and Weissmann, 1996). There are three main sub-types, which are classified according to the phenotype: familial CJD, Gerstmann-Sträussler-Scheinker syndrome (GSS), and fatal familial insomnia (FFI). These diseases account for 10 - 20% of all TSE cases in humans and all of them are inherited in an autosomal dominant fashion (Harder et al., 1999). Over 50 different mutations in the human *PRNP* gene have been found in kindreds with familial CJD. However, only four point mutations, namely at codons 102, 178, 200 and 210, together with insertions of five or six octapeptide repeats, account for 95% of the familial cases (Capellari et al., 2005). Moreover, a polymorphism at codon 129 encodes either methionine or valine, which influences the susceptibility to or the phenotype of human prion diseases (Palmer et al., 1991).

2.2.4.1 Familial CJD

Familial CJD usually has an earlier onset and a prolonged clinical course compared to sporadic CJD. Familial CJD is not associated with distinctive clinical features (Windl et al., 1999). Different *PRNP* mutations have been recorded in patients dying of CJD (Kaneko et al., 2000). In neuropathologically confirmed cases, various point mutations and octapeptide repeat insertions have been described (Goldfarb et al., 1991). In general, penetrance of *PRNP* mutations is high, but the existence of healthy octogenarian carriers of certain mutations indicates that there are additional disease modifiers.

2.2.4.2 Gerstmann-Sträussler-Scheinker disease (GSS)

P102L and G131V mutations are the most common of the *PRNP* mutations that have been described by Gerstmann-Sträussler-Scheinker (GSS). The typical clinical course of this disease is slow and progressive cerebellar ataxia beginning in the fifth or sixth decade paralleled by cognitive decline (Collinge et al., 1989). Patients suffering from GSS share the distinctive and defining neuropathological feature of wide-spread, multicentric amyloid plaques, which are immunoreactive for PrP (Hsiao et al., 1989; Hsiao et al., 1991).

2.2.4.3 Fatal familial insomnia (FFI)

Fatal familial insomnia (FFI) is a genetic human prion disease caused by a mutation at codon 178 of *PRNP*. The mutation results in the substitution of an asparagine for an aspartic acid at this residue (D178N) (Medori et al., 1992; Tateishi et al., 1995). In this disease the normal sleep-wake cycle of patients is profoundly disturbed. Additionally, the disease is characterized by insomnia and sympathetic over-reactivity (Medori et al., 1992). The pathologic characteristics of FFI segregate with the D178N mutation exclusively in combination with methionine homozygosity at codon 129. Onset of the disease is usually in the fifth decade of life, with a clinical course of 13-15 months (McLean et al., 1997; Medori et al., 1992; Zerr et al., 1998).

2.2.4.4 Iatrogenic CJD

Iatrogenic CJD (iCJD) is caused by exposure of individuals to prions during surgical procedures, such as transplantation of human dura mater or corneal grafts. Stereotactically implanted electroencephalography electrodes as well as treatment with pituitary growth hormone and gonadotropins from human cadavers have also been reported to cause this form of human prion disease (Brown P, 2000). Dura mater transplants and pituitary growth hormone administration account for most of these cases. However, prion ingection through contaminated hormones has efficiently been eliminated with the advent of recombinant human

pituitary hormones.

2.3 Prion diseases in animals

2.3.1 Natural and experimental scrapie in sheep

Scrapie is a type of prion disease that affects sheep and goats. The disease is characterized by scraping of fleece, stumbling and behavioral changes of affected animals and has a progressive course, leading to death within 3-6 months (Cuille and Chelle, 1939). Examination of the CNS from affected animals shows TSE-characteristic changes with neuronal loss, vacuolation and gliosis. Scrapie was the first TSE to be experimentally transmitted (Pattison and Millson, 1961). The precise route of transmission is unclear, but lambs exposed in the pasture display infectivity first in tonsils, retropharyngeal lymph nodes, and intestine (Hadlow et al., 1982). Although in animals there are no known genetic cases of prion diseases as there are in humans allelic variations in the sheep *Prnp* sequence do occur, and variation at several residues in the PrP amino acid sequence influences susceptibility to both natural and experimental scrapie infection (Goldmann et al., 1994).

2.3.2 Bovine spongiform encephalopathy (BSE)

In 1985, the first cases of bovine spongiform encephalopathy (BSE; commonly known as “mad cow disease”) were reported in the UK. In the following decade, a rampant epidemic throughout the country affected hundreds of thousands of cattle in the UK (Anderson et al., 1996). The export of cattle and contaminated feed led to the spread of the disease in Europe and to other countries around the world. Even now it is still unclear whether scrapie-infected sheep carcasses or a sporadic case of BSE in cows rendered into bone meal initiated the epidemic. In any case, as a consequence of feeding other animals with prion contamionated meat and bone meal, BSE was subsequently transmitted to exotic felines in zoos and domestic house cats, leading to feline spongiform encephalopathy (FSE) (Lasmezas et al., 1996). The peak of the BSE crisis in cattle occurred in the years 1992 in the UK and in 1995 in Switzerland. Since that time, the BSE incidence has declined due to regulations prohibiting the feeding of ruminant-contaminated meat and bone meal to other ruminants.

2.3.3 Chronic wasting disease (CWD)

Chronic wasting disease (CWD) was initially identified as a fatal wasting disease of captive mule deer in the late 1960s in Colorado and was classified as a TSE in the 1970s (Williams and Young, 1982). CWD has become a serious health problem in farms and wild deer and elk populations in North America and Canada with a current incidence of about 10% in certain wild deer populations in Colorado and Wyoming. Affected

animals become emaciated, experience behavioral changes, unsteadiness and massive salivation. Death occurs within weeks to months, and pathological examination of the brain show widespread spongiform changes in grey matter (Sigurdson and Miller, 2003). Furthermore, inoculation with brain tissue from a CWD-infected mule deer led to the development of a neurodegenerative disease in the host species confirming that CWD is transmissible (Marsh et al., 2005). Studies involving inoculation of CWD in mice have shown transmission in transgenic mice expressing cervid PrP, but not in wild-type mice or transgenic mice expressing human PrP (129MM), which is suggestive that a species barrier still prevents the spread of the infectious particles to humans (Browning et al., 2004).

2.3.4 Transmissible mink encephalopathy (TME)

Trasmissible mink encephalopathy (TME) has culminated as confined outbreaks in various mink ranches mainly in the US and it is assumed that the disease is acquired by feeding animals tissue from scrapie-infected sheep (Hartsough and Burger, 1965). There is some evidence that it might have originally developed from a cattle TSE disease (Marsh et al., 1991). However, TME, but not BSE, has been readily transmitted to hamsters (Kimberlin and Marsh, 1975). Therefore, agents causing TME and BSE are currently believed to be distinct.

2.4 Peripheral prion pathogenesis and neuroinvasion

2.4.1 Prions and the role of the immune system

Following peripheral exposure, many of the acquired TSE agents accumulate and replicate in lymphoid tissues and the lymphoreticular system including the spleen, lymph nodes, Peyers‘s patches (PPs) and tonsils (Beekes and McBride, 2000; Hill et al., 1997b; Hilton et al., 1998; Mabbott and MacPherson, 2006; Mould et al., 1970; Sigurdson et al., 1999; Wadsworth, 2001). TSE agents often persist within the lymphoid tissues for the duration of the infection, but the magnitude and duration of lymphoid tissue involvement can vary considerably depending on the particular TSE agent (Foster et al., 2001). In experimental inoculations in cattle, accumulation of the BSE agent in lymphoid tissues is restricted to the terminal ileum (Terry et al., 2003) and PrP^{Sc} is only detected in the spleens of a proportion of sporadic CJD (sCJD) cases at the clinical stage of disease (Glatzel et al., 2003). Furthermore, the route of administration influences the tissue distribution of extraneuronal PrP^{Sc} accumulation. For example after oral inoculation, the scrapie agent accumulates in the gut-associated lymphoid tissues (GALT), such as the Peyer‘s patches and mesenteric lymph nodes before neuroinvasion (Andreoletti et al., 2000; Beekes and McBride, 2000; Kimberlin and Walker, 1989; Mabbott et al., 2003; Prinz et al., 2003b). In mice, the spatio-temporal prion distribution patterns depend on the type and dose of the prion strain, the application route and the genetic background of the host.

2.4.1.1 Prion and secondary lymphoid tissue

The main function of secondary lymphoid tissues is to provide an optimal microenvironment in which antigen-presenting cells and rare antigen-specific T- and B-lymphocytes can interact to survey all entering or circulating antigens and to initiate an efficient immune response. Secondary lymphoid organs are located at sites where foreign antigens and pathogenic microbes enter the body, either by penetrating the skin, by crossing the mucosal barrier or by entering the blood circulation (e.g. during blood transfusion; Fig. 4). The major secondary lymphoid organs are the spleen, lymph nodes and Peyer‘s patches. Additionally there are secondary lymphoid tissues associated with the surfaces of the gastrointestinal and respiratory tracts. These organs comprise nasopharyngeal-associated lymphoid tissue (NALT) (Fukuyama et al., 2002), cryptopatches (Saito et al., 1998) and isolated lymphoid follicles (Hamada et al., 2002). Although quite different in appearance, the lymph nodes, spleen, and mucosa-associated lymphoid tissues (MALT) share the same basic architecture. They are all highly structured, composed of a stromal matrix providing the optimal environment for B- and T-lymphocytes, antigen presenting cells (APCs) and other accessory cells. The spleen is grossly divided into two compartments. The red pulp is the site of red blood cell disposal interspersed with lymphoid white pulp. The lymphocytes surround the arterioles entering the organ, forming areas of the white pulp, the inner region of which is divided into a periarteriolar lymphoid sheath (PALS), containing mainly T-lymphocytes and a rim of B-lymphocytes. The marginal zone is the zone of lymphocyte entry into the spleen from the blood and contains a layer of reticular cells, macrophages and resident B-lymphocytes that surrounds the PALS and the follicular areas. Primary B-cell follicles are located in the periphery of the PALS. In addition to naive and re-circulating B-lymphocytes, B-cell follicles contain follicular dendritic cells (FDCs), which function as efficient antigen capturing cells. Some of the B-cell follicles include germinal centres, which are then denoted as secondary follicles. There, B-lymphocytes proliferate after encountering their specific antigen and cooperating with T-lymphocytes. The importance of secondary lymphoid tissue for the neuroinvasion of prions was corroborated by findings that showed the stromal compartment to be the site of replication of the scrapie agent (Clarke and Kimberlin, 1984), and that the cells involved in scrapie replication were not mitotically active (Fraser and Dickinson, 1978).

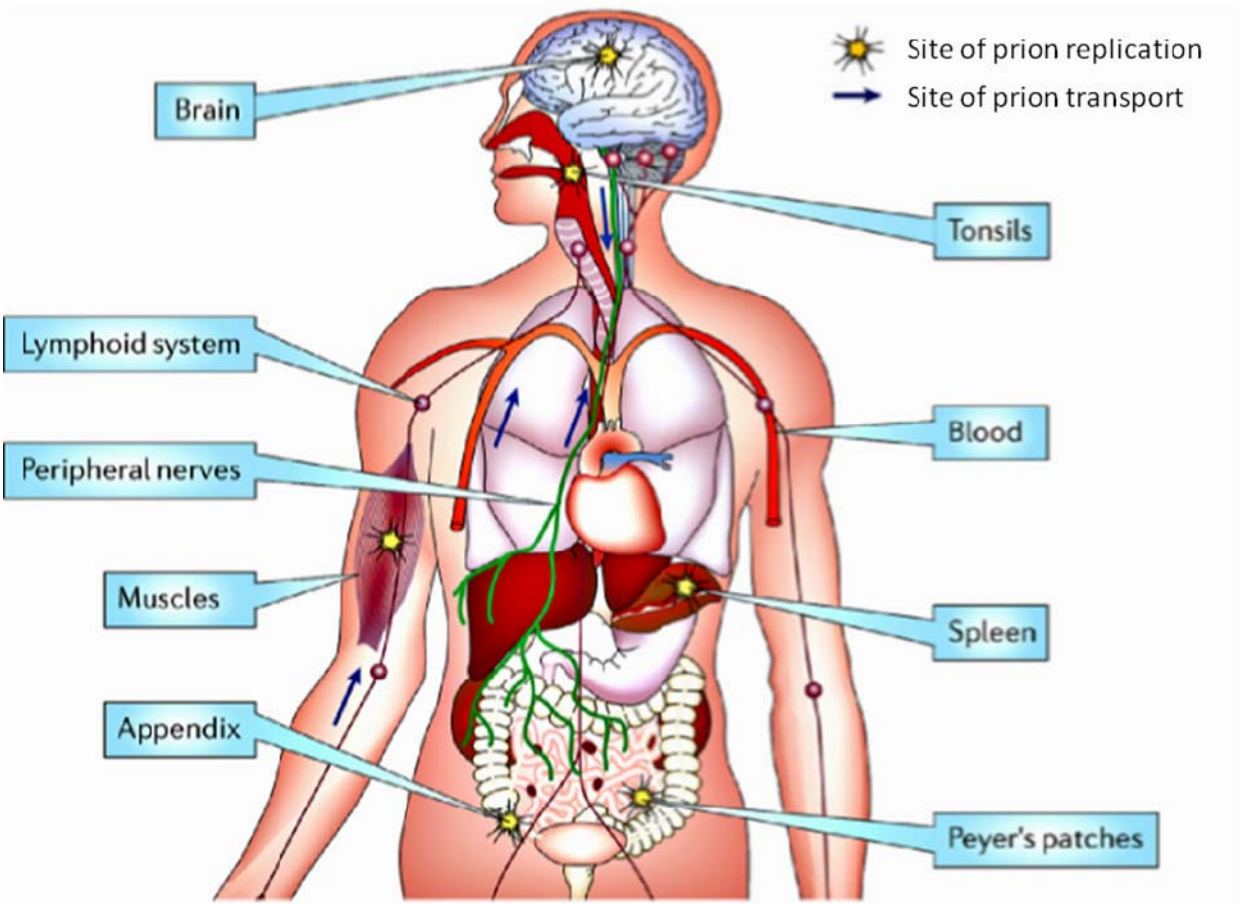

Figure 4. Human tissues involved in propagation and transport of prions. After oral uptake and peripheral replication in the LRS (spleen, appendix, tonsils or other lymphoid tissues), prions are transported to the CNS primarily by peripheral nerves; from (Aguzzi and Heikenwalder, 2006).

2.4.2 Prion propagation from the periphery to the CNS

Neuroinvasion, the transfer of prion infectivity from the sites of prion propagation in the periphery of the body, like spleen or lymph nodes, to the CNS, is crucially dependent on PrP expression in radio-resistant cells (Blättler et al., 1997; Kaeser et al., 2001). Innervation of secondary lymphoid organs is a rate-limiting step in prion neuroinvasion (Glatzel et al., 2001). The distance between FDCs and splenic nerve endings has been shown to have an impact on the speed of neuroinvasion (Prinz et al., 2003a). This was shown experimentally by manipulating the position of FDCs via ablation of the CXCR5 chemokine receptor (Forster et al., 1996). After initial infection and peripheral prion replication, prions migrate from the peripheral nerves of the host to the CNS, setting the stage for the onset of fatal, progressive neurodegeneration.

2. Results

2.5 Experiments to elucidate mechanisms of prion transmission via aerial routes

2.5.1 Aerosol inhalation in WT, PrP transgenic and knockout animals

In a first set of experiments together with my collaborators from Tübingen and under Professor Dr. Lothar Stitz's guidance, aerosols were tested as potential prion vectors. All aerosol-related experiments were performed by Professor Lothar Stitz's group. Mice were exposed to prion aerosols that were produced from RML-infected brain homogenates using a nebulizer device. Thereby, particle sizes capable of reaching upper and lower airways (100% particles below 10 µm with 60% of the particles below 2.5 µm and 52% below 1.2 µm) were generated. Depending on the duration of exposition to aerosols made from a 20% RML6 mouse brain homogenate (1 minute, 5 minutes, 10 minutes), *Tg*a20 mice (overexpressing PrP^{C}) as well as *CD1* and *C57BL/6* control mice developed scrapie (Fig. 5 and 6 A-C). Moreover, all *Tg*a20 mice that had been exposed to prion aerosols generated from a 2.5%, a 5%, a 10% or a 20% brain homogenate resulted in terminal scrapie. *C57BL/6* mice that had been exposed to aerosols of 20% brain homogenates for 10 min also developed scrapie. Western blot and histoblot analysis revealed the presence of PrP^{Sc} in brains of all clinically affected animals (Fig. 6; data not shown). Although the incubation time was prolonged and transmission was slightly less efficient in CD1 compared to *Tg*a20 mice, variation of disease onset among individual *CD1* mice was considerably low.

In addition, at day 360 post-exposure, PrP^{Sc} was detected in the brains of *Tg*a20 mice which had been exposed to aerosolic 0.1% RML infected brain homogenate for 5 minutes (Fig. 6C). However, at that time point mice did not show any clinical signs of prion disease, suggesting preclinical or subclinical disease. From these experiments I conclude that aerosols are efficacious prion vectors.

2.5.2 Prion infection of pulmonary tissue

In a next set of experiments, the amout of prion infectivity reaching the lungs after aerosolic infection was investigated. Lungs of *Tg*a20 mice that were exposed to RML prion-contaminated aerosols contained PK-resistant material when isolated and analyzed immediately after exposure. PrP^{Sc} levels were detected by sodium phosphotungstic-enhanced Western blot analysis (Fischer et al., 1996; Tabaton et al., 2004) (Fig. 6).

Moreover, these results were confirmed using the Misfolded Protein Assay (MPA) (Fig. 6J; courtesy of Rita Moos). To investigate whether the prion infectivity load reaching the pulmonary system would suffice to induce scrapie in mice, two additional experiments were performed. Identical lung homogenates were inoculated i.c. into *Tg*a20 indicator mice. These animals developed scrapie 80±3 dpi, corresponding to a prion titre of approximately 5-6 log LD50/mg of lung tissue, and the brains of these mice contained detectable levels of PrP^{Sc} (Figs. 6E and F).

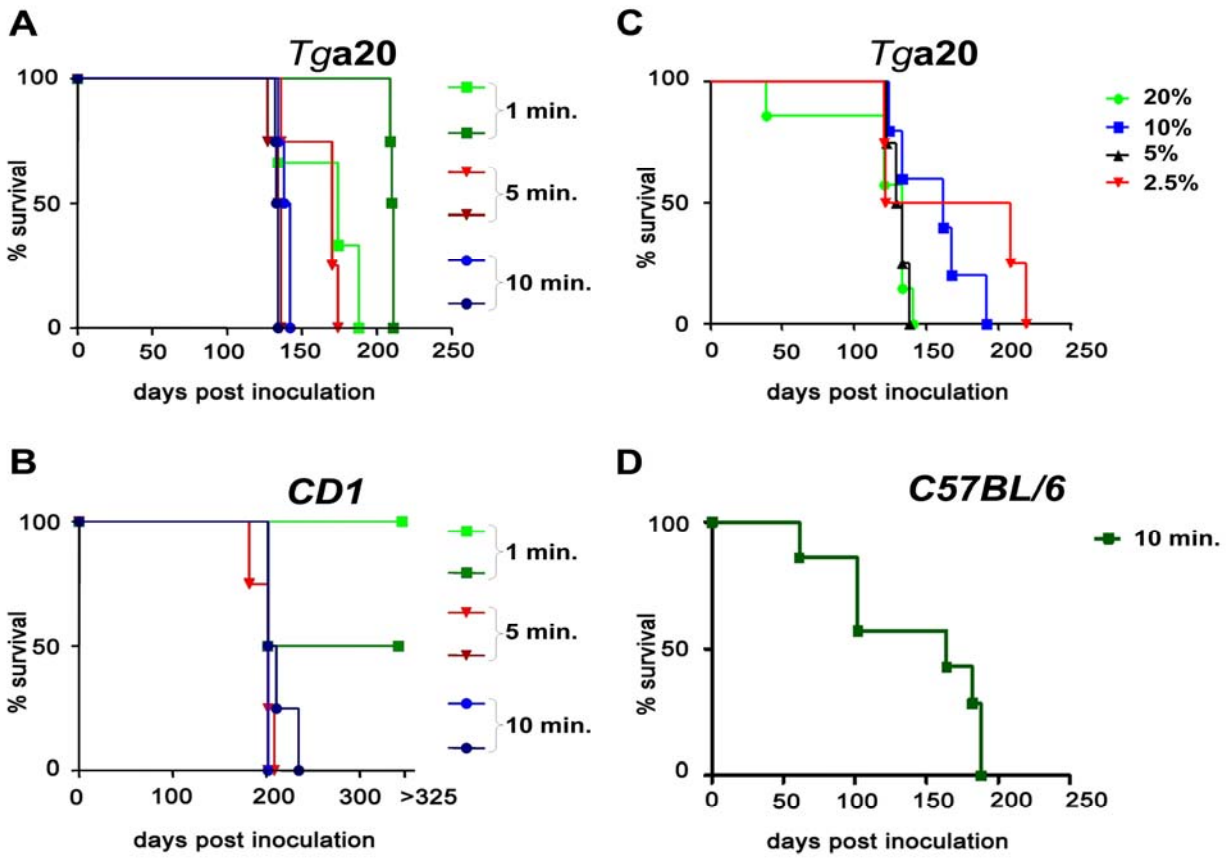

Figure 5: Efficient prion transmission via the aerosol route. (A) *Tg*a20 and **(B)** *CD1* mice were exposed for 1, 5 or 10 minutes to aerosols generated from a 20% RML6 mouse brain homogenate. These experiments were repeated two times. **(C)** *Tg*a20 mice were also exposed to aerosols generated from a 2.5%, 5%, 10% or 20% RML6 mouse brain homogenate for 10 min. **(D)** *C57BL/6* mice were exposed for 10 minutes to aerosols generated from a 20% RML6 mouse brain homogenate. Kaplan-Meier curves describe the percentage of survival after particular time points post prion aerosol treatment (y-axis represents percentage of living mice; x-axis demonstrates survival time in days). Different colors and symbols describe the various experimental groups.

Second, lung homogenates (10%) of aerosol-exposed, terminally sick *Tg*a20 mice were inoculated i.c. into *Tg*a20 indicator mice. This finally resulted in terminal scrapie and the death of the exposed animals. The animals were sacrificed with terminal scrapie after 71 days (n=9; lung homogenates used as inoculum after an exposure to prion aerosols for 10 minutes) or 78 days (n=9; lung homogenates used as inoculum after an aerosol exposition for 1 minute). Again, PrP^{Sc} could be detected in the brains of the affected animals by Western blot analysis (Fig. 6 D; data not shown). These experiments were performed in Tübingen.

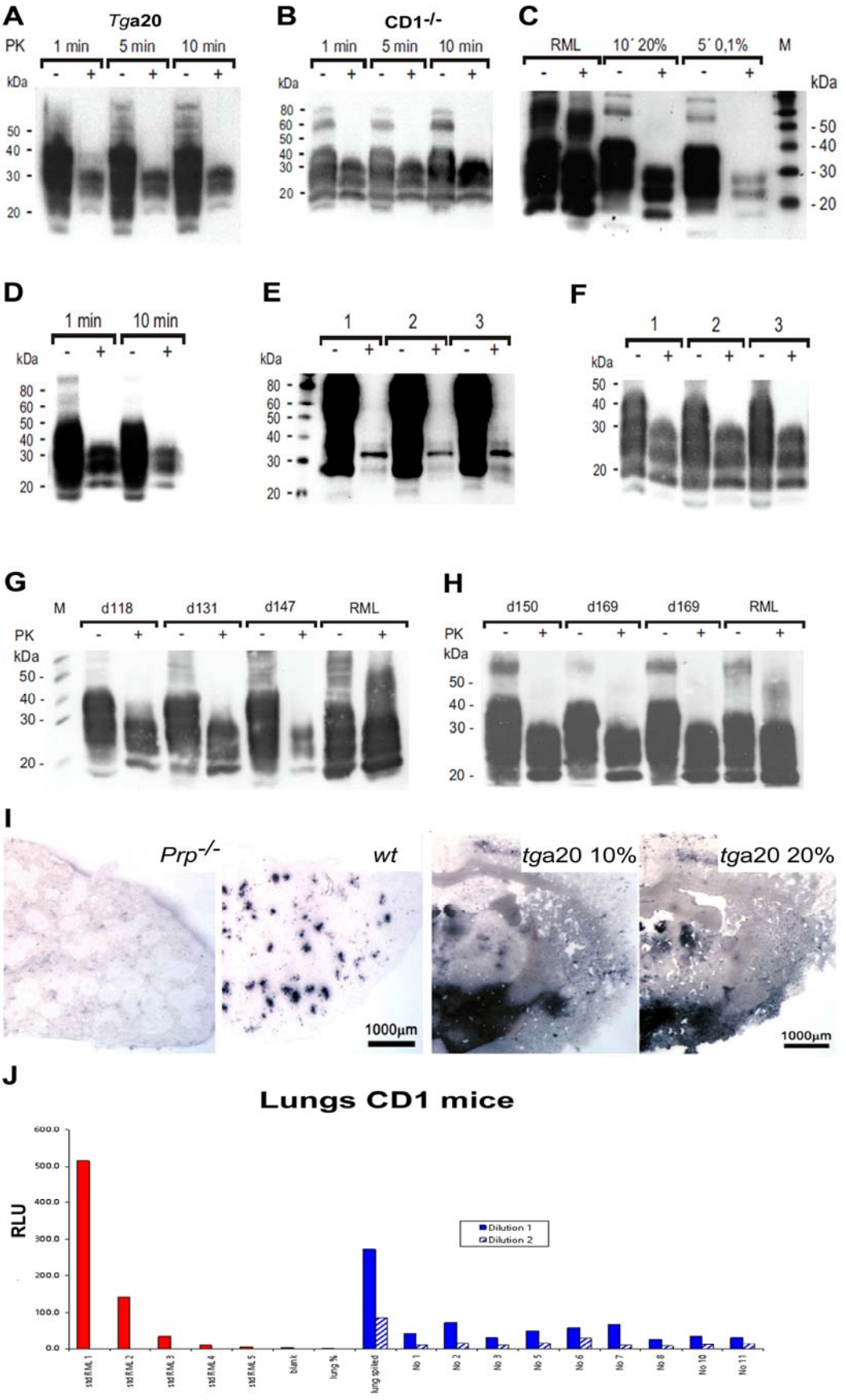

Figure 6: PrP^{Sc} deposition in brains of mice infected with prion aerosol and PrP^{Sc} in brains of *Tg*a20 mice

inoculated i.c. with aerosol exposed lung homogenates.

Brain homogenates (10%;w/v) from **(A)** *Tg*a20 or from (**B**) *CD1* mice which had been exposed to prion aerosols. (**C**) Brain homogenates (10% w/v) from *Tg*a20 mice exposed to prion aerosols from 20% brain homogenate for 10 minutes or 0.1% homogenate for 5 minutes. **(D)** Lung homogenates (10% w/v) from terminally sick *Tg*a20 mice which had been exposed to RML aerosols for 1 or 10 minutes. Homogenates were prepared as a pool from 5 mice and were used for i.c. inoculation into *Tg*a20 mice. **(E)** *Tg*a20 mice that had been exposed to aerosol were sacrificed immediately after the end of aerosol inoculation. Lanes 1-3 represent a pool of lung homogenates (10% w/v) from 5 mice each. **(F)** Brain homogenates (10% w/v) from *Tg*a20 mice inoculated i.c. with lung homogenate from mice which had been exposed to aerosol and were sacrificed immediately after the end of aerosol inoculation. Lanes 1-3 represent individual mice. (**G and H**) Western blot analysis of brains from *Tg*a20 mice inoculated with phosphotungstic acid-precipitated brain homogenate directly intratracheally by means of tracheal tubes. Brains were collected from diseased mice at terminal stage. Different days post inoculations are indicated. **(I)** Histoblot analysis of brains from mice exposed to prion aerosols. As positive and negative controls for histoblot analysis served the spleen of a $Prp^{-/-}$ mouse showing no signal (negative control; outer left panel) and the spleen of a wild type (*C57BL/6*) mouse (positive control; second panel from left) with positive signal in the white pulp follicles. Brains of mice challenged with a 10% (third panel from left) or 20% (right panel) showing deposits of PrP^{Sc} in cortex and mesencephalon. **(J)** Analysis of lung tissues from terminally scrapie sick mice by the "misfolded protein assay" (MPA) reveals positive signals as indicators of Prp^{Sc} deposition in all nine cases investigated (blue). Dilution curve is shown in the left (red) part of the graph. The lung of a $PrP^{0/0}$ and a lung of a clearly infected, terminally sick mouse were used as controls. Y-axis: RLU: Relative (Chemi) Luminescence Units, X-axis: mouse number; two blue columns represent two different dilutions: full represents a 1:10 dilution and the hatched one a 1:40 dilution of a 10% lung homogenate. Data for uninfected lung and brain controls are not shown here, but did not display a positive signal.

2.5.3 Where do prions go after inhalation?

To trace the path of prions after inhalation, mice were exposed to aerosols composed of RML6 mouse brain homogenate (20%) mixed with an equal volume of Coomassie blue (resulting in a 10% inoculum). The paranasal sinuses, the ethmoid bone and the upper part of the trachea were clearly stained. Additionally, in the stomach and in the upper part of the small intestine Coomassie blue could be found, whereas no staining was macroscopically detectable in the lungs. This suggests that only a minimal part of the infectious particles reaches the lungs after aerosolic infection. However, these results also indicate that even this small amount of infectivity is high enough to ultimately cause prion disease (data not shown).

2.5.4 Intratracheal prion inoculation as an efficient infection route

To obtain further evidence that prions can be transmitted aerially, mice were inoculated i.t. by means of small tracheal tubes. These experiments were also performed in Tübingen. *Tg*a20 mice (n=2) exposed to 20 µl of phosphotungstic acid-precipitated brain homogenate (20% w/v) developed disease at 118 and 131 dpi, respectively, whereas mice (n=4) receiving 10 µl of precipitated material were sacrificed with clinical signs

of scrapie between days 147 and 169 after inoculation (days 147, 150, 169, 169) (Fig. 6 G-H). Again, all i.t.-inoculated mice contained PrP^{Sc} (Fig. 6H) in the brain.

2.5.5 Intranasal prion inocualion is also extremely efficient in transmitting prion infectivity

In order to study the aerial transmission pathway, different mouse lines (age matched, 6-8 week-old mice) were inoculated with prions [RML 6.0, low dose, high dose and healthy brain homogenate (HBH) inoculum] by direct application of inocula on the nasal mucosa (Figs. 7-9). It should be mentioned that mice breathe exclusively through their noses, strengthening the relevance of the performed experiments. Mice were sacrificed at various time points up to the terminal stage of the disease, and various organs were subsequently examined. This provided a dynamic overview of the progression of PrP^{Sc} from the respiratory entry portal to the CNS. The following organs were analyzed by histoblot analysis, Western blot analysis, histology and immunohistochemistry: nasal mucosa, lung tissue, bronchial lymph nodes (BLNs), spleen, brain hemispere, olfactory bulb, cerebellum and spinal cord.

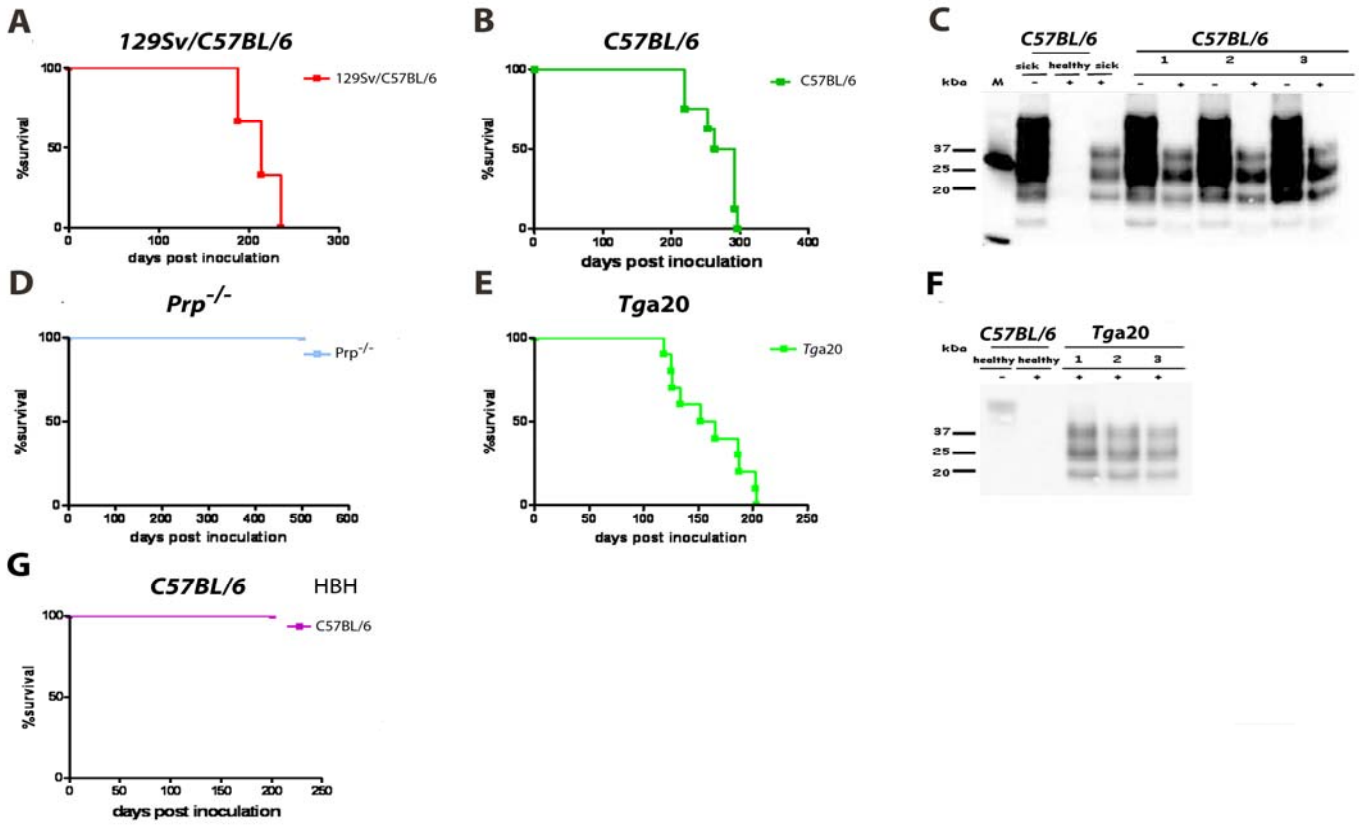

Figure 7: Efficient prion transmission via the intranasal route. Survival curves of **(A)** *129Sv/C57BL/6*, **(B)** *C57BL/6* that were i.n. inoculated with RML6 0.1%. Western blots of **(C)** *C57BL/6* mice that were i.n. inoculated with RML6 0.1%. Survival curves of **(D)** *Prp*$^{-/-}$ and **(E)** *Tg*a20 mice that were i.n. inoculated with RML6 0.1%. Western blots of **(F)** *Tg*a20 mice that were intranasally inoculated with RML6 0.1%. Survival curves of **(G)** *C57BL/6* mice i.n. challenged with HBH. Various mice were analyzed by Western blots for the presence of PrP^{Sc}. Brain homogenates

were analyzed with (+) and without (-) previous proteinase K (PK) treatment as indicated. Homogenate derived from a terminally scrapie-sick mouse served as positive control (sick), and healthy C57BL/6 mouse tissue as negative control (healthy), respectively. Molecular weights are indicated on the left side of the blots. All terminally sick mice showed considerable amounts of PrP^{Sc} in the brain.

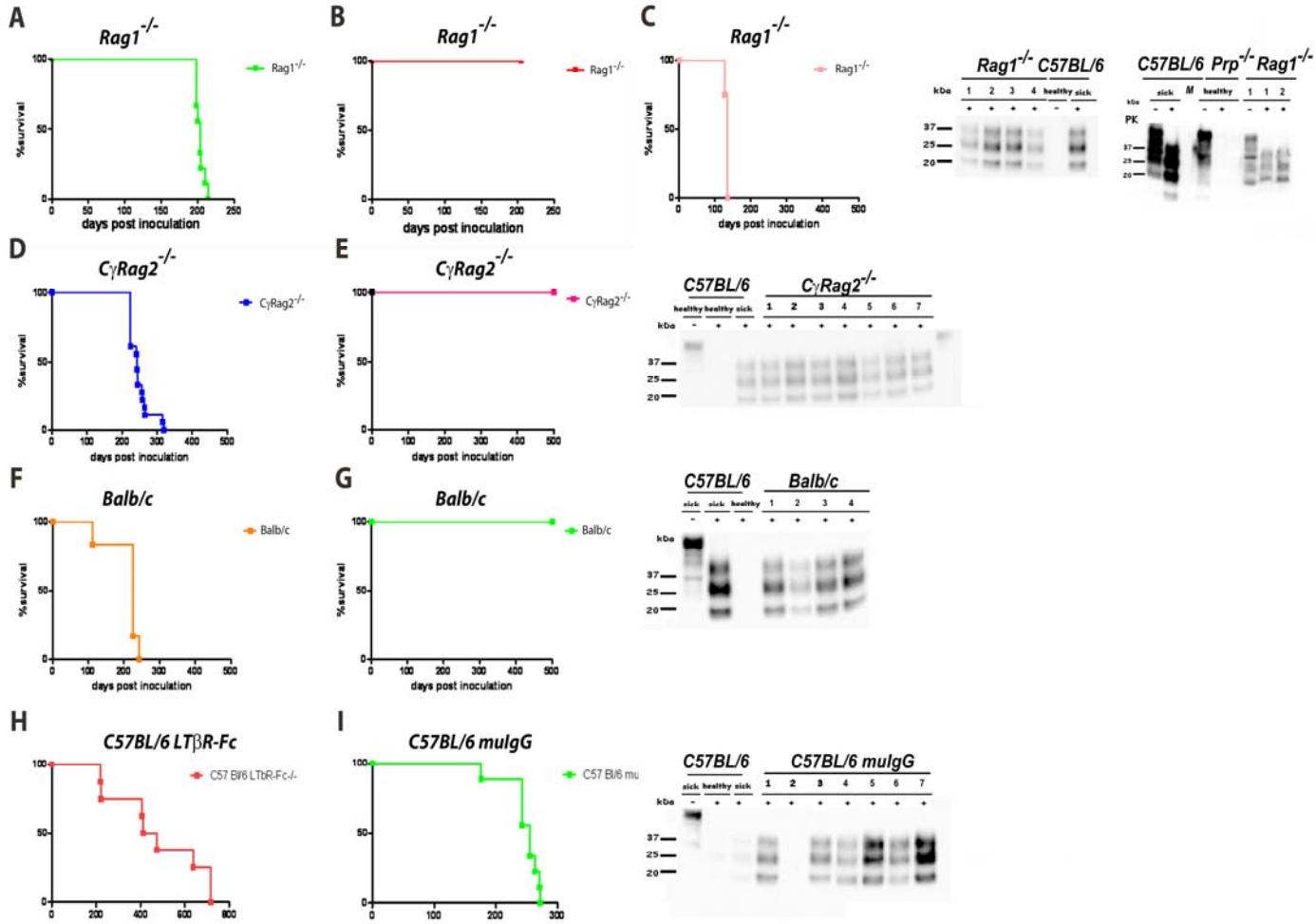

Figure 8: Efficient prion transmission via the intranasal route. Survival curves of **(A)** *Rag1*$^{-/-}$ mice i.n. inoculated with RML6 0.1% or **(B)** with HBH. **(C)** *Rag1*$^{-/-}$ mice i.c. inoculated with RML6 0.1% are shown. Kaplan-Meier curves describe the percentage of survival after particular time points post i.n. prion inoculation (y-axis represents percentage of living animals; x-axis demonstrates survival time in days). **(upper right panel)** Respective Western blots of *Rag1*$^{-/-}$ mice with *C57BL/6* controls are shown. Survival curves of **(D)** *CγRag2*$^{-/-}$ mice i.n. inoculated with RML6 0.1% or **(E)** with HBH. **(second row, right panel)** Respective Western blots of *CγRag2*$^{-/-}$ mice with *C57BL/6* controls are shown. Survival curves of **(F)** *Balb/c* mice i.n. inoculated with RML6 0.1% or **(G)** with HBH. **(third row, right panel)** Respective Western blots are shown. Survival curves of **(H)** *C57BL/6* mice treated with LTβR-Fc or **(I)** with mu-IgG. **(lower right panel)** Respective Western blots are shown. Various mice were analyzed by Western blots for the presence of PrP^{Sc}. Brain homogenates were analyzed with (+) and without (-) previous proteinase K (PK) treatment as indicated. Homogenate derived from a terminally scrapie-sick mouse served as positive control (sick), and healthy *C57BL/6* mouse tissue as negative control (healthy), respectively. Molecular weights are indicated on the left side of the blots.

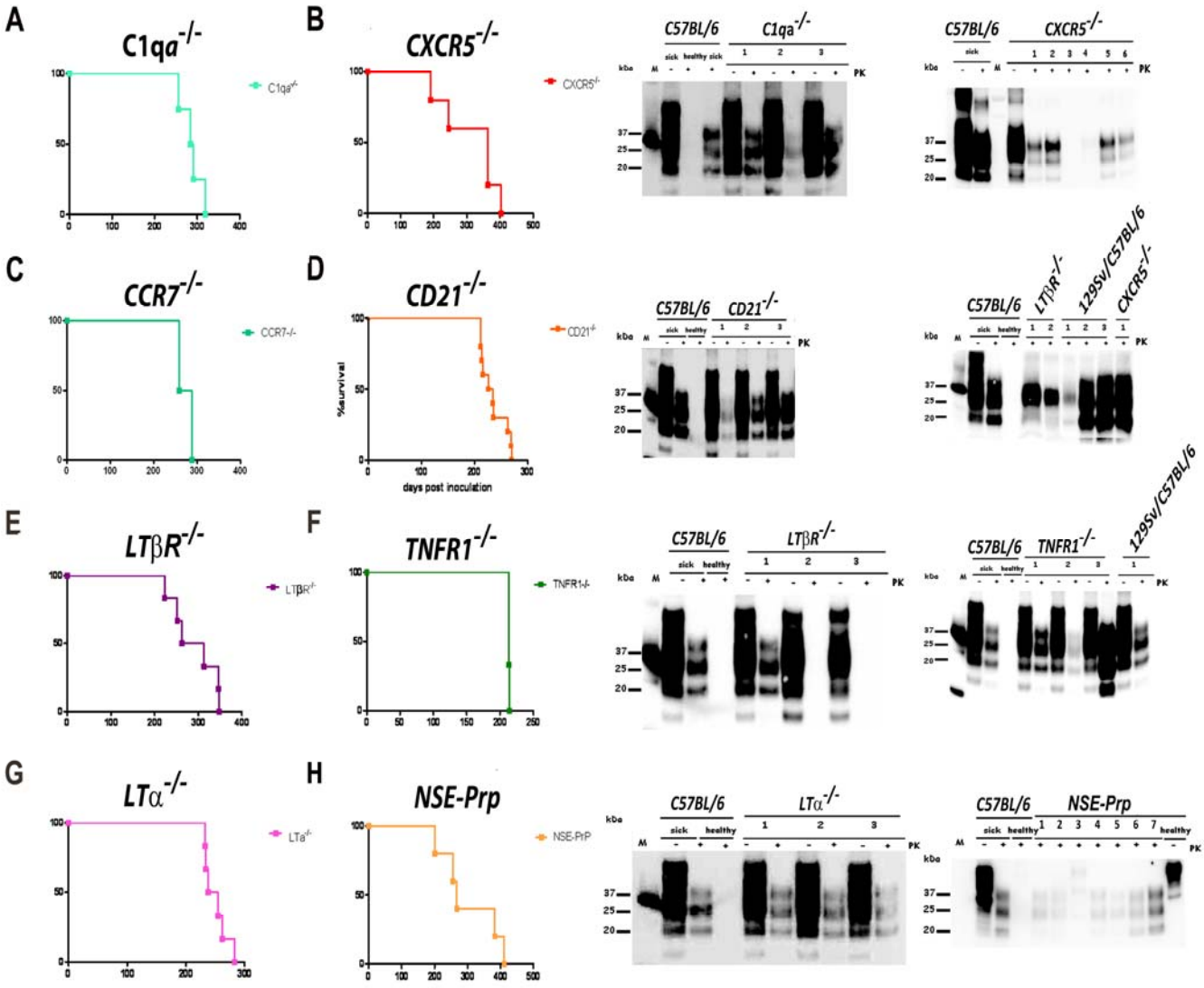

Figure 9: Efficient prion transmission via the intranasal route. **(A)** *C1qa*$^{-/-}$ mice i.n. inoculated with RML6 0.1% and **(B)** *CXCR5*$^{-/-}$ mice i.n. inoculated with RML6 0.1% are shown. Respective Western blots of **(upper row, left panel)** *C1qa*$^{-/-}$ mice i.n. inoculated with RML6 0.1% and **(upper row, right panel)** *CXCR5*$^{-/-}$ mice i.n. inoculated with RML6 0.1% are shown. Survival curves of **(C)** *CCR7*$^{-/-}$ mice i.n. inoculated with RML6 0.1% and **(D)** *CD21*$^{-/-}$ mice i.n. inoculated with RML6 0.1% are shown. Respective Western blots of **(second row, left panel)** *CD21*$^{-/-}$ mice i.n. inoculated with RML6 0.1% and **(second row, right panel)** *CCR7*$^{-/-}$ mice i.n. inoculated with RML6 0.1% are shown. Survival curves of **(E)** *LTβR*$^{-/-}$ mice i.n. inoculated with RML6 0.1% and **(F)** *TNFR1*$^{-/-}$mice i.n. inoculated with RML6 0.1% are shown. Respective Western blots of **(third row, left panel)** *LTβR*$^{-/-}$ mice i.n. inoculated with RML6 0.1% and **(third row, right panel)** *TNFR1*$^{-/-}$ mice i.n. inoculated with RML6 0.1% are shown. Survival curves of **(G)** *LTα*$^{-/-}$ mice i.n. inoculated with RML6 0.1% and **(H)** *NSE-PrP* mice i.n. inoculated with RML6 0.1% are shown. Respective Western blots of **(lower row, left panel)** *LTα*$^{-/-}$ mice i.n. inoculated with RML6 0.1% and **(lower row, right panel)** *NSE-PrP* mice i.n. inoculated with RML6 0.1% are shown.

2.5.5.1 Various mouse strains intranasally infected with prions succumb to scrapie

In order to elucidate the impact of specific cellular comparments, I analyzed as experimental cohorts a "molecular group" with *PrP* $^{-/-}$ (n=11), *Tg*a20 (n=10) and *NSE-PrP* mice (neuron specific PrP^C expression) (n=6), a "deficiency group" with *Rag1*$^{-/-}$ (n=9), *CγRag2*$^{-/-}$ (n=20), LTα$^{-/-}$ (n=6), *LTβR*$^{-/-}$ (n=6), *TNFR1*$^{-/-}$ (n=3), *CD40L*$^{-/-}$ (n=4), *C1qa*$^{-/-}$ (n=4), *CD21*$^{-/-}$ mice (n=10), a "chemokine group" with *CCR7*$^{-/-}$ (n=2), *CXCR5*$^{-/-}$ mice (n=5), respective controls, and an "induced mouse model group" with *C57BL/6* mice treated with LTβR-Fc (n=8) or murine IgG (n=9) as control. *C57BL/6* (n=20) and *C57BL/6129Sv* (n=5) mice served as internal positive controls. *Tg*a20 mice overexpressing PrP^C underlined the role of PrP^C in prion pathogenesis with a shortened incubation time. As negative controls, *Prp*$^{-/-}$ (n=11) mice were used. The results from these experiments are summarized below.

2.5.5.2 Intranasal prion propagation depends on the PrP^C expression levels

*Tg*a20 (PrP^C overexpressing) and *129SvC57BL/6* mice succumbed to scrapie after i.n. prion inoculation with an attack rate of 100% (survival time *Tg*a20 mice: 160 dpi, stdev +/- 28 days). *Tg*a20 mice, displaying a reduced incubation time in comparison to *C57BL/6* mice (survival time *C57BL/6* mice: 259 dpi, stdev +/- 64 days) (Fig. 7) and *129SvC57BL/6* mice (survival time *129SvC57BL/6* mice: 220 dpi, stdev +/- 21 days) (Fig. 7), showed a minimally shortened incubation period when compared to control mice after i.n. inoculation or compared to i.c. inoculation (Fig. 7; data not shown). *NSE-PrP* mice (survival time *NSE-PrP* mice: 291 dpi, stdev +/- 86 days) displayed longer survival times (Fig. 9) compared to control animals, whereas *Prp*$^{-/-}$ mice, lacking PrP^C, remained resistant to prions (Fig. 7D). These findings are consistent with the current understanding of prion pathogenesis. *NSE-PrP* mice are characterized by an almost exclusive expression of PrP^C in neurons within the CNS and display a higher expression level of PrP protein in the CNS when compared to *C57BL/6* mice. All i.n. challenged *NSE-PrP* mice also developed scrapie, although the incubation times were significantly prolonged.

2.5.5.3 Relevance of the complement system for prion pathogenesis after intranasal challenge

The complement system is an important part of immune defense mechanisms and has also been shown to be involved in peripheral prion infection of lymphoid organs. The complement C1q*a* is known to be involved in the binding of PrP^{Sc} to follicular dendritic cells (FDCs), and accordingly, C1qa$^{-/-}$ mice are resistant to prion infection upon low-dose peripheral inoculation. *CD21*$^{-/-}$ mice (complement receptor 2-deficient which also lack the *C3d/C4b*-opsonized antigen receptor), on the other hand, display a normal lymphoid microarchitecture while showing a reduction in germinal centre (GC) size. The incubation time in these mice is greatly increased upon peripheral prion inoculation via the i.p. route. To determine whether complements were involved in prion infection via the intranasal route, C1q*a*$^{-/-}$ and *CD21*$^{-/-}$ were inoculated

i.n. C1q*a*$^{-/-}$ mice (n=6), as well as *CD21*$^{-/-}$ (n=10) mice succumbed to scrapie with an attack rate of 100% after i.n. inoculation (survival time in C1q*a*$^{-/-}$ mice: 288 dpi, stdev +/- 26 days; survival time in *CD21*$^{-/-}$ mice: 235 dpi, stdev +/- 24 days) (Fig. 9). These results indicate that these complement components are not essential for prion propagation following i.n. application. Additionally, I also i.n. inoculated *CD40L*$^{-/-}$ mice with prions. As these mice cannot switch the isotype, they cannot respond with antigen-specific antibodies following prion infection. They also lack GC B-cells; however, small FDCM1^{+} networks are still present. No effect on incubation time upon i.c. prion inoculation and a reduced incubation time following i.p. prion inoculation were previously described in *CD40L*$^{-/-}$ mice. In my experiments, all i.n. challenged *CD40L*$^{-/-}$ mice succumbed to terminal scrapie (survival time *CD40L*$^{-/-}$ mice: 107 dpi, stdev +/- 12 days) (data not shown).

2.5.5.4 CCR7 or CXCR5 deficiency does not protect against intranasally administered prions

CCR7$^{-/-}$ mice show an impaired migration of dendritic cells (DCs) from the periphery, which are exposed to antigens in secondary lymphoid organs. FDCs in *CXCR5*$^{-/-}$ mice are in closer proximity to nerve terminals compared to WT mice. This leads to a reduced incubation time upon peripheral prion inoculation. In contrast, upon i.n. prion inoculation both mouse strains reacted with a prolonged incubation time (survival time *CCR7*$^{-/-}$ mice: 273 dpi, stdev +/- 21 days; survival time *CXCR5*$^{-/-}$ mice: 280 dpi, stdev +/- 119 days) (Fig. 9).

2.5.5.5 Induced mouse models

Treatment of *C57BL/6* mice with LTβR-Fc blocks LTβR signaling and leads to dedifferention of FDCs and ablated GCs. To determine whether inhibition of LTβR signaling would affect the rate of i.n. prion infection, I once again treated *C57BL/6* mice with 100µg LTβR-Fc/mouse prior and post prion challenge (-7 days, 0 days, +7 days). These mice were then tested for their capability of prion infection upon i.n. administration and remarkably, again 100% of the i.n. challenged mice died because of scrapie (survival time *C57BL/6* mice treated with LTβR-Fc: 476 dpi, stdev +/- 200 days) (Fig. 8H). *C57BL/6* mice treated with muIgG (survival time *C57BL/6* mice treated with muIgG: 246 dpi, stdev +/- 29 days) served as control group (Fig. 8I).

2.5.5.6 Mechanisms of neuroinvasion and the role of the immune system

Next, I sought to determine how prions enter the CNS following i.n. application. Is a functional immune system required for neuroinvasion upon i.n. infection with prions? To address this question, I inoculated either *Rag1*$^{-/-}$ mice (n=9), which lack mature B- and T-cells and *C*γ*Rag2*$^{-/-}$ mice (n=20), which lack mature B-, T- and NK-cells either i.n. or (as a control) i.c.. In addition, both mouse strains were also i.n. inoculated

with HBH to exclude the possibility that the inoculation strategy itself impacts the life expectancy of treated mice. None of the mice inoculated with HBH displayed a shortened life span, and none developed clinical signs resembling scrapie. As expected i.c. prion infection very efficiently led to terminal scrapie after approximately 150 days (survival time *Rag1*$^{-/-}$ mice: 131 dpi, stdev +/- 8 days) in *Rag1*$^{-/-}$ (Fig. 8). As *Rag1*$^{-/-}$ mice were generated on a *C57BL/6* background and *CγRag2*$^{-/-}$ mice on a *BalbC* background these mouse strains were also i.n. challenged with RML prions (Fig. 8). As additional controls, *Rag1*$^{-/-}$ and *CγRag2*$^{-/-}$ mice were i.p. inoculated; however in this case the dosage used for the i.n. prion challenge did not suffice to induce scrapie in mice (data not shown). Remarkably, 100% of the i.n. inoculated *Rag1*$^{-/-}$ or *CγRag2*$^{-/-}$ mice i.n. exposed to prions succumbed to scrapie (survival time *Rag1*$^{-/-}$ mice: 203 dpi, stdev +/- 6 days; survival time *CγRag2*$^{-/-}$ mice: 235 dpi, stdev +/- 29 days; survival time *BalbC* mice: 209 dpi, stdev +/- 48 days) (Fig. 8), providing evidence for an LRS-independent mechanism of prion neuroinvasion upon i.n. prion administration. PK-resistant material was present in different regions of the CNS (OB, frontal lobe, temporal and parietal lobe, midbrain, cerebellum, s.c.), but was not detectable in spleens, BLNs, lungs and tracheae of scrapie sick *Rag 1*$^{-/-}$ mice. The onset of scrapie in the absence of a functional immune system favors a direct peripheral transmission route without the involvement of the LRS.

2.5.5.7 TNF superfamily members (TNFR1 and Lymphotoxin) and i.n. applicated prions

Additionally, I also challenged *LTα*$^{-/-}$, *LTβR*$^{-/-}$ and *TNFR1*$^{-/-}$ mice i.n. with RML prions. Both, *LTα*$^{-/-}$ and *LTβR*$^{-/-}$ mice lack Peyer`s patches and lymph nodes as well as an intact NALT. Furthermore, these mice display chronic inflammation of the lungs. Consistent with a role for lymphotoxin signaling in peripheral prion infection, these mice are not capable of efficiently replicating prions upon peripheral administration. On the other hand, *TNFR1*$^{-/-}$ mice lack Peyer`s patches, show an aberrant splenic microarchitecture, an abnormal NALT, but have intact lymph nodes where prion replication can occur. However, the prion replication efficacy in spleen was reduced or absent. These mice die due to scrapie after a prolonged incubation time when peripherally challenged with prions. Interestingly, when i.n. infected, most of these mice efficiently succumbed to scrapie (survival time *LTα*$^{-/-}$ mice: 250 dpi, stdev +/- 20 days; survival time *LTβR*$^{-/-}$ mice: 251 dpi, stdev +/- 52 days; survival time *TNFR1*$^{-/-}$ mice: 213 dpi, stdev +/- 1 days) (Fig. 9). At terminal disease stages, mice were sacrificed and organs were isolated for further examination and scrapie confirmation.

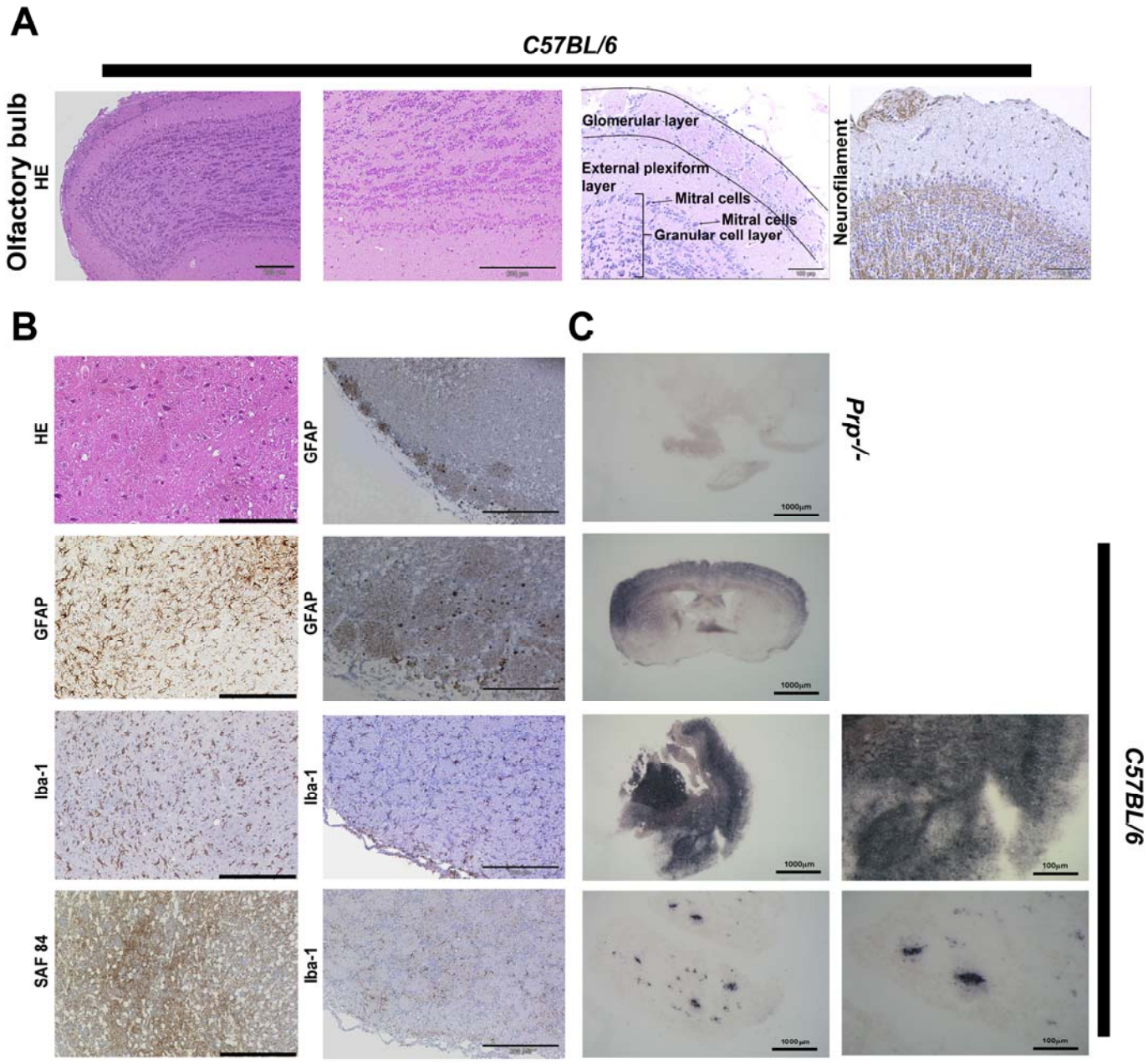

Figure 10: Histological, immunohistochemical and immunoblot confirmation of prion disease. (A) Histological and immunohistochemical characterization of scrapie affected *C57BL/6* mouse brains. Representative olfactory bulbs (HE and Neurofilament stains) are shown. **(B)** Histological and immunohistochemical characterization of scrapie affected *C57BL/6* mouse brains. Representative olfactory bulbs display spongiosis, astrogliosis, microglial activation and Prp^{Sc} deposits (HE, GFAP, Iba-1 and SAF-84 staining). **(C)** Histoblot analysis of prion infected mouse brains. Upper panel: shows healthy brain of a $Prp^{-/-}$ mouse as negative control, other panels demonstrate Prp^{Sc} deposits in *C57BL/6* mice. Arrow bars indicated the sizes of the respective figures.

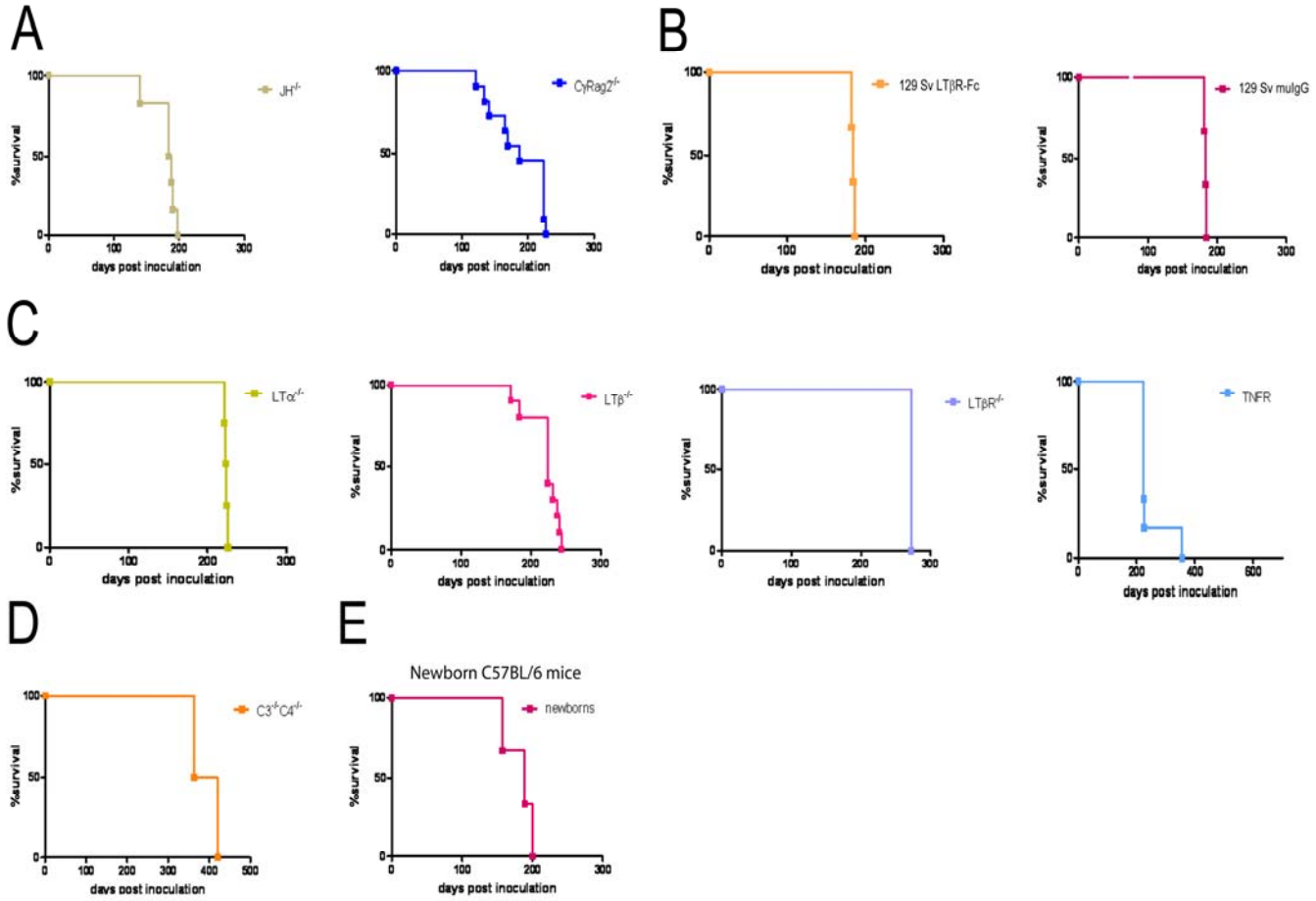

Figure 11: Efficacy of prion transmission through aerosols in immunocompromised and newborn mice. Various mouse strains **(A-D)** were exposed to aerosolized RML infected brain homogenates (*JH*$^{-/-}$, *CγRag2*$^{-/-}$, *129Sv/C57BL/6* treated with LTβR-Fc or with mu-IgG, *LTα*$^{-/-}$, *LTβ*$^{-/-}$, *LTβR*$^{-/-}$, *TNFR1*$^{-/-}$, *C3*$^{-/-}$*C4*$^{-/-}$).(**E**) Newborn C57BL/6 mice were exposed for 10 minutes to aerosols generated from a 20% RML6 mouse brain homogenate. Kaplan-Meier curves describe the percentage of survival after particular time points post prion aerosol treatment. Exposure to aerosols generated from healthy mouse brain homogenates did not have any effect (data not shown).

2.5.6 Experiments with newborn mice argue against an ocular infection

Another possible mechanism of prion transmission via aerosols may be through the ocular route, namely via cornea and/or retina (Safar et al., 1998; Wadsworth, 2001). In order to verify or exclude this possibility, newborn, under one day old, *Tg*a 20 (n=3) and *CD1* (n=3) mice with eyelids still closed were exposed to prion aerosols. These experiments were performed in Tübingen by Lothar Stitz and his co-workers. All these mice developed scrapie and PrP^{Sc} was detectable in their brains when sacrificed at terminal disease stages after an incubation time between 157 (*Tg*a20) and 211 (*CD1*) days (Fig. 11E; data not shown).

These experiments prove that (1) mice have not contracted scrapie via the ocular route, and (2) a functionally active immune system is not essential for aerosolic prion transmission. However, as mice were

exposed to aerosols under saturating conditions in an inhalation chamber, I cannot exclude the possibility that they may have contracted infection via their airways or might have ingested a portion of condensed inoculum, analogously to oral transmission. Nevertheless, in similar experimental setups (e.g. using RML or Me7 prion strains), oral inoculation with prions is much less efficient than aerosol exposure, and it leads to much longer incubation times (Russelakis-Carneiro et al., 1999; Scott et al., 1993) arguing against this possibility.

2.5.7 Evaluation of transmission efficacy and exclusion of side-pathways

The results obtained after aerosol exposition of newborn mice lacking a functional immune system, including gut associated lymphoid tissue (GALT) functions, support the idea of an LRS-independent prion transmission route. In addition, untreated littermates or other sentinels which were reared or housed together with aerosol-treated mice immediately following exposure to aerosols neither showed signs of scrapie nor the presence of PrP^{Sc} in brains, even after 482 dpi. This indicates that prion transmission was the consequence of direct exposure to the particular aerosols rather than the result of transmission by other routes like ingestion of PrP^{Sc} from fur by grooming.

2.5.8 Aerosolic infection occurs independently of a functionally intact immune system

The next question that arose was how important the LRS is for prion infection upon aerosolic challenge in adult immunocompromised mice. Therefore, several immune deficient mouse strains were exposed to aerosolized prion infected brain homogenates. These included *JH*$^{-/-}$ mice (n=6) lacking B- and T-cells, *CγRag2*$^{-/-}$ mice (n=11) lacking mature B-, T- and NK-cells, *LTα*$^{-/-}$ (n=4), *LTβ*$^{-/-}$ (n=10), *LTβR*$^{-/-}$ (n=6), *TNFR1*$^{-/-}$ mice (n=6), *CD40L*$^{-/-}$ mice (n=6) and *C3*$^{-/-}$*C4*$^{-/-}$ (n=3) mice. In addition, *C57BL/6* mice treated with LTβR-Fc displayed a dedifferentiation of mature FDCs paralleled by ablation of GCs. To achieve an immunocompromised state control mice were i.p. treated with 100µg LTβR-Fc/mouse prior and post-prion challenge (-7 days, 0 days, +7 days). Upon application of reduced dosages of prions (RML 5), peripheral prion replication is known to be either decreased or abolished. *C57BL/6* mice that had been treated with LTβR-Fc (n=3) or murine IgG (n=3) as a control were also exposed to RML prions. Even *NSE-PrP* mice (n=4) were susceptible to prion aerosol exposure. Remarkably, all these mouse lines were susceptible to prions given as aerosols to the respective host (Fig. 11; data not shown). This indicates that aerosolic prion infection is an efficient prion transmission route that does not require a preserved immune status.

Additionally, I tried to find differences in the distribution pattern of PrP^{Sc} by evaluating histoblots and Western blots in all mice challenged with prions via the aerial route. Some examples are shown in Fig. 12. No clear differences could be identified with respect to the genetic background.

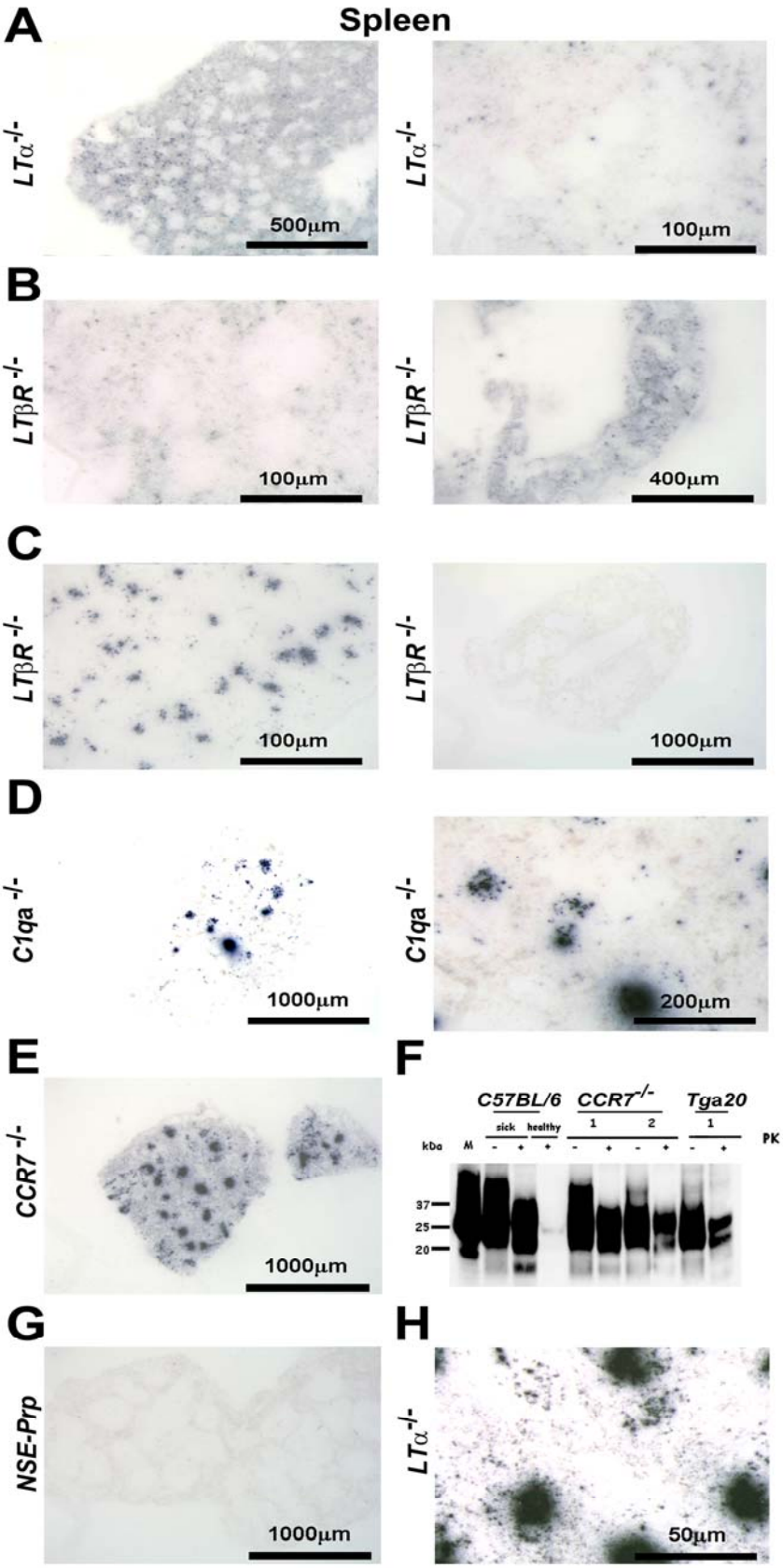

Figure 12: Histoblot profiling of i.n. prion infected mice. (A-E) Histoblot analysis of spleens of *LTα*$^{-/-}$, *LTβR*$^{-/-}$, *C1q*a$^{-/-}$, *CCR7*$^{-/-}$ mice. **(F)** Western blot analysis of spleens of *CCR7*$^{-/-}$ and *Tg*a20 mice. Mice were investigated for the presence of PrP^{Sc}. Spleen homogenates were analyzed with (+) and without (-) previous proteinase K (PK) treatment

as indicated. Homogenate derived from a terminally scrapie-sick mouse served as positive control (pos. ctr.), and healthy C57BL/6 mouse tissue as negative control (neg. ctr.), respectively. Molecular weights are indicated on the left side of the blots. All terminally sick mice showed considerable amounts of PrP^{Sc} in the brain. **(G, H)** Histoblot analysis of spleens of *NSE-PrP* and *LT*$\alpha^{-/-}$ mice. Scale bars: sizes are indicated.

2.6 DISCUSSION

The transmissibility of prion diseases was initially described for scrapie in goats as early as 1939 (Cuille and Chelle, 1939). Since then, numerous natural and experimental transmission routes have been reported. Whereas variant Creutzfeldt-Jakob Disease (vCJD) is transmitted via ingestion of contaminated food from BSE-infected cattle, possible transmission of CJD via blood has also been recently reported (Allain et al., 2009; Choi et al., 2009; Head et al., 2009; Jones et al., 2009; Murray et al., 2009). In addition to well established peripheral routes (oral, i.p., i.c., ocular, intramuscular, transdermal), other experimental routes have revealed the possibility of transmission of prion disease after intraveneous injection and even after exposure of the tongue to PrP^{Sc} (Mulcahy et al., 2004). The aerial transmission route is common for various microbes; however, to my knowledge this has never been investigated for prion aerosols, and incompletely for i.n. applicated prions (Bessen et al., 2009; Corona et al., 2009; DeJoia et al., 2006; Diringer, 1995; Doty, 2008; Hamir et al., 2008; Kincaid and Bartz, 2007; Park et al., 2002; Sbriccoli et al., 2009). Therefore, in collaboration with Prof. Stitz's laboratory, I sought to experimentally evaluate whether prion disease could be transmitted by (1) aerosols and upon (2) contact-mediated i.n. challenge.

For the experimental aerosol infection paradigm, the particle size generated by the nebulizer device ensured that the entire respiratory tract was flooded by the aerosol and that the aerosolized brain homogenate containing the pathological form of the prion protein was able to reach the inner surface of the lung. There prions may colonize airway-associated lymphoid tissues and, thereafter, gain access to the CNS. This prediction was proven correct by the experiments where the pulmonary deposition of PrP^{Sc}-containing inoculum was investigated.

2.6.1 Dissecting prion neuroinvasion after nasal prion administration

I sought to determine whether the reported lack of involvement of the olfactory nerves is a general phenomenon or a strain-dependent feature, as well as to determine the pathways and timelines for dissemination of the infectious agent into the brain upon exposure to prion aerosols or i.n. administration of prions. The experiments clearly demonstrate that transmission of aerosolized, scrapie terminal brain homogenates very efficiently leads to terminal scrapie. In this study, PrP^{C} expression levels and the site of PrP^{C} expression (*NSE-PrP* mice for example) were shown to determine the length of the incubation time upon (1) aerosolic infection and (2) contact-mediated i.n. inoculation.

2.6.2 Prion neuroinvasion after i.n. application in immunocompromised mice

Following peripheral exposure, many of the acquired TSE agents accumulate and replicate in lymphoid tissues and the LRS, including the spleen, lymph nodes, Peyers's patches (PPs) and tonsils (Beekes and McBride, 2000; Hill et al., 1997b; Hilton et al., 1998; Mabbott and MacPherson, 2006; Mould et al., 1970;

Sigurdson et al., 1999; Wadsworth, 2001) After peripheral replication in the LRS, prions are transported to the CNS primarily via peripheral nerves (Aguzzi and Heikenwalder, 2006). It has been shown that innervation of secondary lymphoid organs is a rate-limiting step in prion neuroinvasion (Glatzel et al., 2001). The distance between FDCs and splenic nerve endings has been reported to have an impact on the speed of neuroinvasion (Prinz et al., 2003a).

Remarkably, in these experiments prion transmission occurred in the absence of B-, T- and NK-cells as evidenced by i.n. prion infection of *Rag1*$^{-/-}$ or *CγRag2*$^{-/-}$ mice, indicating a direct transmission route after aerosolic and i.n. prion inoculation. Rather than depending on the LRS, I propose an alternative pathway of direct, contact-mediated prion neuroinvasion which occurs via the dendrites of olfactory neurons extending to the surface of the olfactory epithelium. This is supported by the finding that immunodeficient mice such as newborns, *Rag1*$^{-/-}$ or *CγRag2*$^{-/-}$ mice are equally susceptible to aerosolic and i.n. prion infection as control mice.

Various explanations could underlie these findings: the data either stand in contrast to Sbriccoli`s work (Sbriccoli et al., 2009), or alternatively, the mechanism may also depend on the particular prion strain investigated. However, the data presented here are consistent with recent work by Bessen et al (Bessen et al., 2009) who could show that prion neuroinvasion from the tongue and nasal cavity can occur in the absence of LRS infection. These reported findings partially depended on the strain of the prion agent and/or the host species. This group explained the paucity of Prp^{Sc} deposits in the oral and nasal mucosa from LRS replication-deficient hosts following neuroinvasion by an infection of nerve fibres. These authors hypothesized that the amount of infectivity lies below the detection limit of Prp^{Sc}. Alternatively, they suggest prion transport along cranial nerves without replication (Bessen et al., 2009). Consistent with these data, here I show that horizontal prion transmission can be achieved through airborne infection. I have investigated the transmissibility potential of prions administered by aerosols or i.n.. As prion aerosols may be generated by prion-infected individuals, either of human or of animal origin, prion-contaminated aerosols are highly relevant for horizontal prion transmission. Interestingly, prion transmission occurred in the absence of B-, T- and NK-cells, suggesting a direct transmission route upon i.n. prion inoculation.

Various transgenic mouse models (e.g. *NSE-PrP*; *Tg*a20) expressing the cellular prion protein (PrP^{C}) in specific tissues or cells of the brain or the periphery (e.g. exclusively in the CNS) were investigated to identify the cellular and molecular mechanism(s) of prion invasion via the i.n. route.

In contrast to data provided by others (Bessen et al., 2009), in my hands, *LTα*$^{-/-}$ mice are also infectable with the RML prion agent via the i.n. route. These contradictory results are most probably due to the detection limits of minute amounts of prions. In summary, these results identify aerosols as a highly efficacious mode of prion transmission. In an experimental model of mouse scrapie, I found in collaboration with Prof. Stitz's laboratory that (1) prion aerosols can efficiently transmit the disease in various mouse lines, which depends on the PrP^{C} expression level. In addition, different strains of knock-out and immunodeficient mice were tested for the efficiency of prion transmissibility. These data were reproducible upon (2) i.n. challenge of

mice.

I was also able, despite the limitations of prion diagnostics in mice, to elucidate the cellular and molecular mechanism driving (1) aerosolic and (2) i.n. prion transmission and the subsequent infection of the CNS by prions. A scheme describes the possible ways of the infectious particles after prion infection via the aerial route (Figure 3). Prion transmission to the CNS may occur directly through the nasal mucosa via olfactory nerves (*direct pathway*) involving uptake of prions by the olfactory nerve terminals. Alternatively, uptake mmight require a lymphoid replication phase (*immune mediated pathway*): e.g. in the BLNs, the NALT or the spleen before entering the CNS.

This novel pathway of prion transmission is not only conceptually relevant for the field of prion research, but also highlights a thus far unappreciated risk factor for laboratory personnel and personnel of the meat processing industry. In the light of these findings, it may be appropriate to revise our current prion-related biosafety guidelines and public health standards.

Abbreviations:

AA	amino acid
α1AT	α1-antitrypsin deficiency
ALD	alcoholic liver disease
ALT	alanine aminotransferase
ASH	alcoholic steatohepatitis
AST	aspartate aminotransferase
BLC	B lymphocyte chemoattractant
BM	bone marrow
bp	base pair
CASH	chemotherapy associated steatohepatitis
CCC	Cholangiocellular carcinoma
CD	cluster of differentiation
cDNA	complementary DNA
CH	cholestasis
CJD	Creutzfeldt-Jakob-disease
CNS	central nervous system
cT	threshold cycle
Ctrl	control
CWD	chronic wasting disease
DC	dendritic cell
DNA	Deoxyribonucleic acid
dNTP	Deoxynucleotide
dpi	days post infection
DTT	Dithiothreitol
ECL	enhanced chemiluminescence
EDTA	Ethylendiamintetraacetic acid
ELC	EBl-1 ligand chemokine

Abbreviations

ELISA	Enzyme-linked immunosorbent assay
FDC	follicular dendritic cell
FFI	fatal familial insomnia
FITC	fluorescein isothiocyanate
FLF	focal liver fibrosis
FNH	focal nodular hyperplasia
GALT	gut associated lymphoid tissue
GAPDH	glyceralaldehyde 3-phospate deghydogenase
GC	germinal centre
GFAP	glial acidic fibrilarry protein
GPI	glycosyl-phosphatidyl-inositol
GSS	Gerstmann-Sträussler-Scheinker disease
H&E	hematoxylin and eosin (also HE)
HBV	hepatitis B virus
HCC	hepatocellular carcrinoma
HCV	hepatitis C virus
HE/SID	hemochromatosis/siderosis
Hep	hepatocytes
HEV	hepatitis E virus
HVEM	Herpes virus entry mediator
IFNγ	Interferon gamma
IgG	Immunoglobulin G
IKK	IkB kinase complex
IL	Interleukin
i.n.	intranasal
I.p.	intraperitoneal
IKB	Inhibitor of KB
kD	Kilo dalton

LD	lethal dose
LIGHT	Homologous to lymphotoxins, exhibits inducible expression, and competes with HSV glycoprotein D for HVEM, a receptor expressed by T lymphocytes
LN	Lymph node
LOH	Loss of heterozygosity
LPS	Lipopolysaccharide
LTα	Lymphotoxin α
LTβ	Lymphotoxin β
LT	Lymphotoxin
LT-R	Lymphotoxin receptor
M	Molar
MALT	Mucosa associated lymphoid tissue
MHC	Major histocom patibility com plex
MMP	Matrix metalloproteinase
mRNA	messenger RNA
muIgG	murine IgG
NALT	nasopharyngeal-associated lymphoid tissue
NASH	non alcoholic steatohepatitis
NEMO	NF-κB essential modifier
NF-κB	Nuclear factor of KB
NIK	Nuclear factor of KB inducing kinase
NLS	Nuclear localization signal
NOD	Non obese diabetes
NSAID	Non steroidal anti-inflammatory drug
NVH	non-virus induced HCC
OLD	other liver diseases
ORF	Open Reading Frame
PAGE	Polyacrylamid gel electrophoresis

PBC	primary biliary cirrhosis/ autoimmune cholangitis
PBS	Phosphate-buffered saline
PCR	Polymerase chain reaction
PE	Phycoerythrin
PNA	Peanut agglutinin
PP	Peyers Patch
PTA	Sodium phosphotungstic acid
RML	Rocky mountain laboratory (prion strain)
RNA	Ribonucleic acid
ROS	Reactive oxygen species
RT	Room temperature
RT-PCR	Reverse transcription PCR
SAF	Spongiosis associated fibrils
SDS	Sodium dodecyl sulfate
TCR	T cell receptor
Tg	Transgenic
TLO	Tertiary lymphoid organ
TNF	Tumor necrosis factor
TNFR	TNF receptor
U	unit
VCAM-1	Vascular cell adhesion molecule 1
WD	Wilson`s disease
WHO	world health organization
WT	wild-type
w/v	weight/volume
$^{-/-}$ or $^{0/0}$	knockout
-	negative for
+	positive for

4 Material and Methods

4.1 Human liver tissue

Human liver biopsies were obtained from the University Hospital Zurich, Switzerland, the University Hospital Freiburg, the University Hospital Heidelberg, Germany, the University of Graz, Austria and the University Hospital Grenoble, France. All samples were registered in the respective biobanks and were kept anonymous. The research project was authorized by the ethical committees of the "Gesundheitsdirektion Kanton Zürich" (Ref. Nr. StV 26-2005) Switzerland, Freiburg (Forschungsvorhaben Nr. 299/2001) and Heidelberg (Prof. Bannasch), Germany, "Ethikkomission der medizinischen Universität Graz" (Ref. Nr. Version 1.0 24/11/2008; Prof. Zatloukal) University of Graz, Austria, and by the ethical committee of the University Hospital Grenoble (Ref. Nr. 03/APTF/1, promoter APTFC, Prof. V Leroy). The study protocol was in accordance with the ethical guidelines of the Helsinki declaration and was approved by the review board of the University Hospital Grenoble. Patients were enrolled after giving their written informed consent. HBV- or HCV infected patients suffering from chronic hepatitis were not treated with ribavirin or other immunomodulatory drugs at the time point of needle biopsy.

4.2 Mice

Animals were devoid of any bacterial, viral, and parasitic pathogens listed in the Federation of European Laboratory Animal ScienceAssociations recommendations and were maintained under specific pathogen-free (spf) conditions. Housing and experimental protocols were in accordance with the Swiss Animal Protection Law and mice were held according to the regulations of the Veterinary office of the Canton Zurich. AlbLTαβ transgenic mice were generated as published (Heikenwalder et al., 2005). *Tnfr1*$^{-/-}$, *Tnfr2*$^{-/-}$, *Rag1*$^{-/-}$, *Ltβr*$^{-/-}$, *Ikkα*$^{AA/AA}$ and *Ikkβ*$^{\Delta hep}$ mice were published previously (Alimzhanov et al., 1997; Bluethmann et al., 1994; Browning et al., 1995; Cao et al., 2001; Futterer et al., 1998; Koni et al., 1997; Mackay et al., 1997; Maeda et al., 2005). *Tg*1223, *Tnfr1*$^{-/-}$, *Tnfr2*$^{-/-}$, *Rag1*$^{-/-}$ and *Ikkβ*$^{\Delta hep}$ mice were intercrossed to create *Tg*1223/*Tnfr1*$^{-/-}$, *Tg*1223 /*Tnfr2*$^{-/-}$, *Tg*1223/*Rag1*$^{-/-}$ and *Tg*1223/*Ikkβ*$^{\Delta hep}$.

4.3 Generation of bitransgenic mice overexpressing LTαβ specifically on hepatocytes

As previously published, bitransgenic mice expressing LTα and LTβ in liver under the control of the albumin promoter were generated (Heikenwalder et al., 2005). pBluescript II KS was cut with KpnI, blunted, religated and linearized with BamHI and SahI. A BamHI-SahI restriction product (ca. 5.4 kb) of the PrP 5'HG construct was inserted. The resulting construct was termed AKpnI pBluePrP 5'HG.

The albumin promoter cassette (ca. 2.9 kb) was isolated by digesting pPrP 5‘HGAlbSalI with BamHI and NotI. Murine LTα and LTβ cDNA open reading frames were amplified by PCR from plasmids donated by Prof. Sergei Nedospasov using primers incorporating 50bp and 15bp overhangs with homologous sequences to non-coding regions of *Prnp* (Raeber et al., 1999) as well as MfeI and KpnI restriction sites. LTα primer fwd.: 5’-CGG GGT ACC AGT CCAATT TAG GAG AGC CAA GCA GAC TAT CAT CAT GAC ACT GCT CGG CCG TCT CC-3’. LTβ primer fwd.: 5’-CGG GGT ACC AGT CCA ATT TAG GAG AGC CAA GCA GAC TAT CAT CAT GGG GAC AGG GGA CTG CAG G-3’. LTα primer rev.: 5’-CCACCTCAATTGAATCTACAGTGCAAAGGCTCC-3’. LTβ primer rev.: 5’-CCA CCT CAA TTG AAT TCA CCC CAC CAT CAC CGC-3’. PCR products (610 bps for LTa and 921 bps for LTβ were subcloned into AKpnI pBluePrP5’HG vector. LTα and LTβ ORFs plus flanking regions were sequenced. AKpnI pBluePrP 5‘HGLTFI1. or. FI1. vectors were linearized with BamHI and NotI for the insertion of the promoter cassette. All enzymes were purchased from Roche and New England Biolabs. Fragments were isolated from 0.7% agarose gels (Qiagen, according to the manufacturer’s manual) and dissolved in microinjection buffer. Both constructs were linearized with SahI and NotI and co-injected (equimolar ratio) into male pronuclei of C57BL/6 oocytes. For identification of transgenic mice, the primers below were used: LTα forward primer: (Prp 5‘): 5‘- CTG AGT ATA TTT CAG AAC TG- 3‘. Reverse primer: (LTα rev): 5‘- CAG AGA AAA CCA CCT GGG AG- 3‘. For transgenic LTβ the following primers were used: Primers for LTβ PCR: forward primer (Prp 5‘): 5‘- CTG AGT ATA TTT CAG AAC TG- 3‘. Reverse primer: (LTβ rev): 5‘- GAG TCT CTG AGA GGC TAG AG- 3‘. PCR conditions on a GeneAmp PCR System 9700 (Applied Biosystems) were: 95°C 60 sec. denaturation; 55°C 50 sec. annealing; 72°C 50 sec. elongation; 35 cycles; 72°C 7 mins shoot out; 4°C forever cool down. RNA from wild-type and trangenic mice was isolated in Trizol (Invitrogen) and reverse transcribed using the Geneamp kit (Roche). *C57BL/6-Tg(LTαβ)*1222 and *C57BL/6-Tg(LTαβ)*1223 mouse lines contained one copy per haploid genome of both AlbLTα and AlbLTβ transgenes, with expression restricted to liver and absent from spleen, thymus, mesenteric lymph nodes, pancreas, and kidney. *C57BL/6-Tg(LTαβ)*1223 mice were identified as the highest expressors and were selected for further experiments.

4.3.1 Genomic Southern Blot

For genomic Southern blot analysis mouse tail biopsies were received on dry ice and digested in a lysis buffer containing 100mM Tris-HCl pH 8.5, 5mM EDTA, 0.2% SDS, 20mM NaCl, and 100µg Proteinase K/ml. 10 - 20µg of purified genomic DNA (after Phenol: Chloroform: Isoamylalcohol precipitation) were digested over night and electrophoresed through 0,7% agarose (GIBCO BRL ultra Pure agarose; 15510-027) gels. Genomic digest and DNA separation was checked by ethidium

bromide staining, depurinated by treatment with 1M HCL for 15 mins and 0.4M NaOH for 30mins and transferred to HybondTMN+membranes (Amersham) by vacuum blotting at 50-55 mbar with a Vacu Gene Pump and a Gene XL blotting apparatus (Pharmacia, Biotec) and solutions were used according to the manufacturer's manual (Pharmacia). After the agarose gel was examined for residual DNA, the blot was marked, washed for 5 mins in 2xSSC and prehybridized according to Church and Gilbert (1984). After hybridization (over night at 65°C) with a radioactively labeled probe, the blot was washed and membranes were subjected either to autoradiography using X-ray films (Kodak) or a PhosphorI mager (Molecular Dynamics). Exposed PhosphorImagers were analyzed with a scanner (Aida) and signals were quantified with the Aida 2.41. imaging anaylsis program. To label the probe, template DNA (50ng) was diluted in sterile water and random primer (random Nonamers or Hexamers) were added (Prime-IT® II; Random Primer labeling kit cat# 300385; Stratagene). After gentle mixing, incubation was performed on 95°C for 5 mins. Short centrifugation was followed by 3 mins incubation on ice. This was followed by addition of 5x Primer-buffer (-dCTP), radioactive labeled a32P-dCTP (corresponding to the 25LICi/Amersham Biosciences) and Klenow 5U/µl (Prime-IT® II; Random Primer labeling kit cat# 300385). For purification of the probe a QIAquick PCR-purification kit was used, according to the manufacturer's manual (Quiagen). 10ml sonicated salmon sperm (stock 10µg/ml; Stratagene) were added to the radioactive labeled, purified probe per ml hybridization solution (final conc.: 100µg/ml). The mixture was incubated at 95°C for 5 mins, briefly spinned and chilled on ice for 3 mins before added to the pre-hybridized membrane (2hrs at 65°C). This experiment was performed by Nicolas Zeller and Mathias Heikenwälder.

4.4 TNFα and 3C8 treatment

Twelve to fourteen weeks old male mice (C57BL/6 and various knock-out mice) were i.v. injected with either PBS, murine recombinant TNFα (50µg/kg bodyweight; R&D Systems) and agonistic LTβR antibody (50µg/mouse; clone 3C8; eBioscience) or rat IgG (50µg/mouse; eBioscience) and sacrificed for analysis 45 min post injection. All substances were injected at a total volume of 100µl dissolved in PBS.

4.5 Isolation of intrahepatic murine lymphocytes (IHL)

Mice were anesthetized and liver was perfused with PBS to remove circulating leukocytes. Liver tissue was minced and digested in medium containing collagenase (1mg/ml) and DNase (25µg/ml) at 37°C for 40 min. Cells were centrifuged at 300rpm for 3 min to sediment the majority of hepatocytes. Supernatant was removed and centrifuged again at 1200rpm for 10 min. Cell pellet was resuspended in the 40% fraction of a 40:80 Percoll gradient. Upon centrifugation at 2500rpm for 20 min, IHL were

collected at the interface. IHL were analyzed for surface marker expression by staining with anti-CD4, anti-CD8, anti-TCR-β, anti-NK1.1 or anti-CD19 antibodies, and for cytokine production capacity by intracellular staining with anti-IFNγ and anti-IL17 antibodies (all from eBioscience) upon PMA/Ionomycin stimulation by using a two-laser FACScalibur (BD). Analysis was executed with CellQuest and FlowJo software. Cytokine production by IHL was determined by intracellular staining with anti-IFNγ and anti-IL17 antibodies (all from eBioscience) after 4 hrs stimulation with PMA and Ionomycin.

4.6 Measurement of aminotransferases

The analysis for AST and ALT was performed with mouse serum on a Roche Modular System (Roche Diagnostics) with a commercially available automated colorimetric system at the Institute of Clinical Chemistry at the University Hospital Zurich using a Hitachi P-Modul (Roche).

4.7 RNA isolation from liver tissue

Total RNA from human and mouse liver samples was isolated using RNeasy Mini kit (Qiagen) or RNA-NOW kit (Biogentex-Ozyme). The quantity and quality of the RNA was determined spectroscopically using a nanodrop (Thermo Scientific). For microarray analysis, RNA quality was tested using a bioanalyzer (Agilent). Purified RNA was reversely transcribed into cDNA using Quantitect Reverse Transcription Kit (Qiagen) according to the manufacturer's protocol.

4.8 Real-time RT-PCR

For mRNA expression analysis real-time PCR was performed using Fast Start SYBR Green Master Rox (Roche) or specific TaqMan probes (Applied Biosystems, AB). Primers were custom made by Microsynth or purchased from AB or on a LightCycler® 480 Probes Master (Roche Diagnostics). Real-time PCR was performed on an ABI PRISM 7700 Sequence Detection System or on a 7900 HT Fast Real-Time PCR System (AB). Data were generated and analyzed using SDS 2.3 and RQ manager 1.2 software.

For human *LTβ* and *LTα* Taqman Gene Expression assays from AB were purchased. Hu *LTβ*: Hs00242739_m1(FAM-labelled); probe sequence: 5'-GCC CAC CTC ATA GGC GCT CCG CTG A-3'. Hu *LTα*: Hs00236874 m1(FAM labelled); probe sequence 5'-ACC TCA TTG GAG ACC CCA GCA AGC A-3'. TaqMan analysis for human 18s rRNA was performed with a TaqMan® ribosomal RNA control reagent (VIC™ Probe; AB; Part. No.4308329). mRNA expression levels were

normalized to the housekeeping gene GAPDH (mouse) or 18S rRNA and HPRT (human). Further primers used are listed in the Supplemental material. Efficiency of DNase digest was controlled by PCR of $DNase^{+}RT^{-}$ treated liver RNA samples.

4.8.1 Preparation of mouse-tail lysates for PCR analysis

For PCR screeing of mice, 5-10mm of the tail were cut and lysed in 100Ul lysis buffer containing 50mM Tris-HCl (pH 9.0), 0.5% Nonidet P-40, 0.5% Tween-20 and 0.1mg/ml proteinsae K, at 55°C with agitation over night at 600rpm (Thermomixer 5436, Eppendorf). Following complete digestion, proteinase K was then inactivated by incubation at 95°C for 10 mins. After centrifugation (12000rpm/ 15min/ RT) the lysates were immediately used for PCR or stored at -20°C.

4.8.2 PCR specific for *tg*1222 and *tg*1223 mice

For transgenic LTα the following primers were used: Forward primer: (Prp 5'): 5'-CTG AGT ATA TTT CAG AAC TG-3'. Reverse primer: (LTα rev): 5'-CAG AGA AAA CCA CCT GGG AG-3'. For transgenic LTβ the following primers were used: Forward primer (Prp 5'): 5'-CTG AGT ATA TTT CAG AAC TG-3'. Reverse primer: (LTβ rev): 5'- GAG TCT CTG AGA GGC TAG AG-3'. The following PCR conditions were established on a Gene Amp® PCR System 9700 PCR machine (Applied Biosystems): 95°C 60 sec denaturation; 55°C 50 sec annealing; 72°C 50 sec elongation; 35 cycles.

Gene	fwd-sequence (5'-3')	rev-sequence (5'-3')
ak006094	CGG TTT TAA TCT GAG TGC	GCA ATG AAA GTT TCT TTT AG
ak03 1632	CCT AAT TAG GTT CTA TAG TG	GTT CTA AGA AAC ATC AAA TGC
ak032385	GGA TCC AAC TCT AGT CCT TT	GAT GTGATG GGT TCT AAT C
ak080904	CTT GTC TTT ACT TAC GTC TC	CCT TGG ACT AAA TCA GAA ACC
ak084087	GGT GGT GGA AAT ACT ATC ATG	GCC AAG AAG TAA CAT CTC
arid5a	TCC CGC AGC TTC CTG TAT C	GAC CAG CCT CTC ATA GGT GC
arrdc3	ATG GTG CTG GGA AAG GTA AAG	CGC TAG AAT ACA CGG GGA CAT TA
bc013561	CTG AGG TTT CTT GGT AAT GC	CAC TTT CAA CAG CCA ATT TAA C
Blc	CCA TTT GGC ACG AGG ATT CAC	ATG AGG CTC AGC ACA GCA AC
btg2	ATG AGC CAC GGG AAG AGA AC	GCC CTA CTG AAA ACC TTG AGT C
ccl2	TTA AAA AAC CTG GAT CGG AAC CAA	GCA TTA GCT TCA GAT TTA CGG GT
ccl7	GCT GCT TTC AGC ATC CAA GTG	CCA GGG ACA CCG ACT ACT G
c-fos	AGA CTT CTC ATC TTC AAG TT	AAG ATG GCT GCA GCC AAG T
ch25h	TGC TAC AAC GGT TCG GAG C	AGA AGC CCA CTG AAG TGA TGA T
cxcl1	CTG GGA TTC ACC TCA AGA ACA TC	CAG GGT CAA GGC AAG CCT C
cxcl10	AAG TGC TGC CGT CAT TTT CT	CCT ATG GCC CTC ATT CTC AC
edg8	GCT TTG GTT TGC GCG TGA G	GGC GTC CTA AGC AGT TCC AG
egr1	AGG TTC CCA TGA TCC CTG ACT	GGT ACG GTT CTC CAG ACC CTG
egr2	CAG GAG TGA CGA AAG GAA GC	GAA GAC TGG GCA GAT GGA GG

Elc	GCC TCA GAT TAT CTG CCA T	AGA CAC AGG GCT CCT TCT GGT
e-selectin	CTG CAG TTC TGA CGT GTG GT	GAG CAA TGA GGA CGA TGT CA
extl-1	TTC TGG CTG GCG TTG TCA G	GGG TTC GTC TCA GAC TGG GA
fgf21	CTG CTG GGG GTC TAC CAA G	CTG CGC CTA CCA CTG TTC C
gadd45g	GGG AAA GCA CTG CAC GAA CT	AGC ACG CAA AAG GTC ACA TTG
Gapdh	CCA CCC CAG CAA GGA GAC T	GAA ATT GTG AGG GAG ATG CT
gas1	CCA TCT GCG AAT CGG TCA AAG	GCT CGT CGT CAT ATT CTT CGT C
gpr109b	CTG GAG GTT CGG AGG CAT C	TCG CCA TTT TTG GTC ATC ATG T
g0/g1switch	TAG TGA AGC TAT ACG TTC TGG GC	GTC TCA ACT AGG CCG AGC A
hist1 h1c	AAC CCC AGG CTA AGA AGG C	TGG CTT TAC GGC TTT AGA CGC
hist1h1d	GTG GAG AAG ACA CCT GTG AAG	CCT TGG CTG GAC TCT TTG CT
icam1	TGC GTT TTG GAG CTA GCG GAC CA	CGA GGA CCA TAC AGC ACG TGC CAG
Ifny	TCA AGT GGC ATA GAT GTG GAA GAA	TGG CTC TGC AGG ATT TTC ATG
igfbp1	ATG GGT GCT GCC TGC GGT GTG G	GGT GAG GGC ATG CAG GGG ACG AG
igf1	GGA CCG AGG GCT TTT ACT TCA A	TCG ATA GGG ACG GGG ACT TCT G
igf2	CCG GCT ACC ACA ATG TCC TGC TCT	GCT CCC GCC TGA TGT AAC CTG TCT
Inhbe	AAA AGC CCA GCT CTG GCT AAT	CTG GTT AGG TGC AGT CCC TC
jun-b	TCA CGA CGA CTC TTA CGC AG	CCT TGA GAC CCC GAT AGG GA
Lmln	TGC TGA CGG GCA TTT ACG AAT	TGT CGC ACA TTG TCT GCT AAG
LTα	TCC ACT CCC TCA GAA GCA CT	AGA GAA GCC ATG TCG GAG AA
Ltβ	TAC ACC AGA TCC AGG GGT TC	ACT CAT CCA AGC GCC TAT GA
mkiaaa1 853	GTC TCG GGG CCA GGA GAA G	GAG CTC CGG GCT GTG GAT G
nm025719	ATG TCG CCT GTA TCC CGA TCT	GTA GCG GTC GTT CTC CAG A
nr1d1	TAC ATT GGC TCT AGT GGC TCC	CAG TAG GTG ATG GTG GGA AGT A
Pdxp	ATG AGT CAC ATT CGG GAC CAT	AGG GCA GGA AAT AAG GCC AC
Periplakin	CAA AGG CAA ATA CAG CCC AAC	TTC CAC CTG GTC TGC ATT CTT
p-selectin	GAA AGG GCT GAT TGT GAC CCC	AGT AGT TCC GCA CTG GGT ACA
Rantes	ATG CCG ATT TTC CCA GGA CC	TTT GCC TAC CTC TCC CTA GAG CTG
serpine-1	TTC AGC CCT TGC TTG CCT C	ACA CTT TTA CTC CGA AGT CGG T
Slc	ATG ATG ACT CTG AGC CTC C	GAG CCC TTT CCT TTC TTT CC
socs3	TCC CCG ACT GGG TCT TGA C	GCG GGC ACC TTT CTT ATC C
TNFα	CAT CTT CTC AAA ATT CGA GTG ACA A	TGG GAG TAG ACA AGG TAC AAC CC
TNFαip3	GAA CAG CGA TCA GGC CAG G	GGA CAG TTG GGT GTC TCA CAT T
Vcam	TAC CAG CTC CCA AAA TCC TG	CGG AAT CGT CCC TTT TTG TA
Vmaf	TTC GAC CTT CTC AAG TTC GAC G	TCG AGA TGG GT TTC GGT TCA
xm1 34539	CAC TGG TCA ACT GCT TTT C	CTC TCT ACC TAT ACC CGA TG
adcyap1r1	CTG CGT GCA GAA ATG CTA CTG	AGC CGT AGA GTA ATG GTG GAT AG
baz2a	CAG AGG GTA TGT GTC TGT CTG A	GAA CTC CAC GAT GGT CAA GCA
dmrta1	CCC AAC TTT CGA GGT TTT CCA	CCC AGA GAA TGG TGA TGA GTG TT
Dntt	CTG GCA TTC ATG CGA GCA TC	GAA GGC CCG GCG ATC ATA G
elovl6	GAA AAG CAG TTC AAC GAG AAC G	AGA TGC CGA CCA CCA AAG ATA
fbxl5	TTC AGC AGC GCA GTC AGA C	CAG CAT CTC GGA GAG CTT ATT G
fbxo21	CCT GTA CCT GGC GAT GTA CC	AGC ACC TTC AAG ACA AGA CAG A
hmgcll1	ATG GGG AAT CTA CCA TCT GCT	AGG GAG TCC AGG TAA CTG AGA
nrtk2	CTG GGG CTT ATG CCT GCT G	AGG CTC AGT ACA CCA AAT CCT A
olfr1 508	ACT GTG GTC CTG ATG AGA TTG A	GGG GTA ACA GCA GTG AAA AAC AC
pbef1	GCA GAA GCC GAG TTC AAC ATC	TTT TCA CGG CAT TCA AAG TAG GA
per3	AAC ACG AAG ACC GAA ACA GAA T	CTC GGC TGG GAA ATA CTT TTT CA
phlda3	CCG TGG AGT GCG TAG AGA G	TCT GGA TGG CCT GTT GAT TCT
prm1	CCG TCG CAG ACG AAG ATG TC	CAC CTT ATG GTG TAT GAG CGG

serpina9	AAA CCC AGG TCA GAA TAT CCT CT	GGA CGA GGT ACT CGA AGC C
Slpi	GGC CTT TTA CCT TTC ACG GTG	TAC GGC ATT GTG GCT TCT CAA
srgap3	TCC TGT GAA CAA CTG TCG TCT	CAC GCC CAC AAT TCC CTC C
st8sia3	AGT GTG CTA GGG CTG GTC AT	TGG CGT ACT TGG GAG TGG T
sulf1	TGT GTT CCA CCG TTC GGT C	CAC ATC CTG GTC GTC AGT GAG
Thrsp	ATG CAA GTG CTA ACG AAA CGC	CCT GCC ATT CCT CCC TTG G
tmem45b	ACC ACA AGG GCT TGA AGA ATA AC	GGT GCA GGT GAG GTC CAT C
tmem51	CAA AGC CAA CGG CTC ACA CTA	GCT TAT CCG CAG GGC TGA AA
tnnt2	CAG AGG AGG CCA ACG TAG AAG	CTC CAT CGG GGA TCT TGG GT
ucp2	ATG GTT GGT TTC AAG GCC ACA	CGG TAT CCA GAG GGA AAG TGA T
upp2	GGG AGC GTC CAG AGT ATG G	CTG GTA GGT TGT GTG TTT TGG T
wee1	GTC GCC CGT CAA ATC ACC TT	GAG CCG GAA TCA ATA ACT CGC
Ltβr	TCA AAG CCC AGC ACA ATG TC	TTA TCG CAT AGA AAA CCA GAC TTG C
tnfr1	GCA GTG TCT CAG TTG CAA GAC ATG TCG G	CGT TGG AAC TGG TTC TCC TTA CAG CCA C

4.8.3 Primer sequences used for real-time PCR analysis (murine)

Gene	fwd-sequence (5'-3')	rev-sequence (5'-3')
ak006094	CGG TTT TAA TCT GAG TGC	GCA ATG AAA GTT TCT TTT AG
ak03 1632	CCT AAT TAG GTT CTA TAG TG	GTT CTA AGA AAC ATC AAA TGC
ak032385	GGA TCC AAC TCT AGT CCT TT	GAT GTGATG GGT TCT AAT C
ak080904	CTT GTC TTT ACT TAC GTC TC	CCT TGG ACT AAA TCA GAA ACC
ak084087	GGT GGT GGA AAT ACT ATC ATG	GCC AAG AAG TAA CAT CTC
arid5a	TCC CGC AGC TTC CTG TAT C	GAC CAG CCT CTC ATA GGT GC
arrdc3	ATG GTG CTG GGA AAG GTA AAG	CGC TAG AAT ACA CGG GGA CAT TA
bc013561	CTG AGG TTT CTT GGT AAT GC	CAC TTT CAA CAG CCA ATT TAA C
Blc	CCA TTT GGC ACG AGG ATT CAC	ATG AGG CTC AGC ACA GCA AC
btg2	ATG AGC CAC GGG AAG AGA AC	GCC CTA CTG AAA ACC TTG AGT C
ccl2	TTA AAA AAC CTG GAT CGG AAC CAA	GCA TTA GCT TCA GAT TTA CGG GT
ccl7	GCT GCT TTC AGC ATC CAA GTG	CCA GGG ACA CCG ACT ACT G
c-fos	AGA CTT CTC ATC TTC AAG TT	AAG ATG GCT GCA GCC AAG T
ch25h	TGC TAC AAC GGT TCG GAG C	AGA AGC CCA CTG AAG TGA TGA T
cxcl1	CTG GGA TTC ACC TCA AGA ACA TC	CAG GGT CAA GGC AAG CCT C
cxcl10	AAG TGC TGC CGT CAT TTT CT	CCT ATG GCC CTC ATT CTC AC
edg8	GCT TTG GTT TGC GCG TGA G	GGC GTC CTA AGC AGT TCC AG
egr1	AGG TTC CCA TGA TCC CTG ACT	GGT ACG GTT CTC CAG ACC CTG
egr2	CAG GAG TGA CGA AAG GAA GC	GAA GAC TGG GCA GAT GGA GG
Elc	GCC TCA GAT TAT CTG CCA T	AGA CAC AGG GCT CCT TCT GGT
e-selectin	CTG CAG TTC TGA CGT GTG GT	GAG CAA TGA GGA CGA TGT CA
extl-1	TTC TGG CTG GCG TTG TCA G	GGG TTC GTC TCA GAC TGG GA
fgf21	CTG CTG GGG GTC TAC CAA G	CTG CGC CTA CCA CTG TTC C
gadd45g	GGG AAA GCA CTG CAC GAA CT	AGC ACG CAA AAG GTC ACA TTG
Gapdh	CCA CCC CAG CAA GGA GAC T	GAA ATT GTG AGG GAG ATG CT
gas1	CCA TCT GCG AAT CGG TCA AAG	GCT CGT CGT CAT ATT CTT CGT C
gpr109b	CTG GAG GTT CGG AGG CAT C	TCG CCA TTT TTG GTC ATC ATG T
g0/g1switch	TAG TGA AGC TAT ACG TTC TGG GC	GTC TCA ACT AGG CCG AGC A
hist1 h1c	AAC CCC AGG CTA AGA AGG C	TGG CTT TAC GGC TTT AGA CGC
hist1h1d	GTG GAG AAG ACA CCT GTG AAG	CCT TGG CTG GAC TCT TTG CT
icam1	TGC GTT TTG GAG CTA GCG GAC CA	CGA GGA CCA TAC AGC ACG TGC CAG

Ifny	TCA AGT GGC ATA GAT GTG GAA GAA	TGG CTC TGC AGG ATT TTC ATG
igfbp1	ATG GGT GCT GCC TGC GGT GTG G	GGT GAG GGC ATG CAG GGG ACG AG
igf1	GGA CCG AGG GCT TTT ACT TCA A	TCG ATA GGG ACG GGG ACT TCT G
igf2	CCG GCT ACC ACA ATG TCC TGC TCT	GCT CCC GCC TGA TGT AAC CTG TCT
Inhbe	AAA AGC CCA GCT CTG GCT AAT	CTG GTT AGG TGC AGT CCC TC
jun-b	TCA CGA CGA CTC TTA CGC AG	CCT TGA GAC CCC GAT AGG GA
Lmln	TGC TGA CGG GCA TTT ACG AAT	TGT CGC ACA TTG TCT GCT AAG
LTα	TCC ACT CCC TCA GAA GCA CT	AGA GAA GCC ATG TCG GAG AA
Ltβ	TAC ACC AGA TCC AGG GGT TC	ACT CAT CCA AGC GCC TAT GA
mkiaaa1 853	GTC TCG GGG CCA GGA GAA G	GAG CTC CGG GCT GTG GAT G
nm025719	ATG TCG CCT GTA TCC CGA TCT	GTA GCG GTC GTT CTC CAG A
nr1d1	TAC ATT GGC TCT AGT GGC TCC	CAG TAG GTG ATG GTG GGA AGT A
Pdxp	ATG AGT CAC ATT CGG GAC CAT	AGG GCA GGA AAT AAG GCC AC
Periplakin	CAA AGG CAA ATA CAG CCC AAC	TTC CAC CTG GTC TGC ATT CTT
p-selectin	GAA AGG GCT GAT TGT GAC CCC	AGT AGT TCC GCA CTG GGT ACA
Rantes	ATG CCG ATT TTC CCA GGA CC	TTT GCC TAC CTC TCC CTA GAG CTG
serpine-1	TTC AGC CCT TGC TTG CCT C	ACA CTT TTA CTC CGA AGT CGG T
Slc	ATG ATG ACT CTG AGC CTC C	GAG CCC TTT CCT TTC TTT CC
socs3	TCC CCG ACT GGG TCT TGA C	GCG GGC ACC TTT CTT ATC C
TNFα	CAT CTT CTC AAA ATT CGA GTG ACA A	TGG GAG TAG ACA AGG TAC AAC CC
TNFαip3	GAA CAG CGA TCA GGC CAG G	GGA CAG TTG GGT GTC TCA CAT T
Vcam	TAC CAG CTC CCA AAA TCC TG	CGG AAT CGT CCC TTT TTG TA
Vmaf	TTC GAC CTT CTC AAG TTC GAC G	TCG AGA TGG GT TTC GGT TCA
xm1 34539	CAC TGG TCA ACT GCT TTT C	CTC TCT ACC TAT ACC CGA TG
adcyap1r1	CTG CGT GCA GAA ATG CTA CTG	AGC CGT AGA GTA ATG GTG GAT AG
baz2a	CAG AGG GTA TGT GTC TGT CTG A	GAA CTC CAC GAT GGT CAA GCA
dmrta1	CCC AAC TTT CGA GGT TTT CCA	CCC AGA GAA TGG TGA TGA GTG TT
Dntt	CTG GCA TTC ATG CGA GCA TC	GAA GGC CCG GCG ATC ATA G
elovl6	GAA AAG CAG TTC AAC GAG AAC G	AGA TGC CGA CCA CCA AAG ATA
fbxl5	TTC AGC AGC GCA GTC AGA C	CAG CAT CTC GGA GAG CTT ATT G
fbxo21	CCT GTA CCT GGC GAT GTA CC	AGC ACC TTC AAG ACA AGA CAG A
hmgcll1	ATG GGG AAT CTA CCA TCT GCT	AGG GAG TCC AGG TAA CTG AGA
nrtk2	CTG GGG CTT ATG CCT GCT G	AGG CTC AGT ACA CCA AAT CCT A
olfr1 508	ACT GTG GTC CTG ATG AGA TTG A	GGG GTA ACA GCA GTG AAA AAC AC
pbef1	GCA GAA GCC GAG TTC AAC ATC	TTT TCA CGG CAT TCA AAG TAG GA
per3	AAC ACG AAG ACC GAA ACA GAA T	CTC GGC TGG GAA ATA CTT TTT CA
phlda3	CCG TGG AGT GCG TAG AGA G	TCT GGA TGG CCT GTT GAT TCT
prm1	CCG TCG CAG ACG AAG ATG TC	CAC CTT ATG GTG TAT GAG CGG
serpina9	AAA CCC AGG TCA GAA TAT CCT CT	GGA CGA GGT ACT CGA AGC C
Slpi	GGC CTT TTA CCT TTC ACG GTG	TAC GGC ATT GTG GCT TCT CAA
srgap3	TCC TGT GAA CAA CTG TCG TCT	CAC GCC CAC AAT TCC CTC C
st8sia3	AGT GTG CTA GGG CTG GTC AT	TGG CGT ACT TGG GAG TGG T
sulf1	TGT GTT CCA CCG TTC GGT C	CAC ATC CTG GTC GTC AGT GAG
Thrsp	ATG CAA GTG CTA ACG AAA CGC	CCT GCC ATT CCT CCC TTG G
tmem45b	ACC ACA AGG GCT TGA AGA ATA AC	GGT GCA GGT GAG GTC CAT C
tmem51	CAA AGC CAA CGG CTC ACA CTA	GCT TAT CCG CAG GGC TGA AA
tnnt2	CAG AGG AGG CCA ACG TAG AAG	CTC CAT CGG GGA TCT TGG GT
ucp2	ATG GTT GGT TTC AAG GCC ACA	CGG TAT CCA GAG GGA AAG TGA T
upp2	GGG AGC GTC CAG AGT ATG G	CTG GTA GGT TGT GTG TTT TGG T
wee1	GTC GCC CGT CAA ATC ACC TT	GAG CCG GAA TCA ATA ACT CGC

Ltβr	TCA AAG CCC AGC ACA ATG TC	TTA TCG CAT AGA AAA CCA GAC TTG C
tnfr1	GCA GTG TCT CAG TTG CAA GAC ATG TCG G	CGT TGG AAC TGG TTC TCC TTA CAG CCA C

4.8.4 Primer sequences used for real-time PCR analysis (human)

Gene	fwd-sequence (5'-3')	rev-sequence (5'-3')
ltβR	GAG AAC CAA GGT CTG GTG GA	GAG CAG AAA GAA GGC CAG TG
Light	CTG GCG TCT AGG AGA GAT GG	CTG GGT TGA CCT CGT GAG AC
cd45	CCA ATG CAA AAC TCA ACC CTA	CTC CTC TCT CCT GGG ACA TCT
cytokeratin18	CCC GCT ACG CCC TAC AGA	GCG GGT GGT GGT CTT TTG
CD3	GTG ACC TGG CTT TAT CTA CTG GA	GGT ATC TTG AAG GGG CTC ACT
CD20	AAC AAA ATC TCT ACT TTG ATG	GCA AGG CCT ACT GCT GAG TT
Hprt	GAC CAG TCA ACA GGG GAC AT	GTG TCA ATT ATA TCT TCC ACA ATC AAG
ccl2	CAT TGT GGC CAA GGA GAT CTG	CTT CGG AGT TTG GGT TTG CTT
ccl3	CTC TGC ACC ATG GCT CTC TGC AAC	TGT GGA ATC TGC CGG GAG GTG TAG
ccl5	CCC CTC ACT ATC CTA CC	TCA CGC CAT TCT CCT G
cxcl1	ATG GCC CGC GCT GCT CTC TCC	GTT GGA TTT GTC ACT GTT CAG
cxcl10	TAT TCC TGC AAG CCA ATT TTG TC	TCT TGA TGG CCT TCG ATT CTG
TNFα	CTC TGG CCC AGG CAG TCA GA	GGC GTT TGG GAA GGT TGG AT
tnfr1	CTG CCT CAG CTG CTC CAA A	CGG TCC ACT GTG CAA GAA GAG
LTα	CCA CCC TAC ACC TCC TCC TT	AGT CTG GGC AGC TGA AGG T
Ltβ	GAG GAC TGG TAA CGG AGA CG	GGG CTG AGA TCT GTT TCT GG

4.9 Histology and immunohistochemistry

Paraffin sections (2µm) and frozen sections (5 or 10µm) of livers were stained with haematoxylin/eosin or various primary and secondary antibodies. Paraformaldehyde (4%) fixed and paraffin embedded liver tissue was incubated in Ventana buffer and staining was performed on a NEXES immunohistochemistry robot (Ventana instruments, Switzerland) using an IVIEW DAB Detection Kit (Ventana). Antibodies against $B220^{+}$ B-cells (Pharmingen; 1:400), F4/80 (Serotec, 1:50) for macrophages, CD4 (YTS 191; 1:200) and CD8 for T-cells (YTS 169; 1:50) and CD3 for T-cells (clone SP7, Neomarkers; 1:300) were kindly provided by R. Zinkernagel (Odermatt et al., 1991). Anti human and murine GP73 (both Santa Cruz Biotechnology, Inc.) were used as a tumor marker to characterize HCC. Anti murine Glutamine Synthetase (Abcam, Code ab 16802; 1:500) was also used as tumor marker. Liver micro-architecture was evaluated by Collagen IV (IVIEW DAB Kit; 1:50), oval cell proliferation by A6 staining (1:50), kindly provided by Dr. Valentina Factor; both on a Ventana stainer from Roche. Ki67 (NeoMarkers Code RM-9106-S; 1:200) stained proliferating hepatocytes and lymphocytes. Image acquisition was either performed on an Axiophot-microscope (Zeiss), or an Olympus SZX12, equipped with a JVC digital camera (KY-F70; 3CCD) or on an Olympus BX61TRF fluorescent microscope equipped with an F-View camera and analyzed with the Analysis software.

For prion related experiments the following techniques were used: Paraffin sections (2µm) and frozen sections (5 or 10µm) of spleen or brain were stained with hematoxylin/eosin. Antibodies FDC-M1 for mature FDCs (clone 4C11; 1:50; Becton Dickinson), FDC-M2265 (1:50; Immunokontakt212-M/C-1FDCM2), B220/CD45R for B cells (RA3-6B2, Pharmingen 553084; 1:400 in PBS/0. 15% BSA), CD35 for CR1 (8C12, Pharmingen, San Diego, CA; 1.100), CD4 for T-helper cells (YTS 191; 1:200) and CD8 for cytotoxic T-cells (YTS 169; 1:50), both rat anti-mouse kindly provided by Dr. Rolf Zinkernagel, NLDC-145 for dendritic cells (BMA T-2013; 1:1 '000), PNA for germinal centre B-cells (Vector L-1 070; 1:100), F4/80 (Serotec, 1:50) for macrophages, GFAP (1:300; DAKO, Carpinteris, CA) for astrocytes, and Ki-67 for proliferating cells (NeoMarkers, USA) were applied and visualized using standard methods. Iba-1 was used for highlighting activated microglial cells.

For PrP staining, formalin-fixed brain, renal and pancreatic tissues were treated with concentrated formic acid for 60 min to inactivate prion infectivity. Postfixation in formalin was performed for ~8 hrs and tissues were embedded in paraffin. After deparaffination, sections (1-2 tm) were incubated for 6 min in 98% formic acid and washed in distilled water for 30 min. Sections were heated to 100°C in a steamer in citrate buffer (pH 6.0) for 3 min, and allowed to cool down to room temperature. Sections were incubated in Ventana buffer and stains were performed on a NEXEX immunohistochemistry robot (Ventana instruments, Switzerland) using an IVIEW DAB Detection Kit (Ventana). After incubation with protease 1 (Ventana) for 16 min, sections were incubated with anti-PrP SAF-84 (SPI bio, A03208, 1:200) for 32 min. Sections were counterstained with hematoxylin. GFAP immunohistochemistry for astrocytes (1:1,000 for 24 min; DAKO) and Iba1 (1:2500 for 32 min; Wako Chemicals) for microglia was similarly performed, but with antigen retrieval by heating to

100 °C in EDTA buffer (pH 8.0).

4.10 In situ hybridization

In situ hybridization was performed as recently described in (Prinz et al., 2004). In brief, sense and antisense probes for mLTα, mLTβ derived from a pGEM4 plasmid containing KpnI/ BamHI fragment of mLTα (GenBank: Y00467, corresponding to exon 4 of mLTα) or a pGEM plasmid containing Sau3AI fragment of mLTβ (GenBank: U06950, corresponding mainly to exon 3). Sense and antisense probes for mEGR1 were derived from a pBluescript plasmid containing BglII fragment of mEGR1 cDNA (NM_007913). Sense and antisense probes for CCL2 were derived from a pGEM-1 plasmid containing mCCL2 cDNA (Rollins et al., 1988). Sense and antisense probes for mCXCL10 were derived from a pBluescript plasmid containing 1065bp ofthe mCXCL10 cDNA. Sense and antisense probes were Digoxygenin (DIG) labelled according to the manufacturer's protocol with a DIG-labeling kit (Roche). Efficiency of Dig-labeling was quantified on a dotplot on a positively charged nylon membrane (GE Healthcare, Germany). In situ hybridization was performed on freshly cut frozen

sections (10-20µm, air-dried), post fixed in 4% PFA/PBS. Treatment with 0.1M HCl was performed for Egr1 and Ccl2 for 10 min. Tissues were then acetylated in 300ml of 0.1 M triethanolamine containing 750µl acetic anhydride. Prehybridization was performed 3 hrs at RT (or at 60°C for 6hrs for Cxcl10) in 50% formamide, 5x SSC (5x), 5x Denhardt's solution, 250µg/ml E. coli t-RNA (Roche). Hybridization solutions consisted of prehybridization solution containing 50ng/50µl DIGlabelled RNA sense or antisense probes. Probes were denatured at 85°C for 5 min and then placed on ice. Prehybridization solution was then replaced by hybridization-solution, covered with a cover slip, sealed in a box, heated to 85°C for 30 min. (Egr1, Ccl2) and then incubated over night at 58-60°C. Washing was performed in pre-warmed SSC of different concentrations (and subsequently in PBT for CXCL10). For CXCL10 an RNase treatment (5µg/ml RNase in 2 x SSC) was performed between the washing steps. (Blocking was performed using blocking reagent in buffer 1 (100mM Tris-HCl pH 7.5; 150mMNaCl). Slides were incubated with anti-DIG AP (1:2000, Roche) at RT for 2-3 hrs. After subsequent wash in buffer 1 for 20mins twice, detection was performed in buffer 3 (100mM Tris-HCl pH 9.5; 150mMNaCl; 50mM MgCl2) containing 1mM Levamisol; NBTand BCIP (Sigma, Germany). Reaction was stopped in 10mM Tris pH8.0 and 1mM EDTA. Slides were mounted in DAKO aqueous mounting medium and analyzed on an Axiophot-microscope (Zeiss), or an Olympus SZX12, equipped with a JVC digital camera (KY-F70; 3CCD).

4.11 Multiplex-bead assay

Cytokine protein levels from liver homogenates or sera were measured using a multiplexed particle-based flow cytometric cytokine assay (Vignali, 2000). Bioplex mouse cytokine kits were purchased from BioRad (Ismaning, Germany). The procedures closely followed the manufacturer's instructions. The analysis was conducted using a conventional flow cytometer (FC500 MPL, BeckmanCoulter, Nyon, Switzerland). The detection limits were as follows: CCL2 (12 pg/ml), CXCL1 (1 pg/ml), IL1β (0.3 pg/ml), IL6 (0.3 pg/ml), IFNγ (2.8 pg/ml). The homogenization buffer was tested as a negative control.

4.12 Analysis of different HCV genotypes

Different HCV genotypes were analyzed as recently published (Neumann-Haefelin et al., 2006)

4.13 ELISA

CXCL10 protein levels from liver homogenates or sera were measured using a Quantikine-Elisa-Kit from R&D Systems (Oxon, UK). The procedures closely followed the manufacturer's instructions.

The detection limit was 16 pg/ml. The homogenization buffer was tested as a negative control.

4.14 Cytokine assay for TNFα

Livers were homogenized with a Dispomix (Medic tools) in 10 vol of Tris-HCl buffer (50mM, pH 7.4) with NaCl (0.6M), Triton X-100(0.2%)and bovine serum albumin (0.5%) containing freshly dissolved protease inhibitors: benzamidine (1 mM), phenylmethyl-sulfonylfluoride (0.1mM) and Complete Mini Tablets (protease inhibitor cocktail Tablets; Roche). The supernatants were aliquoted and frozen at -80°C until the cytokine assays were performed. Profiling mouse kit for TNFα was purchased from R&D Systems (Wiesbaden-Nordenstadt, Germany). The procedures closely followed the manufacturer's instructions. The analysis was conducted using a conventional flow cytometer (LSRII from Becton Dickinson). The detection limit for TNFα was 0.4 pg/ml.

4.15 Gene expression microarray experiment and data analysis

An Agilent one-colormicroarray-based gene expression analysis (Mouse DNA Microarray 4x 44K) was performed on 3 and 9 month-old *tg*1223 (n=4) and *IKKβ*$^{\Delta hep}$ (n=4) livers in comparison to age matched *C57BL/6* livers (n=3) according to the manufacturer's protocol. For HCC arising in 12 or 18 month-old *tg*1223 (n=3) or *tg*1223/tnfr1/(n=4) livertissue was compared to non-affected Tg1223 (n=3), non-affected *tg*1223/tnfr1$^{-/-}$ (n=4) liver regions as well as age matched *C57BL/6* livers. In addition to biological replicates technical replicates were investigated.

Gene expression was quantified using Agilent Feature Extraction Software Version 9.5.3.1. Expression values were imported into GeneSpring 7.3 (Agilent Technologies, USA) and following Agilent's recommendation, all values less than 5.0 were set to a value of 5.0. For each sample all values were normalized to the respective 50th percentile. In case of the characterization of the *tg*1223 and *IKKβ*$^{\Delta hep}$ liver samples at 3 and 9 months of age, hierarchical clustering and principal component analysis of the normalized values indicated a slight confounding effect based on different dates for the hybridization of the different samples. In order to compensate this effect, for each gene on each array, the expression values were normalized to the median of the values obtained from the C57BL/6 control samples on the respective day, giving rise to ratio values. Those genes were filtered out that did not have at least 75% present flags in at least one of the *C57BL/6*, *tg*1223 or *IKKβ*$^{\Delta hep}$ conditions at 3 or 9 months. Assuming normal distribution ofthe data, statistically significant, differentially expressed genes in *tg*1223 or *IKKβ*$^{\Delta hep}$ livers were selected using a one-sample t-test that assessed whether the respective ratios did significantly differ from 1. The false discovery rate was controlled at a level of 0.05 using the method of Benjamini and Hochberg (Benjamini, 1995). In the study of individual HCC samples, each value for each sample was normalized to the 50th percentile of all expression values of

the respective sample. For each pair of samples representing tumor-affected and unaffected region of the same liver, for each gene, the values were normalized to the values of the respective sample from the unaffected region. Individual fold changes of the strongest up- and downregulated genes of each HCC samples in comparison to the median values of the *C57BL/6* samples were reported after filtering out genes that did not have a present flag.

4.16 Gene Ontology microarray data analysis

Lists of significantly differentially expressed genes were investigated in respect to enrichment of Gene Ontology categories using the Gene Ontology Browser as implemented in GeneSpring 7.3. A Fisher's exact test was used to show whether more genes belonging to a Gene Ontology category are found in the list under investigation than in a randomized gene list of the same size.

4.17 Array-based Comparative Genomic Hybridization (aCGH)

Agilent oligonucleotide array based CGH for Genomic DNA analysis for FFPE samples (Mouse Genome CGH Microarray 4x44K) was performed on paraffin embedded liver tissues according to the protocol provided by Agilent Technologies. Chromosomal copy number aberration in HCC samples of *tg*1223 livers in relation to C57BL/6 samples was investigated using aCGH (Agilent DNA Analytics 4.0 CGH Module User Guide). Log2-ratios of signal intensity values of C57BL/6 (Cy5) versus signal intensity values of HCC (Cy3) samples were computed with Agilent Feature Extraction software Version 9.5.3.1. Log2 ratios were imported into the DNA Analytics Software 4.0.76 (Agilent Technologies, USA). Saturated and non-uniform data points were filtered out. Values of probes that occurred several times within one chip were combined and averaged. The aCGH data were then normalized in a linear way using DNA Analytics centralization method. Aberrations were detected using the Aberration Detection Method Nr.1 (ADM-1) as implemented in the DNAAnalytics software (Agilent DNAAnalytics 4.0 CGH Module User Guide, Agilent Technologies, Inc. 2008) with standard settings. Those aberrations that were not covered by more than two probes were filtered out. Single log2 ratio intensities, moving average of these ratios and aberration detection results were graphically displayed in the genome browser of the DNA Analytics software.

In addition, the aCGH data were analyzed using Partek® Genomics Suite software, version 6.4 (Copyright © 2008, Partek Inc., St. Louis, USA). After importing the array data into Partek, together with Dr. Stefan Zoller from the Functional Genomics Centre Zürich I transformed it into adjusted copy number data as described in the manual. Amplifications and deletions were detected by applying the genomic segmentation workflow. The optimal segmentation and region report parameters were found by following an iterative procedure (Partek support, personal communication) and finally set as

follows: minimum number of genomic markers = 10, segmentation P-value = 0.001, signal to noise ratio = 0.2, expected range = 0.3, region p-value = 0.01. On the resulting segmentation data, together with Dr. Stefan Zoller, I applied the workflow to find regions in multiple samples, reporting all regions that were significant in at least two samples. The related cytobands are indicated for each chromosome as horizontal bars. Annotations for these regions are available under supplemental online material. The cytoband information was obtained from the UCSC genome bioinformatics database (http://genome.ucsc.edu).

Statistical significance of amplification and deletion patterns in aCGH for monoclonal tumors was calculated by applying a permutation test. The samples were compared pair-wise as follows using an in-house written program. First, the sequence overlap (o) of amplifications/deletions was calculated for the two samples. Then, the amplifications/deletions of one sample were kept but randomly distributed on the other sample and the new overlap (r_i) calculated. This step was repeated n = 1 x 107 times and r = sum (r_i>o) computed. Finally, the p-value for the pair-wise comparison was estimated as p = r/n.

4.17.1 Online data on DNA microarray analysis and aCGH analysis

DNA microarray analysis and aCGH analysis

1. Original DNA-microarray data of differentially regulated mRNAs of 3 month-old *tg*1223, *tg*1223/*IKKβ*$^{\Delta hep}$ and *C57BL/6* livers (normalized version) - analyzed on an Agilent microarray platform. Individual samples analyzed are described in detail in the excel file.

   Accession numbers:

   These data were submitted to the Gene Expression Omnibus (GEO) database.

   “Gene expression microarray data can be retrieved from Arrayexpress database using the accession number E-MEXP-1998”.

2. Original DNA-microarray data of differentially regulated mRNAs of 9 month-old *tg*1223, *tg*1223/*IKKβ*$^{\Delta hep}$ and *C57BL/6* livers (normalized version) - analyzed on an Agilent microarray platform. Individual samples analyzed are described in detail in the excel file.

   Accession numbers:

   These data were submitted to the Gene Expression Omnibus (GEO) database.

   “Gene expression microarray data can be retrieved from Arrayexpress database using the accession number E-MEXP-1998”.

3. Original DNA-microarray data of differentially regulated mRNAs of HCC in 18 month-old

*tg*1223, *tg*1223/tnfr1$^{-/-}$, of unaffected regions of the identical livers and of age matched *tg*1223 and C57BL/6 livers (normalized version) - analyzed on an Agilent microarray platform. Individual samples analyzed are described in detail in the excel file.

Accession numbers:

These data were submitted to the Gene Expression Omnibus (GEO) database.

"Gene expression microarray data can be retrieved from Arrayexpress database using the accession number E-MEXP-1998".

4. aCGH-data of various *tg*1223 HCC and C57BL/6 control liver tissues which demonstrate chromosomal aberrations in autosomes by the use of an Agilent aCGH platform.

   The q-arm of each autosome is shown. Log ratios of *C57BL/6* versus *tg*1223 signal intensities or *C57BL/6* versus *C57BL/6* signal intensities are shown. Negative log ratios represent deletions, positive log ratios amplifications of the respective genetic loci.

   Log ratio of 0.5 corresponds to the background level ofindividual *C57BL/6* liver DNA samples hybridized with other *C57BL/6* liver DNA samples (n=5). Lines represent smoothed moving averages. Estimated copy number aberrations are indicated with colored surfaces.

These data can be directly accessed without any password on: http://www.ncbi.nlm.nih.gov/geo/query/acc.cgi?token=zhwdtmksyosskhm&acc=GSE14467

4.17.2 Statistical evaluation of aCGH results

Statistical significance of amplification and deletion patterns in aCGH for monoclonal tumors was calculated by applying a permutation test. The samples were compared pair-wise using an in-house written program: First, the sequence overlap (o) of amplifications/deletions was calculated for the two samples. Then, the amplifications/deletions of one sample were kept but randomly distributed on the other sample and the new overlap (r_i) calculated. This step was repeated $n = 1 \times 10^7$ times and r = sum ($r_i > o$) computed. Finally, the p-value for the pair-wise comparison was estimated as p = r/n.

4.18.1 Western blot analysis

10% liver homogenates were prepared in RIPA buffer (50mM Tris; 1% NP40; 0.25% Deoxycholic acid sodium salt; 150mM NaCl; 1mM EGTA) containing 1 mM Na_3VO_4 and a protease inhibitor cocktail (Complete Mini Tablets; Roche) and quantified with a BCA protein assay kit (Pierce) according to the manufacturer's manual. 60µg protein were denatured in Laemmli buffer containing 5% b-mercaptoethanol and separated by gel electrophoresis on a 12% Bis-Tris gel (Invitrogen) with a

1 x NuPAGE MES-SDS running buffer (Invitrogen) and blotted by wet blotting onto a nitrocellulose membrane (Protran BA 85 pore size 0.45 mm; Whatman). After blotting the membrane was blocked in Roti-Block (Carl Roth) for 2 hrs at RT. Primary antibody GP73 (sc-48011; Santa Cruz; 1:500 dilution) was incubated at 4°C over night under shaking conditions. Incubation with the secondary antibody (HRP-donkey anti goat IgG H+L; 705.035-147 Lot72963; 1:15000; Jackson) was performed under shaking conditions for 1 hr. Primary antibody AFP (#2137; Cell Signaling; 1:20) was incubated at 4°C over night under shaking conditions. Detection was achieved with Supersignal West chemiluminescent Substrate (Pierce). For signal detection a VersaDoc, standard exposure 15-30 sec was used. To assure equal loading, the membranes were reprobed with anti-13-actin antibody (Sigma) and detected as described above.

For prion experiments tissue homogenates were adjusted up to 50 µg protein and not treated or treated with proteinase K (25-50µg/ml, 30 min, 37^{o}C after denaturation and adding of loading dye). Total protein (up to 50µg) was electrophoresed through 12% SDS-PAGE. Proteins were transferred to nitrocellulose (Schleicher-Schuell, Germany and Protran BA 85 pore size 0.45 mm; Whatman) by wet-blotting. Membranes were blocked with TBS-T containing 5% Topblock (Juro, Switzerland; LuBioScience GmbH), incubated with monoclonal anti-mouse PrP antibody POM1/POM19 in 1% Topblock TBST.

4.19 Liver-cell extraction and freezing

For the isolation and analysis of liver cells I included six patients with histologically proven HCC infection who had undergone curative hepatectomy and proven persistent HCV infection in the University Hospital, Grenoble where the analysis was done by my collaborators. Exclusion criteria included co-infection with human immunodeficiency, hepatitis B or hepatitis delta virus, additional causes of liver disease, alcohol consumption higher than 30g/day, inflammatory syndrome, previous antiviral treatment and previous liver transplantation. Liver and tumor tissues derived from curative hepatectomy were washed twice in a complete medium, containing RPMI 1640 supplemented by 10% Fetal Calf Serum (Gibco), and continuous shaking for 2 min. Tissues were cut into pieces with in Petri dishes containing 10ml complete medium and 100µl DNase (3mg/ml) (Boehringer Mannheim). 10% collagenase D (10mg/ml) (Roche Diagnostic Germany) was added and incubated for 20 to 30 min at 37°C. Cell suspensions were then filtered (100µm mesh) and 10% of fetal calf serum (FCS) was added in the final volume and then centrifuged at 15000 rpm twice to remove debris. The cells were then counted with a hemocytometer and stored in 10% DMSO in liquid nitrogen or on - 80°C.

4.20 Separation of $CD45^+$ and $CD45^-$ cells by microbeads

Frozen cell suspensions were thawn and viability was checked by Acridine/propidium iodide with the help of fluorescent microscope and the percentage of living cells was quantified. Leukocytes numbers were then counted with a hemocytometer. Cell sorting was performed as previously described (Vigan et al., 2003) with the following modifications: Cells were incubated with a biotinylated anti-human CD45 antibody (BD Pharmingen) (1 µl of anti CD45 for 1×10^6 of target cells) for 20 min on ice and in dark followed by a washing step with 10 volumes of PBS to remove unbound antibody. Then, the cells were incubated with streptavidine coupled microbeads (Invitrogen, Norway) in PBS with 0.1% BSA and 2mM EDTA, pH 7.4 for 30 min at 2-8°C with gentle tilting and rotation as manufacturer instructions (50 µl of microbeads for 2.5×10^6 target cells). Cells were then separated into two fractions with a magnetic column i.e. one with cells bound to microbeads (leukocytes) and the second fraction consisting of unbound cells (hepatocytes, tumor cells and others). After performing additional washing steps to remove trapped liver or tumor cells, cells were eluted from the column. Both cell fractions were then used for RNA extraction.

4.21 Counting of proliferating hepatocytes

The total number of $Ki67^+$ hepatocytes was counted (number of $Ki67^+$ hepatocytes/visual field of 2 mm^2). For each mouse/genotype (n=8) 10 visual fields were counted. Statistics was performed (*tg*1223 versus *C57BL/6* mice).

4.22 Statistical evaluation

Human specimens and various mouse groups were compared using a oneway ANOVA with post-hoc Bonferroni test and a Fisher's exact test with Bonferroni correction and a chi-square test with exact P-values to evaluate statistical significance. Analyses were evaluated by using the program SPSS 13.0 (SPSS Inc., Chicago, IL). Student's t-test was used to evaluate the statistical significance of hepatic cytokine and transaminase levels.

4.23 Exposure to prions

- Aerosols: Exposition of *Tg*a20 mice to aerosols was performed in inhalation chambers with a Nebuliser device (Pari GmbH, Munich, Germany) run with a pressure of 1.5 bar generating 100% particles below 10 µm with 60% of the particles below 2.5 µm and 52% below 1.2 µm. Such particle sizes are considered to be able to reach upper and lower airways. Prion material used throughout this study was RML strain obtained from the brains of diseased *CD1* mice in its 6^{th} passage (RML6). Mice

were exposed to aerosolized prion infected brain homogenates for two, five or ten minutes.

- Intracerebral prion inoculation of mice: *Tg*a20 mice serving as indicator mice were inoculated i.c. with brain or lung tissue homogenate using 30 µl volumes.

- Intranasal RML prion application in mice: Mice were anesthetized with Ketamine/Xylazin hydrochloride anaesthesia. 10 µl of RML 6.0 (0.1%) were i.n. inoculated in each nostril and on the nasal epithelium by using a 10 µl pipette. The mice were held horizontally during inoculation process and for 1 minute following the inoculation. The whole procedure was repeated after a break of 20 minutes, reaching a final volume of 40 µl of RML 6.0 (4 log LD50).

Mice were monitored every day, and scrapie was diagnosed according to clinical criteria including ataxia, kyphosis, tail rigidity and hind leg paresis. Mice were sacrificed at the onset of terminal disease. All mice described were maintained under specific pathogen-free conditions. Breeding and experiments were performed in compliance with the guidelines of the Kanton of Zürich.

4.24 Sodium phosphotungstic acid (PTA) precipitation

10% homogenates of spleen, brain, pancreas and kidney were prepared in 0.32 M sucrose or PBS. Gross cellular debris was removed by centrifugation at 80 g for 1 min. 300µl of PBS were added to 200µl of the resultant supernatant, and mixed 1:1 with 4% Sarkosyl in PBS. Samples were incubated for 15 min at 37°C under constant agitation. Benzonase and $MgCl_2$ were added to a final concentration of 50 U/ml and 12.75 mM respectively, and incubated for 30 min at 37°C under continuous agitation. Pre-warmed PTA stock solution (pH 7.4) was added to a final concentration of 0.3% and the sample was incubated at 37°C for 30 min with constant agitation, followed by centrifugation at 37°C for 30 min at maximum speed in an Eppendorf microcentrifuge. The pellet was resuspended in 30µl 0.1% Sarkosyl in PBS and digested with 30Llg/ml proteinase K (PK) for 30 min at 37°C with agitation. The sample was heated at 95°C for 5 min in SDS-containing loading buffer before loading onto 12% or 16% Novex SDS polyacrylamide gels (Invitrogen, USA) (experiments performed in Tübingen).

4.25 Misfolded Protein Assay (MPA)

The assay, which was performed on a 96-well plate is divided into two parts: the PSR1 Capture and an ELISA. For the PSR1 Capture the set up of each reaction was as following: 3µL of PSR1 beads (buffer removed) and 100 µL of 1 x TBSTT were spiked with brain homogenate, incubated at 37°C for 1hr with shaking at 750rpm, the beads were washed on the plate washer (ELX405 Biotek) 8 times with residual 50 µL/well TBST. Then 75 µL/well of denaturing buffer was added. This was incubated at RT for 10min with shaking at 750rpm. Subsequently 30 µL/well of neutralizing buffer were added. An

additional incubation at RT for 5min with shaking at 750rpm followed. The beads were pulled down with a magnet. The ELISA was performed as follows: 150 µL/well of the sample was transferred to an ELISA plate which was coated with POM19. An incubation step at 37°C for 1hr with shaking at 300rpm followed. That was washed 6 times with wash buffer. POM2-AP conjugate had to be diluted to 0.01 µg/mL in conjugate diluent. 150 µL/well of diluted conjugate was added. Incubation at 37°C for 1hr without shaking followed. Washing 6 times with wash buffer was followed by preparation of enhanced substrate by adding 910 µL of enhancer to 10mL of substrate (Lumiphos plus, Lumigen). 150 µL/well of enhanced substrate was added. Incubation at 37°C for 30min was followed by reading by luminometer (Luminoskan Ascent) at default PMT, filter scale=1.

4.26 FACS analysis

Secondary lymphoid tissues were harvested and cells and single cell suspensions were generated by gentle pushing the tissue through a cellstrainer (Becton Dickinson (BD), USA). Alternatively, peripheral blood from the tail vein was collected in pre-cooled FACS-buffer (960 µl PBS, 20µl FCS, 20 µl EDTA 0.5M, 1g NaN_3). Next samples were spun down for 5min at 300g at 4°C and the supernatant was discarded. Cells in the pellet were resuspended in 100 µl of FACS-buffer containing the conjugated antibodies with a concentration based on the manufacturer's recommendations. Samples were gently vortexed and incubated for 20 min at 4°C in the dark. Afterwards samples were washed with FACS-buffer and spun down, supernatant was discarded. In case the primary antibodies were not directly conjugated with fluorochromes the staining step was repeated. Red blood cell lysis was performed with 1 ml of 1x lysis solution (BD). Samples were incubated for 3min at room temperature before the reaction was terminated by adding 3 ml of FACS-buffer. Again samples were spun down and resuspended accordingly to the cell density. FACS was performed at a two-laser FACScalibur (BD). The analysis was executed with cell-quest and flow-jo software.

4.27 Histoblot analysis

Histoblots were performed as described previously (Taraboulos et al., 1992). Frozen brains that were cut into 12-µm-thick slices were mounted on nitrocellulose membranes. Total PrP, as well as PrP^{Sc} after digestion with 50 or 100 µg/ml proteinase K for 4 hrs at 37°C, were detected with the anti‐prion POM1 antibody. (1:10000, NBT/BCIP, Roche Diagnostics).

Curriculum vitae:

Family status: married to Mrs. Mag. rer. nat. Cornelia Haybäck-Thannhauser

Nationality: Austria

Age: 32 years date of birth: 14. 6. 1977

Place of birth: Steyr/Upper Austria

Education

- 1983 – 1987 Primary school: Markt St. Florian, Austria
- 1987 - 1995 Secondary school: Akademisches Gymnasium, Linz, Austria
  School leaving examination (Matura): 26. Juni 1995 with „Gutem Erfolg“
- 10.1995 – 01.2001 Leopold – Franzens – University of Innsbruck, Tyrol, Austria (Medical faculty), Medical School, Termination of specific education in Experimental Pathology: 26.03.1999 (Prof.Wick), University of Innsbruck
- 19.1.2001 Award of academic title Dr. med. univ. (M.D.) - notice of the degree programme in Medicine
- 26.1.2001 Award of Promotion-certificate
- 2.5.2001 – 31.3.2002 Rotation physician at the General Hospital Linz, Austria (Surgical Departments: Viszeral-, Herz-, Gefässchirurgie, Internal Medicine, Pulmonology)
- 1.4.2002 – 31.7.2002 Specialist Registrar at the Institute of Clinical Pathology,at the General Hospital Linz, Austria
- 1.8.2002 - 18.10.2005 Specialist Registrar at the Institute of Clinical Pathology and Neuropathology, Wagner-Jauregg State Hospital Linz, Austria
- 1.6.2005 – 30.6.2005 Department of Pulmonology at the General Hospital Steyr, Austria
- 1.7.2005 – 31.7.2005 Department of Visceral Surgery at the General Hospital Rohrbach,

Curriculum vitae

Austria

- from 1.10.2005 to now: MD-PhD-student (Doktorand): Molecular Biology; University of Zürich, Kanton Zürich, Switzerland (Mathematisch Naturwissenschaftliche Fakultät)
- from 1.10.2005 to now: Research Fellow, Specialist Registrar and Resident at the Institute of Neuropathology, Department of Pathology, University Hospital Zürich, Switzerland
- 28.9.2006: Examination for degree "Specialist in Pathology" (Facharztprüfung zum "Facharzt für Pathologie") – at the University of Graz, Austria
- 28.11.2007: Award "Specialist in General Pathology" ("Facharzt für Pathologie") (Austrian Board of Pathology, Austrian Medical Association)
- since 2008: Responsible person for the National Reference Centre of Prion Diseases (NRPE) of Switzerland at the Institute of Neuropathology and Co-Biosafety officer of the Institute of Neuropathology, Department of Pathology, University Hospital Zürich, Switzerland
- 03.10.2008: Examination for degree "Specialist in Neuropathology" (Facharztprüfung zum "Facharzt für Neuropathologie") – Vienna, Austria
- 23.09.2009: Award "Specialist in Neuropathology" ("Facharzt für Neuropathologie") (Austrian Board of Pathology, Austrian Medical Association)
- 2005 – 2009 Ph.D thesis at the Institute of Neuropathology at the University Hospital Zürich, Switzerland, Director: Prof. Dr. Adriano Aguzzi. Project: "Mechanisms of Inflammation Induced Hepatocarcinogenesis and Efficient Prion Transmission via the Aerial Route"

Publications

Original peer-reviewed articles:

*** Deletion of the anti-apoptotic protein Mcl-1 in murine hepatocytes**

triggers proliferation and hepatocarcinogenesis

Weber A, Boger R, Vick B, Urbanik T, Haybaeck J, Heine S, Zoller S, Teufel A, Krammer PH, Opferman JT, Galle PR, Schuchmann M, Heikenwaelder M, Schulze-Bergkamen H

(accepted for publication in **Hepatology**, 2009)

*** Decreased numbers of hypocretin (orexin) neurons with severe traumatic brain injury**

Christian R. Baumann, Claudio L. Bassetti, Philipp O. Valko, Johannes Haybaeck, Morten Keller, Erika Clark, Silke Ludwig, Markus Tolnay, Thomas E. Scammell

(**Ann Neurol.**, 2009, Oct;66(4):555-559)

*** A Lymphotoxin-driven Pathway to Hepatocellular Carcinoma**

Johannes Haybaeck, Nicolas Zeller, Monika Julia Wolf, Achim Weber, Ulrich Wagner, Michael Odo Kurrer, Juliane Bremer, Giandomenica Iezzi, Rolf Graf, Pierre-Alain Clavien, Robert Thimme, Hubert Blum, Sergei A. Nedospasov, Kurt Zatloukal, Muhammad Ramzan, Sandra Ciesek, Thomas Pietschmann, Patrice N. Marche, Michael Karin, Manfred Kopf, Jeffrey L. Browning, Adriano Aguzzi and Mathias Heikenwalder.

(**Cancer CELL**, 2009, Oct 6; 16(4):295-308)

*** Prion Immune activation strongly increases the susceptibility to peripherally administered prions**

Juliane Bremer[*], Mathias Heikenwalder[*], Johannes Haybaeck[*], Cinzia Tiberi, Michael Kurrer, and Adriano Aguzzi

[*] These authors contributed equally to this work

(**PLos One**, 2009, Sep 25; 4(9))

*** "Case report: Rapidly progressive and lethal septicemia due to infection with Pasteurella multocida in an infant"**

Haybaeck J, Schindler C, Braza P, Willinger B, Drlicek M

(**Wien Klin Wochenschr., The Middle European Journal of Medicine**, 2009 Mar;121(5-6):216-219)

*** Lymphotoxin-dependent prion replication in inflammatory cells of granulomas**

Mathias Heikenwalder, Ilan Margalith, Michael Kurrer, Christian Julius*, Magdalini Polymenidou, Johannes Haybaeck, Nicolas Zeller, Petra Schwarz, Matthias Matter, Jan Kranich, Juliane Bremer, Walker Jackson, Susan Lindquist, Christina J. Sigurdson and Adriano Aguzzi.

(**Immunity**, 2008, Dec 19; 29(6):998-1008.)

*** Immunohistochemical tracking of an immune response in mammary paget's disease**

Thomas Brunhuber, Johannes Haybaeck, Georg Schäfer, Gregor Mikuz, Eric Langhoff, Sem Saeland, Serge Lebecque, Nikolaus Romani, Peter Obrist

(**Cancer Lett.**, 2008 Oct. 6)

*** Severe hypoxia and mesencephalic infarctions mimicking Creutzfeldt-Jakob disease** Michel Mittelbronn, David Capper, Benedikt Bader, Jens Schittenhelm, Johannes Haybaeck, Petra Weber, Richard Meyermann, Horst Wiethölter

(**Folia Neuropathol**, 2008, 46(2):149-53)

*** Dural Arachnoid Granulations and "Giant" Arachnoid Granulations**

Johannes Haybaeck, Rene Silye, Dov Soffer

(**Surgical and Radiologic Anatomy**, 2008 Jul; 30(5):417-21)

*** Expression of Cellular Prion Protein (Prp^C) in Schizophrenia, Bipolar Disorder, and Depression**

Serge Weis, Johannes Haybaeck, Jeanette R. Dulay, Ida C. Llenos

(**Journal of Neural Transmission**, 2008 May; 115(5):761-71)

*** Germinal centre B cells are dispensable in prion transport and neuroinvasion**

Mathias Heikenwalder, Christian Federau, Lotta von Boehmer, Petra Schwarz, Mareike Wagner, Nicolas Zeller, Johannes Haybaeck, Marco Prinz, Burkhard Becher and Adriano Aguzzi

(**Journal of Neuroimmunology**, 2007 Dec; 192(1-2):113-23)

* STAT-1 expression in human glioblastoma and peritumoral tissue

Haybaeck J., Schindler C., Spizzo G., Obrist P., Doppler W.

(**Anticancer Research**, 2007 Nov-Dec; 27(6B):3829-35)

Review articles:

*** Crystal arthropathies**

Fuerst M, Haybaeck J, Zustin J, Rüther W.

(**Orthopade.** 2009 Jun; 38(6):501-10. German)

Original peer-reviewed articles in review:

*** Expression of O^6-Methylguanine-DNA Methyltransferase in Childhood Medulloblastoma**

Denis Faoro, André O. von Bueren, Tarek Shalaby, Marie-Louise Hürlimann, Lucia Arnold, Nicolas Gerber, Johannes Haybaeck, Michel Mittelbronn, Stefan Rutkowski, Monika Hegi and Michael A. Grotzer

(in review for publication in **Pediatric Brain, Blood and Cancer**, 2009)

*** Randomized Tree Ensembles for Object Detection\newline in Computational Pathology**

Thomas Fuchs, Johannes Haybaeck, Peter Wild, Holger Moch, Mathias Heikenwalder, Adriano Aguzzi, Joachim Buhmann

(in review for publication in **Med Image Comput Comput Assist Interv Int Conf Med Image Comput Comput Assist Interv.**, presented at the "International Symposium on Visual Computing" 2009)

*** TAK1 suppresses a NEMO-dependent, but NF-κB independent pathway to liver cancer**

Kira Bettermann, Mihael Vucur, Christiane Koppe, Felix Heymann, Johannes Haybaeck, Achim Weber, Ralf Weiskirchen, Christian Liedtke, Nikolaus Gassler, Michael Müller, Shizuo Akira, Frank Tacke, Mathias Heikenwalder, Christian Trautwein and Tom Luedde

Publications

(in review for publication in **Cancer CELL**, 2009)

Published abstracts (peer reviewed journals), CDs:

* Lymphotoxin-driven hepatocellular cancer

Johannes Haybaeck, Nicolas Zeller, Monika Julia Wolf, Ulrich Wagner, Michael Odo Kurrer, Juliane Bremer, Achim Weber, Giandomenica Iezzi, Rolf Graf6, Pierre-Alain Clavien, Robert Thimme, Hubert Blum, Sergei Nedospasov, Kurt Zatloukal, Michael Karin, Manfred Kopf, Adriano Aguzzi, and Mathias Heikenwalder. (2009 Virchow`s Archive [Abstr.])

* Hepatitis induced liver carcinogenesis

Johannes Haybaeck, Nicolas Zeller, Monika Julia Wolf, Ulrich Wagner, Michael Kurrer, Achim Weber, Juliane Bremer, Manfred Kopf, Giandomenica Iezzi, Rolf Graf, Pierre-Alain Clavien, Robert Thimme, Hubert Blum, Michael Karin, Adriano Aguzzi and Mathias Heikenwalder.

(October Issue 2008 of Anticancer Research, [Abstr.])

* De novo expression of CD163 in human brain lesions is not associated with hemorrhages K. Holfelder, J. Schittenhelm, J. Haybaeck, R. Meyermann, R. Beschorner

(October Issue 2008 of Acta Neuropahologica, 116: 339-357 [Abstr.])

* Efficient prion transmission via the intranasal and aerosolic route in the absence of an intact immune system

J. Haybaeck*, M. Heikenwalder*, I. Margalith, N. Zeller, D. Marino, P. Schwarz, C. Bridel, K. Mertz, E. Gagulić, L. Stitz and A. Aguzzi. *contributed equally

(October Issue 2008 of Acta Neuropahologica, 116: 339-357 [Abstr.])

* STAT-1 immunohistochemistry in human glioblastoma

Haybaeck J., Obrist P., Schindler C., Spiegl-Kreinecker S., Pichler J., Doppler W.

(October Issue 2006 of Neuro-Oncology,Volume 8,Issue 4 [Abstr.])

* Regional differences in incidence of chondrocalcinosis. Schindler C., Haybaeck J., Kaiser A., Fischer J., Kaiser A., Kuchelemeister K.

Publications

(Acta Neuropathologica (2005), pg.19, 110: 339 [Abstr.], Verlag: SPRINGER)

* Intraoperative Hirntumorzytologie, authors: J. Haybäck, C. Schindler, Verhandlungen der Deutschen Gesellschaft für Zytologie, 24. Tagung, 2005, Wien, Herausgeber: N. Freudenberg, H. Wiener, W. Höbling, E. Bayer-Pietsch, M. Arnabold, H. Köppl, Verlag: ELSEVIER - Urban & Fischer

* CD-ROM to the topic „Intraoperative Hirntumorzytologie“ zur Dreiländertagung für Zytologie, Wien, 2005: authors: J. Haybäck, C. Schindler , presentation: 9.9.2005

* Post-poliomyelitis myopathy, J. Haybäck, K. Stieglbauer, C. Schindler; (published as Abstract in Journal of Clinical Neuropathology, March/April 2005;24:94[Abstr.])

* CD-ROM to the topic „Intraoperative Hirntumorzytologie“: authors: Haybäck J.,

Schindler C., in cooperation with Spiegl-Kreinecker S., Fellner F., Presentation 23.4.2004

* Abstract for 4th European Cytogenetics Conference, September 6-9. 2003, Bologna, Italy, Title: Mosaicism for maternal isodisomy 22 and trisomy 22 in a fetus with malformation; AH.-Ch. Duba, K. Kirchmayr, R. Silye, J. Haybäck, A. Janecke, B. Günther and W. Arzt

(Annales de Génétiques (2003), [Abstr.], Verlag: ELSEVIER)

Scientific prizes

*Poster prize for the best poster in the field of Neurosciences together with Mathias Heikenwalder entitled “Efficient prion transmission via the intranasal or aerosolic route in the absence of a functional immune system” at the 8th DAY OF CLINICAL RESEARCH of the University Hospital Zürich, April 16, 2009, Centre of Medical Research (CMR) University Zürich, Switzerland

*Young Investigator Award bestowed by the Charles Rodolphe Brupbacher Foundation for Cancer Research (a biennial prize for young investigators) price for work entitled “A lymphotoxin driven pathway to chronic hepatitis and hepatocellular carcinoma” at the 9th Charles Rodolphe Brupbacher Symposium, February 11 - 13, 2009, Lecture Hall Nord, University Hospital Zurich, Switzerland

*Poster prize for the best poster in the cancer field together with Mathias Heikenwalder entitled “Liver specific expression of lymphotoxin causes chronic hepatitis induced hepatocellular carcinoma” at the 7th Day of Clinical Research Zürich, March 27, 2008, Centre of Medical Research (CMR) University Zürich

Acknowledgements

I want to thank and acknowledge all people with whom I had the pleasure to share my time during working on my thesis in Adriano Aguzzi‘s laboratory. These personalities continuously supported me intellectually as well as by technical help. I was able to discuss new and exciting experimental data with them in a lot of fruitful collaborations. I received an incredible load of positive inputs every day from my colleagues in the lab as well as from collaboration partners from other laboratories.

First of all I like to thank Prof. Dr. Adriano Aguzzi who offered me to accomplish my PhD thesis in his great, well-equipped and outstanding Institute of Neuropathology. I particularly want to thank him for his generosity and intellectual as well as financial support, and his valuable suggestions throughout the whole time in his institute. I could spend a great time in his lab for what I am really enormously grateful. Adriano‘s criticism was always grounded on a scientific basis for what I will always have to thank him because finally this led to my personal development as a scientist. I always received a lot of input and helpful answers whenever I asked.

Moreover I would like to thank him for giving me the exclusive possibility to spend my training time in Neuropathology in parallel to doing my studies in molecular biology and my research work at his laboratory. Adriano, thanks a lot for your support!

I would like to express my warmest thanks to Dr. Mathias Heikenwälder who always was the person who guided me through the for me so far unknown areas of research and who always, from the first day on when I came to Adriano Aguzzi‘s lab, took care of my steady development. On a daily basis he tried to push our research activities some steps forward and that is what really makes him an excellent scientist. I am very thankful for giving me the opportunity to work with him, not only on the projects that lead to my thesis but also many other exciting projects where we together stepped into new grounds of basic research. On the other hand it was always a pleasure for me to feel as working in a real team when studying so far unknown molecular and cellular mechanism together with him. With time Mathias did not only become my favorite collaborator but a friend for what I really thank him. Mathias, thanks a lot for being my partner in the lab and for being my friend! If you once need anything you can count on me as I can count on you. Thanks a lot for everything!

In particular I want to acknowledge the generation of the *tg*1223 mice and the successful and continuous collaboration.

We had a real great time together in the lab and at various congresses that we attended together. I am absolutely sure that we will also collaborate on interesting and exciting projects in the future as well.

Moreover, I would like to thank Dr. Nicolas Zeller for his support and work during the starting period of the liver project. We worked together in a quite efficient manner, also due to kindly providing me all his knowledge on the various mouse lines, his protocols and data sheets. He said: “Then it stays in the family”, meaning that all together we really felt like working in a scientific family.

Sincere thanks are given to Prof. Dr. Manfred Kopf and Prof. Dr. Burkhard Becher for their support as members of my PhD-committee. In addition we have started some other fruitful collaborative efforts which are still ongoing and that will also lead to exciting results. It was extremely helpful that whenever I had questions I had the possibility to ask, and even better I knew that I would always get important, clear and honest inputs.

Monika Julia Wolf I want to thank for her support whenever we did experiments with various groups of many animals. Also endless seeming experiments were much fun because of her humor. Our collaborations, which will still continue in the future as well, were very efficient and fruitful. We had great times laughing a lot and that made our work very enjoyable. Monika, it was and still is nice working with you!

With Dr. Juliane Bremer I have been working and I am still working on many interesting projects. I want to thank her for her constant input and friendly support. We shared a lot of fascinating and exciting new scientific findings. In addition we always met each other as often being the last persons in the lab. Thereby, we motivated each other and our collaborative efforts turned out to be quite fruitful. For our future shared research collaborations I really hope that the past success will continue, and I am pretty sure that we will be able to still finish many good projects. Thanks Juliane for everything, you are a great colleague.

I want to thank a lot Birgit Riepl and Gitta Seleznik as the ”core people” of our “inflammation induced carcinogenesis group” for their steady intellectual and technical help. It was always a pleasure to work with you and to help each other as a real, very effective team. I believe that the atmosphere in our lab would not have been that good without your positive, helpful and productive spirit.

I am extremely grateful for Dr. Giandomenica Iezzi‘s support with the isolation of intrahepatic lymphocytes. She was very helpful and it was very nice to collaborate with her. The data which came out of our experiments were really important as it is still a matter of debate in the field which lymphocytic subtypes are most critical for the initiation and maintenance of hepatitis and which cells are beside hepatocytes crucial for HCC development. Therefore I am very glad that I gad the opportunity to work with Giando who is a real expert in isolation of intrahepatic lymphocytes.

Dr. Uli Wagner and Dr. Stefan Zoller, as my contact persons for questions on bioinformatics, were always extremely supportive. The frequent discussions with them at the Functional Genomics Centre Zürich were always very productive and fruitful. Especially their input in designing the DNA-microarray and the aCGH experiments was essential for a reasonable and efficient data collection with the following stringent analysis. We really had a very good time. Finally our collaborations led to successful work. In addition, the next collaborations are already set up and will lead to success as well.

With Ilan Margalith I shared not only my office room for a long time but also many exciting projects. Therefore, I want to express my warmest thanks for all his input and support.

My sincere thanks I want to express to all members of the Institute of Neuropathology especially to Mareike Schroff, Petra Schwarz and Rita Moos for their excellent technical expertise and support. Moreover they always were the good spirits when things did not work that well as expected. Without their enormous, high-quality technical support the daily work in our lab would not have been possible in such an efficient way.

I am very grateful to PD Dr. Rolf Graf from the Department of Visceral Surgery for fruitful scientific

discussion and for his incredible, unusually high support. With time Rolf became a really good friend. It was always a great pleasure when Rolf came to our office and laboratory. We had a lot of fun and we will continue our fruitful collaborative efforts. Thank you Rolf!

PD Dr. Achim Weber and PD Dr. Michael Odo Kurrer I want to thank for many animating scientific discussions, their intellectual input and for all past and current collaborations. I believe that we will be able to continue our collaborations which will for sure help to elucidate interesting questions related to pathomechanisms.

In addition I am grateful to Prof. Dr. Wolfram Jochum from the Department of Clinical Pathology for fruitful scientific discussion and support.

I would like to thank our animal care technician Mirzet Delic, the animal care takers and the members of the BZL for their high quality work.

Also I would like to thank all collaborators including Prof. Dr. Michael Karin, Prof. Dr. Kurt Zatloukal, Prof. Dr. Helmut Blum, Prof. Dr. Robert Thimme, Prof. Snorri Thorgeirsson, Dr. Valentina Factor and Dr. Eli Pikarsky for intensive collaboration, exchanging ideas, stimulating discussions and for providing of antibodies, tissue samples or any other kind of support.

I thank Marianne König, Rita Moos, Udo Ungethüm, Mirzet Delic, Urs Egli, Silvia Behnke, André Fitsche, Andrea Patrignani, Marie-Ange Thelu and Manja Barthel for excellent technical assistance.

I am gratful to Sergei A. Nedospasov, Muhammad Ramzan, Sandra Ciesek, Thomas Pietschmann, Patrice N. Marche, Kurt Zatloukal and Jeffrey L. Browning for their support.

I also want to thank Norbert Wey and Monika Bieri for excellent technical assistance.

With respect to the second part of my thesis I am very grateful to Professor Lothar Stitz, Dr. Kirsten Mertz, Dr. Elizabeta Gagulić and Dr. Oliver Planz from the Institute of Immunology, Friedrich-Loeffler-Institute, Paul-Ehrlich-Strasse 28, D-72076 Tübingen, Germany. Dr. Claire Bridel and Dr. Kirsten Mertz were involved in the frist i.n. inoculations. Kirsten also worked on the aerosol experiments for which I am very grateful. I also want to thank Silke Gaedt for excellent technical assistance and Petra Reinhold for advice on aerosol treatment. I am grateful to Dr. Tobias Junt for discussions.

This work was supported in part by EU-CT-2001-01925 and the TSE-Forschungsprogramm des Landes Baden-Württemberg, Germany. This work was also supported in part by grants from the UK Department of Environment, Food and Rural Affairs (A.A.) an EU Framework Programme 6 STREP grant (A.A.).

Finally I wish to express my deepest gratitude to my family. All of this would also not have been possible without the constant and unconditioned support of my wife, my parents, my grandmother, my aunts and uncles.

I am deeply indebted in particular to my wife Cornelia who accepted my decision to become a student for a second time after already having studied medicine and having worked as pathologist and to go abroad for doing research as well as for becoming neuropathologist. Cornelia, you are absolutely the best wife I can imagine! Thank you very much!

References

Aggarwal, B.B. (2003). Signalling pathways of the TNF superfamily: a double-edged sword. Nat Rev Immunol *3*, 745-756.

Aguzzi, A. (2004). Understanding the diversity of prions. Nat Cell Biol *6*, 290-292.

Aguzzi, A., and Glatzel, M. (2006). Prion infections, blood and transfusions. Nat Clin Pract Neurol *2*, 321-329.

Aguzzi, A., and Haass, C. (2003). Games played by rogue proteins in prion disorders and Alzheimer's disease. Science *302*, 814-818.

Aguzzi, A., and Heikenwalder, M. (2006). Pathogenesis of prion diseases: current status and future outlook. Nat Rev Microbiol *4*, 765-775.

Aguzzi, A., Heikenwalder, M., and Polymenidou, M. (2007). Insights into prion strains and neurotoxicity. Nat Rev Mol Cell Biol *8*, 552-561.

Aguzzi, A., and Polymenidou, M. (2004). Mammalian prion biology: one century of evolving concepts. Cell *116*, 313-327.

Aguzzi, A., and Sigurdson, C.J. (2004). Antiprion immunotherapy: to suppress or to stimulate? Nat Rev Immunol *4*, 725-736.

Aguzzi, A., and Weissmann, C. (1996). Sleepless in Bologna: transmission of fatal familial insomnia. Trends Microbiol *4*, 129-131.

Akerman, P., Cote, P., Yang, S.Q., McClain, C., Nelson, S., Bagby, G.J., and Diehl, A.M. (1992). Antibodies to tumor necrosis factor-alpha inhibit liver regeneration after partial hepatectomy. Am J Physiol *263*, G579-585.

Akhurst, B., Matthews, V., Husk, K., Smyth, M.J., Abraham, L.J., and Yeoh, G.C. (2005). Differential lymphotoxin-beta and interferon gamma signaling during mouse liver regeneration induced by chronic and acute injury. Hepatology *41*, 327-335.

Akira, S., Takeda, K., and Kaisho, T. (2001). Toll-like receptors: critical proteins linking innate and acquired immunity. Nat Immunol *2*, 675-680.

Akiyama, T. (2000). Wnt/beta-catenin signaling. Cytokine Growth Factor Rev *11*, 273-282.

Akowitz, A., Sklaviadis, T., Manuelidis, E.E., and Manuelidis, L. (1990). Nuclease-resistant polyadenylated RNAs of significant size are detected by PCR in highly purified Creutzfeldt-Jakob disease preparations. Microb Pathog *9*, 33-45.

Akowitz, A., Sklaviadis, T., and Manuelidis, L. (1994). Endogenous viral complexes with long RNA cosediment with the agent of Creutzfeldt-Jakob disease. Nucleic Acids Res *22*, 1101-1107.

Akriviadis, E.A., Llovet, J.M., Efremidis, S.C., Shouval, D., Canelo, R., Ringe, B., and Meyers, W.C. (1998). Hepatocellular carcinoma. Br J Surg *85*, 1319-1331.

Alimzhanov, M.B., Kuprash, D.V., Kosco-Vilbois, M.H., Luz, A., Turetskaya, R.L., Tarakhovsky, A., Rajewsky, K., Nedospasov, S.A., and Pfeffer, K. (1997). Abnormal development of secondary lymphoid tissues in lymphotoxin beta-deficient mice. Proc Natl Acad Sci U S A *94*, 9302-9307.

Allain, J.P., Stramer, S.L., Carneiro-Proietti, A.B., Martins, M.L., Lopes da Silva, S.N., Ribeiro, M., Proietti, F.A., and Reesink, H.W. (2009). Transfusion-transmitted infectious diseases. Biologicals *37*, 71-77.

Alonzi, T., Maritano, D., Gorgoni, B., Rizzuto, G., Libert, C., and Poli, V. (2001). Essential role of STAT3 in the control of the acute-phase response as revealed by inducible gene inactivation [correction of activation] in the liver. Mol Cell Biol *21*, 1621-1632.

Alpini, G., Ulrich, C.D., 2nd, Phillips, J.O., Pham, L.D., Miller, L.J., and LaRusso, N.F. (1994). Upregulation

of secretin receptor gene expression in rat cholangiocytes after bile duct ligation. Am J Physiol *266*, G922-928.

Alvaro, D., Alpini, G., Jezequel, A.M., Bassotti, C., Francia, C., Fraioli, F., Romeo, R., Marucci, L., Le Sage, G., Glaser, S.S.*, et al.* (1997). Role and mechanisms of action of acetylcholine in the regulation of rat cholangiocyte secretory functions. J Clin Invest *100*, 1349-1362.

Amir, R.E., Haecker, H., Karin, M., and Ciechanover, A. (2004). Mechanism of processing of the NF-kappa B2 p100 precursor: identification of the specific polyubiquitin chain-anchoring lysine residue and analysis of the role of NEDD8-modification on the SCF(beta-TrCP) ubiquitin ligase. Oncogene *23*, 2540-2547.

An, M.M., Fan, K.X., Cao, Y.B., Shen, H., Zhang, J.D., Lu, L., Gao, P.H., and Jiang, Y.Y. (2006). Lymphtoxin beta receptor-Ig protects from T-cell-mediated liver injury in mice through blocking LIGHT/HVEM signaling. Biol Pharm Bull *29*, 2025-2030.

Anand, S., Wang, P., Yoshimura, K., Choi, I.H., Hilliard, A., Chen, Y.H., Wang, C.R., Schulick, R., Flies, A.S., Flies, D.B.*, et al.* (2006). Essential role of TNF family molecule LIGHT as a cytokine in the pathogenesis of hepatitis. J Clin Invest *116*, 1045-1051.

Anderson, R.M., Donnelly, C.A., Ferguson, N.M., Woolhouse, M.E., Watt, C.J., Udy, H.J., MaWhinney, S., Dunstan, S.P., Southwood, T.R., Wilesmith, J.W.*, et al.* (1996). Transmission dynamics and epidemiology of BSE in British cattle. Nature *382*, 779-788.

Andreoletti, O., Berthon, P., Marc, D., Sarradin, P., Grosclaude, J., van Keulen, L., Schelcher, F., Elsen, J.M., and Lantier, F. (2000). Early accumulation of PrP(Sc) in gut-associated lymphoid and nervous tissues of susceptible sheep from a Romanov flock with natural scrapie. J Gen Virol *81 Pt 12*, 3115-3126.

Andrews, N.J., Farrington, C.P., Ward, H.J., Cousens, S.N., Smith, P.G., Molesworth, A.M., Knight, R.S., Ironside, J.W., and Will, R.G. (2003). Deaths from variant Creutzfeldt-Jakob disease in the UK. Lancet *361*, 751-752.

Ansel, K.M., Ngo, V.N., Hyman, P.L., Luther, S.A., Forster, R., Sedgwick, J.D., Browning, J.L., Lipp, M., and Cyster, J.G. (2000). A chemokine-driven positive feedback loop organizes lymphoid follicles. Nature *406*, 309-314.

Arenzana-Seisdedos, F., Turpin, P., Rodriguez, M., Thomas, D., Hay, R.T., Virelizier, J.L., and Dargemont, C. (1997). Nuclear localization of I kappa B alpha promotes active transport of NF-kappa B from the nucleus to the cytoplasm. J Cell Sci *110 (Pt 3)*, 369-378.

Avantaggiati, M.L., Natoli, G., Balsano, C., Chirillo, P., Artini, M., De Marzio, E., Collepardo, D., and Levrero, M. (1993). The hepatitis B virus (HBV) pX transactivates the c-fos promoter through multiple cis-acting elements. Oncogene *8*, 1567-1574.

Bachert, C., Fimmel, C., and Linstedt, A.D. (2007). Endosomal trafficking and proprotein convertase cleavage of cis Golgi protein GP73 produces marker for hepatocellular carcinoma. Traffic *8*, 1415-1423.

Baeuerle, P.A., and Baltimore, D. (1996). NF-kappa B: ten years after. Cell *87*, 13-20.

Baffet, G., Braciak, T.A., Fletcher, R.G., Gauldie, J., Fey, G.H., and Northemann, W. (1991). Autocrine activity of interleukin 6 secreted by hepatocarcinoma cell lines. Mol Biol Med *8*, 141-156.

Banner, D.W., D'Arcy, A., Janes, W., Gentz, R., Schoenfeld, H.J., Broger, C., Loetscher, H., and Lesslauer, W. (1993). Crystal structure of the soluble human 55 kd TNF receptor-human TNF beta complex: implications for TNF receptor activation. Cell *73*, 431-445.

Barbara, J.A., Smith, W.B., Gamble, J.R., Van Ostade, X., Vandenabeele, P., Tavernier, J., Fiers, W., Vadas, M.A., and Lopez, A.F. (1994). Dissociation of TNF-alpha cytotoxic and proinflammatory activities by p55 receptor- and p75 receptor-selective TNF-alpha mutants. Embo J *13*, 843-850.

Bartz, J.C., Kincaid, A.E., and Bessen, R.A. (2003). Rapid prion neuroinvasion following tongue infection. J Virol *77*, 583-591.

Basler, K., Oesch, B., Scott, M., Westaway, D., Walchli, M., Groth, D.F., McKinley, M.P., Prusiner, S.B., and Weissmann, C. (1986). Scrapie and cellular PrP isoforms are encoded by the same chromosomal gene. Cell

46, 417-428.

Baumann, F., Tolnay, M., Brabeck, C., Pahnke, J., Kloz, U., Niemann, H.H., Heikenwalder, M., Rulicke, T., Burkle, A., and Aguzzi, A. (2007). Lethal recessive myelin toxicity of prion protein lacking its central domain. Embo J *26*, 538-547.

Beekes, M., and McBride, P.A. (2000). Early accumulation of pathological PrP in the enteric nervous system and gut-associated lymphoid tissue of hamsters orally infected with scrapie. Neurosci Lett *278*, 181-184.

Bendheim, P.E., Brown, H.R., Rudelli, R.D., Scala, L.J., Goller, N.L., Wen, G.Y., Kascsak, R.J., Cashman, N.R., and Bolton, D.C. (1992). Nearly ubiquitous tissue distribution of the scrapie agent precursor protein. Neurology *42*, 149-156.

Benjamin, L.E., Golijanin, D., Itin, A., Pode, D., and Keshet, E. (1999). Selective ablation of immature blood vessels in established human tumors follows vascular endothelial growth factor withdrawal. J Clin Invest *103*, 159-165.

Benjamini, Y.a.H., Y. (1995). Controlling the False Discovery Rate: A Practical and Powerful Approach to Multiple Testing. J R Statist Soc B *57*, 289-300.

Berasain, C., Castillo, J., Perugorria, M.J., Latasa, M.U., Prieto, J., and Avila, M.A. (2009). Inflammation and liver cancer: new molecular links. Ann N Y Acad Sci *1155*, 206-221.

Bessen, R.A., Martinka, S., Kelly, J., and Gonzalez, D. (2009). Role of the lymphoreticular system in prion neuroinvasion from the oral and nasal mucosa. J Virol *83*, 6435-6445.

Biacabe, A.G., Laplanche, J.L., Ryder, S., and Baron, T. (2004). Distinct molecular phenotypes in bovine prion diseases. EMBO Rep *5*, 110-115.

Biron, C.A. (2001). Interferons alpha and beta as immune regulators--a new look. Immunity *14*, 661-664.

Black, R.A., Rauch, C.T., Kozlosky, C.J., Peschon, J.J., Slack, J.L., Wolfson, M.F., Castner, B.J., Stocking, K.L., Reddy, P., Srinivasan, S.*, et al.* (1997). A metalloproteinase disintegrin that releases tumour-necrosis factor-alpha from cells. Nature *385*, 729-733.

Blättler, T., Brandner, S., Raeber, A.J., Klein, M.A., Voigtländer, T., Weissmann, C., and Aguzzi, A. (1997). PrP-expressing tissue required for transfer of scrapie infectivity from spleen to brain. Nature *389*, 69-73.

Blight, K.J., McKeating, J.A., and Rice, C.M. (2002). Highly permissive cell lines for subgenomic and genomic hepatitis C virus RNA replication. J Virol *76*, 13001-13014.

Blomhoff, R., and Wake, K. (1991). Perisinusoidal stellate cells of the liver: important roles in retinol metabolism and fibrosis. Faseb J *5*, 271-277.

Bluethmann, H., Rothe, J., Schultze, N., Tkachuk, M., and Koebel, P. (1994). Establishment of the role of IL-6 and TNF receptor 1 using gene knockout mice. J Leukoc Biol *56*, 565-570.

Bocharova, O.V., Breydo, L., Parfenov, A.S., Salnikov, V.V., and Baskakov, I.V. (2005). In vitro conversion of full-length mammalian prion protein produces amyloid form with physical properties of PrP(Sc). J Mol Biol *346*, 645-659.

Bosch, F.X., Ribes, J., and Borras, J. (1999). Epidemiology of primary liver cancer. Semin Liver Dis *19*, 271-285.

Bounhar, Y., Zhang, Y., Goodyer, C.G., and LeBlanc, A. (2001). Prion protein protects human neurons against Bax-mediated apoptosis. J Biol Chem *276*, 39145-39149.

Boutros, M., Paricio, N., Strutt, D.I., and Mlodzik, M. (1998). Dishevelled activates JNK and discriminates between JNK pathways in planar polarity and wingless signaling. Cell *94*, 109-118.

Brandel, J.P., Delasnerie-Laupretre, N., Laplanche, J.L., Hauw, J.J., and Alperovitch, A. (2000). Diagnosis of Creutzfeldt-Jakob disease: effect of clinical criteria on incidence estimates [In Process Citation]. Neurology *54*, 1095-1099.

Brandner, S., Raeber, A., Sailer, A., Blattler, T., Fischer, M., Weissmann, C., and Aguzzi, A. (1996). Normal host prion protein (PrPC) is required for scrapie spread within the central nervous system. Proc Natl Acad Sci

U S A *93*, 13148-13151.

Brown, D.R., Qin, K., Herms, J.W., Madlung, A., Manson, J., Strome, R., Fraser, P.E., Kruck, T., von Bohlen, A., Schulz-Schaeffer, W.*, et al.* (1997). The cellular prion protein binds copper in vivo. Nature *390*, 684-687.

Brown, H.R., Goller, N.L., Rudelli, R.D., Merz, G.S., Wolfe, G.C., Wisniewski, H.M., and Robakis, N.K. (1990). The mRNA encoding the scrapie agent protein is present in a variety of non-neuronal cells. Acta Neuropathol Berl *80*, 1-6.

Brown, P. (1990). Transmissible spongiform encephalopathies in humans: kuru, Creutzfeldt-Jakob disease and Gerstmann-Straussler-Scheinker disease. Can J Vet Res *54*, 38-41.

Brown, P., Cervenakova, L., McShane, L., Goldfarb, L.G., Bishop, K., Bastian, F., Kirkpatrick, J., Piccardo, P., Ghetti, B., and Gajdusek, D.C. (1998). Creutzfeldt-Jakob disease in a husband and wife. Neurology *50*, 684-688.

Brown, P., and Gajdusek, D.C. (1991). Survival of scrapie virus after 3 years' interment. Lancet *337*, 269-270.

Brown P, P.M., Brandel JP, Sato T, McShane L, Zerr I, Fletcher A, Will RG, Pocchiari M, Cashman NR, d'Aignaux JH, Cervenakova L, Fradkin J, Schonberger LB, Collins SJ (2000). Iatrogenic Creutzfeldt-Jakob disease at the millennium. Neurology *55*, 1075-1081.

Browning, J.L., Dougas, I., Ngam-ek, A., Bourdon, P.R., Ehrenfels, B.N., Miatkowski, K., Zafari, M., Yampaglia, A.M., Lawton, P., Meier, W.*, et al.* (1995). Characterization of surface lymphotoxin forms. Use of specific monoclonal antibodies and soluble receptors. J Immunol *154*, 33-46.

Browning, J.L., and French, L.E. (2002). Visualization of lymphotoxin-beta and lymphotoxin-beta receptor expression in mouse embryos. J Immunol *168*, 5079-5087.

Browning, J.L., Ngam-ek, A., Lawton, P., DeMarinis, J., Tizard, R., Chow, E.P., Hession, C., O'Brine-Greco, B., Foley, S.F., and Ware, C.F. (1993). Lymphotoxin beta, a novel member of the TNF family that forms a heteromeric complex with lymphotoxin on the cell surface. Cell *72*, 847-856.

Browning, J.L., Sizing, I.D., Lawton, P., Bourdon, P.R., Rennert, P.D., Majeau, G.R., Ambrose, C.M., Hession, C., Miatkowski, K., Griffiths, D.A.*, et al.* (1997). Characterization of lymphotoxin-alpha beta complexes on the surface of mouse lymphocytes. J Immunol *159*, 3288-3298.

Browning, S.R., Mason, G.L., Seward, T., Green, M., Eliason, G.A., Mathiason, C., Miller, M.W., Williams, E.S., Hoover, E., and Telling, G.C. (2004). Transmission of prions from mule deer and elk with chronic wasting disease to transgenic mice expressing cervid PrP. J Virol *78*, 13345-13350.

Bruce, M.E., Will, R.G., Ironside, J.W., McConnell, I., Drummond, D., Suttie, A., McCardle, L., Chree, A., Hope, J., Birkett, C.*, et al.* (1997). Transmissions to mice indicate that 'new variant' CJD is caused by the BSE agent Nature *389*, 498-501.

Budhu, A., and Wang, X.W. (2006). The role of cytokines in hepatocellular carcinoma. J Leukoc Biol *80*, 1197-1213.

Büeler, H.R., Aguzzi, A., Sailer, A., Greiner, R.A., Autenried, P., Aguet, M., and Weissmann, C. (1993). Mice devoid of PrP are resistant to scrapie. Cell *73*, 1339-1347.

Büeler, H.R., Fischer, M., Lang, Y., Bluethmann, H., Lipp, H.P., DeArmond, S.J., Prusiner, S.B., Aguet, M., and Weissmann, C. (1992). Normal development and behaviour of mice lacking the neuronal cell-surface PrP protein. Nature *356*, 577-582.

Campbell, J.S., Hughes, S.D., Gilbertson, D.G., Palmer, T.E., Holdren, M.S., Haran, A.C., Odell, M.M., Bauer, R.L., Ren, H.P., Haugen, H.S.*, et al.* (2005). Platelet-derived growth factor C induces liver fibrosis, steatosis, and hepatocellular carcinoma. Proc Natl Acad Sci U S A *102*, 3389-3394.

Campbell, J.S., Prichard, L., Schaper, F., Schmitz, J., Stephenson-Famy, A., Rosenfeld, M.E., Argast, G.M., Heinrich, P.C., and Fausto, N. (2001). Expression of suppressors of cytokine signaling during liver regeneration. J Clin Invest *107*, 1285-1292.

Cao, Y., Bonizzi, G., Seagroves, T.N., Greten, F.R., Johnson, R., Schmidt, E.V., and Karin, M. (2001). IKKalpha provides an essential link between RANK signaling and cyclin D1 expression during mammary

gland development. Cell *107*, 763-775.

Capellari, S., Cardone, F., Notari, S., Schinina, M.E., Maras, B., Sita, D., Baruzzi, A., Pocchiari, M., and Parchi, P. (2005). Creutzfeldt-Jakob disease associated with the R208H mutation in the prion protein gene. Neurology *64*, 905-907.

Carr, B.I., and Van Thiel, D.H. (1990). Hormonal manipulation of human hepatocellular carcinoma. A clinical investigative and therapeutic opportunity. J Hepatol *11*, 287-289.

Cashman, N.R., Loertscher, R., Nalbantoglu, J., Shaw, I., Kascsak, R.J., Bolton, D.C., and Bendheim, P.E. (1990). Cellular isoform of the scrapie agent protein participates in lymphocyte activation. Cell *61*, 185-192.

Castilla, J., Saa, P., Hetz, C., and Soto, C. (2005). In vitro generation of infectious scrapie prions. Cell *121*, 195-206.

Cervenakova, L., Goldfarb, L.G., Garruto, R., Lee, H.S., Gajdusek, D.C., and Brown, P. (1998). Phenotype-genotype studies in kuru: implications for new variant Creutzfeldt-Jakob disease. Proc Natl Acad Sci U S A *95*, 13239-13241.

Chang, M.L., Yeh, C.T., Chen, J.C., Huang, C.C., Lin, S.M., Sheen, I.S., Tai, D.I., Chu, C.M., Lin, W.P., Chang, M.Y.*, et al.* (2008). Altered expression patterns of lipid metabolism genes in an animal model of HCV core-related, nonobese, modest hepatic steatosis. BMC Genomics *9*, 109.

Chen, C.M., You, L.R., Hwang, L.H., and Lee, Y.H. (1997). Direct interaction of hepatitis C virus core protein with the cellular lymphotoxin-beta receptor modulates the signal pathway of the lymphotoxin-beta receptor. J Virol *71*, 9417-9426.

Chen, Y.W., Jeng, Y.M., Yeh, S.H., and Chen, P.J. (2002). P53 gene and Wnt signaling in benign neoplasms: beta-catenin mutations in hepatic adenoma but not in focal nodular hyperplasia. Hepatology *36*, 927-935.

Cheng, W.S., Govindarajan, S., and Redeker, A.G. (1992). Hepatocellular carcinoma in a case of Wilson's disease. Liver *12*, 42-45.

Chesebro, B. (1998). BSE and prions: uncertainties about the agent. Science *279*, 42-43.

Chesebro, B. (2003). Introduction to the transmissible spongiform encephalopathies or prion diseases. Br Med Bull *66*, 1-20.

Chiarini, L.B., Freitas, A.R., Zanata, S.M., Brentani, R.R., Martins, V.R., and Linden, R. (2002). Cellular prion protein transduces neuroprotective signals. Embo J *21*, 3317-3326.

Chisari, F.V., Pinkert, C.A., Milich, D.R., Filippi, P., McLachlan, A., Palmiter, R.D., and Brinster, R.L. (1985). A transgenic mouse model of the chronic hepatitis B surface antigen carrier state. Science *230*, 1157-1160.

Choi, E.M., Geschwind, M.D., Deering, C., Pomeroy, K., Kuo, A., Miller, B.L., Safar, J.G., and Prusiner, S.B. (2009). Prion proteins in subpopulations of white blood cells from patients with sporadic Creutzfeldt-Jakob disease. Lab Invest *89*, 624-635.

Chung, C.D., Liao, J., Liu, B., Rao, X., Jay, P., Berta, P., and Shuai, K. (1997). Specific inhibition of Stat3 signal transduction by PIAS3. Science *278*, 1803-1805.

Chung, R.T., He, W., Saquib, A., Contreras, A.M., Xavier, R.J., Chawla, A., Wang, T.C., and Schmidt, E.V. (2001). Hepatitis C virus replication is directly inhibited by IFN-alpha in a full-length binary expression system. Proc Natl Acad Sci U S A *98*, 9847-9852.

Clarke, M.C., and Kimberlin, R.H. (1984). Pathogenesis of mouse scrapie: distribution of agent in the pulp and stroma of infected spleens. Vet Microbiol *9*, 215-225.

Cohen, F.E., Pan, K.M., Huang, Z., Baldwin, M., Fletterick, R.J., and Prusiner, S.B. (1994). Structural clues to prion replication Science *264*, 530-531.

Collinge, J., Harding, A.E., Owen, F., Poulter, M., Lofthouse, R., Boughey, A.M., Shah, T., and Crow, T.J. (1989). Diagnosis of Gerstmann-Straussler syndrome in familial dementia with prion protein gene analysis. Lancet *2*, 15-17.

Collinge, J., Whitfield, J., McKintosh, E., Beck, J., Mead, S., Thomas, D.J., and Alpers, M.P. (2006). Kuru in the 21st century--an acquired human prion disease with very long incubation periods. Lancet *367*, 2068-2074.

Collins, S.J., Lawson, V.A., and Masters, C.L. (2004). Transmissible spongiform encephalopathies. Lancet *363*, 51-61.

Coope, H.J., Atkinson, P.G., Huhse, B., Belich, M., Janzen, J., Holman, M.J., Klaus, G.G., Johnston, L.H., and Ley, S.C. (2002). CD40 regulates the processing of NF-kappaB2 p100 to p52. Embo J *21*, 5375-5385.

Corona, C., Porcario, C., Martucci, F., Iulini, B., Manea, B., Gallo, M., Palmitessa, C., Maurella, C., Mazza, M., Pezzolato, M.*, et al.* (2009). Olfactory system involvement in natural scrapie disease. J Virol *83*, 3657-3667.

Crawford, D.H., Leggett, B.A., and Powell, L.W. (1998). Haemochromatosis. Baillieres Clin Gastroenterol *12*, 209-225.

Creutzfeldt, H.G. (1920). Über eine eigenartige herdförmige Erkrankung des Zentralnervensystems. Z ges Neurol Psychiatr *57*, 1-19.

Cuille, J., and Chelle, P.L. (1939). Experimental transmission of trembling to the goat. C R Seances Acad Sci *208*, 1058-1160.

Cupedo, T., Jansen, W., Kraal, G., and Mebius, R.E. (2004). Induction of secondary and tertiary lymphoid structures in the skin. Immunity *21*, 655-667.

DeArmond, S.J., Mobley, W.C., DeMott, D.L., Barry, R.A., Beckstead, J.H., and Prusiner, S.B. (1987). Changes in the localization of brain prion proteins during scrapie infection [published erratum appears in Neurology 1987 Nov;37(11):1770]. Neurology *37*, 1271-1280.

Decker, K. (1990). Biologically active products of stimulated liver macrophages (Kupffer cells). Eur J Biochem *192*, 245-261.

Dejardin, E., Droin, N.M., Delhase, M., Haas, E., Cao, Y., Makris, C., Li, Z.W., Karin, M., Ware, C.F., and Green, D.R. (2002). The lymphotoxin-beta receptor induces different patterns of gene expression via two NF-kappaB pathways. Immunity *17*, 525-535.

DeJoia, C., Moreaux, B., O'Connell, K., and Bessen, R.A. (2006). Prion infection of oral and nasal mucosa. J Virol *80*, 4546-4556.

Deleault, N.R., Geoghegan, J.C., Nishina, K., Kascsak, R., Williamson, R.A., and Supattapone, S. (2005). Protease-resistant prion protein amplification reconstituted with partially purified substrates and synthetic polyanions. J Biol Chem *280*, 26873-26879.

Deugnier, Y.M., Guyader, D., Crantock, L., Lopez, J.M., Turlin, B., Yaouanq, J., Jouanolle, H., Campion, J.P., Launois, B., Halliday, J.W.*, et al.* (1993). Primary liver cancer in genetic hemochromatosis: a clinical, pathological, and pathogenetic study of 54 cases. Gastroenterology *104*, 228-234.

Devereux, T.R., Stern, M.C., Flake, G.P., Yu, M.C., Zhang, Z.Q., London, S.J., and Taylor, J.A. (2001). CTNNB1 mutations and beta-catenin protein accumulation in human hepatocellular carcinomas associated with high exposure to aflatoxin B1. Mol Carcinog *31*, 68-73.

Dickinson, A.G., Stamp, J.T., and Renwick, C.C. (1974). Maternal and lateral transmission of scrapie in sheep. J Comp Pathol *84*, 19-25.

Diringer, H. (1995). Proposed link between transmissible spongiform encephalopathies of man and animals. Lancet *346*, 1208-1210.

Doi, S., Ito, M., Shinagawa, M., Sato, G., Isomura, H., and Goto, H. (1988). Western blot detection of scrapie-associated fibril protein in tissues outside the central nervous system from preclinical scrapie-infected mice. J Gen Virol *69*, 955-960.

Donne, D.G., Viles, J.H., Groth, D., Mehlhorn, I., James, T.L., Cohen, F.E., Prusiner, S.B., Wright, P.E., and Dyson, H.J. (1997). Structure of the recombinant full-length hamster prion protein PrP(29- 231): the N terminus is highly flexible. Proc Natl Acad Sci U S A *94*, 13452-13457.

Doty, R.L. (2008). The olfactory vector hypothesis of neurodegenerative disease: is it viable? Ann Neurol *63*,

7-15.

Drayton, D.L., Ying, X., Lee, J., Lesslauer, W., and Ruddle, N.H. (2003). Ectopic LT alpha beta directs lymphoid organ neogenesis with concomitant expression of peripheral node addressin and a HEV-restricted sulfotransferase. J Exp Med *197*, 1153-1163.

Eagon, P.K., Porter, L.E., Francavilla, A., DiLeo, A., and Van Thiel, D.H. (1985). Estrogen and androgen receptors in liver: their role in liver disease and regeneration. Semin Liver Dis *5*, 59-69.

El-Serag, H.B. (2002). Hepatocellular carcinoma: an epidemiologic view. J Clin Gastroenterol *35*, S72-78.

El-Serag, H.B., Lau, M., Eschbach, K., Davila, J., and Goodwin, J. (2007). Epidemiology of hepatocellular carcinoma in Hispanics in the United States. Arch Intern Med *167*, 1983-1989.

El-Serag, H.B., and Rudolph, K.L. (2007). Hepatocellular carcinoma: epidemiology and molecular carcinogenesis. Gastroenterology *132*, 2557-2576.

Ember, J.A., and Hugli, T.E. (1997). Complement factors and their receptors. Immunopharmacology *38*, 3-15.

Erdman, S.E., Rao, V.P., Poutahidis, T., Ihrig, M.M., Ge, Z., Feng, Y., Tomczak, M., Rogers, A.B., Horwitz, B.H., and Fox, J.G. (2003). CD4(+)CD25(+) regulatory lymphocytes require interleukin 10 to interrupt colon carcinogenesis in mice. Cancer Res *63*, 6042-6050.

Fargion, S., Fracanzani, A.L., Piperno, A., Braga, M., D'Alba, R., Ronchi, G., and Fiorelli, G. (1994). Prognostic factors for hepatocellular carcinoma in genetic hemochromatosis. Hepatology *20*, 1426-1431.

Fattori, E., Cappelletti, M., Costa, P., Sellitto, C., Cantoni, L., Carelli, M., Faggioni, R., Fantuzzi, G., Ghezzi, P., and Poli, V. (1994). Defective inflammatory response in interleukin 6-deficient mice. J Exp Med *180*, 1243-1250.

Fausto, N. (1999). Lessons from genetically engineered animal models. V. Knocking out genes to study liver regeneration: present and future. Am J Physiol *277*, G917-921.

Fausto, N. (2000). Liver regeneration. J Hepatol *32*, 19-31.

Feldstein, A.E., Canbay, A., Angulo, P., Taniai, M., Burgart, L.J., Lindor, K.D., and Gores, G.J. (2003a). Hepatocyte apoptosis and fas expression are prominent features of human nonalcoholic steatohepatitis. Gastroenterology *125*, 437-443.

Feldstein, A.E., Canbay, A., Guicciardi, M.E., Higuchi, H., Bronk, S.F., and Gores, G.J. (2003b). Diet associated hepatic steatosis sensitizes to Fas mediated liver injury in mice. J Hepatol *39*, 978-983.

Fernandez Rodriguez, C.M., and Alonso Lopez, S. (2009). [Treatment optimization in chronic hepatitis C virus infection.]. Gastroenterol Hepatol.

Ferrara, N., and Davis-Smyth, T. (1997). The biology of vascular endothelial growth factor. Endocr Rev *18*, 4-25.

Fischer, M., Rülicke, T., Raeber, A., Sailer, A., Moser, M., Oesch, B., Brandner, S., Aguzzi, A., and Weissmann, C. (1996). Prion protein (PrP) with amino-proximal deletions restoring susceptibility of PrP knockout mice to scrapie. EMBO J *15*, 1255-1264.

Ford, M.J., Burton, L.J., Li, H., Graham, C.H., Frobert, Y., Grassi, J., Hall, S.M., and Morris, R.J. (2002a). A marked disparity between the expression of prion protein and its message by neurones of the CNS. Neuroscience *111*, 533-551.

Ford, M.J., Burton, L.J., Morris, R.J., and Hall, S.M. (2002b). Selective expression of prion protein in peripheral tissues of the adult mouse. Neuroscience *113*, 177-192.

Forster, R., Mattis, A.E., Kremmer, E., Wolf, E., Brem, G., and Lipp, M. (1996). A putative chemokine receptor, BLR1, directs B cell migration to defined lymphoid organs and specific anatomic compartments of the spleen. Cell *87*, 1037-1047.

Foster, J., McKenzie, C., Parnham, D., Drummond, D., Chong, A., Goldman, W., and Hunter, N. (2006a). Lateral transmission of natural scrapie to scrapie-free New Zealand sheep placed in an endemically infected UK flock. Vet Rec *159*, 633-634.

Foster, J., McKenzie, C., Parnham, D., Drummond, D., Goldmann, W., Stevenson, E., and Hunter, N. (2006b). Derivation of a scrapie-free sheep flock from the progeny of a flock affected by scrapie. Vet Rec *159*, 42-45.

Foster, J.D., Parnham, D.W., Hunter, N., and Bruce, M. (2001). Distribution of the prion protein in sheep terminally affected with BSE following experimental oral transmission. J Gen Virol *82*, 2319-2326.

Fotin-Mleczek, M., Henkler, F., Samel, D., Reichwein, M., Hausser, A., Parmryd, I., Scheurich, P., Schmid, J.A., and Wajant, H. (2002). Apoptotic crosstalk of TNF receptors: TNF-R2-induces depletion of TRAF2 and IAP proteins and accelerates TNF-R1-dependent activation of caspase-8. J Cell Sci *115*, 2757-2770.

Fournier, J., Escaig-Haye, F., Billette de Villemeur, T., Robain, O., Lasmezas, C.I., Deslys, J.P., Dormont, D., and Brown, P. (1998). Distribution and submicroscopic immunogold localization of cellular prion protein (PrPc) in extracerebral tissues. Cell Tissue Res *292*, 77-84.

Fox, E.S., Thomas, P., and Broitman, S.A. (1987). Comparative studies of endotoxin uptake by isolated rat Kupffer and peritoneal cells. Infect Immun *55*, 2962-2966.

Fraser, H., and Dickinson, A.G. (1978). Studies of the lymphoreticular system in the pathogenesis of scrapie: the role of spleen and thymus. J Comp Pathol *88*, 563-573.

Fraser, R., Dobbs, B.R., and Rogers, G.W. (1995). Lipoproteins and the liver sieve: the role of the fenestrated sinusoidal endothelium in lipoprotein metabolism, atherosclerosis, and cirrhosis. Hepatology *21*, 863-874.

Fu, Y.-X., Huang, G., Wang, Y., and Chaplin, D.D. (1998a). B Lymphocytes induce the formation of follicular dendritic cell clusters in a Lymphotoxin a-dependent fashion. J Exp Med *187*, 1009-1018.

Fu, Y.X., Huang, G., Wang, Y., and Chaplin, D.D. (1998b). B lymphocytes induce the formation of follicular dendritic cell clusters in a lymphotoxin alpha-dependent fashion. J Exp Med *187*, 1009-1018.

Fujiwara, D., Hino, K., Yamaguchi, Y., Kubo, Y., Yamashita, S., Uchida, K., Konishi, T., Nakamura, H., Korenaga, M., Okuda, M*., et al.* (2004). Type I interferon receptor and response to interferon therapy in chronic hepatitis C patients: a prospective study. J Viral Hepat *11*, 136-140.

Fukuyama, S., Hiroi, T., Yokota, Y., Rennert, P.D., Yanagita, M., Kinoshita, N., Terawaki, S., Shikina, T., Yamamoto, M., Kurono, Y*., et al.* (2002). Initiation of NALT organogenesis is independent of the IL-7R, LTbetaR, and NIK signaling pathways but requires the Id2 gene and CD3(-)CD4(+)CD45(+) cells. Immunity *17*, 31-40.

Futterer, A., Mink, K., Luz, A., Kosco-Vilbois, M.H., and Pfeffer, K. (1998). The lymphotoxin beta receptor controls organogenesis and affinity maturation in peripheral lymphoid tissues. Immunity *9*, 59-70.

Gajdusek, D.C. (1977). Unconventional viruses and the origin and disappearance of kuru. Science *197*, 943-960.

Gajdusek, D.C. (1988). Transmissible and non-transmissible amyloidoses: autocatalytic post-translational conversion of host precursor proteins to beta-pleated sheet configurations. J Neuroimmunol *20*, 95-110.

Gajdusek, D.C., Gibbs, C.J., and Alpers, M. (1966). Experimental transmission of a Kuru-like syndrome to chimpanzees. Nature *209*, 794-796.

Gajdusek, D.C., and Zigas, V. (1957). Degenerative disease of the central nervous system in New Guinea - the endemic occurrence of 'kuru' in the native population. N Engl J Med *257*, 974-978.

Geller, S.A., Nichols, W.S., Kim, S., Tolmachoff, T., Lee, S., Dycaico, M.J., Felts, K., and Sorge, J.A. (1994). Hepatocarcinogenesis is the sequel to hepatitis in Z#2 alpha 1-antitrypsin transgenic mice: histopathological and DNA ploidy studies. Hepatology *19*, 389-397.

Georgsson, G., Sigurdarson, S., and Brown, P. (2006). Infectious agent of sheep scrapie may persist in the environment for at least 16 years. J Gen Virol *87*, 3737-3740.

Getchell, M.L., and Getchell, T.V. (1992). Fine structural aspects of secretion and extrinsic innervation in the olfactory mucosa. Microsc Res Tech *23*, 111-127.

Ghebranious, N., and Sell, S. (1998). Hepatitis B injury, male gender, aflatoxin, and p53 expression each contribute to hepatocarcinogenesis in transgenic mice. Hepatology *27*, 383-391.

Giles, F.J. (2001). The vascular endothelial growth factor (VEGF) signaling pathway: a therapeutic target in patients with hematologic malignancies. Oncologist *6 Suppl 5*, 32-39.

Glatzel, M., Abela, E., Maissen, M., and Aguzzi, A. (2003). Extraneural pathologic prion protein in sporadic Creutzfeldt-Jakob disease. N Engl J Med *349*, 1812-1820.

Glatzel, M., Heppner, F.L., Albers, K.M., and Aguzzi, A. (2001). Sympathetic innervation of lymphoreticular organs is rate limiting for prion neuroinvasion. Neuron *31*, 25-34.

Glatzel, M., Rogivue, C., Ghani, A., Streffer, J.R., Amsler, L., and Aguzzi, A. (2002). Incidence of Creutzfeldt-Jakob disease in Switzerland. Lancet *360*, 139-141.

Glover, J.R., Kowal, A.S., Schirmer, E.C., Patino, M.M., Liu, J.J., and Lindquist, S. (1997). Self-seeded fibers formed by Sup35, the protein determinant of [PSI+], a heritable prion-like factor of S. cerevisiae. Cell *89*, 811-819.

Goldenring, J.R., and Nomura, S. (2006). Differentiation of the gastric mucosa III. Animal models of oxyntic atrophy and metaplasia. Am J Physiol Gastrointest Liver Physiol *291*, G999-1004.

Goldfarb, L.G., Brown, P., McCombie, W.R., Goldgaber, D., Swergold, G.D., Wills, P.R., Cervenakova, L., Baron, H., Gibbs, C.J., Jr., and Gajdusek, D.C. (1991). Transmissible familial Creutzfeldt-Jakob disease associated with five, seven, and eight extra octapeptide coding repeats in the PRNP gene. Proc Natl Acad Sci U S A *88*, 10926-10930.

Goldfarb, L.G., Petersen, R.B., Tabaton, M., Brown, P., LeBlanc, A.C., Montagna, P., Cortelli, P., Julien, J., Vital, C., Pendelbury, W.W*., et al.* (1992). Fatal familial insomnia and familial Creutzfeldt-Jakob disease: disease phenotype determined by a DNA polymorphism. Science *258*, 806-808.

Goldmann, W., Hunter, N., Smith, G., Foster, J., and Hope, J. (1994). PrP genotype and agent effects in scrapie: change in allelic interaction with different isolates of agent in shee. JGenVirol

Journal of General Virology *75*, 989-995.

Gomes, L.I., Esteves, G.H., Carvalho, A.F., Cristo, E.B., Hirata, R., Jr., Martins, W.K., Marques, S.M., Camargo, L.P., Brentani, H., Pelosof, A*., et al.* (2005). Expression profile of malignant and nonmalignant lesions of esophagus and stomach: differential activity of functional modules related to inflammation and lipid metabolism. Cancer Res *65*, 7127-7136.

Gommerman, J.L., and Browning, J.L. (2003). Lymphotoxin/light, lymphoid microenvironments and autoimmune disease. Nat Rev Immunol *3*, 642-655.

Gommerman, J.L., Mackay, F., Donskoy, E., Meier, W., Martin, P., and Browning, J.L. (2002). Manipulation of lymphoid microenvironments in nonhuman primates by an inhibitor of the lymphotoxin pathway. J Clin Invest *110*, 1359-1369.

Grell, M., Becke, F.M., Wajant, H., Mannel, D.N., and Scheurich, P. (1998a). TNF receptor type 2 mediates thymocyte proliferation independently of TNF receptor type 1. Eur J Immunol *28*, 257-263.

Grell, M., Wajant, H., Zimmermann, G., and Scheurich, P. (1998b). The type 1 receptor (CD120a) is the high-affinity receptor for soluble tumor necrosis factor. Proc Natl Acad Sci U S A *95*, 570-575.

Grell, M., Zimmermann, G., Gottfried, E., Chen, C.M., Grunwald, U., Huang, D.C., Wu Lee, Y.H., Durkop, H., Engelmann, H., Scheurich, P*., et al.* (1999). Induction of cell death by tumour necrosis factor (TNF) receptor 2, CD40 and CD30: a role for TNF-R1 activation by endogenous membrane-anchored TNF. Embo J *18*, 3034-3043.

Greten, F.R., Eckmann, L., Greten, T.F., Park, J.M., Li, Z.W., Egan, L.J., Kagnoff, M.F., and Karin, M. (2004). IKKbeta links inflammation and tumorigenesis in a mouse model of colitis-associated cancer. Cell *118*, 285-296.

Greten, F.R., and Karin, M. (2004). The IKK/NF-kappaB activation pathway-a target for prevention and treatment of cancer. Cancer Lett *206*, 193-199.

Griffith, J.S. (1967). Self-replication and scrapie. Nature *215*, 1043-1044.

Gupta, R.A., and Dubois, R.N. (2001). Colorectal cancer prevention and treatment by inhibition of

cyclooxygenase-2. Nat Rev Cancer *1*, 11-21.

Hadlow, W.J., Kennedy, R.C., and Race, R.E. (1982). Natural infection of Suffolk sheep with scrapie virus. J Infect Dis *146*, 657-664.

Hamada, H., Hiroi, T., Nishiyama, Y., Takahashi, H., Masunaga, Y., Hachimura, S., Kaminogawa, S., Takahashi-Iwanaga, H., Iwanaga, T., Kiyono, H.*, et al.* (2002). Identification of multiple isolated lymphoid follicles on the antimesenteric wall of the mouse small intestine. J Immunol *168*, 57-64.

Hamir, A.N., Kunkle, R.A., Richt, J.A., Miller, J.M., and Greenlee, J.J. (2008). Experimental transmission of US scrapie agent by nasal, peritoneal, and conjunctival routes to genetically susceptible sheep. Vet Pathol *45*, 7-11.

Hanahan, D., and Weinberg, R.A. (2000). The hallmarks of cancer. Cell *100*, 57-70.

Harder, A., Jendroska, K., Kreuz, F., Wirth, T., Schafranka, C., Karnatz, N., Theallier-Janko, A., Dreier, J., Lohan, K., Emmerich, D.*, et al.* (1999). Novel twelve-generation kindred of fatal familial insomnia from germany representing the entire spectrum of disease expression. Am J Med Genet *87*, 311-316.

Hartsough, G., and Burger, D. (1965). Encephalopathy of mink. I. Epizootiologic and clinical observations. J Infect Dis *115*, 387-392.

Haybaeck, J., Zeller, N., Wolf, M.J., Weber, A., Wagner, U., Kurrer, M.O., Bremer, J., Iezzi, G., Graf, R., Clavien, P.A.*, et al.* (2009). A lymphotoxin-driven pathway to hepatocellular carcinoma. Cancer Cell *16*, 295-308.

Head, M.W., Yull, H.M., Ritchie, D.L., Bishop, M.T., and Ironside, J.W. (2009). Pathological investigation of the first blood donor and recipient pair linked by transfusion-associated variant CJD transmission. Neuropathol Appl Neurobiol.

Heikenwalder, M., Julius, C., and Aguzzi, A. (2007). Prions and peripheral nerves: A deadly rendezvous. J Neurosci Res.

Heikenwalder, M., Kurrer, M.O., Margalith, I., Kranich, J., Zeller, N., Haybaeck, J., Polymenidou, M., Matter, M., Bremer, J., Jackson, W.S.*, et al.* (2008). Lymphotoxin-dependent prion replication in inflammatory stromal cells of granulomas. Immunity *29*, 998-1008.

Heikenwalder, M., Zeller, N., Seeger, H., Prinz, M., Klohn, P.C., Schwarz, P., Ruddle, N.H., Weissmann, C., and Aguzzi, A. (2005). Chronic lymphocytic inflammation specifies the organ tropism of prions. Science *307*, 1107-1110.

Heindryckx, F., Colle, I., and Van Vlierberghe, H. (2009). Experimental mouse models for hepatocellular carcinoma research. Int J Exp Pathol *90*, 367-386.

Heinrich, P.C., Behrmann, I., Haan, S., Hermanns, H.M., Muller-Newen, G., and Schaper, F. (2003). Principles of interleukin (IL)-6-type cytokine signalling and its regulation. Biochem J *374*, 1-20.

Heppner, F.L., Christ, A.D., Klein, M.A., Prinz, M., Fried, M., Kraehenbuhl, J.P., and Aguzzi, A. (2001). Transepithelial prion transport by M cells. Nat Med *7*, 976-977.

Herms, J., Tings, T., Gall, S., Madlung, A., Giese, A., Siebert, H., Schurmann, P., Windl, O., Brose, N., and Kretzschmar, H. (1999). Evidence of presynaptic location and function of the prion protein. J Neurosci *19*, 8866-8875.

Herzog, C., Sales, N., Etchegaray, N., Charbonnier, A., Freire, S., Dormont, D., Deslys, J.P., and Lasmezas, C.I. (2004). Tissue distribution of bovine spongiform encephalopathy agent in primates after intravenous or oral infection. Lancet *363*, 422-428.

Hill, A.F., Butterworth, R.J., Joiner, S., Jackson, G., Rossor, M.N., Thomas, D.J., Frosh, A., Tolley, N., Bell, J.E., Spencer, M.*, et al.* (1999). Investigation of variant Creutzfeldt-Jakob disease and other human prion diseases with tonsil biopsy samples. Lancet *353*, 183-189.

Hill, A.F., Desbruslais, M., Joiner, S., Sidle, K.C., Gowland, I., Collinge, J., Doey, L.J., and Lantos, P. (1997a). The same prion strain causes vCJD and BSE. Nature *389*, 448-450, 526.

Hill, A.F., Zeidler, M., Ironside, J., and Collinge, J. (1997b). Diagnosis of new variant Creutzfeldt-Jakob

disease by tonsil biopsy. Lancet *349*, 99.

Hilton, D.A., Fathers, E., Edwards, P., Ironside, J.W., and Zajicek, J. (1998). Prion immunoreactivity in appendix before clinical onset of variant Creutzfeldt-Jakob disease Lancet *352*, 703-704.

Hodgson, H.J. (1987). Fibrolamellar cancer of the liver. J Hepatol *5*, 241-247.

Hommel, J.D., Sears, R.M., Georgescu, D., Simmons, D.L., and DiLeone, R.J. (2003). Local gene knockdown in the brain using viral-mediated RNA interference. Nat Med *9*, 1539-1544.

Houston, F., Foster, J.D., Chong, A., Hunter, N., and Bostock, C.J. (2000). Transmission of BSE by blood transfusion in sheep. Lancet *356*, 999-1000.

Hsiao, K., Baker, H.F., Crow, T.J., Poulter, M., Owen, F., Terwilliger, J.D., Westaway, D., Ott, J., and Prusiner, S.B. (1989). Linkage of a prion protein missense variant to Gerstmann-Sträussler syndrome. Nature *338*, 342-345.

Hsiao, K.K., Cass, C., Schellenberg, G.D., Bird, T., Devine Gage, E., Wisniewski, H., and Prusiner, S.B. (1991). A prion protein variant in a family with the telencephalic form of Gerstmann-Straussler-Scheinker syndrome. Neurology *41*, 681-684.

Hu, K.Q., Yu, C.H., and Vierling, J.M. (1992). Up-regulation of intercellular adhesion molecule 1 transcription by hepatitis B virus X protein. Proc Natl Acad Sci U S A *89*, 11441-11445.

Huang, H., Fujii, H., Sankila, A., Mahler-Araujo, B.M., Matsuda, M., Cathomas, G., and Ohgaki, H. (1999). Beta-catenin mutations are frequent in human hepatocellular carcinomas associated with hepatitis C virus infection. Am J Pathol *155*, 1795-1801.

Huang, Q., Liu, D., Majewski, P., Schulte, L.C., Korn, J.M., Young, R.A., Lander, E.S., and Hacohen, N. (2001). The plasticity of dendritic cell responses to pathogens and their components. Science *294*, 870-875.

Hutter, G., Heppner, F.L., and Aguzzi, A. (2003). No Superoxide Dismutase Activity of Cellular Prion Protein in vivo. Biol Chem *384*, 1279-1285.

Itzkowitz, S.H., and Yio, X. (2004). Inflammation and cancer IV. Colorectal cancer in inflammatory bowel disease: the role of inflammation. Am J Physiol Gastrointest Liver Physiol *287*, G7-17.

Jackson, G.S., Hosszu, L.L., Power, A., Hill, A.F., Kenney, J., Saibil, H., Craven, C.J., Waltho, J.P., Clarke, A.R., and Collinge, J. (1999). Reversible conversion of monomeric human prion protein between native and fibrilogenic conformations. Science *283*, 1935-1937.

Jaeschke, H., Farhood, A., and Smith, C.W. (1994). Contribution of complement-stimulated hepatic macrophages and neutrophils to endotoxin-induced liver injury in rats. Hepatology *19*, 973-979.

Jakob, A. (1921). Über eigenartige Erkrankungen des Zentralnervensystems mit bemerkenswertem anatomischem Befunde. (Spastische Pseudosklerose-Encephalomyelopathie mit disseminierten Degenerationsherden). Z ges Neurol Psychiatr *64*, 147-228.

Jarrett, J.T., and Lansbury, P.T., Jr. (1993). Seeding "one-dimensional crystallization" of amyloid: a pathogenic mechanism in Alzheimer's disease and scrapie? Cell *73*, 1055-1058.

Jeng, Y.M., Wu, M.Z., Mao, T.L., Chang, M.H., and Hsu, H.C. (2000). Somatic mutations of beta-catenin play a crucial role in the tumorigenesis of sporadic hepatoblastoma. Cancer Lett *152*, 45-51.

Johnson, C.J., Phillips, K.E., Schramm, P.T., McKenzie, D., Aiken, J.M., and Pedersen, J.A. (2006). Prions adhere to soil minerals and remain infectious. PLoS Pathog *2*, e32.

Johnson, R.T. (2005). Prion diseases. Lancet Neurol *4*, 635-642.

Johnson, R.T., and Gibbs, C.J., Jr. (1998). Creutzfeldt-Jakob disease and related transmissible spongiform encephalopathies. N Engl J Med *339*, 1994-2004.

Jones, M., Peden, A.H., Yull, H., Wight, D., Bishop, M.T., Prowse, C.V., Turner, M.L., Ironside, J.W., MacGregor, I.R., and Head, M.W. (2009). Human platelets as a substrate source for the in vitro amplification of the abnormal prion protein (PrP) associated with variant Creutzfeldt-Jakob disease. Transfusion *49*, 376-384.

Kaeser, P.S., Klein, M.A., Schwarz, P., and Aguzzi, A. (2001). Efficient lymphoreticular prion propagation requires PrP(c) in stromal and hematopoietic cells. J Virol *75*, 7097-7106.

Kaldor, J.M., and Bosch, F.X. (1990). Multistage theory of carcinogenesis: the epidemiological evidence for liver cancer. Bull Cancer *77*, 515-519.

Kaneko, K., Ball, H.L., Wille, H., Zhang, H., Groth, D., Torchia, M., Tremblay, P., Safar, J., Prusiner, S.B., DeArmond, S.J.*, et al.* (2000). A synthetic peptide initiates Gerstmann-Straussler-Scheinker (GSS) disease in transgenic mice. J Mol Biol *295*, 997-1007.

Karin, M. (1999). How NF-kappaB is activated: the role of the IkappaB kinase (IKK) complex. Oncogene *18*, 6867-6874.

Karin, M. (2006). Nuclear factor-kappaB in cancer development and progression. Nature *441*, 431-436.

Karin, M., Cao, Y., Greten, F.R., and Li, Z.W. (2002). NF-kappaB in cancer: from innocent bystander to major culprit. Nat Rev Cancer *2*, 301-310.

Karin, M., and Greten, F.R. (2005). NF-kappaB: linking inflammation and immunity to cancer development and progression. Nat Rev Immunol *5*, 749-759.

Karin, M., and Lin, A. (2002). NF-kappaB at the crossroads of life and death. Nat Immunol *3*, 221-227.

Kato, T., Jr., Delhase, M., Hoffmann, A., and Karin, M. (2003). CK2 Is a C-Terminal IkappaB Kinase Responsible for NF-kappaB Activation during the UV Response. Mol Cell *12*, 829-839.

Katze, M.G., He, Y., and Gale, M., Jr. (2002). Viruses and interferon: a fight for supremacy. Nat Rev Immunol *2*, 675-687.

Kawase, T., Ohki, R., Shibata, T., Tsutsumi, S., Kamimura, N., Inazawa, J., Ohta, T., Ichikawa, H., Aburatani, H., Tashiro, F.*, et al.* (2009). PH domain-only protein PHLDA3 is a p53-regulated repressor of Akt. Cell *136*, 535-550.

Kern, P.M., Keilholz, L., Kalden, J.R., and Herrmann, M. (2001). Apoptotic UV-irradiated lymphocytes undergo protease mediated shedding of L-selectin in vitro. Transfus Apher Sci *24*, 99-101.

Khoruts, A., Stahnke, L., McClain, C.J., Logan, G., and Allen, J.I. (1991). Circulating tumor necrosis factor, interleukin-1 and interleukin-6 concentrations in chronic alcoholic patients. Hepatology *13*, 267-276.

Kimberlin, R.H., and Marsh, R.F. (1975). Comparison of scrapie and transmissible mink encephalopathy in hamsters. I. Biochemical studies of brain during development of disease. J Infect Dis *131*, 97-103.

Kimberlin, R.H., and Walker, C.A. (1989). Pathogenesis of scrapie in mice after intragastric infection. Virus Res *12*, 213-220.

Kincaid, A.E., and Bartz, J.C. (2007). The nasal cavity is a route for prion infection in hamsters. J Virol *81*, 4482-4491.

King, C.Y., and Diaz-Avalos, R. (2004). Protein-only transmission of three yeast prion strains. Nature *428*, 319-323.

Knight, B., Yeoh, G.C., Husk, K.L., Ly, T., Abraham, L.J., Yu, C., Rhim, J.A., and Fausto, N. (2000). Impaired preneoplastic changes and liver tumor formation in tumor necrosis factor receptor type 1 knockout mice. J Exp Med *192*, 1809-1818.

Koike, K., Moriya, K., Iino, S., Yotsuyanagi, H., Endo, Y., Miyamura, T., and Kurokawa, K. (1994). High-level expression of hepatitis B virus HBx gene and hepatocarcinogenesis in transgenic mice. Hepatology *19*, 810-819.

Kojiro, M., Nakahara, H., Sugihara, S., Murakami, T., Nakashima, T., and Kawasaki, H. (1984). Hepatocellular carcinoma with intra-atrial tumor growth. A clinicopathologic study of 18 autopsy cases. Arch Pathol Lab Med *108*, 989-992.

Koni, P.A., Sacca, R., Lawton, P., Browning, J.L., Ruddle, N.H., and Flavell, R.A. (1997). Distinct roles in lymphoid organogenesis for lymphotoxins alpha and beta revealed in lymphotoxin beta-deficient mice. Immunity *6*, 491-500.

Konold, T., Moore, S.J., Bellworthy, S.J., and Simmons, H.A. (2008). Evidence of scrapie transmission via milk. BMC Vet Res *4*, 14.

Koo, J.S., Seong, J.K., Park, C., Yu, D.Y., Oh, B.K., Oh, S.H., and Park, Y.N. (2005). Large liver cell dysplasia in hepatitis B virus x transgenic mouse liver and human chronic hepatitis B virus-infected liver. Intervirology *48*, 16-22.

Kopf, M., Baumann, H., Freer, G., Freudenberg, M., Lamers, M., Kishimoto, T., Zinkernagel, R., Bluethmann, H., and Kohler, G. (1994). Impaired immune and acute-phase responses in interleukin-6-deficient mice. Nature *368*, 339-342.

Kovacs, T., Beck, J.A., Papp, M.I., Lantos, P.L., Aranyi, Z., Szirmai, I.G., Farsang, M., Stuke, A., Csillik, A., and Collinge, J. (2007). Familial prion disease in a Hungarian family with a novel 144-base pair insertion in the prion protein gene. J Neurol Neurosurg Psychiatry *78*, 321-323.

Kratz, A., Campos-Neto, A., Hanson, M.S., and Ruddle, N.H. (1996). Chronic inflammation caused by lymphotoxin is lymphoid neogenesis. J Exp Med *183*, 1461-1472.

Kulkarni, A.P., Getchell, T.V., and Getchell, M.L. (1994). Neuronal nitric oxide synthase is localized in extrinsic nerves regulating perireceptor processes in the chemosensory nasal mucosae of rats and humans. J Comp Neurol *345*, 125-138.

Kunz, B., Sandmeier, E., and Christen, P. (1999). Neurotoxicity of prion peptide 106-126 not confirmed FEBS Lett *458*, 65-68.

Kurschner, C., Morgan, J.I., Yehiely, F., Bamborough, P., Da Costa, M., Perry, B.J., Thinakaran, G., Cohen, F.E., Carlson, G.A., and Prusiner, S.B. (1995). The cellular prion protein (PrP) selectively binds to Bcl-2 in the yeast two-hybrid system: identification of candidate proteins binding to prion protein. Brain Res Mol Brain Res *30*, 165-168.

Kuwahara, C., Takeuchi, A.M., Nishimura, T., Haraguchi, K., Kubosaki, A., Matsumoto, Y., Saeki, K., Matsumoto, Y., Yokoyama, T., Itohara, S.*, et al.* (1999). Prions prevent neuronal cell-line death. Nature *400*, 225-226.

Ladogana, A., Puopolo, M., Croes, E.A., Budka, H., Jarius, C., Collins, S., Klug, G.M., Sutcliffe, T., Giulivi, A., Alperovitch, A.*, et al.* (2005). Mortality from Creutzfeldt-Jakob disease and related disorders in Europe, Australia, and Canada. Neurology *64*, 1586-1591.

Lasmezas, C.I., Deslys, J.P., Demaimay, R., Adjou, K.T., Lamoury, F., Dormont, D., Robain, O., Ironside, J., and Hauw, J.J. (1996). BSE transmission to macaques. Nature *381*, 743-744.

Laurent-Puig, P., Legoix, P., Bluteau, O., Belghiti, J., Franco, D., Binot, F., Monges, G., Thomas, G., Bioulac-Sage, P., and Zucman-Rossi, J. (2001). Genetic alterations associated with hepatocellular carcinomas define distinct pathways of hepatocarcinogenesis. Gastroenterology *120*, 1763-1773.

Laurent-Puig, P., and Zucman-Rossi, J. (2006). Genetics of hepatocellular tumors. Oncogene *25*, 3778-3786.

Lee, F.I. (1966). Cirrhosis and hepatoma in alcoholics. Gut *7*, 77-85.

Lee, H.S., Brown, P., Cervenakova, L., Garruto, R.M., Alpers, M.P., Gajdusek, D.C., and Goldfarb, L.G. (2001). Increased susceptibility to Kuru of carriers of the PRNP 129 methionine/methionine genotype. J Infect Dis *183*, 192-196.

Lee, I.Y., Westaway, D., Smit, A.F., Wang, K., Seto, J., Chen, L., Acharya, C., Ankener, M., Baskin, D., Cooper, C.*, et al.* (1998). Complete genomic sequence and analysis of the prion protein gene region from three mammalian species. Genome Res *8*, 1022-1037.

Lee, J.S., Heo, J., Libbrecht, L., Chu, I.S., Kaposi-Novak, P., Calvisi, D.F., Mikaelyan, A., Roberts, L.R., Demetris, A.J., Sun, Z.*, et al.* (2006). A novel prognostic subtype of human hepatocellular carcinoma derived from hepatic progenitor cells. Nat Med *12*, 410-416.

Lee, S.H., Park, S.G., Lim, S.O., and Jung, G. (2005). The hepatitis B virus X protein up-regulates lymphotoxin alpha expression in hepatocytes. Biochim Biophys Acta *1741*, 75-84.

Lee, T.H., Finegold, M.J., Shen, R.F., DeMayo, J.L., Woo, S.L., and Butel, J.S. (1990). Hepatitis B virus

transactivator X protein is not tumorigenic in transgenic mice. J Virol *64*, 5939-5947.

Lehmann, S., and Harris, D.A. (1996). Mutant and infectious prion proteins display common biochemical properties in cultured cells. J Biol Chem *271*, 1633-1637.

Ligios, C., Sigurdson, C.J., Santucciu, C., Carcassola, G., Manco, G., Basagni, M., Maestrale, C., Cancedda, M.G., Madau, L., and Aguzzi, A. (2005). PrPSc in mammary glands of sheep affected by scrapie and mastitis. Nat Med *11*, 1137-1138.

Lo, J.C., Wang, Y., Tumanov, A.V., Bamji, M., Yao, Z., Reardon, C.A., Getz, G.S., and Fu, Y.X. (2007). Lymphotoxin beta receptor-dependent control of lipid homeostasis. Science *316*, 285-288.

Locksley, R.M., Killeen, N., and Lenardo, M.J. (2001). The TNF and TNF receptor superfamilies: integrating mammalian biology. Cell *104*, 487-501.

Loeppen, S., Schneider, D., Gaunitz, F., Gebhardt, R., Kurek, R., Buchmann, A., and Schwarz, M. (2002). Overexpression of glutamine synthetase is associated with beta-catenin-mutations in mouse liver tumors during promotion of hepatocarcinogenesis by phenobarbital. Cancer Res *62*, 5685-5688.

Loffreda, S., Rai, R., Yang, S.Q., Lin, H.Z., and Diehl, A.M. (1997). Bile ducts and portal and central veins are major producers of tumor necrosis factor alpha in regenerating rat liver. Gastroenterology *112*, 2089-2098.

Lowes, K.N., Croager, E.J., Abraham, L.J., Olynyk, J.K., and Yeoh, G.C. (2003). Upregulation of lymphotoxin beta expression in liver progenitor (oval) cells in chronic hepatitis C. Gut *52*, 1327-1332.

Lu, H., Ouyang, W., and Huang, C. (2006). Inflammation, a key event in cancer development. Mol Cancer Res *4*, 221-233.

Luedde, T., Beraza, N., Kotsikoris, V., van Loo, G., Nenci, A., De Vos, R., Roskams, T., Trautwein, C., and Pasparakis, M. (2007). Deletion of NEMO/IKKgamma in liver parenchymal cells causes steatohepatitis and hepatocellular carcinoma. Cancer Cell *11*, 119-132.

Ma, J., Wollmann, R., and Lindquist, S. (2002). Neurotoxicity and Neurodegeneration When PrP Accumulates in the Cytosol. Science *298:*, 1781-1785.

Mabbott, N.A., and MacPherson, G.G. (2006). Prions and their lethal journey to the brain. Nat Rev Microbiol *4*, 201-211.

Mabbott, N.A., Young, J., McConnell, I., and Bruce, M.E. (2003). Follicular dendritic cell dedifferentiation by treatment with an inhibitor of the lymphotoxin pathway dramatically reduces scrapie susceptibility. Journal of Virology *77*, 6845-6854.

Mackay, F., Majeau, G.R., Lawton, P., Hochman, P.S., and Browning, J.L. (1997). Lymphotoxin but not tumor necrosis factor functions to maintain splenic architecture and humoral responsiveness in adult mice. Eur J Immunol *27*, 2033-2042.

MacSween, R.N. (1982). Alcohol and cancer. Br Med Bull *38*, 31-33.

MacSween, R.N., and Anthony, R.S. (1982). Immune mechanisms in alcoholic liver disease. J Clin Lab Immunol *9*, 1-5.

Maeda, S., Kamata, H., Luo, J.L., Leffert, H., and Karin, M. (2005). IKKbeta couples hepatocyte death to cytokine-driven compensatory proliferation that promotes chemical hepatocarcinogenesis. Cell *121*, 977-990.

Maeda, S., and Omata, M. (2008). Inflammation and cancer: role of nuclear factor-kappaB activation. Cancer Sci *99*, 836-842.

Maignien, T., Lasme Zas, C.I., Beringue, V., Dormont, D., and Deslys, J.P. (1999). Pathogenesis of the oral route of infection of mice with scrapie and bovine spongiform encephalopathy agents [In Process Citation]. J Gen Virol *80*, 3035-3042.

Malatjalian, D.A., and Graham, C.H. (1982). Liver adenoma with granulomas. The appearance of granulomas in oral contraceptive-related hepatocellular adenoma and in the surrounding nontumorous liver. Arch Pathol Lab Med *106*, 244-246.

Malhi, H., Gores, G.J., and Lemasters, J.J. (2006). Apoptosis and necrosis in the liver: a tale of two deaths?

Hepatology *43*, S31-44.

Mallucci, G.R., Ratte, S., Asante, E.A., Linehan, J., Gowland, I., Jefferys, J.G., and Collinge, J. (2002). Post-natal knockout of prion protein alters hippocampal CA1 properties, but does not result in neurodegeneration. Embo J *21*, 202-210.

Manson, J.C., Clarke, A.R., Hooper, M.L., Aitchison, L., McConnell, I., and Hope, J. (1994). 129/Ola mice carrying a null mutation in PrP that abolishes mRNA production are developmentally normal. Mol Neurobiol *8*, 121-127.

Manson, J.C., Jamieson, E., Baybutt, H., Tuzi, N.L., Barron, R., McConnell, I., Somerville, R., Ironside, J., Will, R., Sy, M.S.*, et al.* (1999). A single amino acid alteration (101L) introduced into murine PrP dramatically alters incubation time of transmissible spongiform encephalopathy. EMBO J *18*, 6855-6864.

Manuelidis, L., Sklaviadis, T., Akowitz, A., and Fritch, W. (1995). Viral particles are required for infection in neurodegenerative Creutzfeldt-Jakob disease. Proc Natl Acad Sci U S A *92*, 5124-5128.

Marrero, J.A., and Lok, A.S. (2004). Newer markers for hepatocellular carcinoma. Gastroenterology *127*, S113-119.

Marrero, J.A., Romano, P.R., Nikolaeva, O., Steel, L., Mehta, A., Fimmel, C.J., Comunale, M.A., D'Amelio, A., Lok, A.S., and Block, T.M. (2005). GP73, a resident Golgi glycoprotein, is a novel serum marker for hepatocellular carcinoma. J Hepatol *43*, 1007-1012.

Marsh, R.F., Bessen, R.A., Lehmann, S., and Hartsough, G.R. (1991). Epidemiological and experimental studies on a new incident of transmissible mink encephalopathy. J Gen Virol *72 (Pt 3)*, 589-594.

Marsh, R.F., Kincaid, A.E., Bessen, R.A., and Bartz, J.C. (2005). Interspecies transmission of chronic wasting disease prions to squirrel monkeys (Saimiri sciureus). J Virol *79*, 13794-13796.

Mathiason, C.K., Powers, J.G., Dahmes, S.J., Osborn, D.A., Miller, K.V., Warren, R.J., Mason, G.L., Hays, S.A., Hayes-Klug, J., Seelig, D.M.*, et al.* (2006). Infectious prions in the saliva and blood of deer with chronic wasting disease. Science *314*, 133-136.

Matthews, W.B., and Will, R.G. (1981). Creutzfeldt-Jakob disease in a lifelong vegetarian [letter]. Lancet *2*, 937.

McClary, H., Koch, R., Chisari, F.V., and Guidotti, L.G. (2000). Relative sensitivity of hepatitis B virus and other hepatotropic viruses to the antiviral effects of cytokines. J Virol *74*, 2255-2264.

McKinley, M.P., Bolton, D.C., and Prusiner, S.B. (1983). A protease-resistant protein is a structural component of the scrapie prion. Cell *35*, 57-62.

McLean, C.A., Storey, E., Gardner, R.J., Tannenberg, A.E., Cervenakova, L., and Brown, P. (1997). The D178N (cis-129M) "fatal familial insomnia" mutation associated with diverse clinicopathologic phenotypes in an Australian kindred. Neurology *49*, 552-558.

Mead, S., Stumpf, M.P., Whitfield, J., Beck, J.A., Poulter, M., Campbell, T., Uphill, J.B., Goldstein, D., Alpers, M., Fisher, E.M.*, et al.* (2003a). Balancing selection at the prion protein gene consistent with prehistoric kurulike epidemics. Science *300*, 640-643.

Mead, S., Stumpf, M.P., Whitfield, J., Beck, J.A., Poulter, M., Campbell, T., Uphill, J.B., Goldstein, D., Alpers, M., Fisher, E.M.*, et al.* (2003b). Balancing selection at the prion protein gene consistent with prehistoric kurulike epidemics. Science *300*, 640-643.

Mebius, R.E., Rennert, P., and Weissman, I.L. (1997). Developing lymph nodes collect CD4+CD3- LTbeta+ cells that can differentiate to APC, NK cells, and follicular cells but not T or B cells. Immunity *7*, 493-504.

Medina, J., Caveda, L., Sanz-Cameno, P., Arroyo, A.G., Martin-Vilchez, S., Majano, P.L., Garcia-Buey, L., Sanchez-Madrid, F., and Moreno-Otero, R. (2003). Hepatocyte growth factor activates endothelial proangiogenic mechanisms relevant in chronic hepatitis C-associated neoangiogenesis. J Hepatol *38*, 660-667.

Medori, R., Tritschler, H.J., LeBlanc, A., Villare, F., Manetto, V., Chen, H.Y., Xue, R., Leal, S., Montagna, P., Cortelli, P.*, et al.* (1992). Fatal familial insomnia, a prion disease with a mutation at codon 178 of the prion protein gene N Engl J Med *326*, 444-449.

Meireles, S.I., Cristo, E.B., Carvalho, A.F., Hirata, R., Jr., Pelosof, A., Gomes, L.I., Martins, W.K., Begnami, M.D., Zitron, C., Montagnini, A.L.*, et al.* (2004). Molecular classifiers for gastric cancer and nonmalignant diseases of the gastric mucosa. Cancer Res *64*, 1255-1265.

Melia, W.M., Johnson, P.J., Neuberger, J., Zaman, S., Portmann, B.C., and Williams, R. (1984). Hepatocellular carcinoma in primary biliary cirrhosis: detection by alpha-fetoprotein estimation. Gastroenterology *87*, 660-663.

Mellen, J.S., Xia, V.W., Hashemzadeh, M., Imagawa, D., Jamal, M., Hoefs, J., and Hu, K.Q. (2009). The Clinical Presentation of Chronic Hepatitis B Virus (HBV) Infection in Asian Americans: A Single Center Retrospective Study. J Clin Gastroenterol.

Michalopoulos, G.K., and DeFrances, M.C. (1997). Liver regeneration. Science *276*, 60-66.

Miele, G., Alejo Blanco, A.R., Baybutt, H., Horvat, S., Manson, J., and Clinton, M. (2003). Embryonic activation and developmental expression of the murine prion protein gene. Gene Expr *11*, 1-12.

Miller, M.W., and Williams, E.S. (2003). Prion disease: horizontal prion transmission in mule deer. Nature *425*, 35-36.

Miller, M.W., Williams, E.S., Hobbs, N.T., and Wolfe, L.L. (2004). Environmental sources of prion transmission in mule deer. Emerg Infect Dis *10*, 1003-1006.

Monga, S.P., Pediaditakis, P., Mule, K., Stolz, D.B., and Michalopoulos, G.K. (2001). Changes in WNT/beta-catenin pathway during regulated growth in rat liver regeneration. Hepatology *33*, 1098-1109.

Mouillet-Richard, S., Ermonval, M., Chebassier, C., Laplanche, J.L., Lehmann, S., Launay, J.M., and Kellermann, O. (2000). Signal transduction through prion protein. Science *289*, 1925-1928.

Mould, D.L., Dawson, A.M., and Rennie, J.C. (1970). Very early replication of scrapie in lymphocytic tissue. Nature *228*, 779-780.

Mulcahy, E.R., Bartz, J.C., Kincaid, A.E., and Bessen, R.A. (2004). Prion infection of skeletal muscle cells and papillae in the tongue. J Virol *78*, 6792-6798.

Muller, U., Jongeneel, C.V., Nedospasov, S.A., Lindahl, K.F., and Steinmetz, M. (1987). Tumour necrosis factor and lymphotoxin genes map close to H-2D in the mouse major histocompatibility complex. Nature *325*, 265-267.

Murdoch, G.H., Sklaviadis, T., Manuelidis, E.E., and Manuelidis, L. (1990). Potential retroviral RNAs in Creutzfeldt-Jakob disease. J Virol *64*, 1477-1486.

Murray, K., Peters, J., Stellitano, L., Winstone, A., Verity, C., and Will, R. (2009). Is there evidence of vertical transmission of variant CJD? J Neurol Neurosurg Psychiatry.

Naas, T., Ghorbani, M., Alvarez-Maya, I., Lapner, M., Kothary, R., De Repentigny, Y., Gomes, S., Babiuk, L., Giulivi, A., Soare, C.*, et al.* (2005). Characterization of liver histopathology in a transgenic mouse model expressing genotype 1a hepatitis C virus core and envelope proteins 1 and 2. J Gen Virol *86*, 2185-2196.

Nakamoto, Y., Guidotti, L.G., Kuhlen, C.V., Fowler, P., and Chisari, F.V. (1998). Immune pathogenesis of hepatocellular carcinoma. J Exp Med *188*, 341-350.

Nakanuma, Y., and Ohta, G. (1985). Is mallory body formation a preneoplastic change? A study of 181 cases of liver bearing hepatocellular carcinoma and 82 cases of cirrhosis. Cancer *55*, 2400-2404.

Nakanuma, Y., and Ohta, G. (1986). Expression of Mallory bodies in hepatocellular carcinoma in man and its significance. Cancer *57*, 81-86.

Nakanuma, Y., Terada, T., Doishita, K., and Miwa, A. (1990). Hepatocellular carcinoma in primary biliary cirrhosis: an autopsy study. Hepatology *11*, 1010-1016.

Naslavsky, N., Stein, R., Yanai, A., Friedlander, G., and Taraboulos, A. (1997). Characterization of detergent-insoluble complexes containing the cellular prion protein and its scrapie isoform. J Biol Chem *272*, 6324-6331.

Neumann-Haefelin, C., McKiernan, S., Ward, S., Viazov, S., Spangenberg, H.C., Killinger, T., Baumert, T.F.,

Nazarova, N., Sheridan, I., Pybus, O.*, et al.* (2006). Dominant influence of an HLA-B27 restricted CD8+ T cell response in mediating HCV clearance and evolution. Hepatology *43*, 563-572.

Ng, T.I., Mo, H., Pilot-Matias, T., He, Y., Koev, G., Krishnan, P., Mondal, R., Pithawalla, R., He, W., Dekhtyar, T.*, et al.* (2007). Identification of host genes involved in hepatitis C virus replication by small interfering RNA technology. Hepatology *45*, 1413-1421.

Ngo, V.N., Korner, H., Gunn, M.D., Schmidt, K.N., Riminton, D.S., Cooper, M.D., Browning, J.L., Sedgwick, J.D., and Cyster, J.G. (1999). Lymphotoxin alpha/beta and tumor necrosis factor are required for stromal cell expression of homing chemokines in B and T cell areas of the spleen. J Exp Med *189*, 403-412.

Nicholes, K., Guillet, S., Tomlinson, E., Hillan, K., Wright, B., Frantz, G.D., Pham, T.A., Dillard-Telm, L., Tsai, S.P., Stephan, J.P.*, et al.* (2002). A mouse model of hepatocellular carcinoma: ectopic expression of fibroblast growth factor 19 in skeletal muscle of transgenic mice. Am J Pathol *160*, 2295-2307.

Niederau, C., Erhardt, A., Haussinger, D., and Strohmeyer, G. (1999). Haemochromatosis and the liver. J Hepatol *30 Suppl 1*, 6-11.

Nilsson, J.A., and Cleveland, J.L. (2003). Myc pathways provoking cell suicide and cancer. Oncogene *22*, 9007-9021.

Nunziante, M., Gilch, S., and Schatzl, H.M. (2003). Essential role of the prion protein N terminus in subcellular trafficking and half-life of cellular prion protein. J Biol Chem *278*, 3726-3734.

Odermatt, B., Eppler, M., Leist, T.P., Hengartner, H., and Zinkernagel, R.M. (1991). Virus-triggered acquired immunodeficiency by cytotoxic T-cell-dependent destruction of antigen-presenting cells and lymph follicle structure. Proc Natl Acad Sci U S A *88*, 8252-8256.

Oh, J.D., Karam, S.M., and Gordon, J.I. (2005). Intracellular Helicobacter pylori in gastric epithelial progenitors. Proc Natl Acad Sci U S A *102*, 5186-5191.

Ohnishi, S., Murakami, T., Moriyama, T., Mitamura, K., and Imawari, M. (1986). Androgen and estrogen receptors in hepatocellular carcinoma and in the surrounding noncancerous liver tissue. Hepatology *6*, 440-443.

Okuda, K. (1992). Hepatocellular carcinoma: recent progress. Hepatology *15*, 948-963.

Okuda, K. (1997). Hepatocellular carcinoma: clinicopathological aspects. J Gastroenterol Hepatol *12*, S314-318.

Omata, M. (1987). Current perspectives on hepatocellular carcinoma in Oriental and African countries compared to developed western countries. Dig Dis *5*, 97-115.

Paitel, E., Fahraeus, R., and Checler, F. (2003). Cellular Prion Protein Sensitizes Neurons to Apoptotic Stimuli through Mdm2-regulated and p53-dependent Caspase 3-like Activation. J Biol Chem *278*, 10061-10066.

Palmer, M.S., Dryden, A.J., Hughes, J.T., and Collinge, J. (1991). Homozygous prion protein genotype predisposes to sporadic Creutzfeldt-Jakob disease. Nature *352*, 340-342.

Pan, K.M., Baldwin, M., Nguyen, J., Gasset, M., Serban, A., Groth, D., Mehlhorn, I., Huang, Z., Fletterick, R.J., Cohen, F.E.*, et al.* (1993). Conversion of alpha-helices into beta-sheets features in the formation of the scrapie prion proteins. ProcNatlAcadSciUSA.

Park, C.H., Ishinaka, M., Takada, A., Kida, H., Kimura, T., Ochiai, K., and Umemura, T. (2002). The invasion routes of neurovirulent A/Hong Kong/483/97 (H5N1) influenza virus into the central nervous system after respiratory infection in mice. Arch Virol *147*, 1425-1436.

Park, Y.N., Kim, Y.B., Yang, K.M., and Park, C. (2000). Increased expression of vascular endothelial growth factor and angiogenesis in the early stage of multistep hepatocarcinogenesis. Arch Pathol Lab Med *124*, 1061-1065.

Pattison, I.H., and Millson, G.C. (1961). Experimental transmission of scrapie to goats and sheep by the oral route. J Comp Pathol *71*, 171-176.

Pattison, J.H. (1965). Experiments with scrapie with special reference to the nature of the agent and the pathology of the disease (Washington D.C., US. Governement Printing Office).

Pennisi, E. (1998). How a growth control path takes a wrong turn to cancer. Science *281*, 1438-1439, 1441.

Perez-Carreras, M., Del Hoyo, P., Martin, M.A., Rubio, J.C., Martin, A., Castellano, G., Colina, F., Arenas, J., and Solis-Herruzo, J.A. (2003). Defective hepatic mitochondrial respiratory chain in patients with nonalcoholic steatohepatitis. Hepatology *38*, 999-1007.

Perrier, V., Kaneko, K., Safar, J., Vergara, J., Tremblay, P., DeArmond, S.J., Cohen, F.E., Prusiner, S.B., and Wallace, A.C. (2002). Dominant-negative inhibition of prion replication in transgenic mice. Proc Natl Acad Sci U S A *99*, 13079-13084.

Picarella, D.E., Kratz, A., Li, C.B., Ruddle, N.H., and Flavell, R.A. (1992). Insulitis in transgenic mice expressing tumor necrosis factor beta (lymphotoxin) in the pancreas. Proc Natl Acad Sci U S A *89*, 10036-10040.

Pietschmann, T., Kaul, A., Koutsoudakis, G., Shavinskaya, A., Kallis, S., Steinmann, E., Abid, K., Negro, F., Dreux, M., Cosset, F.L.*, et al.* (2006). Construction and characterization of infectious intragenotypic and intergenotypic hepatitis C virus chimeras. Proc Natl Acad Sci U S A *103*, 7408-7413.

Pikarsky, E., Porat, R.M., Stein, I., Abramovitch, R., Amit, S., Kasem, S., Gutkovich-Pyest, E., Urieli-Shoval, S., Galun, E., and Ben-Neriah, Y. (2004). NF-kappaB functions as a tumour promoter in inflammation-associated cancer. Nature *431*, 461-466.

Pinna, A.D., Iwatsuki, S., Lee, R.G., Todo, S., Madariaga, J.R., Marsh, J.W., Casavilla, A., Dvorchik, I., Fung, J.J., and Starzl, T.E. (1997). Treatment of fibrolamellar hepatoma with subtotal hepatectomy or transplantation. Hepatology *26*, 877-883.

Polakis, P. (2000). Wnt signaling and cancer. Genes Dev *14*, 1837-1851.

Pomerantz, J.L., and Baltimore, D. (2002). Two pathways to NF-kappaB. Mol Cell *10*, 693-695.

Porter, L.E., Van Thiel, D.H., and Eagon, P.K. (1987). Estrogens and progestins as tumor inducers. Semin Liver Dis *7*, 24-31.

Poser, C.M. (2002). Notes on the history of the prion diseases. Part I. Clin Neurol Neurosurg *104*, 1-9.

Prinz, M., Heikenwalder, M., Junt, T., Schwarz, P., Glatzel, M., Heppner, F.L., Fu, Y.X., Lipp, M., and Aguzzi, A. (2003a). Positioning of follicular dendritic cells within the spleen controls prion neuroinvasion. Nature *425*, 957-962.

Prinz, M., Huber, G., Macpherson, A.J., Heppner, F.L., Glatzel, M., Eugster, H.P., Wagner, N., and Aguzzi, A. (2003b). Oral Prion Infection Requires Normal Numbers of Peyer's Patches but Not of Enteric Lymphocytes. Am J Pathol *162*, 1103-1111.

Prinz, M., Montrasio, F., Furukawa, H., van der Haar, M.E., Schwarz, P., Rülicke, T., Giger, O., Häusler, K.G., Glatzel, M., and Aguzzi, A. (2004). Intrinsic resistance of oligodendrocytes to prion infection. J Neurosci *24*, 5974-5981.

Priola, S.A., and Chesebro, B. (1995). A single hamster PrP amino acid blocks conversion to protease-resistant PrP in scrapie-infected mouse neuroblastoma cells. J Virol *69*, 7754-7758.

Prusiner, S.B. (1982). Novel proteinaceous infectious particles cause scrapie. Science *216*, 136-144.

Prusiner, S.B. (1991). Molecular biology of prion diseases. Science *252*, 1515-1522.

Prusiner, S.B., Groth, D.F., Bolton, D.C., Kent, S.B., and Hood, L.E. (1984). Purification and structural studies of a major scrapie prion protein. Cell *38*, 127-134.

Prusiner, S.B., Scott, M., Foster, D., Pan, K.M., Groth, D., Mirenda, C., Torchia, M., Yang, S.L., Serban, D., Carlson, G.A.*, et al.* (1990). Transgenetic studies implicate interactions between homologous PrP isoforms in scrapie prion replication. Cell *63*, 673-686.

Puglielli, M.T., Browning, J.L., Brewer, A.W., Schreiber, R.D., Shieh, W.J., Altman, J.D., Oldstone, M.B., Zaki, S.R., and Ahmed, R. (1999). Reversal of virus-induced systemic shock and respiratory failure by blockade of the lymphotoxin pathway. Nat Med *5*, 1370-1374.

Radovanovic, I., Braun, N., Giger, O.T., Mertz, K., Miele, G., Prinz, M., Navarro, B., and Aguzzi, A. (2005).

Truncated prion protein and Doppel are myelinotoxic in the absence of oligodendrocytic PrPC. J Neurosci *25*, 4879-4888.

Raeber, A.J., Klein, M.A., Frigg, R., Flechsig, E., Aguzzi, A., and Weissmann, C. (1999). PrP-dependent association of prions with splenic but not circulating lymphocytes of scrapie-infected mice. EMBO J *18*, 2702-2706.

Rennert, P.D., Browning, J.L., Mebius, R., Mackay, F., and Hochman, P.S. (1996). Surface lymphotoxin alpha/beta complex is required for the development of peripheral lymphoid organs. J Exp Med *184*, 1999-2006.

Reuber, M., Al-Din, A.S., Baborie, A., and Chakrabarty, A. (2001). New variant Creutzfeldt-Jakob disease presenting with loss of taste and smell. J Neurol Neurosurg Psychiatry *71*, 412-413.

Rieger, R., Edenhofer, F., Lasmezas, C.I., and Weiss, S. (1997). The human 37-kDa laminin receptor precursor interacts with the prion protein in eukaryotic cells. Nat Med *3*, 1383-1388.

Riek, R., Hornemann, S., Wider, G., Billeter, M., Glockshuber, R., and Wüthrich, K. (1996). NMR structure of the mouse prion protein domain PrP(121-231). Nature *382*, 180-182.

Riek, R., Hornemann, S., Wider, G., Glockshuber, R., and Wüthrich, K. (1997). NMR characterization of the full-length recombinant murine prion protein, mPrP(23-231). FEBS Lett *413*, 282-288.

Riek, R., Wider, G., Billeter, M., Hornemann, S., Glockshuber, R., and Wüthrich, K. (1998). Prion protein NMR structure and familial human spongiform encephalopathies. Proc Natl Acad Sci U S A *95*, 11667-11672.

Riesner, D., Kellings, K., Wiese, U., Wulfert, M., Mirenda, C., and Prusiner, S.B. (1993). Prions and nucleic acids: search for "residual" nucleic acids and screening for mutations in the PrP-gene. Dev Biol Stand *80*, 173-181.

Ringe, B., Wittekind, C., Weimann, A., Tusch, G., and Pichlmayr, R. (1992). Results of hepatic resection and transplantation for fibrolamellar carcinoma. Surg Gynecol Obstet *175*, 299-305.

Rivera-Milla, E., Stuermer, C.A., and Malaga-Trillo, E. (2003). An evolutionary basis for scrapie disease: identification of a fish prion mRNA. Trends Genet *19*, 72-75.

Roberts, S.K., Ludwig, J., and Larusso, N.F. (1997). The pathobiology of biliary epithelia. Gastroenterology *112*, 269-279.

Rollins, B.J., Morrison, E.D., and Stiles, C.D. (1988). Cloning and expression of JE, a gene inducible by platelet-derived growth factor and whose product has cytokine-like properties. Proc Natl Acad Sci U S A *85*, 3738-3742.

Ross, R.K., Yuan, J.M., Yu, M.C., Wogan, G.N., Qian, G.S., Tu, J.T., Groopman, J.D., Gao, Y.T., and Henderson, B.E. (1992). Urinary aflatoxin biomarkers and risk of hepatocellular carcinoma. Lancet *339*, 943-946.

Rubel, L.R., Ishak, K.G., Benjamin, S.B., and Knuff, T.E. (1982). alpha 1-Antitrypsin deficiency and hepatocellular carcinoma. Association with cirrhosis, copper storage, and Mallory bodies. Arch Pathol Lab Med *106*, 678-681.

Ruddell, R.G., Knight, B., Tirnitz-Parker, J.E., Akhurst, B., Summerville, L., Subramaniam, V.N., Olynyk, J.K., and Ramm, G.A. (2009). Lymphotoxin-beta receptor signaling regulates hepatic stellate cell function and wound healing in a murine model of chronic liver injury. Hepatology *49*, 227-239.

Ruddle, N.H., and Waksman, B.H. (1967). Cytotoxic effect of lymphocyte-antigen interaction in delayed hypersensitivity. Science *157*, 1060-1062.

Russelakis-Carneiro, M., Betmouni, S., and Perry, V.H. (1999). Inflammatory response and retinal ganglion cell degeneration following intraocular injection of ME7 [In Process Citation]. Neuropathol Appl Neurobiol *25*, 196-206.

Saborio, G.P., Soto, C., Kascsak, R.J., Levy, E., Kascsak, R., Harris, D.A., and Frangione, B. (1999). Cell-lysate conversion of prion protein into its protease-resistant isoform suggests the participation of a cellular chaperone. Biochem Biophys Res Commun *258*, 470-475.

Safar, J., Wille, H., Itri, V., Groth, D., Serban, H., Torchia, M., Cohen, F.E., and Prusiner, S.B. (1998). Eight prion strains have PrP(Sc) molecules with different conformations. Nat Med *4*, 1157-1165.

Safar, J.G., Kellings, K., Serban, A., Groth, D., Cleaver, J.E., Prusiner, S.B., and Riesner, D. (2005). Search for a prion-specific nucleic acid. J Virol *79*, 10796-10806.

Saito, H., Kanamori, Y., Takemori, T., Nariuchi, H., Kubota, E., Takahashi-Iwanaga, H., Iwanaga, T., and Ishikawa, H. (1998). Generation of intestinal T cells from progenitors residing in gut cryptopatches. Science *280*, 275-278.

Sakamoto, M. (2009). Early HCC: diagnosis and molecular markers. J Gastroenterol *44 Suppl 19*, 108-111.

Salman, M.D. (2003). Chronic wasting disease in deer and elk: scientific facts and findings. J Vet Med Sci *65*, 761-768.

Santuccione, A., Sytnyk, V., Leshchyns'ka, I., and Schachner, M. (2005). Prion protein recruits its neuronal receptor NCAM to lipid rafts to activate p59fyn and to enhance neurite outgrowth. J Cell Biol *169*, 341-354.

Sawcer, S.J., Yuill, G.M., Esmonde, T.F., Estibeiro, P., Ironside, J.W., Bell, J.E., and Will, R.G. (1993). Creutzfeldt-Jakob disease in an individual occupationally exposed to BSE. Lancet *341*, 642.

Sbriccoli, M., Cardone, F., Valanzano, A., Lu, M., Graziano, S., De Pascalis, A., Ingrosso, L., Zanusso, G., Monaco, S., Bentivoglio, M*., et al.* (2009). Neuroinvasion of the 263K scrapie strain after intranasal administration occurs through olfactory-unrelated pathways. Acta Neuropathol *117*, 175-184.

Schieferdecker, H.L., Schlaf, G., Jungermann, K., and Gotze, O. (2001). Functions of anaphylatoxin C5a in rat liver: direct and indirect actions on nonparenchymal and parenchymal cells. Int Immunopharmacol *1*, 469-481.

Schlitt, H.J., Neipp, M., Weimann, A., Oldhafer, K.J., Schmoll, E., Boeker, K., Nashan, B., Kubicka, S., Maschek, H., Tusch, G*., et al.* (1999). Recurrence patterns of hepatocellular and fibrolamellar carcinoma after liver transplantation. J Clin Oncol *17*, 324-331.

Schmitt-Ulms, G., Legname, G., Baldwin, M.A., Ball, H.L., Bradon, N., Bosque, P.J., Crossin, K.L., Edelman, G.M., DeArmond, S.J., Cohen, F.E*., et al.* (2001). Binding of neural cell adhesion molecules (N-CAMs) to the cellular prion protein. J Mol Biol *314*, 1209-1225.

Schmitz, M.L., and Baeuerle, P.A. (1991). The p65 subunit is responsible for the strong transcription activating potential of NF-kappa B. Embo J *10*, 3805-3817.

Schnur, J., Olah, J., Szepesi, A., Nagy, P., and Thorgeirsson, S.S. (2004). Thioacetamide-induced hepatic fibrosis in transforming growth factor beta-1 transgenic mice. Eur J Gastroenterol Hepatol *16*, 127-133.

Scott, J.R., Foster, J.D., and Fraser, H. (1993). Conjunctival instillation of scrapie in mice can produce disease. Vet Microbiol *34*, 305-309.

Seeger, H., Heikenwalder, M., Zeller, N., Kranich, J., Schwarz, P., Gaspert, A., Seifert, B., Miele, G., and Aguzzi, A. (2005). Coincident scrapie infection and nephritis lead to urinary prion excretion. Science *310*, 324-326.

Seidel, B., Thomzig, A., Buschmann, A., Groschup, M.H., Peters, R., Beekes, M., and Terytze, K. (2007). Scrapie Agent (Strain 263K) can transmit disease via the oral route after persistence in soil over years. PLoS ONE *2*, e435.

Sekhon, S.S., Tan, X., Micsenyi, A., Bowen, W.C., and Monga, S.P. (2004). Fibroblast growth factor enriches the embryonic liver cultures for hepatic progenitors. Am J Pathol *164*, 2229-2240.

Sell, S., Hunt, J.M., Dunsford, H.A., and Chisari, F.V. (1991). Synergy between hepatitis B virus expression and chemical hepatocarcinogens in transgenic mice. Cancer Res *51*, 1278-1285.

Selzner, N., Selzner, M., Odermatt, B., Tian, Y., Van Rooijen, N., and Clavien, P.A. (2003). ICAM-1 triggers liver regeneration through leukocyte recruitment and Kupffer cell-dependent release of TNF-alpha/IL-6 in mice. Gastroenterology *124*, 692-700.

Sen, R., and Baltimore, D. (1986a). Inducibility of kappa immunoglobulin enhancer-binding protein Nf-kappa B by a posttranslational mechanism. Cell *47*, 921-928.

Sen, R., and Baltimore, D. (1986b). Multiple nuclear factors interact with the immunoglobulin enhancer sequences. Cell *46*, 705-716.

Senftleben, U., Cao, Y., Xiao, G., Greten, F.R., Krahn, G., Bonizzi, G., Chen, Y., Hu, Y., Fong, A., Sun, S.C., *et al.* (2001). Activation by IKKalpha of a second, evolutionary conserved, NF-kappa B signaling pathway. Science *293*, 1495-1499.

Shakhov, A.N., Lyakhov, I.G., Tumanov, A.V., Rubtsov, A.V., Drutskaya, L.N., Marino, M.W., and Nedospasov, S.A. (2000). Gene profiling approach in the analysis of lymphotoxin and TNF deficiencies. J Leukoc Biol *68*, 151-157.

Shaw, I.C. (1995a). BSE and farmworkers. Lancet *346*, 1365.

Shaw, I.C. (1995b). BSE and farmworkers [letter]. Lancet *346*, 1365.

Shimoda, K., Mori, M., Shibuta, K., Banner, B.F., and Barnard, G.F. (1999). Vascular endothelial growth factor/vascular permeability factor mRNA expression in patients with chronic hepatitis C and hepatocellular carcinoma. Int J Oncol *14*, 353-359.

Shmerling, D., Hegyi, I., Fischer, M., Blattler, T., Brandner, S., Gotz, J., Rulicke, T., Flechsig, E., Cozzio, A., von Mering, C., *et al.* (1998). Expression of amino-terminally truncated PrP in the mouse leading to ataxia and specific cerebellar lesions. Cell *93*, 203-214.

Sigurdson, C.J., and Miller, M.W. (2003). Other animal prion diseases. Br Med Bull *66*, 199-212.

Sigurdson, C.J., Williams, E.S., Miller, M.W., Spraker, T.R., O'Rourke, K.I., and Hoover, E.A. (1999). Oral transmission and early lymphoid tropism of chronic wasting disease PrPres in mule deer fawns (Odocoileus hemionus). J Gen Virol *80*, 2757-2764.

Simonetti, R.G., Camma, C., Fiorello, F., Politi, F., D'Amico, G., and Pagliaro, L. (1991). Hepatocellular carcinoma. A worldwide problem and the major risk factors. Dig Dis Sci *36*, 962-972.

Simonic, T., Duga, S., Strumbo, B., Asselta, R., Ceciliani, F., and Ronchi, S. (2000). cDNA cloning of turtle prion protein. FEBS Lett *469*, 33-38.

Siso, S., Gonzalez, L., Jeffrey, M., Martin, S., Chianini, F., and Steele, P. (2006a). Prion protein in kidneys of scrapie-infected sheep. Vet Rec *159*, 327-328.

Siso, S., Hanzlicek, D., Fluehmann, G., Kathmann, I., Tomek, A., Papa, V., and Vandevelde, M. (2006b). Neurodegenerative diseases in domestic animals: a comparative review. Vet J *171*, 20-38.

Smith, P.E., Zeidler, M., Ironside, J.W., Estibeiro, P., and Moss, T.H. (1995). Creutzfeldt-Jakob disease in a dairy farmer. Lancet *346*, 898.

Solforosi, L., Criado, J.R., McGavern, D.B., Wirz, S., Sanchez-Alavez, M., Sugama, S., DeGiorgio, L.A., Volpe, B.T., Wiseman, E., Abalos, G., *et al.* (2004). Cross-linking cellular prion protein triggers neuronal apoptosis in vivo. Science *303*, 1514-1516.

Soto, C., and Castilla, J. (2004). The controversial protein-only hypothesis of prion propagation. Nat Med *10 Suppl*, S63-67.

Spencer, M.D., Knight, R.S., and Will, R.G. (2002). First hundred cases of variant Creutzfeldt-Jakob disease: retrospective case note review of early psychiatric and neurological features. BMJ (Clinical research ed *324*, 1479-1482.

Spraker, T.R., O'Rourke, K.I., Balachandran, A., Zink, R.R., Cummings, B.A., Miller, M.W., and Powers, B.E. (2002a). Validation of monoclonal antibody F99/97.6.1 for immunohistochemical staining of brain and tonsil in mule deer (Odocoileus hemionus) with chronic wasting disease. J Vet Diagn Invest *14*, 3-7.

Spraker, T.R., Zink, R.R., Cummings, B.A., Wild, M.A., Miller, M.W., and O'Rourke, K.I. (2002b). Comparison of histological lesions and immunohistochemical staining of proteinase-resistant prion protein in a naturally occurring spongiform encephalopathy of free-ranging mule deer (Odocoileus hemionus) with those of chronic wasting disease of captive mule deer. Vet Pathol *39*, 110-119.

Stahl, N., Borchelt, D.R., Hsiao, K., and Prusiner, S.B. (1987). Scrapie prion protein contains a phosphatidylinositol glycolipid. Cell *51*, 229-240.

Steele, A.D., Emsley, J.G., Ozdinler, P.H., Lindquist, S., and Macklis, J.D. (2006). Prion protein (PrPc) positively regulates neural precursor proliferation during developmental and adult mammalian neurogenesis. Proc Natl Acad Sci U S A *103*, 3416-3421.

Streetz, K., Leifeld, L., Grundmann, D., Ramakers, J., Eckert, K., Spengler, U., Brenner, D., Manns, M., and Trautwein, C. (2000). Tumor necrosis factor alpha in the pathogenesis of human and murine fulminant hepatic failure. Gastroenterology *119*, 446-460.

Strumbo, B., Ronchi, S., Bolis, L.C., and Simonic, T. (2001). Molecular cloning of the cDNA coding for Xenopus laevis prion protein. FEBS Letters *508*, 170-174.

Su, G.L. (2002). Lipopolysaccharides in liver injury: molecular mechanisms of Kupffer cell activation. Am J Physiol Gastrointest Liver Physiol *283*, G256-265.

Subrata, L.S., Lowes, K.N., Olynyk, J.K., Yeoh, G.C., Quail, E.A., and Abraham, L.J. (2005). Hepatic expression of the tumor necrosis factor family member lymphotoxin-beta is regulated by interleukin (IL)-6 and IL-1beta: transcriptional control mechanisms in oval cells and hepatoma cell lines. Liver Int *25*, 633-646.

Tabaton, M., Monaco, S., Cordone, M.P., Colucci, M., Giaccone, G., Tagliavini, F., and Zanusso, G. (2004). Prion deposition in olfactory biopsy of sporadic Creutzfeldt-Jakob disease. Ann Neurol *55*, 294-296.

Tai, D.I., Tsai, S.L., Chen, Y.M., Chuang, Y.L., Peng, C.Y., Sheen, I.S., Yeh, C.T., Chang, K.S., Huang, S.N., Kuo, G.C.*, et al.* (2000). Activation of nuclear factor kappaB in hepatitis C virus infection: implications for pathogenesis and hepatocarcinogenesis. Hepatology *31*, 656-664.

Takaoka, A., and Yanai, H. (2006). Interferon signalling network in innate defence. Cell Microbiol *8*, 907-922.

Takenaka, K., Yamamoto, K., Taketomi, A., Itasaka, H., Adachi, E., Shirabe, K., Nishizaki, T., Yanaga, K., and Sugimachi, K. (1995). A comparison of the surgical results in patients with hepatitis B versus hepatitis C-related hepatocellular carcinoma. Hepatology *22*, 20-24.

Talarmin, H., Rescan, C., Cariou, S., Glaise, D., Zanninelli, G., Bilodeau, M., Loyer, P., Guguen-Guillouzo, C., and Baffet, G. (1999). The mitogen-activated protein kinase kinase/extracellular signal-regulated kinase cascade activation is a key signalling pathway involved in the regulation of G(1) phase progression in proliferating hepatocytes. Mol Cell Biol *19*, 6003-6011.

Tanaka, M., Chien, P., Naber, N., Cooke, R., and Weissman, J.S. (2004). Conformational variations in an infectious protein determine prion strain differences. Nature *428*, 323-328.

Taraboulos, A., Jendroska, K., Serban, D., Yang, S.L., DeArmond, S.J., and Prusiner, S.B. (1992). Regional mapping of prion proteins in brain. Proc Natl Acad Sci U S A *89*, 7620-7624.

Tateishi, J., Brown, P., Kitamoto, T., Hoque, Z.M., Roos, R., Wollman, R., Cervenakova, L., and Gajdusek, D.C. (1995). First experimental transmission of fatal familial insomnia. Nature *376*, 434-435.

Taub, R. (2003). Hepatoprotection via the IL-6/Stat3 pathway. J Clin Invest *112*, 978-980.

Terada, T., Hoso, M., and Nakanuma, Y. (1989). Development of cavernous vasculatures in livers with hepatocellular carcinoma. An autopsy study. Liver *9*, 172-178.

Terradillos, O., Billet, O., Renard, C.A., Levy, R., Molina, T., Briand, P., and Buendia, M.A. (1997). The hepatitis B virus X gene potentiates c-myc-induced liver oncogenesis in transgenic mice. Oncogene *14*, 395-404.

Terry, L.A., Marsh, S., Ryder, S.J., Hawkins, S.A., Wells, G.A., and Spencer, Y.I. (2003). Detection of disease-specific PrP in the distal ileum of cattle exposed orally to the agent of bovine spongiform encephalopathy. Vet Rec *152*, 387-392.

Thieringer, F., Maass, T., Czochra, P., Klopcic, B., Conrad, I., Friebe, D., Schirmacher, P., Lohse, A.W., Blessing, M., Galle, P.R.*, et al.* (2008). Spontaneous hepatic fibrosis in transgenic mice overexpressing PDGF-A. Gene *423*, 23-28.

Thorgeirsson, S.S., and Santoni-Rugiu, E. (1996). Transgenic mouse models in carcinogenesis: interaction of c-myc with transforming growth factor alpha and hepatocyte growth factor in hepatocarcinogenesis. Br J Clin Pharmacol *42*, 43-52.

Tobler, I., Deboer, T., and Fischer, M. (1997). Sleep and sleep regulation in normal and prion protein-deficient mice. J Neurosci *17*, 1869-1879.

Tobler, I., Gaus, S.E., Deboer, T., Achermann, P., Fischer, M., Rülicke, T., Moser, M., Oesch, B., McBride, P.A., and Manson, J.C. (1996). Altered circadian activity rhythms and sleep in mice devoid of prion protein. Nature *380*, 639-642.

Tonjes, R.R., Lohler, J., O'Sullivan, J.F., Kay, G.F., Schmidt, G.H., Dalemans, W., Pavirani, A., and Paul, D. (1995). Autocrine mitogen IgEGF cooperates with c-myc or with the Hcs locus during hepatocarcinogenesis in transgenic mice. Oncogene *10*, 765-768.

Toyosaka, A., Okamoto, E., Mitsunobu, M., Oriyama, T., Nakao, N., and Miura, K. (1996). Pathologic and radiographic studies of intrahepatic metastasis in hepatocellular carcinoma; the role of efferent vessels. HPB Surg *10*, 97-103; discussion 103-104.

Trautwein, C., Rakemann, T., Brenner, D.A., Streetz, K., Licato, L., Manns, M.P., and Tiegs, G. (1998). Concanavalin A-induced liver cell damage: activation of intracellular pathways triggered by tumor necrosis factor in mice. Gastroenterology *114*, 1035-1045.

Tumanov, A.V., Koroleva, E.P., Christiansen, P.A., Khan, M.A., Ruddy, M.J., Burnette, B., Papa, S., Franzoso, G., Nedospasov, S., Fu, Y.X.*, et al.* (2008). T Cell-Derived Lymphotoxin Regulates Liver Regeneration. Gastroenterology.

Tumanov, A.V., Kuprash, D.V., and Nedospasov, S.A. (2003). The role of lymphotoxin in development and maintenance of secondary lymphoid tissues. Cytokine Growth Factor Rev *14*, 275-288.

Vainer, G.W., Pikarsky, E., and Ben-Neriah, Y. (2008). Contradictory functions of NF-kappaB in liver physiology and cancer. Cancer Lett.

Vascellari, M., Nonno, R., Mutinelli, F., Bigolaro, M., Di Bari, M.A., Melchiotti, E., Marcon, S., D'Agostino, C., Vaccari, G., Conte, M.*, et al.* (2007). PrPSc in Salivary Glands of Scrapie-Affected Sheep. J Virol *81*, 4872-4876.

Vey, M., Pilkuhn, S., Wille, H., Nixon, R., Dearmond, S.J., Smart, E.J., Anderson, R.G.W., Taraboulos, A., and Prusiner, S.B. (1996). Subcellular Colocalization of the Cellular and Scrapie Prion Proteins in Caveolae-Like Membranous Domains. Proceedings of the National Academy of Sciences of the United States of America *93*, 14945-14949.

Vidal, E., Marquez, M., Ordonez, M., Raeber, A.J., Struckmeyer, T., Oesch, B., Siso, S., and Pumarola, M. (2005). Comparative study of the PrPBSE distribution in brains from BSE field cases using rapid tests. J Virol Methods *127*, 24-32.

Vigan, I., Jouvin-Marche, E., Leroy, V., Pernollet, M., Tongiani-Dashan, S., Borel, E., Delachanal, E., Colomb, M., Zarski, J.P., and Marche, P.N. (2003). T lymphocytes infiltrating the liver during chronic hepatitis C infection express a broad range of T-cell receptor beta chain diversity. J Hepatol *38*, 651-659.

Vignali, D.A. (2000). Multiplexed particle-based flow cytometric assays. J Immunol Methods *243*, 243-255.

Wadsworth, J.D.F., Joiner, S., Hill, A.F., Campbell, T.A., Desbruslais, M., Luthert, P.J., Collinge, J. (2001). Tissue distribution of protease resistant prion protein in variant CJD using a highly sensitive immuno-blotting assay. Lancet *358*, 171-180.

Wang, Y., Wang, J., Sun, Y., Wu, Q., and Fu, Y.X. (2001). Complementary effects of TNF and lymphotoxin on the formation of germinal center and follicular dendritic cells. J Immunol *166*, 330-337.

Ware, C.F. (2005). Network communications: lymphotoxins, LIGHT, and TNF. Annu Rev Immunol *23*, 787-819.

Wasley, A., Miller, J.T., and Finelli, L. (2007). Surveillance for acute viral hepatitis--United States, 2005. MMWR Surveill Summ *56*, 1-24.

Watanabe, S., Horie, Y., Kataoka, E., Sato, W., Dohmen, T., Ohshima, S., Goto, T., and Suzuki, A. (2007). Non-alcoholic steatohepatitis and hepatocellular carcinoma: lessons from hepatocyte-specific phosphatase and tensin homolog (PTEN)-deficient mice. J Gastroenterol Hepatol *22 Suppl 1*, S96-S100.

Watarai, M., Kim, S., Erdenebaatar, J., Makino, S., Horiuchi, M., Shirahata, T., Sakaguchi, S., and Katamine, S. (2003). Cellular prion protein promotes Brucella infection into macrophages. J Exp Med *198*, 5-17.

Waxman, D.J., and Azaroff, L. (1992). Phenobarbital induction of cytochrome P-450 gene expression. Biochem J *281 (Pt 3)*, 577-592.

Weiss, S., Proske, D., Neumann, M., Groschup, M.H., Kretzschmar, H.A., Famulok, M., and Winnacker, E.L. (1997). RNA aptamers specifically interact with the prion protein PrP. J Virol *71*, 8790-8797.

Weissmann, C., Enari, M., Klohn, P.C., Rossi, D., and Flechsig, E. (2002). Transmission of prions. J Infect Dis *186 Suppl 2*, S157-165.

Wen, S., Felley, C.P., Bouzourene, H., Reimers, M., Michetti, P., and Pan-Hammarstrom, Q. (2004). Inflammatory gene profiles in gastric mucosa during Helicobacter pylori infection in humans. J Immunol *172*, 2595-2606.

Will, R.G., Ironside, J.W., Zeidler M., Cousens S.N., Estibeiro K., Alperovitch A., Poser S., Pocchiari M., Hofman A., and Smith, P.G. (1996). A new variant of Creutzfeldt-Jakob disease in the UK. Lancet *347*, 921-925.

Willett, W.C., and MacMahon, B. (1984). Diet and cancer--an overview. N Engl J Med *310*, 633-638.

Williams, A.O., and Knapton, A.D. (1996). Hepatic silicosis, cirrhosis, and liver tumors in mice and hamsters: studies of transforming growth factor beta expression. Hepatology *23*, 1268-1275.

Williams, E.S., and Young, S. (1982). Spongiform encephalopathy of Rocky Mountain elk. JWildlDis *18*, 465-471.

Windl, O., Giese, A., Schulz-Schaeffer, W., Zerr, I., Skworc, K., Arendt, S., Oberdieck, C., Bodemer, M., Poser, S., and Kretzschmar, H.A. (1999). Molecular genetics of human prion diseases in Germany. Hum Genet *105*, 244-252.

Worm, M., and Geha, R.S. (1994). CD40 ligation induces lymphotoxin alpha gene expression in human B cells. Int Immunol *6*, 1883-1890.

Wu, C.G., Salvay, D.M., Forgues, M., Valerie, K., Farnsworth, J., Markin, R.S., and Wang, X.W. (2001). Distinctive gene expression profiles associated with Hepatitis B virus x protein. Oncogene *20*, 3674-3682.

Xiao, G., Harhaj, E.W., and Sun, S.C. (2001). NF-kappaB-inducing kinase regulates the processing of NF-kappaB2 p100. Mol Cell *7*, 401-409.

Yamada, Y., Kirillova, I., Peschon, J.J., and Fausto, N. (1997). Initiation of liver growth by tumor necrosis factor: deficient liver regeneration in mice lacking type I tumor necrosis factor receptor. Proc Natl Acad Sci U S A *94*, 1441-1446.

Yamagiwa, Y., Marienfeld, C., Tadlock, L., and Patel, T. (2003). Translational regulation by p38 mitogen-activated protein kinase signaling during human cholangiocarcinoma growth. Hepatology *38*, 158-166.

Yamaguchi, R., Yano, H., Iemura, A., Ogasawara, S., Haramaki, M., and Kojiro, M. (1998). Expression of vascular endothelial growth factor in human hepatocellular carcinoma. Hepatology *28*, 68-77.

Yoshida, H., Honda, K., Shinkura, R., Adachi, S., Nishikawa, S., Maki, K., Ikuta, K., and Nishikawa, S.I. (1999). IL-7 receptor alpha+ CD3(-) cells in the embryonic intestine induces the organizing center of Peyer's patches. Int Immunol *11*, 643-655.

You, L.R., Chen, C.M., and Lee, Y.H. (1999). Hepatitis C virus core protein enhances NF-kappaB signal pathway triggering by lymphotoxin-beta receptor ligand and tumor necrosis factor alpha. J Virol *73*, 1672-1681.

Yuki, K., Hirohashi, S., Sakamoto, M., Kanai, T., and Shimosato, Y. (1990). Growth and spread of hepatocellular carcinoma. A review of 240 consecutive autopsy cases. Cancer *66*, 2174-2179.

Zanata, S.M., Lopes, M.H., Mercadante, A.F., Hajj, G.N., Chiarini, L.B., Nomizo, R., Freitas, A.R., Cabral, A.L., Lee, K.S., Juliano, M.A.*, et al.* (2002). Stress-inducible protein 1 is a cell surface ligand for cellular prion that triggers neuroprotection. Embo J *21*, 3307-3316.

Zandi, E., Chen, Y., and Karin, M. (1998). Direct phosphorylation of IkappaB by IKKalpha and IKKbeta: discrimination between free and NF-kappaB-bound substrate. Science *281*, 1360-1363.

Zanusso, G., Ferrari, S., Cardone, F., Zampieri, P., Gelati, M., Fiorini, M., Farinazzo, A., Gardiman, M., Cavallaro, T., Bentivoglio, M.*, et al.* (2003). Detection of pathologic prion protein in the olfactory epithelium in sporadic Creutzfeldt-Jakob disease. N Engl J Med *348*, 711-719.

Zebrowski, B.K., Liu, W., Ramirez, K., Akagi, Y., Mills, G.B., and Ellis, L.M. (1999). Markedly elevated levels of vascular endothelial growth factor in malignant ascites. Ann Surg Oncol *6*, 373-378.

Zeremski, M., Petrovic, L.M., and Talal, A.H. (2007). The role of chemokines as inflammatory mediators in chronic hepatitis C virus infection. J Viral Hepat *14*, 675-687.

Zerr, I., Giese, A., Windl, O., Kropp, S., Schulz-Schaeffer, W., Riedemann, C., Skworc, K., Bodemer, M., Kretzschmar, H.A., and Poser, S. (1998). Phenotypic variability in fatal familial insomnia (D178N-129M) genotype. Neurology *51*, 1398-1405.

Zhang, C.C., Steele, A.D., Lindquist, S., and Lodish, H.F. (2006). Prion protein is expressed on long-term repopulating hematopoietic stem cells and is important for their self-renewal. Proc Natl Acad Sci U S A *103*, 2184-2189.

Zhang H, K.K., Nguyen JT, et al. (1995). Conformational transitions in peptides containing two putative alpha-helices of the prion protein. J Mol Biol *250*, 514-526.

Zhang, J., Chen, L., Zhang, B.Y., Han, J., Xiao, X.L., Tian, H.Y., Li, B.L., Gao, C., Gao, J.M., Zhou, X.B.*, et al.* (2004). Comparison study on clinical and neuropathological characteristics of hamsters inoculated with scrapie strain 263K in different challenging pathways. Biomed Environ Sci *17*, 65-78.

Zhu, N., Khoshnan, A., Schneider, R., Matsumoto, M., Dennert, G., Ware, C., and Lai, M.M. (1998). Hepatitis C virus core protein binds to the cytoplasmic domain of tumor necrosis factor (TNF) receptor 1 and enhances TNF-induced apoptosis. J Virol *72*, 3691-3697.

Zigas, V., and Gajdusek, D.C. (1957). Kuru: Clinical study of a new syndrome resembling paralysis agitans in natives of the Eastern Highlands of Australian New Guinea. Med J Austral *2*, 745-754.